

PHD THESIS



Heterocycle-based redox active, electrochromic organic materials

PhD School Director:
Prof. Gianpaolo Brivio

Supervisor:
Dr. Luca Beverina

Candidate:
Mauro Sassi
040824

Abstract

ELECTROCHROMIC MATERIALS represent a special and intriguing class of redox active compounds, characterized by a drastic change in their optical properties upon reduction or oxidation. Many aromatic organic molecules, monomeric or polymeric, are electrochromic, and some of them can even outperform their inorganic counterparts in some aspects. In particular, the ability to easily tune the colour of the redox states, represent an invaluable asset of this class of compounds. Among the many different organic electrochromic materials, those possessing a highly transmissive colourless state have gained much attention for their potential application in smart windows, self-darkening eyeglasses, anti-glare car rearview mirrors, etc. Moreover, a neutral tint of the coloured form is desired for these applications in order to avoid colour distortion.

This work develops a novel class of discrete and polymeric electrochromic materials based on the violene structural motif. In particular, the class of diazinium ethenes has been explored and the electrochromic properties of the derivatives have been evaluated by electrochemical measures. These compounds have shown to undergo a reversible two-electron transfer, accompanied by a colourless \rightleftharpoons coloured electrochromic behaviour with high contrast in the 450-550 nm region.

The new violene discrete electrochromes were then incorporated in a poly(3,4-ethylenedioxythiophene) (PEDOT) matrix, developing an hybrid multichromophoric system that take advantage of the characteristics of both systems to achieve a panchromatic absorption in the reduced state and a very high contrast value. In particular, the incorporation of the violene electrochromes has been obtained linking them, through a tether, to an EDOT moiety, and subsequently polymerizing (chemically or electrochemically) the modified monomers (ISOx). The obtained polymers, poly(ISOx), display colourless highly transmissive oxidized states and reduced states with an extended colour palette (violet-red, purple and brown). Moreover, an impressive electrochromic contrast in the visible region has been achieved, with calculated luminance variations as high

as 72%. This result represent a big improvement compared to the literature reported 52% for a system with comparable spectral characteristics.

In the last chapter, a novel and versatile synthon for EDOT derivatization, *exo*-methylene-EDOT, is described and characterized along with some of its derivatives. This compound readily react with alcohols under acid catalysis to give Markovnikov addition products, and with thiols, in presence of radical initiators or photochemically, to give sulfides (anti-Markovnikov products). The latter reactivity proved to be very interesting for the extreme rapidity and high conversions achieved. An EDOT derivative with a pendant trialkoxysilane moiety has been prepared using 3-mercaptopropyltrimetoxysilane as thiol counterpart. This compound was subsequently tested as reagent for the functionalization of surfaces with EDOT moieties. An alternative approach, relying on an *in situ* thiol-ene reaction between *exo*-methylene-EDOT and a thiol functionalized surface, was also tested to achieve such functionalization. Both procedures have demonstrated to provide the desired surface modification. This kind of ultra thin films could find application as coupling layers for the deposition of PEDOT-like polymers on metal oxides, solving the adhesion problems that hamper the long-term operation of the devices.

Acknowledgements

First, I would like to thank Prof. Giorgio Pagani, for his wise and experienced guidance during these last 7 years. He allowed me to pursue the research presented in this dissertation, keeping me on the right track with a right balance of encouragement and objective criticism. With no less sincerity, I would also like to thank Dr. Luca Beverina, a supervisor and an endless source of inspiration. His insight and advice played a key role in determining the success of this research project. In addition, I am thankful to Prof. Milko van der Boom from the Weizmann Institute of Science in Rehovot, Israel for hosting me in his group during my 6-months research period there, permitting the attainment of the results exposed in section 4.5.

I would like also to acknowledge the people I collaborated with, and who helped in the realization of the work presented in this dissertation: Dr. Matteo Salamone and Dr. Riccardo Ruffo for the electrochemical characterization of all the compounds, Dr. Giorgio Patriarca for acquiring high resolution NMR spectra of the compounds, Dr. Marco Vettigli for his support in the synthesis of some of the compounds, Dr. Uwe Posset and his collaborators from the Fraunhofer ISC in Würzburg, Germany for teaching me the techniques used in the deposition of PEDOT-based thin films.

A special thank goes to Dr. Alessandro Sanguineti, Dr. Norberto Manfredi and all those people who contributed to make our lab a nice and stimulating workplace. I extend these thanks to all the wonderful people in Milko van der Boom group for their help, their patience and most of all their friendship.

Finally, I'd like to thank Laura, my family and all my friends for their support, understanding, and unwavering patience during these years.

Contents

1	Introduction to Electrochromic Materials	1
1.1	Electrochromism	1
1.2	Electrochromic materials: Performance Evaluation	2
1.2.1	Contrast Ratio	2
1.2.2	Coloration Efficiency	5
1.2.3	Electrochromic Memory Effect	6
1.2.4	Response Time	6
1.2.5	Write-Erase Efficiency	7
1.2.6	Cycle Life	7
1.2.7	Colour Analysis	8
1.2.7.1	Introduction to the CIE System	8
1.2.7.2	Chromaticity Coordinates	11
1.2.7.3	CIELAB and CIELUV uniform color spaces	12
1.2.7.4	Colorimetry of ECDs	15
1.3	Inorganic Electrochromic Materials	16
1.3.1	Metal Oxides	16
1.3.2	Prussian Blue	18
1.4	Organic Electrochromic Materials	21
1.4.1	Conjugated Polymers	21
1.4.1.1	Polyanilines	24
1.4.1.2	Polycarbazoles	26
1.4.1.3	Polypyrroles	27
1.4.1.4	Polythiophenes	28
1.4.1.5	Poly(3,4-alkylenedioxythiophene)s	30
1.4.1.6	Poly(3,4-alkylenedioxyppyrole)s	35
1.4.1.7	Donor-acceptor Polymers	36
1.4.1.8	Polymerization methods	39
1.4.2	Discrete Reversible Organic Redox Systems	44

1.4.2.1	Violenes	45
1.4.2.2	Violene/Cyanine Hybrids	55
1.4.2.3	Electrochromic systems based on intramolecular redox switching of bonds	58
1.4.3	Metal Coordination Complexes	61
1.4.4	Composite multichromophoric polymeric systems	65
2	Two step reversible discrete electrochromes switching from coloured to highly transmissive	69
2.1	Introduction	69
2.2	Concepts of molecular design of violenes	70
2.3	Novel electrochromes based on heteroaromatic diazinium ethenes	73
2.3.1	Synthesis of the electrochromes	76
2.3.1.1	1,2-bis(10-methylacridin-9(10 <i>H</i>)-ylidene)ethane	76
2.3.1.2	Quinolinium/isoquinolinium substituted ethenes	77
2.3.2	Electrochemical and Spectroelectrochemical Properties . .	84
2.3.2.1	(<i>E</i>)-1-hexyl-4-(2-(1-methylpyridinium-4-yl)vinyl)-pyridinium iodide trifluoromethanesulfonate . .	84
2.3.2.2	1,2-bis(10-methylacridin-9(10 <i>H</i>)-ylidene)ethane	84
2.3.2.3	Quinolinium/isoquinolinium substituted ethenes	87
2.3.2.4	(<i>E</i>)-3-methyl-2-(2-(1-methylquinolinium-4-yl)vinyl)-benzo[<i>d</i>]thiazol-3-ium trifluoromethanesulfonate	94
2.4	Conclusions	94
3	Novel EDOT functionalized diazinium ethenes (ISOx) and polymers thereof	96
3.1	Introduction to multichromophoric polymeric systems	96
3.2	Incorporation of violenes in a PEDOT matrix	98
3.3	Novel poly(ISOx) electrochromic polymers	99
3.3.1	Synthesis of the monomers (ISOx)	101
3.3.2	Electrochemical characterization of ISOx and p(ISOx) compounds	105
3.3.2.1	Electrochemical polymerization	105
3.3.2.2	<i>In situ</i> chemical polymerization of ISOx derivatives	112
3.3.2.3	Electrochromic properties of polyISOx polymers	113
3.4	Conclusions	118

4	emEDOT: a versatile new entry in EDOT chemistry	121
4.1	Introduction	121
4.2	Synthesis of exomethylene-EDOT (emEDOT)	122
4.3	Reactivity of the <i>exo</i> -methylene group	123
4.3.1	Acid catalyzed isomerization	123
4.3.2	Acid catalyzed addition of alcohols	124
4.3.3	Radical addition of thiols	124
4.4	Electrochemical characterization of the derivatives	129
4.4.1	emEDOT and methyl-VDOT	129
4.4.2	2-alkoxy-2-methyl-2,3-dihydrothieno[3,4- <i>b</i>][1,4]dioxines	131
4.4.3	EDOT-(methyl)(3-(trimethoxysilyl)propyl)sulfide	132
4.5	Surface functionalizations	133
4.6	Conclusions	136
	References	138
A	Experimental procedures	158
A.1	General procedure for <i>in situ</i> chemical polymerization of ISOx monomers	160
A.2	Procedures for surface functionalizations	161
A.3	Synthetic procedures	161

Chapter 1

Introduction to Electrochromic Materials

1.1 Electrochromism

The phenomenon of electrochromism can be macroscopically defined as the change, evocation or bleaching of colour as a consequence of an electron transfer (redox) process occurring in a material. For practical applications this process is required to be reversible.¹⁻³ When an electrochromic material is incorporated in an electrochromic device, it is able to change its optical properties upon application of a small electrical voltage and change them back to the initial state upon inversion of the applied potential.⁴ For a material to be electrochromic it has to show:

- multiple stable, accessible redox states;
- absorption bands in the visible region (at least in one state);
- generation of different visible region electronic absorption bands on switching between redox states.

Electrochromism results from the generation of different visible region electronic absorption bands on switching between redox states. The colour change is commonly between a transmissive (bleached) state and an absorptive coloured one, or between two absorptive coloured states with different hues. In cases

where more than two redox states are electrochemically available, the electrochromic material may exhibit several colours and be termed polyelectrochromic.

Likely applications of electrochromic materials include their use in:

- controllable light-reflective or light-transmissive devices for optical information and storage,
- anti-glare car rear-view mirrors,
- sunglasses,
- protective eyewear for the military,
- controllable aircraft canopies,
- glare-reduction systems for offices,
- smart windows for use in cars.

Of these, electrochromic car rear-view mirrors have already achieved considerable commercial success. These safety devices prevent mirror-reflected glare which causes an after image to stay on the eye's retina.

1.2 Electrochromic materials: Performance Evaluation

In order to allow the comparison of the performances of different electrochromic materials, we will briefly introduce some of the more common quantities adopted in the literature. For most of them, a standardization of the measuring techniques does not exist. Nevertheless, a clear understanding of them is of central importance to correctly evaluate the right material for a certain application.

1.2.1 Contrast Ratio

The contrast ratio CR is a commonly employed measure denoting the intensity of colour formed electrochemically as seen by eye (Eq. 1.1):

$$CR = \frac{R_0}{R_x} \quad (1.1)$$

where R_x is the intensity of light reflected diffusely through the coloured state of a display, and R_o is the intensity reflected similarly but from a non-shiny white card. The ratio CR is best quoted at a specific wavelength usually at λ_{max} of the coloured state.

As in practice, a CR of less than about 3 is almost impossible to see by eye, and an as high as possible value is desirable. Typical values of 60:1 can be obtained in devices based on heptyl viologen radical cation, or 10:1 for the cell $WO_3|electrolyte|NiO$.^{1,5} In the case of a transmissive device of the type employed in smart windows, sunglasses, etc., Eq. 1.1 can be reformulated considering the ratio between transmitted light in coloured and bleached states at a certain wavelength (Eq. 1.2):

$$CR = \frac{T_b}{T_c} = e^{(\alpha_c - \alpha_b)L} \quad (1.2)$$

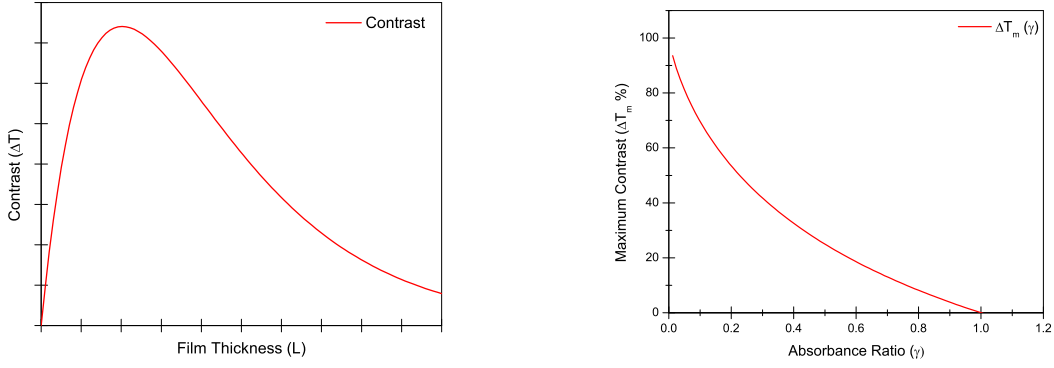
where T_b and T_c are the transmittances of the device in bleached and coloured state respectively. Another way to evaluate contrast is to use absorbance variation $\Delta A = \log(CR)$ between the two states.

However, both these expressions for contrast suffer from some limitations since most of the applications of electrochromic materials (windows, sunglasses, etc.) deal with the concept of color (or brightness) as perceived by human beings. As a consequence, a good contrast parameter should take into account the physiology of vision and color perception. As an example one should consider that when the EC film is extremely thin, the brightness of an EC device in the bleached state and in the colored state are indistinguishable as the film appears almost colourless in both states, while the opposite happens for a very thick film as both states are fully absorbing. Thus, in accordance with eye-perception, the maximum contrast of an EC film is achieved at some intermediate thickness while both CR from Eq. 1.2 and ΔA show a monotonical increase with layer thickness L . A simple way to solve this problem is to express contrast of an EC device as transmittance variation between the two states (Eq. 1.3):

$$\Delta T(\lambda, L) = T_b(\lambda, L) - T_c(\lambda, L) = e^{-\alpha_b(\lambda)L} - e^{-\alpha_c(\lambda)L} \quad (1.3)$$

obtaining a quantity that shows a maximum at a certain thickness $L_m(\lambda)$ (Fig. 1.1a).^{6,7}

The expression in Eq. 1.3 is valid if the film is uniform and colouration efficiency is constant, so that Lambert-Beer law $A = \epsilon cL = \alpha L$ can be applied. The optimum value of thickness $L_m(\lambda)$ can thus be calculated easily solving



(a) ΔT as a function of film thickness (L) for fixed wavelength λ and value of γ .

(b) Maximum achievable contrast ΔT_m as a function of absorbance ratio (γ)

Figure 1.1

$d(\Delta T)/dT = 0$ obtaining:

$$L_m(\lambda) = \frac{\ln\left(\frac{\alpha_b}{\alpha_c}\right)}{\alpha_b - \alpha_c} = \frac{1}{\alpha_b} \cdot \frac{\ln(\gamma)\gamma}{\gamma - 1} \quad (1.4)$$

where $\gamma(\lambda) = \alpha_b(\lambda)/\alpha_c(\lambda) = A_b(\lambda)/A_c(\lambda)$, and is dependent on the chosen wavelength λ . From Eq. 1.3 and 1.4 follows that the maximum contrast achievable at a certain wavelength λ is:

$$\Delta T_m(\lambda) = \left(\frac{1}{\gamma} - 1\right) \cdot \left(\frac{1}{\gamma}\right)^{\frac{1}{\gamma-1}} \quad (1.5)$$

where $\gamma(\lambda)$ is simply the ratio of the absorbance spectra ($0 < \gamma < 1$, Fig. 1.1b). From the experimental point of view, values close to the optimal value are easy to obtain since plotting $\Delta T/\Delta T_m(L/L_m)$ for some values of γ one can see that the function is quite "flat" near the optimal thickness value (Fig. 1.2). As a matter of facts ΔT is the most widespread parameter encountered in the literature for the evaluation of electrochromic contrast. Nevertheless, it's a rough approximation that relies on a single wavelength measure, ignoring the rest of spectral data and human color perception. Consequently, it appears to be a simple way to evaluate performance of ECDs exhibiting the same or a very similar visible absorption band, but cannot be used for comparisons between electrochromes with different spectral behaviour. In these cases the best parameter for contrast evaluation is lightness variation ΔL^* between the two states, where lightness L^* is a colorimetric coordinate in CIE 1976 $L^*a^*b^*$ color space. A short introduction to this color space will follow in section 1.2.7.3

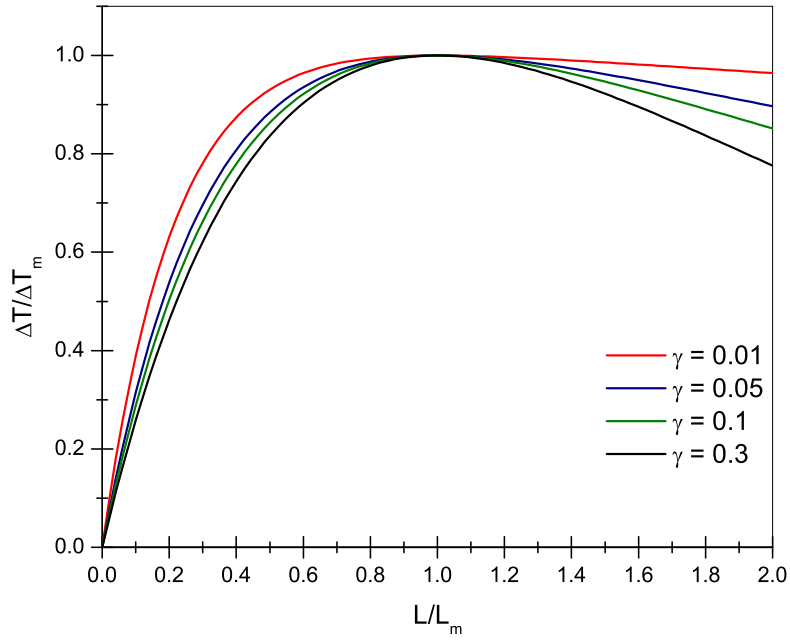
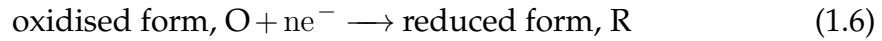


Figure 1.2 $\Delta T/\Delta T_m$ as a function of L/L_m for some values of γ

1.2.2 Coloration Efficiency

During the operation of the ECD, the electrochemical process occurring at the electrode can be depicted as in Eq. 1.6 where the electrochrome, in its oxidised form O , accepts n electrons from the electrode changing to its reduced form R .



Following Faraday's first law, the number of color centres formed is hence proportional to the amount of electrochemical charge passed for unit area Q , and one has, considering Lambert-Beer law, $\Delta A \propto Q$. This faradaic charge equals total charge only in the absence of 'non-faradaic' processes in the cell, and in the absence of unwanted side reactions. Even in the presence of a 100% efficient process at the electrode, some deviations from Eq. 1.6 can be observed in solid state systems because both the shape of the absorption band and the position of its maximum can change somewhat with the extent of charge insertion.¹ The proportionality factor between ΔA and Q is called *colouration efficiency* (Eq. 1.7) and is clearly dependent on the optical pathlength.

$$\eta = \frac{\Delta A}{Q} \left[\text{cm}^2 \text{C}^{-1} \right] \quad (1.7)$$

Colouration efficiencies must be determined at a fixed, cited, wavelength; η is defined as positive if colour is generated cathodically, but negative if colour is generated anodically. Organic electrochromes usually show higher colouration efficiencies when compared to inorganic counterparts as a consequence of the different nature of the electronic transitions responsible for the colouration. Typical values of η for different electrochromes are listed in table 1.1.

Table 1.1 Colouration efficiencies of different electrochromes

Electrochrome	λ_{max}	η	Ref.
	nm	cm ² C ⁻¹	
WO ₃	630–633	36–115	8–10
NiO	630	-37	11
Methyl Viologen	604	176	1,12
Indigo Blue	608	-158	1,12
Methylene Blue	661	-417	1,12
Safranin O	530	-274	1,12
Poly(3,4-propylenedioxyppyrrrole)	480	-520	1,12
Poly(3,4-propylenedioxythiophene)	551	275	1,12
Poly(3,4-ethylenedioxythiophene)	585	183	13

1.2.3 Electrochromic Memory Effect

In ECDs, colour is generated upon application of an external voltage which causes charges (electrons and counterions) to flow. As a consequence, in such a device colour can be easily modulated and controlled monitoring the applied potential and the amount of charge passed. In the absence of defects (e.g.: electronic conduction in the electrolyte), when the external circuit is open electron flow is inhibited, and hence the device preserves its state (bleached or coloured). As a consequence, ECDs don't need a continuously applied voltage (unlike liquid crystal based devices), and consume power only during the switching process (*memory effect*).

1.2.4 Response Time

The response time (or switching time) τ is the time required to the ECD to change from one redox state to the other and vice versa. This parameter is especially important for applications like displays and ophthalmic lenses where

a rapid colour change is desirable. It is usually defined as the time required for some fraction of the final colour to form. Calculation is performed on single-wavelength chronoabsorptometric and chronocoulometric data from an electrochemical kinetic experiment where the device is switched from fully reducing to fully oxidizing potential values (potential steps). A lot of different factors contribute in the determination of the kinetic of the ECD thus affecting τ , but their role is very dependent on the class of materials under study, preparation/deposition technique, device structure, nature of the electrolyte, etc. For electrochromic devices based on conjugated polymers ionic diffusion inside the electrolyte and inside the electrochromic polymeric layer play a dominant role as shown by Anson plots of chronocoulometric data.¹⁴ Reynolds *et al.*^{13,15} reported values of 0.36s and 2.2s/4.4s for PEDOT oxidation and for Prussian Blue oxidation/reduction processes respectively.

1.2.5 Write-Erase Efficiency

The write-erase efficiency is the fraction of the originally formed colour that can be subsequently electrobleached. Values lower than 100% can result from the presence of non-reversible processes at the electrode or when the electrochrome is soluble, at least in one of its redox states, in the electrolytic solution and hence able to diffuse away from the electrode.

1.2.6 Cycle Life

Cycle life represents the number of write-erase cycles that an ECD can perform before any significant extent of performance degradation has occurred. The measure of cycle life is usually performed switching the device repeatedly with double potential steps between its coloured and bleached states with pulses duration greater than τ . Since ECDs are quite complex, many different factors can contribute to lower cycle life, and the determination of dominant ones is a key aspect of the optimization process. Where organic electrochromes are employed, long term stability of both redox states to operational conditions must be carefully considered, and observed cycle lives are usually lower than those of inorganic counterparts. Cycle lives in the order of 10^5 cycles are usually required for applications.

1.2.7 Colour Analysis

The ability to describe, measure and compare colours is a pivotal tool in all those research areas where light interaction with human eye is somewhat involved, and concepts like *hue*, *lightness*, *brightness*, *saturation* play a crucial role. Electrochromic materials make no exception since color of light transmitted or reflected by ECDs have to be considered in most of their applications (e.g.: smart windows, sunglasses, etc.). Since colour is a visual perceptual property, its measure is not directly possible. To solve this problem, the International Commission on Illumination (*Commission Internationale de l'Éclairage*, CIE) has developed the so called CIE colorimetry, which looks back over an evolution of 75 years. CIE colorimetry deals with the measure of the stimulus that causes colour perception and can thus be defined as the metric of the psychophysical color stimulus.^{1,16}

1.2.7.1 Introduction to the CIE System

Light sensation is produced by visible radiation; electromagnetic radiation falling within the wavelength limits of 380nm and 780nm. Radiation from the short wavelength range of this radiation usually produces the sensation of blue light; radiation with wavelengths between 520nm and 550nm is seen as green light, and above about 650nm we usually perceive the light to be of red color. These limits are not well defined, and the actual perception depends strongly on the adaptation state of the eye and on light stimuli surrounding the test object. Basic colorimetry, the description of the results of color matching experiments, is built on additive color mixing and obeys to the following empirical rules:

1. Three independent variables are necessary and sufficient for the specification of a color match.
2. For an additive mixture of color stimuli, only their tristimulus values are relevant, not their spectral compositions.
3. If one or more components of the mixture are gradually changed, the resulting tristimulus values also change gradually.

Once a colour matching experiment (Fig. 1.3) is performed between a tested colour and three properly selected stimuli (e.g. monochromatic red, green and blue lights with variable intensity), the colour can be characterized by the three luminance values of the matching stimuli reaching the eye of the observer. The

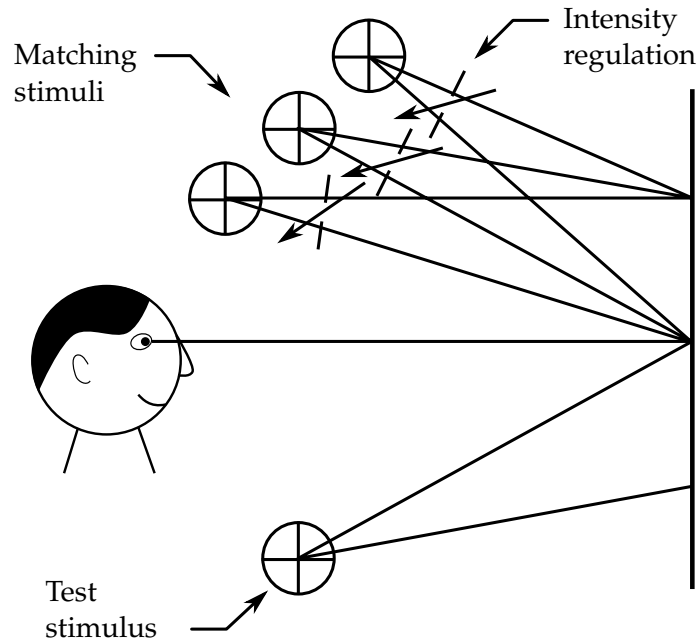


Figure 1.3 Basic color matching experiment

spectral power distributions (SPDs) of the test stimulus and of the additive mixture of the three matching stimuli are usually different. In such cases we speak about metameric colors: they look alike to the human observer (having equal tristimulus values), but their SPD is different. It is apparent that, defining clearly the matching stimuli (spectral composition, intensity units), is possible to describe a color match in the form:

$$[C] \equiv R[R] + G[G] + B[B] \quad (1.8)$$

where $[C]$ is the unknown stimulus and $[R]$, $[G]$, $[B]$ are the matching stimuli. The equation can be rewritten, for a nonmonochromatic test color stimulus, in the form:

$$[C] = \int_{380\text{nm}}^{780\text{nm}} \bar{r}(\lambda)P(\lambda) d\lambda \cdot [R] + \int_{380\text{nm}}^{780\text{nm}} \bar{g}(\lambda)P(\lambda) d\lambda \cdot [G] + \int_{380\text{nm}}^{780\text{nm}} \bar{b}(\lambda)P(\lambda) d\lambda \cdot [B] \quad (1.9)$$

where $\bar{r}(\lambda)$, $\bar{g}(\lambda)$ and $\bar{b}(\lambda)$ are the *color matching functions* (CMFs), and represent the amounts of the three matching stimuli needed to match the monochromatic constituent of the equienergy spectrum at wavelength λ . The CIE 1931 standard defines a standard observer and the spectral composition of the primaries (single monochromatic wavelengths: 700nm for the red, 546.1 for the green and 435.8 for the blue). The requirement that, for an equienergy spectrum, the addition of unit amounts of the three primaries gives the colour match leads to

the following expression for luminance of a colour stimulus with tristimulus values R, G, B :

$$L = 1.0000R + 4.5907G + 0.0601B \quad (1.10)$$

as a consequence of the different energy content of the three monochromatic radiations. Performing colour matching with the stated primaries, CMFs illustrated in figure 1.4a are obtained.

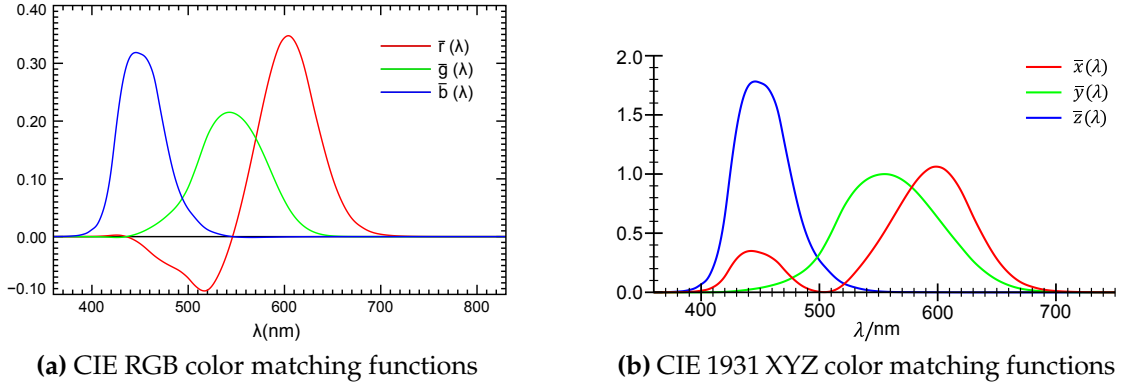


Figure 1.4

Negative lobes indicate that in some part of the spectrum a match can be obtained only adding the matching function to the test stimulus. To avoid this problem in 1931 CIE decided to transform from the real $[R], [G], [B]$ primaries to a set of imaginary primaries $[X], [Y], [Z]$ where CMFs have no negative lobes (Fig. 1.4b). Further requirements were that the tristimulus values of an equienergy stimulus should be equal ($X = Y = Z$), that one of the tristimulus values should provide a photometric quantity, and that the volume of the tetrahedron set by the new primaries should be as small as possible. The transformation is described by Eq. 1.11.

$$\begin{pmatrix} X \\ Y \\ Z \end{pmatrix} = \begin{pmatrix} 2.768892 & 1.751748 & 1.130160 \\ 1.000000 & 4.590700 & 0.060100 \\ 0 & 0.056508 & 5.594292 \end{pmatrix} \cdot \begin{pmatrix} R \\ G \\ B \end{pmatrix} \quad (1.11)$$

In connection with Eq. 1.8 the amounts of primaries needed to achieve the colour match are the tristimulus values. In CIE-XYZ system they are defined

as:

$$\begin{aligned}
 X &= k \int_{380\text{nm}}^{780\text{nm}} \phi_{\lambda}(\lambda) \bar{x}(\lambda) d\lambda, \\
 Y &= k \int_{380\text{nm}}^{780\text{nm}} \phi_{\lambda}(\lambda) \bar{y}(\lambda) d\lambda, \\
 Z &= k \int_{380\text{nm}}^{780\text{nm}} \phi_{\lambda}(\lambda) \bar{z}(\lambda) d\lambda;
 \end{aligned}
 \tag{1.12}$$

where $\phi_{\lambda}(\lambda)$ is the colour stimulus function seen by the observer.

Colorimetry makes distinction between two different classes of color stimuli:

- stimuli reaching the observer directly from a primary light source (e.g. sunlight, color monitor etc.);
- stimuli reaching the observer from a reflective or transmissive material;

and the constant k in Eq. 1.12 assumes different values for the two cases. Our interest is focused on non-self-luminous objects, called secondary light sources, where light coming from a primary source falls on a transmitting/reflecting material and part of it reaches the observer. Being the spectral reflection and transmission described by spectral reflectance $R(\lambda)$ and spectral transmittance $T(\lambda)$, we can write the colour stimulus function as:

$$\phi_{\lambda}(\lambda) = R(\lambda) \cdot S(\lambda) \text{ or } \phi_{\lambda}(\lambda) = T(\lambda) \cdot S(\lambda)
 \tag{1.13}$$

where $R(\lambda)$ is the spectral reflectance factor and $T(\lambda)$ the spectral transmittance factor of the object color (evaluated following a standard geometric condition), and $S(\lambda)$ is the relative SPD of the illuminant (possibly one of those standardized by CIE).

1.2.7.2 Chromaticity Coordinates

Since the colour stimulus is fully described by the tristimulus values X, Y, Z , a full plot all visible colours is a 3D figure. However, it is possible to divide the concept of colour in two parts: *brightness* and *chromaticity*. For example, grey and white are considered to have the same chromaticity but different brightness. In CIE XYZ color space Y parameter is designed to measure brightness (or luminance) of colour while chromaticity is measured by two derived pa-

parameters x and y defined inside a derived colour space:

$$\begin{aligned} x &= \frac{X}{X+Y+Z}, \\ y &= \frac{Y}{X+Y+Z}, \\ z &= \frac{Z}{X+Y+Z} = 1 - x - y. \end{aligned} \tag{1.14}$$

The diagram that represents all the chromaticities visible to the average person (gamut of human vision), is called chromaticity diagram and is represented in figure 1.5. The curved edge of the gamut is called the spectral locus and corresponds to monochromatic light, with wavelengths listed in μm .

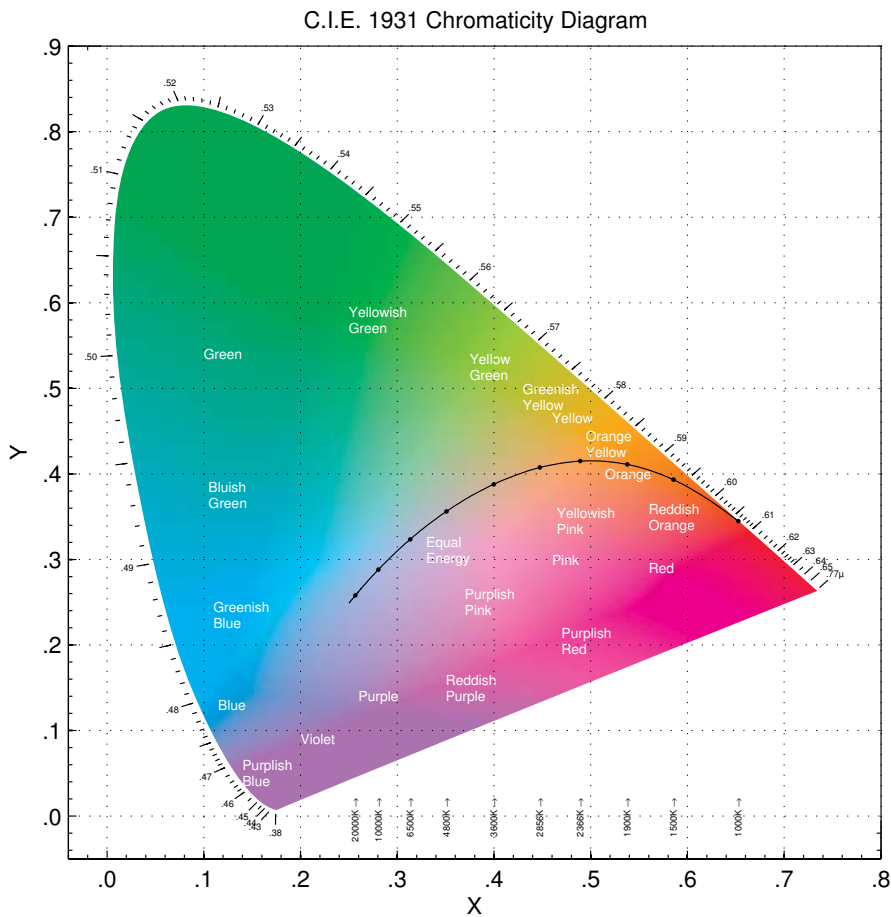


Figure 1.5 CIE 1931 color space chromaticity diagram

1.2.7.3 CIELAB and CIELUV uniform color spaces

CIE Y,x,y color space is well suited to describe colour stimuli. However some problems arise when looking to color differences (*e.g.* if someone want to know

if two different samples will be indistinguishable by visual observation or not). In 1942, Macadam¹⁷ showed that the chromaticity difference that corresponds to a just noticeable color difference will be different in different areas of the x,y chromaticity diagram, and that at one point in the diagram equal chromaticity differences in different directions represent visual color differences of different magnitudes (Fig. 1.6). In order to solve this problem and obtain a uniform

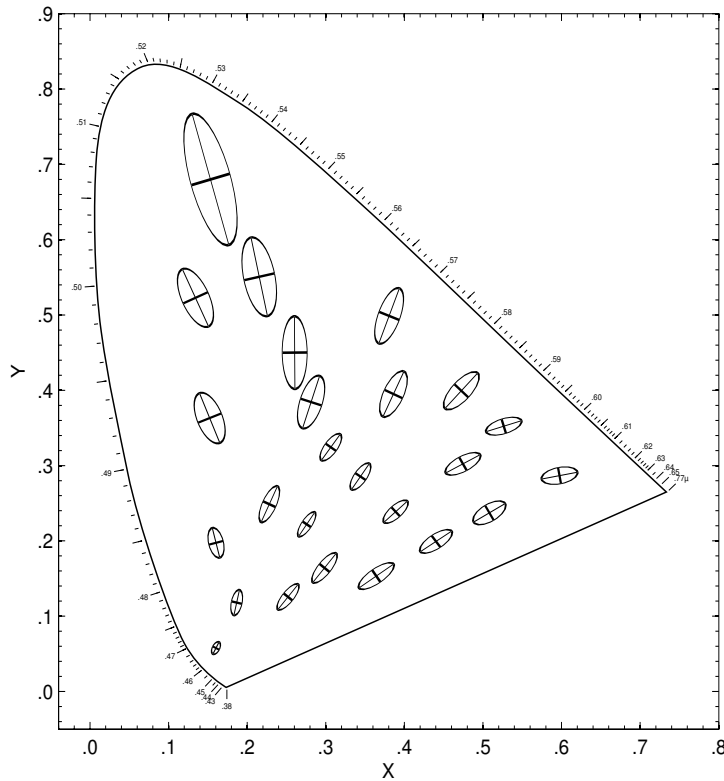


Figure 1.6 Ten times just noticeable chromaticity differences according to MacAdam's determination¹⁷

chromaticity diagram, different transformation of CIE Yxy were attempted but none was perfect. The following transformation for the *uniform chromaticity scale diagram* (CIE 1960 UCS diagram) was recommended by CIE in 1959 (and amended in 1976, Fig. 1.7):

$$\begin{aligned} u' &= \frac{4X}{X + 15Y + 3Z} = \frac{4x}{-2x + 12y + 3}, \\ v' &= \frac{9Y}{X + 15Y + 3Z} = \frac{9y}{-2x + 12y + 3}. \end{aligned} \tag{1.15}$$

However, colour stimuli are three dimensional, and the request to extend the UCS into a three dimensional space was already expressed at the time the 1960 UCS diagram. In 1976, CIE amended the UCS diagram and recommended two

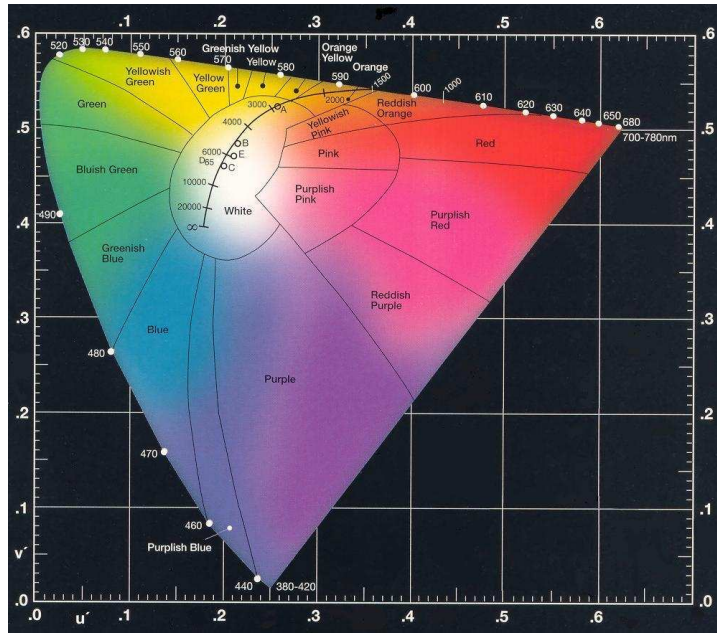


Figure 1.7 CIE 1976 uniform chromaticity scale diagram (UCS)

new color spaces: CIELAB and CIELUV. These new colour spaces are called *uniform colour spaces* and are formulated in such a way that equal distances correspond to colours that are perceptually equidistant. Both spaces can be used with the CIE 1931 standard colorimetric observer if the samples are seen within a visual angle between 1° and 4° .

CIELAB color space This color space is defined by the following equations:

$$\begin{aligned}
 L^* &= 116f(Y/Y_n) - 16, \\
 a^* &= 500[f(X/X_n) - f(Y/Y_n)], \\
 b^* &= 200[f(Y/Y_n) - f(Z/Z_n)].
 \end{aligned}
 \tag{1.16}$$

where

$$f(t) = \begin{cases} t^{1/3}, & \text{if } t > (\frac{6}{29})^3 \\ \frac{1}{3}(\frac{29}{6})^2 t + \frac{4}{29}, & \text{if } t \leq (\frac{6}{29})^3 \end{cases}
 \tag{1.17}$$

and where $X; Y; Z$ are the tristimulus values of the test object color stimulus considered, and X_n, Y_n, Z_n are the tristimulus values of a specified white object color stimulus. In most cases, the specified white object color stimulus should be light reflected from a perfect reflecting diffuser illuminated by the same light source as the test object. In this color space the positive a^* axis points approxi-

mately in the direction of red color stimuli, the negative axis approximately in the direction of green stimuli; positive b^* points approximately in the direction of yellow stimuli and negative b^* approximately in the direction of blue stimuli. L^* is coupled to the luminance of the stimulus, thus it is a crude correlate of lightness. Therefore one can construct approximate correlates of the perceived attributes lightness, chroma, and hue in the following form:

$$\text{CIE 1976 lightness : } L^* \text{ as in Eq. 1.16} \quad (1.18)$$

$$\text{CIELAB chroma : } C_{ab}^* = (a^{*2} + b^{*2})^{(1/2)} \quad (1.19)$$

$$\text{CIELAB hue angle : } h_{ab} = \arctan(b^*/a^*) \quad (1.20)$$

The CIE $L^*a^*b^*$ space is a standard commonly used in the paint, plastic and textile industries.

CIELUV color space In 1976, the CIE was unable to select only one single color space as representative "uniform color space", and agreed to a second one as well: CIELUV. The $L^*u^*v^*$ colour space is now used as a standard in television, video and the display industries. The L^* function of the CIELUV space is the same as that of the CIELAB space, thus equations 1.16 and 1.17 describe CIE 1976 lightness also in the CIELUV space. In a three-dimensional Euclidian space, the other two coordinates are:

$$\begin{aligned} u^* &= 13L^*(u' - u'_n), \\ v^* &= 13L^*(v' - v'_n). \end{aligned} \quad (1.21)$$

where $u'; v'$ are the CIE 1976 UCS coordinates of the test stimulus (Eq. 1.15, and $u_n; v_n$ are those of a specified white object color stimulus. In the CIELUV space, correlates of chroma, hue and saturation can be defined as follows:

$$\text{CIELUV saturation: } s_{uv} = 13 \left[(u' - u'_n)^2 + (v' - v'_n)^2 \right] \quad (1.22)$$

$$\text{CIELUV chroma : } C_{uv}^* = (u^{*2} + v^{*2})^{(1/2)} = L^* \cdot s_{uv} \quad (1.23)$$

$$\text{CIELUV hue angle : } h_{uv} = \arctan(v^*/u^*) \quad (1.24)$$

1.2.7.4 Colorimetry of ECDs

When it comes to electrochromic materials, it is clear that their properties are better described with the tools of colorimetry, and numerous examples of their application can be found in literature^{15,18-21}. Considering all the assets and

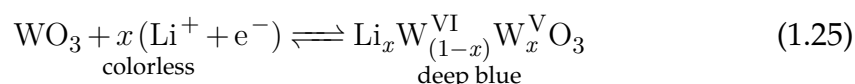
drawbacks of the three different colour spaces, generally in situ colorimetric results are expressed graphically in the CIE 1931 Yxy colour space system. (In addition, due to the common use of the CIELAB system, values of $L^*a^*b^*$ are also often reported). As a consequence, electrochromic contrast can be better described by luminance variation ΔL^* since it is a far better representation of lightness when compared to transmittance variation (described in section 1.2.1). Colorimetric measures on electrochromic films deposited on optically transparent electrodes are usually performed under potential control in a spectroelectrochemical cell, mounting the sample inside a light box, and using a commercial colorimeter (e.g. Minolta CS-100 Chroma Meter) in a 0/0 geometry. In this way, rather than simply measuring spectral absorption bands, the human eye's sensitivity to light across the whole visible spectral region is taken into account, and a numerical description of a particular colour is given. As an alternative one could calculate the colorimetric quantities starting from UV/Vis absorption data as described in ASTM E308 standard using a simple numerical spreadsheet. In this case, a calibrated light source that can be software corrected to represent the standard illuminants suggested by the CIE is required. Colour of ECDs in their redox states play a central role in many of their possible applications (e.g.: sunglasses, smart windows, displays). The need to expand the available color palette has driven most of the research on electrochromics in the last 10 years.²⁵ Full color display applications require materials switching from an highly transmissive state to an absorptive one with high color purity.^{19,26,27} On the other hand, the development of electrochromic materials able to change from an highly transmissive state to absorptive one with a neutral hue (located near the white point of the chromaticity diagram) is desired for some applications (windows, sunglasses, rearview mirrors) since this eliminates problems of colour distortion. However, this has remained a challenge owing to the extra requirement for simultaneous and efficient electrochemical bleaching of all absorption bands over the visible region, and there are only few examples of this type in literature.^{20,21}

1.3 Inorganic Electrochromic Materials

1.3.1 Metal Oxides

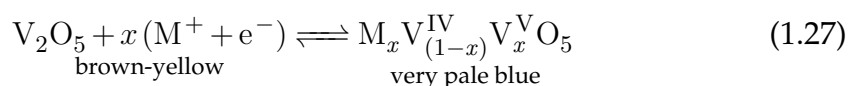
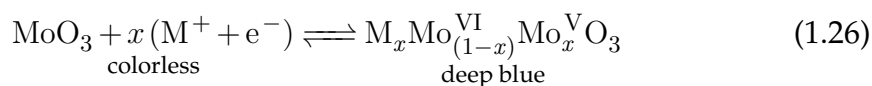
Among inorganic electrochromic materials, transition metal oxides occupy a central role since many of them can be electrochemically switched to non-stoichiometric

redox states with an intense electronic absorption band due to optical intervalence charge transfer. Metal oxides showing electrochromism include those of: cerium, chromium, cobalt, copper, iridium, iron, manganese, molybdenum, nickel, niobium, palladium, praseodymium, rhodium, ruthenium, tantalum, titanium, tungsten and vanadium. The coloured forms of these materials usually show blue or grey to black colouration, and it is much less common for transition-metal oxides to form other colours by intervalence transitions. The oxides of tungsten, molybdenum, iridium and nickel show the most intense electrochromic colour changes. The oxides IrO_2 , MoO_3 , Nb_2O_5 , TiO_2 , NiO , RhO_2 and WO_3 possess a colourless redox state, so allowing the electrochromic transition: colourless (clear) \rightleftharpoons coloured. This property is especially interesting, as stated in section 1.2.7.4, and finds application in on-off or light-intensity modulation roles.^{1,2,28} Tungsten trioxide (WO_3), a high-bandgap d^0 semiconductor, is the most widely studied electrochromic material. In 1815, Berzelius reported that pure WO_3 changed its colour from pale yellow when heated under a flow of H_2 gas²⁹, and the first recorded color change following an electrochemical reduction of WO_3 was in 1930³⁰. Thin-films of WO_3 with all tungsten sites in oxidation state W^{VI} are colourless or very pale yellow. On electrochemical reduction, W^{V} sites are generated, electrons and protons (or monovalent cations) are injected from the electrolyte, and colour change follows. In the case of Li^+ cations, which are often employed as the electrolyte cation, the reaction can be written as:

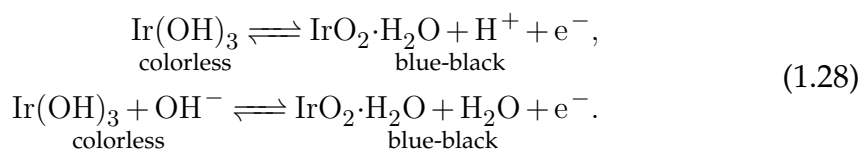


At low x the films have a deep blue color likely caused by photo-effected intervalence charge transfer (IVCT) between adjacent W^{V} and W^{VI} sites. At higher x , insertion irreversibly forms a metallic "bronze" that is red or golden. The details of the colouration mechanism in WO_3 are fairly complicated. Deb³¹ underlined the critical role played by defects (oxygen vacancies) along with the involvement of four other mechanisms: (a) IVCT, (b) polaronic absorption, (c) interband excitations, and (d) transitions from the valence band to the split-off W^{V} state. As a consequence of its interesting electrochromic properties and the many possible commercial applications, numerous production methods for WO_3 coatings were developed to produce thin (0.2-0.5 μm) even films on conductive substrates. These include a number of different deposition techniques: thermal evaporation in vacuum, electrochemical oxidation of tungsten

metal, chemical vapour deposition (CVD), sol-gel methods (spray pyrolysis, dip and spin coating), sputtering in vacuum (DC magnetron, electron beam, RF radiation), Langmuir-Blodgett deposition.¹ As stated above, many other metal oxides are electrochromic. As an example, molybdenum and vanadium oxides generate an intensely coloured redox state upon reduction with concurrent cation insertion (Eq. 1.26 and 1.27).



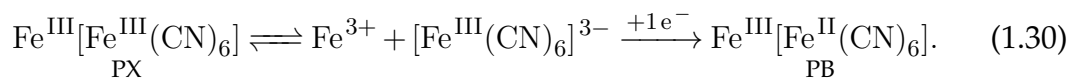
In contrast, group VIII oxides offer an example of anodically colouring electrochromic materials; as in the case of hydrated iridium oxide and hydrated nickel oxide. The former follows one of the two mechanisms proposed in Eq. 1.28 while the latter, in basic electrolytes, follows the mechanism depicted in Eq. 1.29.



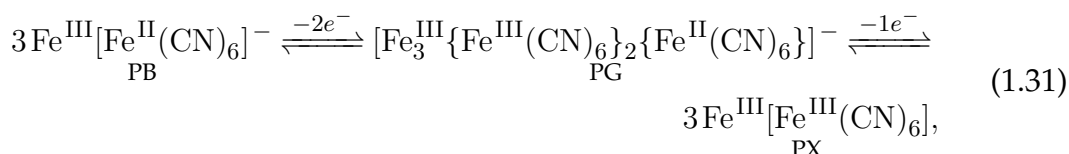
1.3.2 Prussian Blue

Prussian Blue [PB; Iron(III) hexacyanoferrate(II)], one of the first synthetic pigments (firstly prepared by Diesbach in Berlin in 1704³²) is the prototype of a number of polynuclear transition metal hexacyanometallates which form an important class of insoluble mixed-valence compounds with general formula $\text{M}'_k[\text{M}''(\text{CN})_6]_l$ (k, l integers), where M' and M'' are transition metals with different formal oxidation numbers. Prussian Blue is extensively used as a pigment in the formulation of paints, lacquers and printing inks. Since its intense blue colour arises from IVCT between the mixed-valence iron oxidation states³³, it follows that it can be removed by reduction or oxidation showing electrochromic properties. In 1978, a first report concerning the electrochemistry of PB thin films was reported by Neff³⁴, and extensive investigation of its properties followed, including applications in ECDs as primary or secondary

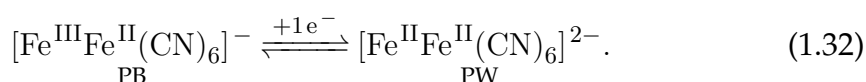
electrochrome. The preparation of PB thin films is usually performed by electrochemical reduction (Eq. 1.30) of solutions of the brown-yellow soluble complex Prussian Brown (PX, $\text{Fe}^{\text{III}}[\text{Fe}^{\text{III}}(\text{CN})_6]$) which is present as an adduct in equilibrium with free $\text{Fe}^{\text{III}}[\text{Fe}^{\text{III}}(\text{CN})_6]$ ions in solution (Eq. 1.30).



A subsequent three-stage electrodeposition mechanism for PB films has been established, with a nucleation stage where small PB nuclei cover the substrate surface, and the following stages where the growth becomes three dimensional, and is limited by diffusion of electroactive species (fall in growth rate is observed).³⁵ The obtained PB thin films can be either oxidized or reduced. Oxidation electrochemistry is illustrated in the following equation (1.31):



where the intermediate oxidation state, Prussian green (PG), has the composition shown in Eq. 1.31 in the case of bulk material, but it is believed that a continuous composition range exist, in the case of thin films; from PB to PX.³⁶ In contrast, electrochemical reduction of PB leads to Prussian white (PW) (Eq. 1.32) which appears colorless in thin films, a characteristic that make this redox process the most interesting from the point of view of ECDs.



The cyclic voltammetry showing the sharply peaked PB \rightarrow PW transition and the electrochemistry showing the PW, PB, PG and PX states are illustrated in Fig. 1.8. A broad current peak characterizes the PB \rightarrow PX transition, supporting the involvement of a range of different compositions. Although there are examples in literature where PB has been used as a sole electrochromic material to build an ECD^{37,38}, its use in conjunction with a complementary electrochromic material is more common. An example of this latter case is represented by the use of PB in conjunction with WO_3 since they are anodically and cathodically colouring electrochromes respectively.³⁹⁻⁴¹ In these complementary devices, both cathode and anode are electrochromic, and are simulta-

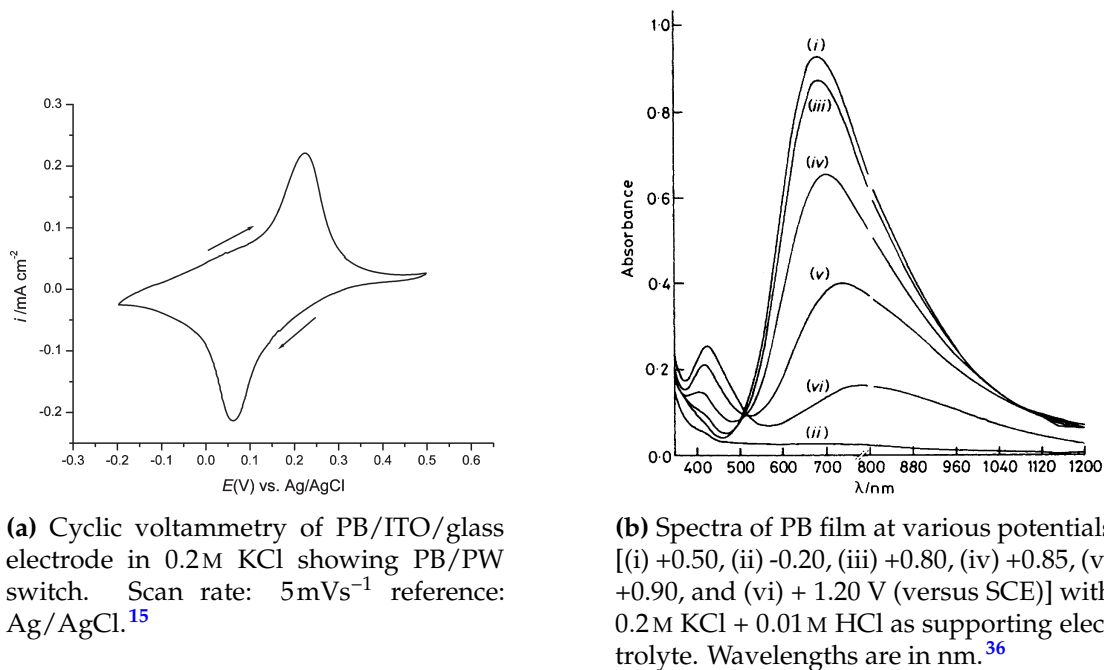


Figure 1.8

neously bleached/coloured switching the polarity with a synergistic effect on contrast. The same approach has been applied with conjugated polymers using PB as a colouring counter electrode for polymeric electrochromic films of polyaniline⁴²⁻⁴⁴, PEDOT⁴⁵ and PProDOT⁴⁶.

1.4 Organic Electrochromic Materials

Many aromatic organic molecules exhibit multiple stable redox states with different UV/Vis absorption spectra, thus being electrochromic. Some of these compounds show very good electrochromic properties that can even outperform their inorganic counterparts in some aspects. The main advantages of organic EC materials over inorganic ones are:

1. extended colour palette;
2. ability to easily tune the colour of the two states through functionalization;
3. easy processability into thin films (at least for some of them);
4. potentially low cost.

As a consequence, the research on electrochromic materials, has focused a big part of its efforts on organic electrochromes during the last 20 years. Many different classes of these materials have been developed. Some of them are molecular materials that are soluble, in one or both redox states, in the electrolyte. Electrochromic materials of these types are classified as Type II and I respectively.^{1,47} A lot of small molecular organic electrochromic systems fall in one of these two classes (viologens, TMPDs, TCNQs, quinones, TTFs, etc.). On the other hand, Type III materials are those that are solid in all their redox states. This last group represent the most interesting one from the point of view of ECDs since these materials possess higher write-erase efficiency, higher cycle lives, high memory effect, and can be applied to all-solid-state devices (*e.g.* using a polymeric electrolyte). Conjugated polymers and metallophthalocyanines represent typical examples of Type III organic electrochromes. Different strategies to immobilize discrete electrochromes have been developed, in order to extend their applicability to devices.

1.4.1 Conjugated Polymers

After the discovery and rationalization of the properties of polyacetylene,^{48–50} the interest in the study of these fascinating materials rise rapidly. They soon found numerous applications, based on their unique conducting, semiconducting and electrochemical properties: sensors, solar cells, transistors, organic light emitting devices (OLEDs) and, of course, electrochromic devices. Conjugated

polymers are electroactive compounds since upon oxidation positive charges are generated on the polymer backbone, balanced by negatively charged counterions, and a so called *p-doped state* is reached. The positive charges are able to migrate along the polymeric chain and to nearby chains being responsible for conductivity of the doped polymer. In conjugated polymers with a non-degenerate ground state (like poly(heterocycles)), these positively charged states are termed bipolarons, and corresponds to localized levels inside the gap of the polymer.⁵¹ At very low doping levels, an ESR signal can be recorded from samples of conjugated polymers, and is attributed to polaron states. These are monocationic radicalic states that represent the first step of the oxidation process. After polaron formation a structural relaxation take place causing a local distortion of the chain in the vicinity of the charge that leads to a quinoid-like structure in which single bonds assume double bonding character (Fig. 1.9a). Further oxidation leads to the formation of bipolarons since they are predicted to have a ~ 0.4 eV energy gain when compared to two polarons (lower oxidation potential), despite the coulomb repulsion between similar charges.⁵² The pres-

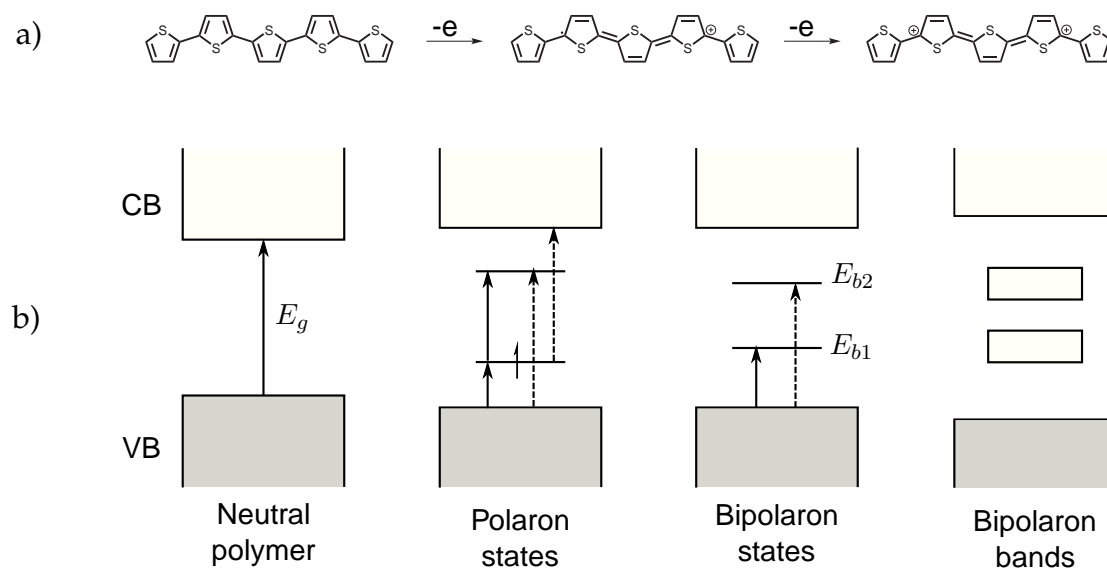


Figure 1.9 Band diagrams for bipolarons and polarons, in poly(heterocycles), showing the localized gap states and their occupancy.⁵²

ence of mid-gap levels in doped (oxidized) polymers deeply influences their spectroscopic properties that become dominated by two sub-gap (low energy) transitions from the valence band to the localized bipolaronic states (E_{b1} and E_{b2} in Fig. 1.9). This behaviour is the origin of the electrochromism in conjugated polymers since it result in a huge change in their absorption spectrum. The main optical absorption band in the reduced neutral conjugated polymers is determined by a $\pi - \pi^*$ transition through the band gap, hence falling in the

UV/Vis region, while the low energy bipolaronic transitions determine absorption bands located at longer wavelengths. The observed color change is dependent on the energy gap of the polymer. Thin films of polymers with $E_g > 3\text{ eV}$ are colourless in the undoped states while their doped form is coloured because of absorption in the visible region. In contrast, those with lower band gaps ($E_g \sim 1.5\text{ eV}$) show coloured reduced forms, but possess faintly coloured or colourless doped forms, as an effect of absorption bands shifted to the NIR region with just small residual absorption in the visible.

The main advantages of conjugated polymers over other electrochromic systems are:

- high colouration efficiency;
- good mechanical properties;
- ease of color tuning via structural modifications on the monomers;
- low switching times;
- potentially low cost;
- ease of processing.

The tuning of colour (hue) is certainly one of the most desired characteristics in electrochromic materials, and the possibility to accomplish this task is surely the most remarkable characteristic of conjugated polymers. Many research efforts have been devoted, over years, to the expansion of the "colour palette" of electrochromic conjugated polymers, and several approaches have been adopted. These include:

- modification of the HOMO and LUMO positions of the building blocks incorporated in the repeating unit;
- variation of the backbone planarity (π -overlap) using sterically hindering substituents
- increase of the conjugation lengths using ring fused heterocycles that change the bond length alternation
- use of a donor-acceptor structure in the repeating unit

A detailed review on electrochromic conjugated polymers and the different approaches to tune their colour has been recently published by Reynolds *et al.*⁵³,

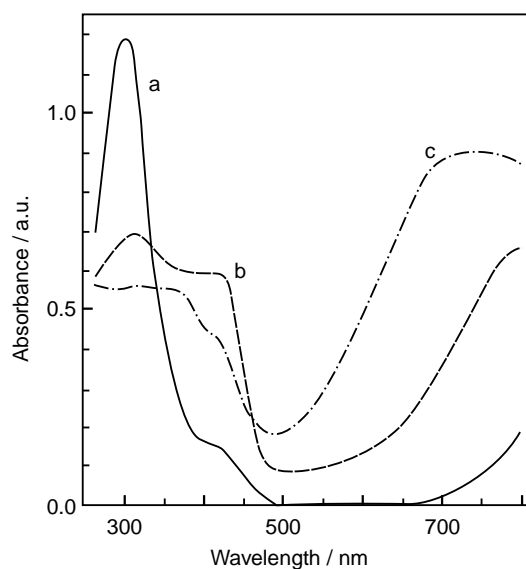
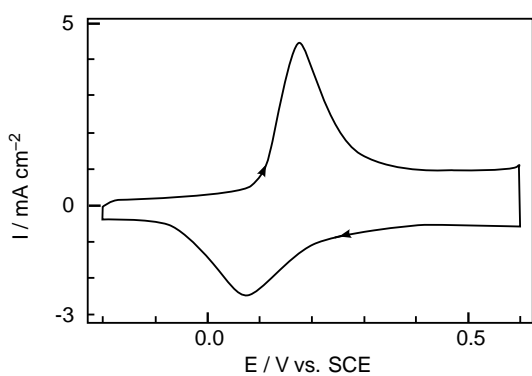
and consequently the following discussion will cover only the most representative examples. A classification based on the nature of the parent monomer will be adopted. An exception is represented by 3,4-alkylenedioxythiophenes and 3,4-alkylenedioxy pyrroles that will be treated as separate from pyrroles and thiophenes, as a consequence of their peculiar characteristics and their central role in the literature of electrochromics. A final section will be devoted to donor-acceptor systems since they recently gained popularity among electrochromic polymers for their uncommon optical properties.

1.4.1.1 Polyanilines

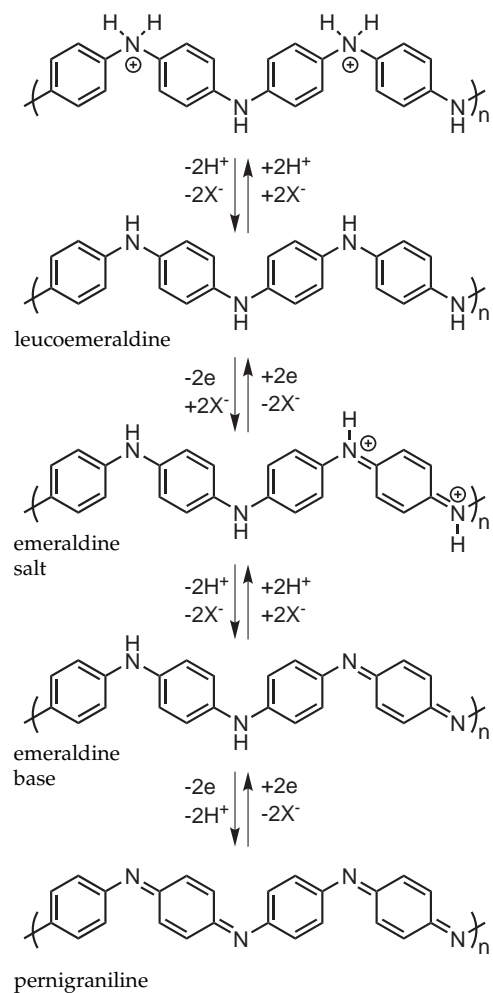
In 1862, Letheby, a chemistry professor in the College of London Hospital, reported about the formation of a layer of bluish-green pigment on a Pt electrode by oxidation of a solution of aniline in sulfuric acid.⁵⁴ This probably represents the first report on the electrochemical synthesis of a conjugated polymer. Polyaniline (PANI) can be prepared by anodic polymerization, with the best results obtained by galvanostatic technique in aqueous acidic solutions.⁵⁵ The electrochemical behavior of PANI in aqueous acidic solutions involve both redox and acid/base equilibria being rather complicated, and several slightly different mechanisms have been proposed. The structures of the various states are depicted in Fig. 1.10b.

The fully reduced PANI form is called leucoemeraldine, and has a transmissive yellow colour. This form can be oxidized to the green emeraldine form, in equilibrium with its protonated form, thanks to the acidic conditions, becoming conductive. This redox process is rather stable and located between -0.2 and 0.6 V vs. SCE (see Fig. 1.10a).^{55,57} Further oxidation in the 1-4 pH range leads to the fully reduced deep blue form pernigraniline. If the same film is placed in solutions of $\text{pH} > 4$, polyaniline turns black and no longer switches. Nevertheless, cyclic stabilities up to 10^6 cycles for the yellow \rightleftharpoons green transition have been claimed.⁵⁵

Numerous substituted derivatives of PANI have been investigated. As an example, the polymerization of *o*- and *m*-toluidine leads to the corresponding polymers that have proved to possess enhanced stability when compared to PANI. In these derivatives the absorption maxima and the redox potentials are shifted, as an effect of the lower conjugation length, while the response time on switching is longer than in PANI.^{58,59} A variety of polyanilines, substituted with methoxy, methyl and hydroxymethyl functionalities, have been investigated by D'Aprano *et al.*⁶⁰ In their investigation they found that both the *o*-



(a) Steady-state cyclic voltammogram of a PANI coated Pt electrode in 1 M HCl, in the range from -0.2 to 0.6 V vs. SCE (up); and spectroelectrogram of the same on Pt-coated quartz substrate at -0.2 V (a), 0.15 V (b), and 0.6 V (c) vs. SCE in 1 M HCl. Adapted from Kobayashi *et al.* ^{55,56}



(b) Schematic representation of the different redox states of polyaniline.

Figure 1.10

methyl and *o*-methoxy substituted monomers can be easily polymerized electrochemically at a lower potential than aniline. The methoxy derivative was found to possess a slightly red shifted absorption maximum as a result of the electron donating effect of the substituents. The small entity of this shift is due to the steric effect of the 2-substitution itself that induce an higher torsional angle, and reduce the conjugation, inducing a blue shift of the maximum (as observed for the methyl derivative). A stronger reduction of the band gap is observed with 2,5-dimethoxyaniline that has an absorption maximum shifted to 350nm. Copolymerization of aniline with *o*-anisidine was tested obtaining better electrochromic properties.⁶¹ Gazotti *et al.* prepared soluble poly(*o*-methoxyaniline) polymerizing the monomer in presence of a variety of organic acids, and studied the electrochromic properties of films obtained by casting solutions of the same.⁶² A more recent approach to soluble polyaniline involve polymerization using an inverse emulsion technique to obtain a soluble material with good conductivities.⁶³ The use of poly(*p*-styrenesulfonate) (PSS) during aqueous polymerization with ammonium persulfate has allowed the preparation of water dispersible nanoparticles of PANI-PSS with diameters in the 25-30nm range.^{64,65}

Several examples of electrochromic devices employing PANI are present in literature. Mastragostino *et al.* reported of a solid state electrochromic device based on prussian blue and PANI, using a polymeric electrolyte, but poor cycling stability was achieved.^{42,43} Electrochromic smart windows using PANI, in combination with prussian blue and WO₃, have been reported.⁶⁶ These dual-electrochrome devices show a better cycling stability retaining 90% of their initial performance after 3700 cycles.

1.4.1.2 Polycarbazoles

Thin films of unsubstituted poly(carbazole) can be obtained by anodic polymerization. They show a reversible p-doping process at relatively low potential, accompanied by a colour transition from yellow to green.⁶⁷ Functionalization on the *N*-position has proved to slightly hypsochromically shift the absorption band of the reduced form. Chevrot *et al.* demonstrated a colorless \rightleftharpoons green-blue transition in *N*-butyl- and *N*-dodecyl-substituted derivatives.^{68,69} They also obtained an *N*-oligoether-functionalized carbazole monomer that once polymerized demonstrates a very good stability on cycling in acidic water solutions (95% of the initial charge density was maintained after 7000 cycles). Poly(carbazole)s with enhanced water solubilities have also been obtained using chains car-

rying sulfonate terminal groups.⁷⁰ A carbazole analogous, fluorene, has been recently investigated for electrochromic devices. Bezgin *et al.*⁷¹ obtained films of poly(9-fluorenicarboxylic acid) by electrochemical polymerization in $\text{BF}_3 \cdot \text{Et}_2\text{O}$. The obtained polymer has a high band-gap of 3.1 eV and shows a colorless \rightarrow orange-brown transition upon p-doping, with colouration efficiencies up to $232 \text{ cm}^2\text{C}^{-1}$. The polymer was used to build a dual electrochrome device with PEDOT as a cathodically colouring material with a resulting dark blue \rightleftharpoons colorless transition.

1.4.1.3 Polypyrroles

Pyrrole is an electron-rich heterocycle and hence possesses a low-oxidation potential. As a consequence, poly(pyrrole) can be easily obtained by oxidative polymerization both chemically and electrochemically. The films of the parent polymer have yellow colour in their undoped state ($E_g \sim 2.7 \text{ eV}$) and blue-to-violet in their doped conductive state (Fig. 1.11).⁷² In an effort to improve me-

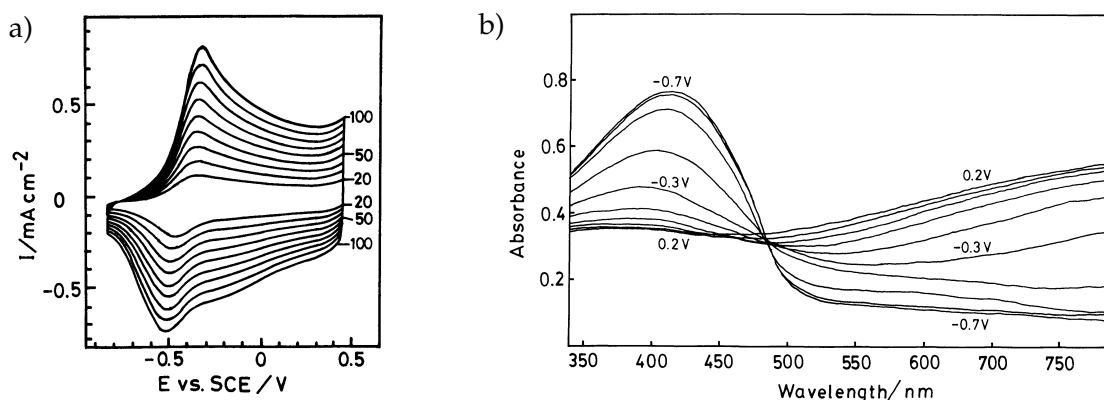


Figure 1.11 Cyclic voltammograms of poly(pyrrole) at various sweep rates (in 0.5 M KCl, Pt electrodes, vs. SCE, sweep rates in mV s^{-1}) (a), and spectroelectrochromogram on SnO_2 coated glass electrode with 0.1 V potential intervals (b) in the same electrolyte.⁷²

chanical properties of polypyrrole polymer films in aqueous solutions, pyrrole has been electropolymerized in presence of surfactants such as sodium dodecylsulfate.⁷³ Obtained films switched from transmissive yellow in the neutral state to violet in a partially oxidized state and brown when fully oxidized, and showed remarkable cycling stabilities up to 2×10^4 cycles with a decay to the 75% of the initial contrast.⁷⁴

Functionalized derivatives, either at the nitrogen or at the 3- and/or 4- positions, have been prepared. Interestingly the *N*-functionalization with alkyl

or phenyl groups proved to have almost no influence on the band gap and on the hue of the doped and undoped states, testifying clearly the small entity of the substituent-induced steric hindrance along the backbone.⁷⁵ On the other hand, the *N*-substitution proved to rise the monomers oxidation threshold and to reduce the conductivity measured on the doped polymers. Dimers of *N*-methylpyrrole, possessing a lower oxidation potential than the parent monomer, can be electropolymerized easier without risk of overoxidation in the growing polymer. Using *N,N'*-dimethyl-2,2'-bipyrrole, an hypsochromic shift of the optical absorption in the dedoped form of the resulting polymer has been observed, along with higher conductivity in doped state and lower oxidation potential. The resultant enhancement of the transmissivity of the bleached form allowed the obtainment of a pale yellow \rightleftharpoons gray blue transition.⁷⁶⁻⁷⁸ Literature describing the redox properties of *C*-substituted poly(pyrrole)s is limited, as a consequence of the low air stability of the monomers and the corresponding polymers under atmospheric conditions. Nevertheless, the whole series of pure *N*-methyl- and 3-methylpyrrole, monomethyl-substituted 2,2'-dipyrroles (three substrates) and dimethyl-substituted 2,2'-dipyrroles (four substrates) were prepared and studied by Zottiet *al.* under comparable experimental conditions that allow a comparison of the results.^{77,78} Their findings demonstrate that *C*-substitution is more efficient than *N*-substitution in electron injection on the ring. The loss of planarity, due to the methyl substitution in positions adjacent to the interannular bond, leads to an increase in λ_{max} and a decrease in conductivity. Furthermore, some new synthetic approaches, aimed to the obtainment of monomers with a further functionalizable alkyl-chain, have been developed.⁷⁹⁻⁸¹

1.4.1.4 Polythiophenes

Poly(thiophene)s have attracted a lot of interest for electrochromic applications. This can be attributed to their environmental stability, processability and ease of electrochemical synthesis. In addition, further functionalization of the parent monomer has proved to be easily achievable. A huge variety of examples are present in literature with particular emphasis on poly(3-substituted thiophene)s and poly(3,4-disubstituted thiophene)s.⁸² The application of PTs as electrochromes was first suggested by Garnier *et al.*^{83,84} and Druy and Seymour⁸⁵. Their findings reveal that the parent poly(thiophene) films are blue in the reduced state (λ_{max} =730nm) and red (λ_{max} =470nm) in the undoped form. A high cycling stability for poly(3-methylthiophene), with an 80% retainment of

the electroactivity after 1.2×10^5 cycles, have been reported. This latter compound was more extensively studied, as a consequence of its lower oxidation potential, that prevents the polymer overoxidation during electrochemical synthesis, and leads to lower switching potentials. Furthermore, the substitution in the 3-position partially prevents the occurrence of insulative $\alpha - \beta'$ couplings during the polymerization, leading to an increased conjugation length and an higher conductivity.⁸² Poly(3-methylthiophene) is purple when neutral with an absorption maximum at 530nm (2.34eV), and turns pale blue upon oxidation.⁸⁶ The comparison between poly(thiophene) and poly(3-methylthiophene) clearly demonstrates the possibility to achieve a control over the optical properties of poly(thiophene) derivatives through functionalization on the 3- and 4-positions of the monomer. This tunability of colour properties, as already pointed out, represents one of the main advantages in the use of conjugated polymers as electrochromes. Nevertheless, a simple increment on the length of the alkyl chain in the 3-position of thiophene does not lead to any significant change in electrochromic properties of the resulting polymers, but is beneficial for solution-processability.⁸⁷ On the other hand, a drastic variation of conjugation length and optical properties is observed moving from nonregioregular 3-substituted poly(thiophene)s (with both head to head (HH) and head to tail (HT) configurations) to regioregular ones (only HT configurations).^{88,89} The effect of regiochemistry on electrochromic properties was further demonstrated by Arbizzani *et al.*⁹⁰ that obtained poly(3-hexylthiophene)s with pale-green reduced states through electropolymerization of 3-3' and 4,4'-dihexyl-2,2'-bithiophenes. The use of oligomers, as in this latter example, represents another common strategy to lower the oxidation potential and avoid overoxidation during electropolymerization.⁸³⁻⁸⁵ Other possibilities include the replacement of common organic solvents with strong Lewis acids. In particular, homogeneous and smooth films of poly(thiophene) and poly(3-methylthiophene) have been obtained by Reynolds *et al.*⁹¹ with the use of $\text{BF}_3 \cdot \text{Et}_2\text{O}$ as a solvent (Fig. 1.12). A huge variety of different functional groups have been attached, either directly or through an alkyl tether, to the 3- and/or 4-positions of thiophene in order to modify its properties. These include fluorinated chains⁹², esters^{93,94}, carboxylic acids⁹⁵ and aromatic groups⁹⁶⁻⁹⁸.

In the class of ring-fused heterocyclic derivatives of thiophene, a representative example of low band gap polymer has to be quoted, namely polyisothiophene (PITN). This material was developed following the idea of narrowing the energy gap reducing the bond length alternation by the use of aromatic

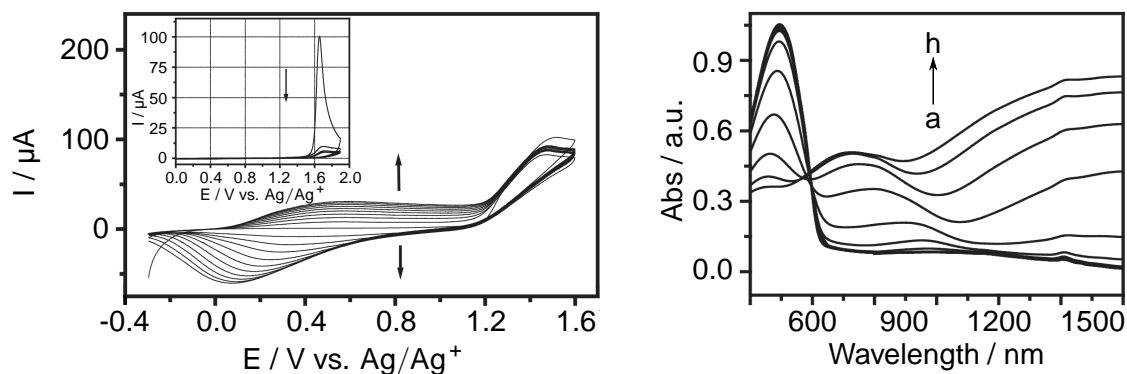


Figure 1.12 Cyclic voltammogram of thiophene (0.01 M) in $\text{BF}_3 \cdot \text{Et}_2\text{O}$ (vs. Ag/Ag^+ , scan rate 100 mV s^{-1}) with inset showing the behaviour in $0.1 \text{ M Bu}_4\text{NPF}_6/\text{MeCN}$ (left) and spectrovoltammogram of the obtained poly(thiophene) in the same electrolyte. Spectra were recorded at the following potentials: a: -0.20 , b: 0.50 , c: 0.60 , d: 0.70 , e: 0.80 , f: 0.90 , g: 1.0 , h: $1.1 \text{ V vs. Ag}/\text{Ag}^+$ (right). Adapted from Reynolds *et al.*⁹¹

systems with high resonance energies.^{99,100} Polyisothianaphtene, with a 1 eV energy gap, was the first reported example of cathodically colouring polymer since it poses an highly transmissive greenish-yellow conductive state, and switches to blue upon reduction. Nonetheless, it poses low stability to ambient conditions and a bad processability as a result of its insolubility. Another

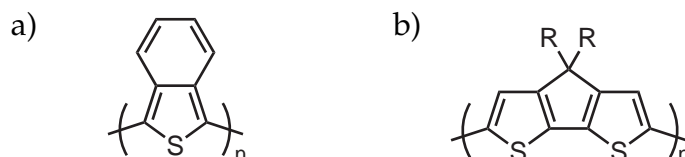


Figure 1.13 Structures of: a) poly(isothianaphtene) and b) poly(cyclopentadithiophene).

approach to obtain a gap reduction in PTs and hence a bathochromic shift of the absorption is the development of systems in which the heterocyclic rings are forced to planarity.¹⁰¹ An example of this type is represented by substituted poly(cyclopentadithiophene)s (pCPDT). A derivative, (4,4'-dioctyl-cyclopenta[2,1-b:3,4-b']-dithiophene, with a 1.73 eV , show a switching between deep blue and highly transmissive with high colouration efficiency ($932 \text{ cm}^2 \text{ C}^{-1}$) and good cycling stability (8% contrast loss after 1000 cycles).¹⁰²

1.4.1.5 Poly(3,4-alkylenedioxythiophene)s

Poly(thiophene)s have attracted a lot of interest for their possible application in electrochromic systems. The reason is that they possess an ideal combination of

electronic properties and stability to environmental condition. Their moderate band gap make the π - π^* transition to fall inside the visible region giving them an highly coloured reduced form. Nevertheless, as discussed previously, an electrochromic material possessing a completely colorless form (highly transmissive) is highly desirable. The achievement of such a result with polythiophenes require the NIR absorption band of the oxidized form to be shifted further toward low energies. Furthermore, the onset of this band should also be located in the NIR region, and tailing in the visible limited.

A poly(thiophene) derivative, poly(3,4-ethylenedioxythiophene) (PEDOT), fulfilling all these constraints was discovered in 1987-1988 by the chemists working at Bayer AG.¹⁰³ In fact, this alkoxy-substituted poly(thiophene) show a reduced band gap (~ 1.6 eV) and a dark blue to highly transmissive sky-blue transition upon oxidation. Furthermore, its oxidized form is highly conductive and stable in air up to very high temperatures, to humidity including moist air, also at elevated temperatures, and, after only a few years of further development, it demonstrated to be even processable in water. In those years, the main interest was to find highly conductive polymers that could overcome the numerous problems of the existing ones. In fact, despite the advances and the scientific steps that followed the discovery of poly(acetylene), the existing polymers still suffered from very limited environmental stabilities and insufficient conductivity half-life values.¹⁰⁴ The development of alkoxy-substituted thiophenes started as an attempt to overcome these difficulties. The idea was to take advantage of the electron donating effect of the substituent to lower the band gap, and stabilize the radical-cationic species (see Fig. 1.14). This class of compounds

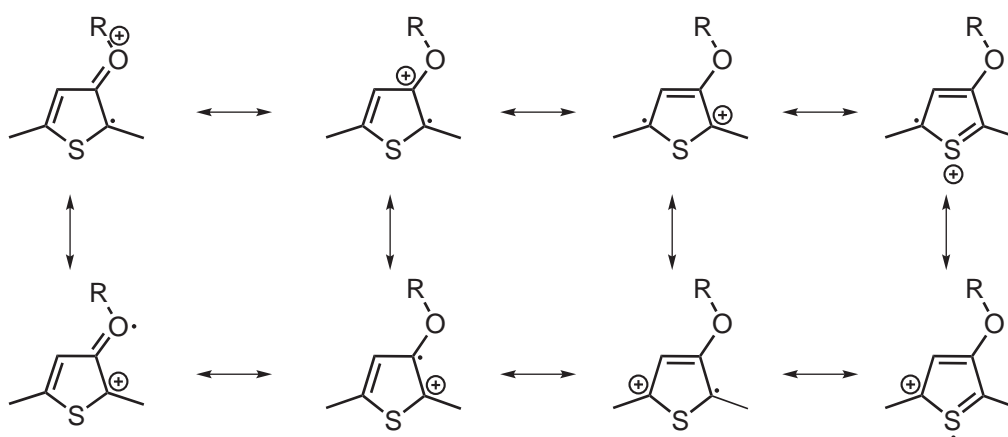


Figure 1.14 Radical cation (polaron) mesomeric stabilization with oxygen contribution.

was initially studied by chemist at Hoechst AG in 1986-1988. In particular, they

investigated the electrochemical polymerization of 3-alkoxythiophenes.¹⁰⁵⁻¹⁰⁷ Their initial results with 3-alkoxythiophenes were quite poor, but later, with the introduction of a methyl group on the 4-position, a clear improvement of conductivities was achieved.¹⁰⁸ This observation is clearly due to the blocking of the 4-position, that inhibits α - β' and β - β' couplings to occur during the polymerization. Later studies, that included both 3-alkoxy-4 methylthiophenes and 3,4-dialkoxythiophenes, revealed the existence of a clear structural relationship in this class of compounds.¹⁰⁹⁻¹¹¹ In particular, dimethoxythiophene possesses high conductivity, but this conductivity falls when *n*-butoxythiophene is considered, as a consequence of steric interaction between the substituents that lowers the conjugation length. Furthermore, their stability to air and humidity was not adequate for practical applications. Nevertheless, the key-factor was to exploit the stabilization effect of the oxygen-bearing substituents minimizing the adverse effect represented by steric hindrance between them (reduction of conjugation). A technical breakthrough was achieved when the Bayer researchers Friedrich Jonas and Gerhard Heywang decided to extend the thiophene structures to bicyclic ring systems. In other words, ring closure of two alkoxy substituents had to be accomplished to form dioxolane-, dioxane-, or dioxepane 3,4-anellated thiophenes.¹¹² They initially tried to synthesize, without success, 3,4-methylenedioxythiophene, and then extended the ring size of the anellated dioxolane to the six-membered dioxane ring in 3,4-ethylenedioxythiophene (EDOT). The new monomer was found to be easily polymerizable (with FeCl_3), and the obtained doped polymer was highly conductive and stable to environmental conditions. A long list of patent applications, claiming its application to capacitors and rechargeable batteries, was deposited. More relevant to electrochromics, the so-called *in situ* polymerization technique was invented, permitting to circumvent the complete insolubility of doped PEDOT by forming it during processing and hence allowing the deposition of thin-films of the polymer. A further breakthrough came with the development of PEDOT:PSS complex, as a result of a collaboration between Bayer AG and Agfa-Gavaert. This water dispersion of PEDOT, with poly(styrenesulfonic acid) as stabilizer, opened the way to easy solution processing of conductive polymeric films, and is currently sold under the trade name of Clevios PTM (formerly Baytron PTM). In the context of electrochromics, the use of PEDOT prevails over PEDOT:PSS due to the fact that the former can be easier dedoped. As formerly mentioned, PEDOT possesses a relatively stable and highly transmissive sky-blue oxidized state, an invaluable characteristic for

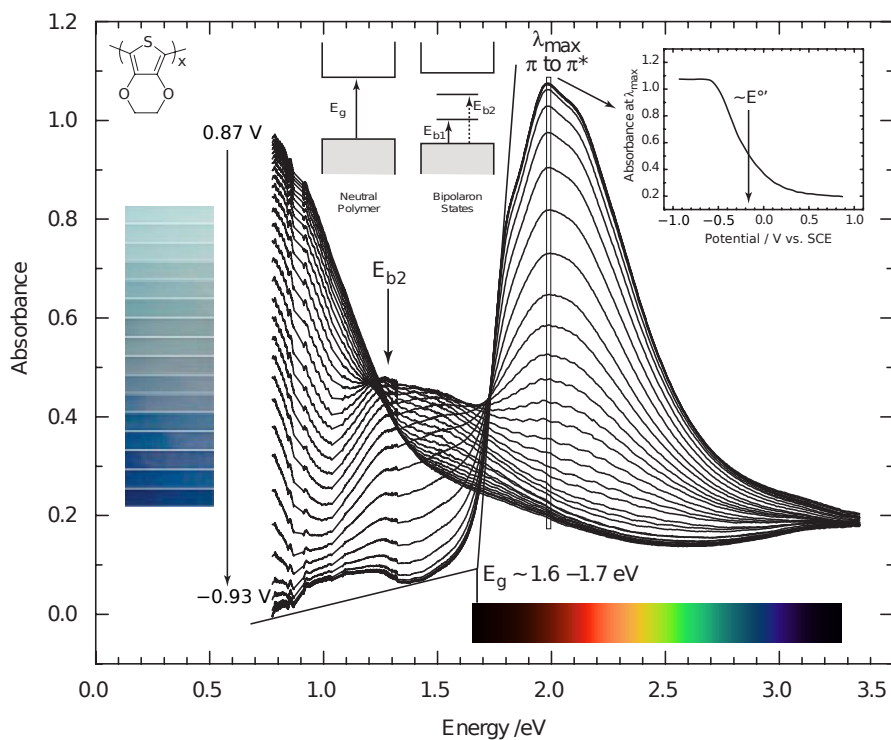


Figure 1.15 Spectroelectrogram of a poly[3,4-(ethylenedioxy)thiophene] (PEDOT) film on ITO/glass. The film was electrochemically deposited from 0.3M EDOT and 0.1M $\text{Bu}_4\text{ClO}_4/\text{PC}$ and switched in 0.1M $\text{Bu}_4\text{ClO}_4/\text{ACN}$. Inset shows absorbance at λ_{max} versus potential. The bandgap is determined by extrapolating the onset of the $\pi - \pi^*$ transition to the background absorbance. Adapted from Mortimer²⁸.

a polymer based ECD. This was soon demonstrated with the realization of the first electrochemically prepared PEDOT-based ECDs by Inganäs *et al.*⁹⁶. As can be noted from figure 1.15, the absorption band of reduced PEDOT lies in the NIR region of the visible spectrum giving its distinctive dark blue-colour, and its doped form has minimal tailing in the visible from its charged carriers transitions. A variety of PEDOT derivatives with appended solubilizing chains were soon prepared along with the first examples of soluble PEDOTs (with longer chains, namely $-C_8H_{17}$ and $-C_{14}H_{29}$).^{113–117} The latter were usually obtained by reduction of partially doped polymer with hydrazine. These substituents proved to allow the modulation of PEDOT's band gap in a way similar to what had been observed for poly(thiophene)s. Furthermore, a drastic enhancement of switching properties was obtained with a reduction of switching times (to the 12s range), along with a more effective depletion of the absorption of the neutral state on full-oxidation. This was attributed to the ability of the lateral chains to facilitate inward/outward migration of the dopant counterions.¹¹⁸ The solubilizing chains proved to have an important influence also on cycling stability, with PEDOT- C_{14} withstanding 16000 cycles retaining 60% of its electroactivity, compared to the 65% of parent PEDOT after 6000 cycles.¹¹⁶ A further advantage, in the use of chemically synthesized soluble PEDOTs, is the possibility to purify them from the oligomers that are inevitably formed during the oxidative polymerization. These species (having four to six monomer units) are trapped inside the polymeric film during electrochemical polymerization (or *in situ* polymerization) and impair the optical properties. In particular, they reduce the transmissivity of the doped state.¹¹⁹

A selenium analogue of EDOT, 3,4-(ethylenedioxy)selenophene (EDOS), has been also synthesized and investigated. The obtained polymer (PEDOS), have been electrochemically prepared by Cava *et al.*¹²⁰ EDOS, being more electron-rich than EDOT, possesses a lower oxidation potential (1.22V vs. Fc/Fc^+), and the corresponding PEDOS has a narrower band gap when compared to PEDOT (~ 1.4 eV). Electrochemical properties of PEDOS and its simple derivatives have been recently reinvestigated by Bendikov *et al.*^{121–123} This polymer and its derivatives prove to possess very interesting electrochromic properties. As an example, PEDOS- C_6 is claimed to possess a very high contrast ratio ($\Delta T=89\%$ at 763nm), a fast switching time (0.7s), a colouration efficiency of $773\text{ cm}^2\text{ C}^{-1}$ and a cycling stability comparable to that of PEDOT derivatives (ΔT decays to 48% after 10000 cycles).¹²³

Derivatives of PEDOT with expanded alkylene bridges have been tested (Fig.

1.16). The size of this bridge was found to play an important role in determining

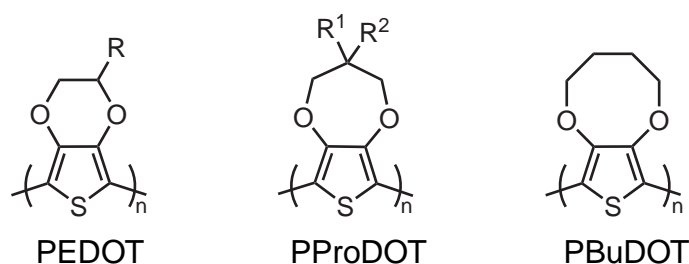


Figure 1.16 Structures of substituted PEDOT analogues with expanded alkylene bridges.

redox and optical properties. In particular, a systematic study of the structure-electrochromic properties relationship of a series of polymers, differing by the size of the alkylene bridge and the nature of the substituents, was carried out by Reynolds *et al.*¹²⁴ The comparison clearly shows that, upon switching from the ethylenedioxy bridge of PEDOT to the propylenedioxy (PProDOT) and to butylenedioxy (PBuDOT), better properties are obtained, namely: better resolved redox features in CVs, higher contrast and shorter switching times. This effect was again attributed to the more open morphology induced by the larger bridges that facilitates the diffusion of counterions.¹²⁵ Moreover, the insertion of extra methylenes in the EDOT ring disrupts its coplanarity with the adjacent aromatic center, and alters its electron-donating effect. As a result, the polymer HOMO is lowered relative to the air-oxidation threshold, enhancing its environmental stability. A large library of different PProDOT derivatives was developed by Reynolds *et al.*¹²⁶⁻¹²⁸ This comprises examples of highly homogeneous electrochromic films deposited by spray-casting using an airbrush. In these examples, an increment of electrochromic contrast ($\Delta T=51\%$ for dibutyl-substituted PProDOT-Bu₂, $\Delta T=70\%$ for dihexyl-substituted PProDOT-n-Hex₂ and $\Delta T=79\%$ for the bis(2-ethylhexyl)-substituted PProDOT-EtHex₂) was observed elongating the alkyl substituents, with a red-purple to transmissive sky-blue color transition. Nonetheless, a threshold exists, as testified by the worse performances of PProDOT-(MeOC₁₈)₂.¹²⁸

1.4.1.6 Poly(3,4-alkylenedioxythiophene)s

Since the introduction of the 3,4-alkylenedioxy bridges on thiophene brought to a drastic enhancement of the stability and electrochromic properties of the resulting polymer, it is no surprise that the same approach was later extended

to pyrrole. The resulting 3,4-alkylenedioxy pyrrole can be polymerized exclusively through its 2- and 5-positions, leading to a much more regioregular polymer than poly(pyrrole). Moreover, the obtained poly(3,4-alkylenedioxy pyrrole)s (PXDOPE) possess an highly tunable optical and electrochemical behaviour. This tuning results from the structural modification of the parent monomers with substituents on the alkylene bridge (as seen for PEDOT) and, in this case, even on the nitrogen atom.¹²⁹ As expected, PEDOPs have a low oxidation potential when compared to poly(pyrrole)s and an improved ambient stability in the doped state. A comparison with PEDOT reveals a wider band gap (~ 2.0 eV vs. ~ 1.6 eV) owing to the energy difference between the LUMOs.^{130,131} PEDOP shows a transition from bright red to transmissive blue-gray upon oxidation with contrasts as high as 59%.¹³⁰ The propylenedioxy substituted analogue PProDOP, has a band gap of ~ 2.2 eV and shows enhanced electrochromic properties, with higher optical contrast and transmissivity of the oxidized state. This effect is due to the bathochromic shift of the polaronic and bipolaronic bands observed with ring expansion.¹³² The parent PProDOP exhibits colour transition from orange to brown on partial oxidation to light grey-blue upon full oxidation, with an impressive cycling stability (10% loss of electroactivity after 40000 cycles on Pt electrode). Substituents on the alkylene bridge allow to fine tune the colour of the redox states and modify solubility of the resulting polymers. However, *N*-substitution have a greater effect on the electronic properties, as they alter steric hindrance, planarity and hence conjugation length. As a result, PProDOPs with band gaps as wide as 3.4 eV were obtained with this strategy (see Fig. 1.17). The resulting polymers can be anodically colouring with the coloured oxidized state determined by the absorption from the charged carriers transitions, or even transmissive in both states, with electrochromism confined in the UV and NIR regions.¹³⁴ A detailed report on this interesting class of electrochromic polymers have been published in 2003 by Reynolds *et al.*¹³³

1.4.1.7 Donor-acceptor Polymers

This class of polymers is characterized by a repeating unit containing both electron donating (high lying energy levels) and electron withdrawing (low lying energy levels) moieties. Structures of this type have been extensively investigated with the aim of obtaining polymers with very low band gaps, in order to obtain intrinsic conductivity.¹³⁵ This concept predicts that structures of this type are expected to have very small band gaps and wide bands, follow-

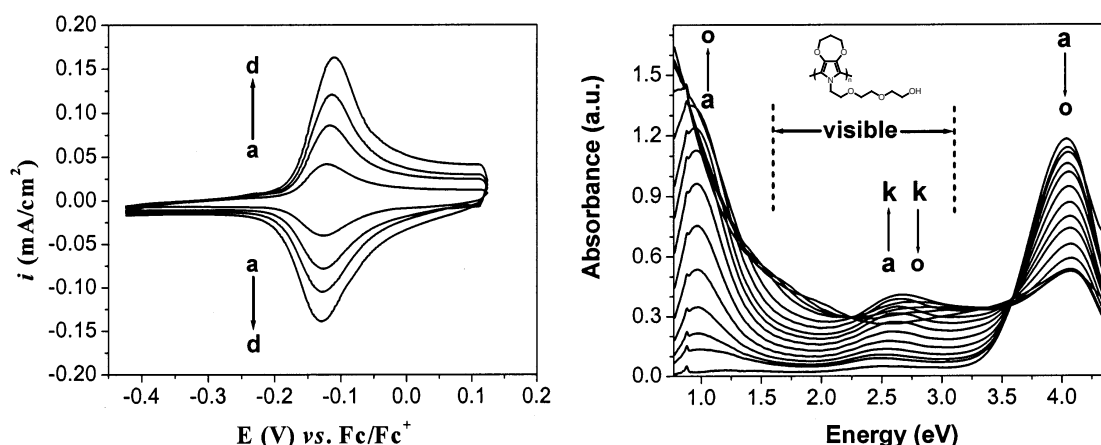


Figure 1.17 Cyclic voltammograms (left) of *N*-Gly-PProDOP in monomer-free solution of 0.1 M LiClO₄/PC at different scan rates: a) 50 b) 100 c) 150 d) 200 mV s⁻¹, and its spectroelectrogram (right) at applied potentials of (a) -200, (b) -70, (c) -60, (d) -50, (e) -40, (f) -30, (g) -20, (h) -10, (i) 0, (j) 20, (k) 60, (l) 200, (m) 300, (n) 400 and (o) 700 mV.¹³³

ing the idea that the valence band is formed close to the HOMO of the donor, while the conduction band is close to the LUMO of the acceptor. This idea has been strongly criticized since, considering perturbation theory, band formation requires strong interaction, the latter being inversely proportional to the energy difference between the orbitals of the fragments.¹³⁶ As an example, copolymers of 4-(Dicyanomethylene)-4*H*-cyclopenta[2,1-*b*:3,4-*b'*]dithiophene and EDOT possess a wide valence band and a very narrow conduction band, better described as low-lying localized acceptor levels.¹³⁷ As a consequence, the copolymer presents a mobility ratio of 500 between p-type and n-type charge carriers and a very low n-type conductivity. From the point of view of electrochromics, the presence of narrow bands and of accessible localized states can be beneficial, since this makes possible to obtain a polymer with 2 absorption bands in its neutral state. It has to be considered, in fact, that this latter condition represents the way to obtain a saturated green hue. A donor-acceptor (DA) polymer with these characteristics was prepared for the first time by Wudl *et al.*¹⁹ in 2004. The polymer was obtained by electrochemical polymerization of 2,3-dithien-3-yl-5,7-dithien-2-yl-thieno[3,4-*b*]pyrazine (DDTP) and switches from a green reduced state to a pale green one upon oxidation. The cycling stability also proved to be quite high with 1.5% loss in redox activity after 10000 cycles, but the observed contrast was quite poor (23% at 370 nm and 12% at 725 nm) as a consequence of the incomplete bleaching of the band associated

with the localized acceptor transition and the tailing of the polaronic band in the visible region. It was soon realized that it was possible to obtain a two-band absorption from DA polymers without the need to incorporate a secondary chromophoric unit in broken conjugation with the main chain. This possibility had been already predicted by Salzner *et al.*^{136–138} calculating the band structure of DA polymers. In 2007, Toppare *et al.* reinvestigated the previously reported BisEDOT-benzothiadiazole system (PBDT).^{139–141} The electrochemi-

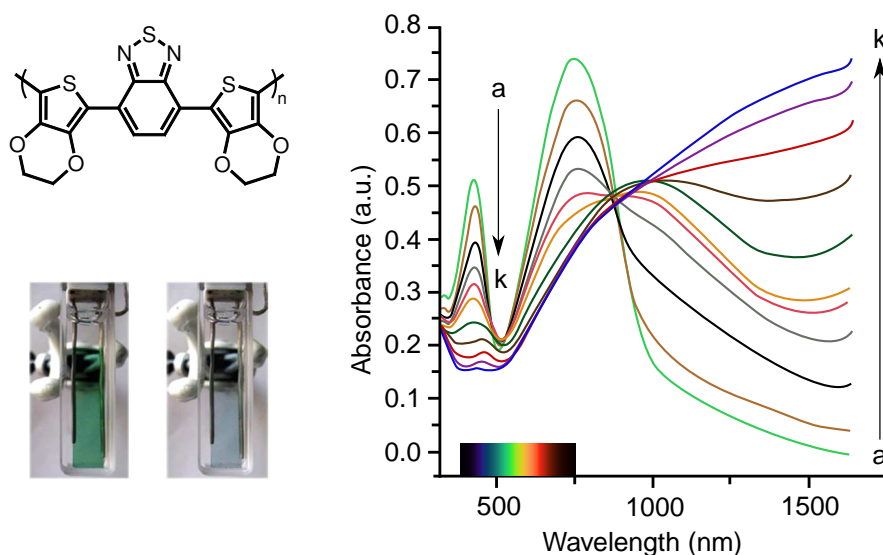


Figure 1.18 Colors of PBDT film on an ITO coated glass slide in the neutral and oxidized states (left) and spectroelectrochromogram of PBDT film on an ITO coated glass slide in monomer-free, 0.1 M $\text{Bu}_4\text{PF}_6/\text{MeCN}$ electrolyte/solvent couple at applied potentials: (a) -0.8 , (b) -0.5 , (c) -0.2 , (d) -0.15 , (e) 0.0 , (f) 0.1 (g) 0.3 , (h) 0.5 , (i) 0.7 , (j) 0.9 , (k) 1.1 V (right). Adapted from Durmus *et al.*¹⁴²

cally synthesized polymeric film was found to switch between a neutral green state and a transmissive light blue one with high cycling stability (Fig. 1.18).¹⁴² The residual blue hue of the oxidized form can be ascribed to the tailing of the NIR centered polaronic transition into the visible region. Numerous variations on this basic structure followed, using either benzothiadiazole or substituted quinoxaline as acceptors.^{143–145} With a slightly different approach, Reynolds *et al.* prepared the polymers in figure 1.19 by oxidative polymerization of the pentameric oligomers constituting the repeating units. In these molecules a benzothiadiazole acceptor unit is symmetrically functionalized with thiophene derivatives (ProDOT, EDOT, and thiophene). With this approach two different green hues were obtained and, more importantly, highly transmissive oxidized states were achieved, but a residual absorption due to the tailing of charge carriers band was still present. Nevertheless, contrast values as high as 44% were

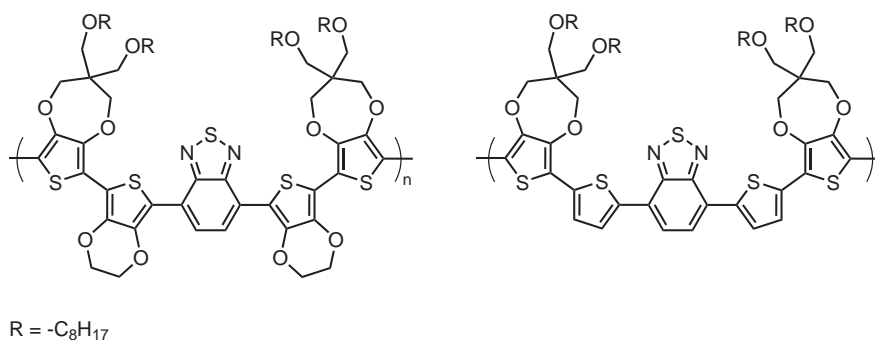


Figure 1.19 Structures of the DA polymers developed by Reynolds *et al.*¹⁴⁶

achieved.¹⁴⁶ Further development of these oligomeric units allowed to prepare a library of polymers absorbing in different region of the visible spectrum. In particular Reynolds *et al.* demonstrated the possibility to tune the intensity and the overlap of the two transitions, associated with this class of DA polymers, varying the contribution of donors and acceptors in the repeating unit. They further showed that copolymerization of one of these oligomers (a trimer), with a ProDOT based monomer, leads to a material with a broad absorption over the whole visible spectrum with a resulting black hue (Fig. 1.20). This material was still switchable to a highly transmissive oxidized form with an electrochromic contrast of 50% at the absorption maximum. Colorimetric measures showed a luminance variation as high as 52% with an L^* value of 85 for the colorless form.²⁰

1.4.1.8 Polymerization methods

Although most of it can be extended to other electrochromic conjugated polymers, the forthcoming discussion will be focused on polymerization methods used in the synthesis of PEDOT, which is by far the most popular of them.

Electrochemical Polymerization The controlled anodic oxidation of suitable electron-rich monomers represent the most important electrochemical method for the preparation of conducting polymers. The process involves a complex reaction sequence in which the activated coupling of different species is involved. The observed electrochemical stoichiometries range from 2.07 to 2.6F mol⁻¹. The polymerization consumes 2F mol⁻¹, but an additional charge is required for the oxidation of the formed polymer. Since the oxidation potentials of polymeric oligomeric species is lower than the one required for monomer oxidation, these processes occur simultaneously.¹⁴⁷ The first step of electrochemical

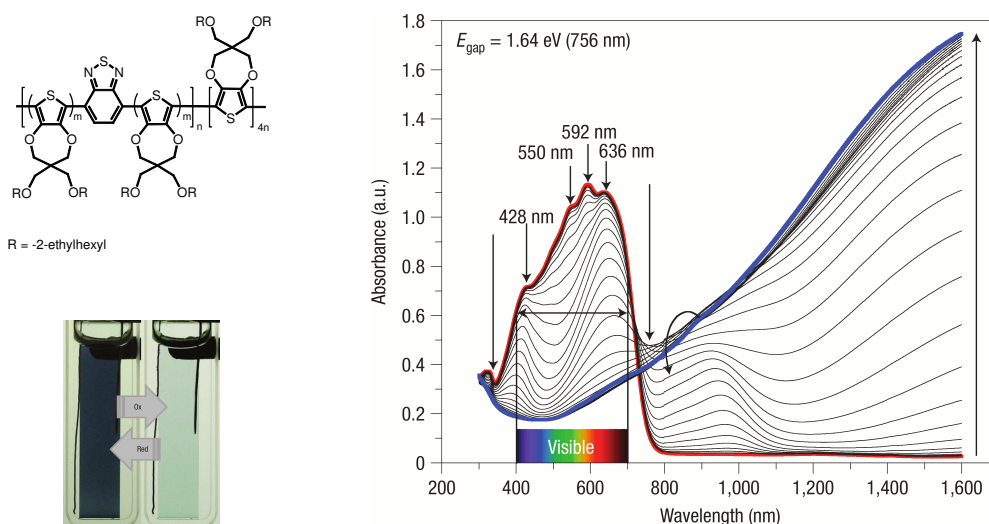


Figure 1.20 Spectroelectrogram of the black to transmissive switching donor-acceptor polymer developed by Reynolds *et al.* Polymeric film was spray-cast onto ITO-coated glass from solution (4 mg ml^{-1}) in toluene. The applied potential was increased in 25 mV steps: $0.04\text{ V} \rightarrow 0.74\text{ V}$. The picture shows the colours obtained on electrochemical switching both in the neutral state (left) and on full oxidation (right).²⁰

deposition of conjugated polymers films involve oligomerization in solution and nucleation on the electrode surface. Diaz suggested that the mechanism of chain growth involve the initial formation of radical cations of the monomer, followed by their dimerization.^{148,149} In the case of pyrroles and thiophenes this dimerization occurs at the α position. This dimerization leads to the formation of the so called σ -dimer that further evolves eliminating protons, and forming an aromatic neutral dimer. This dimer, having lower oxidation potential than the starting monomer, is immediately oxidized to its radical cation, and undergoes the next coupling step. Although it was initially believed that the successive coupling steps involves the reaction of the growing oligomers with monomeric species, it has now been accepted that the growth takes place via successive "dimerization" steps leading from dimers to a tetramers and then to octameric coupling products (Fig. 1.21).¹⁴⁷ At higher concentrations of the starting species, additional coupling reactions may occur which produce intermediates such as trimers, hexamers, and so on. Electrochemical deposition of polymers like poly(pyrrole)s and poly(thiophene)s on the electrode surface, usually follow a mechanism involving (2D or 3D) nucleation and 3D growth.^{150,151} The processes can be monitored using potentiodynamic, potentiostatic and galvanostatic techniques. In particular, potentiodynamic experiments, can provide simple information on the growth rate (increase in current

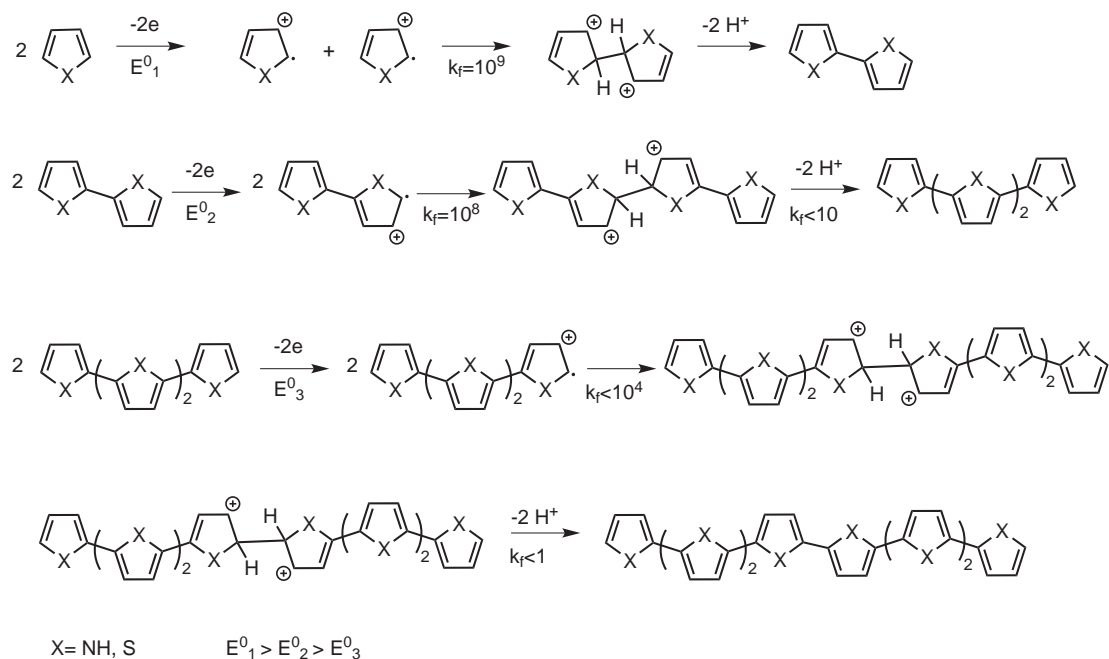


Figure 1.21 Initial steps of electropolymerization taking place via σ -bonded intermediates. Only α - α' couplings has been shown. ¹⁴⁷

with each cycle in cyclic voltammograms), but no informations on nucleation and growth mechanism can be obtained. This happens because, with this technique, the growing process is interrupted at each cycle. To summarize, the electrochemical polymerization of conjugated polymers involves three different steps:

- Oxidation of the monomer at the electrode and formation of soluble oligomers in the diffusion layer (by successive dimerization steps);
- Deposition of oligomers, involving nucleation and growth processes;
- Solid state polymerization, producing longer chains and cross-linked material.

***In situ* Oxidative Polymerization** PEDOT and its derivatives can be easily polymerized chemically by the action of FeCl_3 . In the case of PEDOT, this was one of the first oxidant employed since its use was already known to be effective for the synthesis of poly(pyrrole)s. Treatment of EDOT solutions with FeCl_3 rapidly yields the polymer as insoluble powder with very high conductivity. When performed in boiling acetonitrile (bp 82°C), this reaction yield PEDOT tetrachloroferrate with conductivities (15 S cm^{-1}) 3000 times higher than those

of polypyrrole prepared under the same conditions. Better results can be obtained using an higher boiling solvent such as benzonitrile (bp 188 °C). Several other oxidants have been tested. These include: MnO_2 ^{152,153}, Ce (IV) salts¹⁵⁴, CuCl_2 ¹⁵⁵, phosphomolybdic acid¹⁵⁶ and Fe (III) sulfonates¹⁵⁷. An example of this latter class of compounds is iron (III) *p*-toluenesulfonate ($\text{Fe}(\text{OTs})_3$). Aliphatic alcohols are able to dissolve large amounts of $\text{Fe}(\text{OTs})_3$ yielding stable solutions. Moreover, mixtures of EDOT and these oxidant solutions are metastable (do not give immediate reaction with polymer precipitation), but with very limited pot life. The addition of organic bases (*e.g.* imidazole^{158,159} or pyridine¹⁶⁰) have proved to enhance the stability of the solutions. This observation is related to the buffering of the *p*-toluenesulfonic acid produced during the polymerization. The presence of acidity can, in fact, have catalytic effect on the polymerization. Peroxides are also used as oxidants for PEDOT in aqueous environment. They are usually employed in the synthesis of PEDOT aqueous dispersions such as PEDOT:PSS. The most popular oxidants for this purpose being peroxodisulfates in the presence of catalytic amounts of iron salts (Fe^{II} or Fe^{III}). The presence of iron salts provide the catalytic decomposition of peroxodisulfate at defined reaction rates and are pivotal for a high and reproducible conductivity of the final product.

The metastability of some EDOT/oxidant solutions opened the way to *in situ* polymerization for preparation conductive thin films of the polymer. In this technique the freshly prepared solution of monomer, oxidant, stabilizers, adhesion promoters and other additives in a suitable solvent (usually lower alcohols, up to butanol) is deposited by spin-coating (or another technique) on the substrate as a thin film. The film is then subjected to thermal treatment (curing process), so that polymerization take place forming a conductive polymeric film. Up to now, *in situ* PEDOT is the polythiophene with the highest achievable electric conductivity, although PEDOT:PSS is catching up. This explains why *in situ* PEDOT is of great practical and commercial value. The oxidants of choice for this process are iron (III) or manganese (IV) ions, or other metal ions in an higher oxidation state. Among these, the most popular are iron salts of sulfonic acids. In particular, $\text{Fe}(\text{OTs})_3$ is the most widely used for its good solubility and reactivity.

The polymerization mechanism can be imagined as consisting of two steps. In the first one, the monomer is polymerized to the neutral undoped form of PEDOT, with the formation of TsOH and $\text{Fe}(\text{OTs})_2$ as byproducts (Fig. 1.22). As a consequence, 1:2 stoichiometry ratio exists. In the second step, the neutral

PEDOT is readily oxidized by the excess of $\text{Fe}(\text{OTs})_3$ to its doped form, consuming about 0.25-0.33 additional equivalents of oxidant. More $\text{Fe}(\text{OTs})_2$ is formed during this step, and the released tosylate ion act as a counterion for the positively charged PEDOT. Nevertheless, as discussed previously, in practice these two steps occurs simultaneously as a consequence of the lower oxidation potential of the formed oligomers. The byproducts are then removed from the formed polymeric film rinsing with a polar solvent (water, alcohol). Kinetic studies^{112,161} reveal that the initial formation of EDOT radical cation represent the slowest rate-determining step. Once formed, the radical cation rapidly dimerize. The dimers and oligomers are then rapidly oxidized and

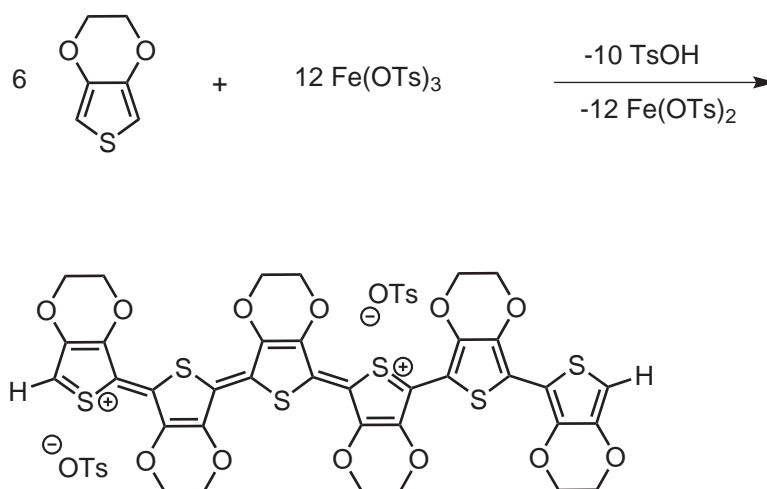


Figure 1.22 Scheme for the polymerization of PEDOT tosylate. An hexamer is shown as example.

their recombination leads to chain growth. As a consequence, reactions of bis-EDOT derivatives (or longer structures) experience an enormous acceleration in reaction rate (20000 times faster). This makes impossible to obtain stable, processable solutions of these derivatives containing an oxidant, limiting the application of *in situ* polymerization technique to derivatives with only one isolated EDOT moiety.

Typical recipes involve the deposition of an adhesion layer on the substrate prior to the deposition of the EDOT/oxidant solution. This is usually represented by a layer of PEDOT:PSS or a layer of γ -glycidoxypropyltrimethoxysilane.¹¹² The standard receipts allow to prepare PEDOT layers with conductivities as high as 500 S cm^{-1} with an easy solution based process. Higher values have been reported using different oxidants, such as iron (III) camphor-sulphonate instead of tosylate.¹⁶² *In situ* PEDOT:Tos layers tend to be mechanically brittle. This problem can be solved adding alcohol soluble polymers to

the formulation as plasticizers.^{103,163} An investigation on the influence of the different parameters on the properties of *in situ* PEDOT has been published in 2004.¹⁶⁴ In this report, a very good conductivity performance (900 S cm^{-1}) from an EDOT derivative, EDOT-MeOH, can be found. This good result has been ascribed to the ability of this compound to inhibit crystallization of the oxidant ($\text{Fe}(\text{OTs})_3$) during polymerization, facilitating the formation of highly homogeneous films. A similar effect has been observed in vapour phase deposited films: addition of PEG-*ran*-PPG to the layer of $\text{Fe}(\text{OTs})_3$ suppress the formation of crystallites, allowing formation of better films with higher conductivities.¹⁶⁵

Reductive Polymerization It has been demonstrated that 2,5-dihalogeno-EDOT compounds tend to undergo spontaneous homopolymerization to produce the polymer.^{166,167} These compounds can also be polymerized using organometallic reactions. The first example of this type of polymerization was reported by Yamamoto *et al.* in 1999. In this case, 2,5-Dichloro-EDOT was dehalogenated in presence of a nickel(0) complex.^{168,169} They claimed the obtainment of neutral undoped PEDOT using this new method. However, the black colour of the product and its insolubility in organic solvents rise suspects over the presence of residual charges or crosslinking in the polymer. With a modified reaction protocol (Fig. 1.23), Chevrot *et al.* prepared a soluble PEDOT. This material was not completely halogen-free (1.84% residual bromine was reported), but soluble in organic solvents. The presence of residual bromine was ascribed to the presence of PEDOT oligomers with bromine end-groups instead of long polymeric chains.^{170,171}

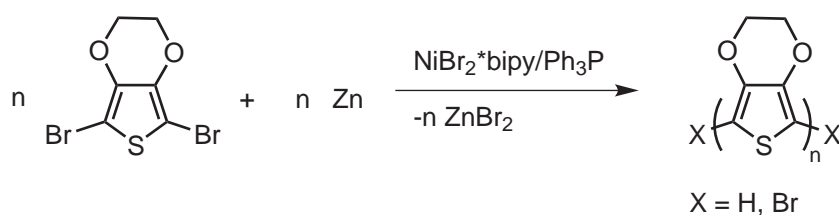


Figure 1.23 Organometallic PEDOT synthesis developed by Chevrot *et al.*¹⁷⁰

1.4.2 Discrete Reversible Organic Redox Systems

Many different types of organic and metal-organic compounds are able to undergo reversible redox processes. In some of them this process is accompanied by a modification of the UV/Vis absorption spectrum, making them elec-

trochromic. Such compounds have been used for more than a century as indicators for titration procedures, mostly on a semi-empirical basis. A special position is occupied by those compound that can undergo reversible redox reactions without involvement of hydrogen ions since these compounds don't have a pH dependent standard potential, and can be easily used with aprotic organic solvents. In fact, the use of these solvent is highly desirable because they present a larger potential window and minimize the possible side reaction of the electrochromic material with O_2 and H_2 coming from water electrolysis. For these reasons the forthcoming discussion will be restricted to these type of electrochromes.

1.4.2.1 Violenes

The first report of a compound belonging to this class dates back to 1879 when Wurster discovered the dye depicted in figure 1.24b, whose structure was lately recognized by Weitz in 1925.¹⁷²⁻¹⁷⁵ A similar reaction, is the one depicted in Fig. 1.24a for 1,4-benzoquinone. The existence of the semiquinone radical anion as the first step of this reduction was discovered only in 1938 due to the complication imposed by quinhydrone formation during the process.¹⁷⁶

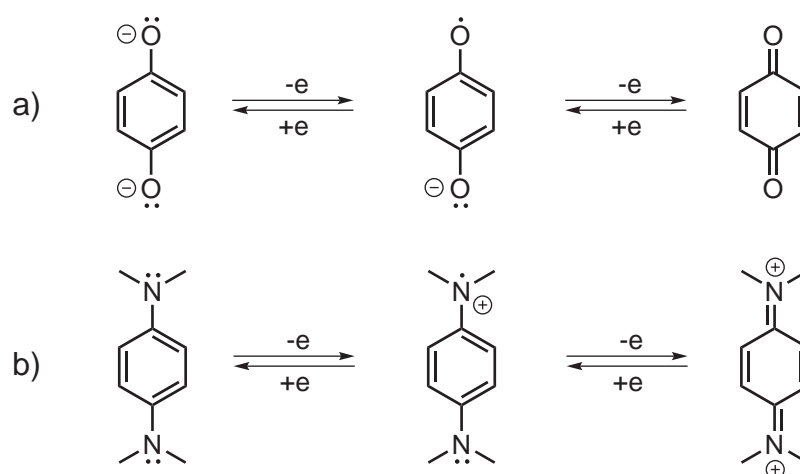


Figure 1.24 Structure and electrochemistry of: a) 1,4-benzoquinone b) Wurster's salt

From 1964 to 1999 Hünig *et al.* published an impressive number of papers about a large class of aromatic redox active compounds called "violenes", and derived a general structural principle for the compounds that have the capacity of two-stage electron transfer.^{177,178} It has been found that a great variety of organic compounds, derived from the general structural types depicted in figure

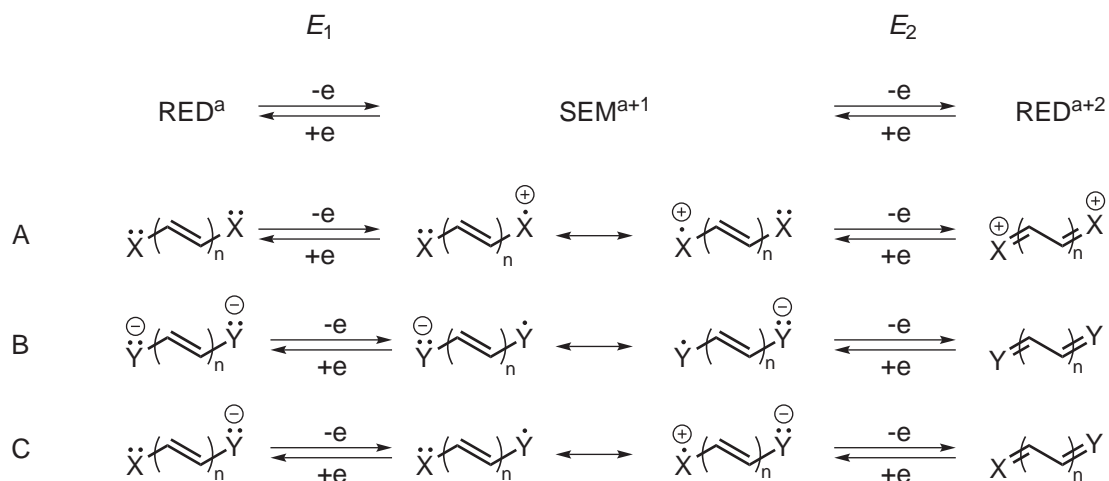


Figure 1.25 General structures for two-step reversible redox systems

1.25, are able to transfer two electrons in a stepwise fashion. The intermediate oxidation state SEM represents radical cations, radical anions and neutral radicals for A, B and C type respectively. The structural requirements for such a compound to reversibly transfer two electrons in two stages can be summarized as follows:

- the end groups of the reduced form (RED) have free electron pairs or π -systems available ($X, Y = \text{N, O, S, Se, P, } \pi\text{-systems}$);
- the end groups are connected by vinylene groups ($n=0,1,2,\dots$), which can be substituted, partially or completely, by ring systems. Aza substitution of methine groups is also possible.

Although the structures of the intermediate radical cations in pictures 1.24 and 1.25 are depicted with a fixed unpaired electron, they are strongly delocalized. As a consequence, low energy absorption bands are present in the UV/Vis spectra of SEM form, and a thermodynamic stabilization is expected in comparison to similar undelocalized radicals. In the case of type C violenes (Fig. 1.25), formally obtained by "crossing" systems A and B, a neutral SEM state is present. In systems of this type the radical is said to be merostabilized, and a lower stability in comparison with type A and B is expected as an effect of its dissymmetry.¹⁷⁹

Among compounds possessing these structural motifs, a further classification can be made:

1. *Open-chain redox systems*: neither the end groups nor the vinylene groups belong to a cyclic π -system;

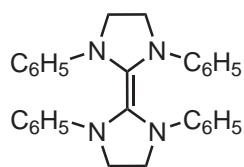
2. *Wurster-type redox systems*: end groups are located outside a cyclic π -system that has aromatic character in the reduced form;
3. *Inverse Wurster-type redox systems*: end groups are located outside a cyclic π -system that has aromatic character in the oxidized form;
4. *Weitz-type redox systems*: end groups are part of a cyclic π -system that has aromatic character in the oxidized form;
5. *Inverse Weitz-type redox systems*: end groups are part of a cyclic π -system that has aromatic character in the reduced form;
6. *Semi-Weitz redox systems*: one end group is part of a cyclic π -system that has aromatic character in the oxidized form.

Few examples, taken from the different subgroups, are depicted in figure 1.26. Between them, it is worth to mention TCNQs (compound f in Fig. 1.26) and TTFs (compound n in Fig. 1.26), which are widely used as acceptor and donor compounds respectively in materials science and supramolecular chemistry.¹⁸⁰⁻¹⁸² Viologens (structure m.), which are simple and easily accessible Weitz type electrochromes, represent another important group.¹⁸³ They will be discussed further in the next paragraph.

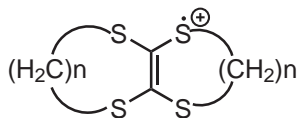
The reactivity of violenes is peculiar since at the equilibrium an amount of all the three redox states is present, and available for reactions. In particular, the RED form is sensitive to electrophiles, as a consequence of the presence of non-bonded electron pairs and an electron rich π -system. This property is expected to be more pronounced the more negative is the potential of the RED/SEM couple. The opposite is valid for the OX form, which is sensitive to nucleophiles; an effect that is increased at higher SEM/OX potentials.

Viologens Viologens, 1,1'-disubstituted-4,4'-bipyridinium dications, have a special importance among other Weitz type violene compounds. Since their discovery in 1933,¹⁸⁴ these redox active organic compounds have been studied in detail over the years. At the beginning, they were investigated as redox indicators, but later several different applications have been found. As an example, they represent the parent compounds, of the "paraquat" herbicides family. However, the interest in these compounds and their applications are mainly related to their remarkable electrochemical properties. Beside ECDs, viologens has been applied as redox switchable moieties in supramolecular chemistry,^{185,186} or more generally as acceptor units.^{187,188}

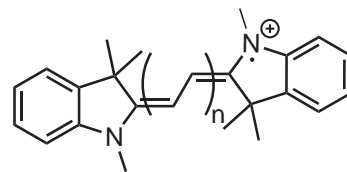
Open chain



a.

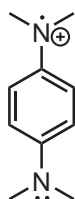


b. $n = 2, 3$

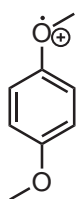


c. $n = 1-5$

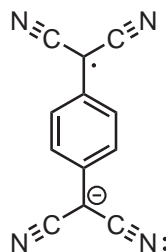
Wurster type



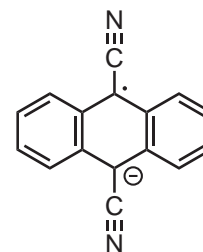
d.



e.

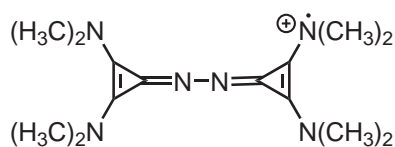


f.

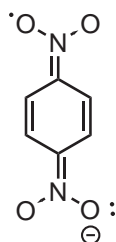


g.

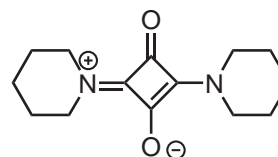
Inverse Wurster type



h.



i.

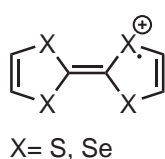


l.

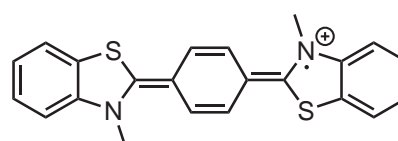
Weitz type



m.

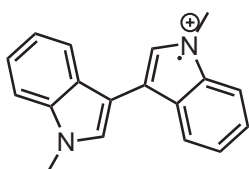


n.

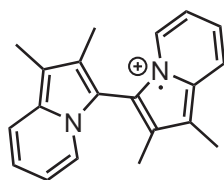


o.

Inverse Weitz type

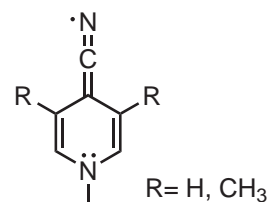


p.



q.

Semi Weitz type



r.

Figure 1.26 Examples of the different types of viologene systems

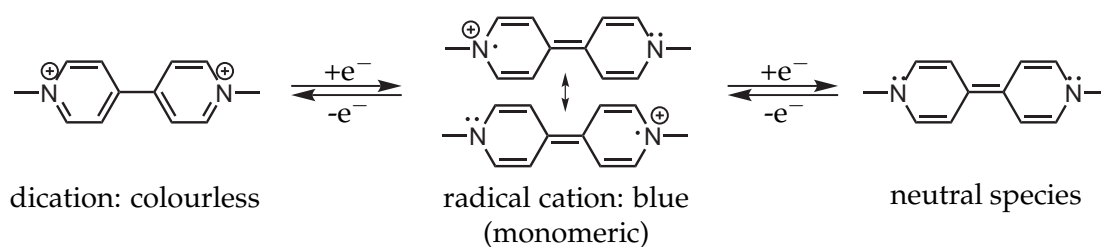


Figure 1.27 Methyl viologen (MV) electrochemistry

The simplest viologen is 1,1'-dimethyl-4,4'-bipyridinium, known as methyl viologen (MV). A radical cation, stabilized by delocalization throughout the π -system, is formed upon reduction (Fig. 1.27). This form is intensely coloured, as an effect of the presence of a charge transfer transition, with an absorption band that can be slightly modulated changing the 1 and 1' substituents. Simple alkyl groups promote a blue/violet colour of the radical cation, whereas aryl groups tend to impart a green hue (as in 1,1'-cyanophenyl-4,4'-bipyridinium, $\epsilon=83\,300\text{ Lmol}^{-1}\text{ cm}^{-1}$ at $\lambda_{max}=674\text{ nm}$ in MeCN). Viologens radical cations can dimerize in solution to form a diamagnetic dimer. This species possesses different spectral properties to the monomer (*e.g.* MV dimer is red) and has a slower oxidation kinetic, giving a quasi-reversible behaviour.^{189,190} The di-reduced redox state has very low colour intensity since it lacks any intense optical transition in the visible region. As a consequence of their reversible electrochemical behaviour and intense electrochromism, viologens soon appeared to be good candidates for electrochromic devices. The first reported viologen-based ECD dates back to 1973, as an outcome of Philips Laboratories's research on displays.¹⁹¹ In the same period IBM and Texas Instruments were also working on displays based on this type of materials.^{47,192} The development of these technologies was then apparently abandoned, as an effect of the competition with the better performing liquid crystal displays (LCDs).

The simplest viologen based ECDs make use of a solution phase Type I system. To attain better performances, viologens with longer alkyl chains were adopted in order to obtain insoluble radical cation species. In this way a type II system with enhanced write erase efficiency was obtained, using heptyl viologen dibromide (HV) as the compound of choice.¹⁹¹ These devices had a maroon colour due to incorporation of dimeric species in the deposited insoluble material and had ageing problems due to the crystallization of the radical cation inside the film.¹⁹³ Formation of the HV⁰ species was also found to affect write-erase efficiency.¹⁹⁴

The Gentex Corporation's patented Night Vision Safety (NVS) mirrors employ

viologen electrochemistry.¹⁹⁵ In this system a proprietary gel formulation, containing a viologen and an anodically colouring electrochrome (thiazine or phenylene diamine), is placed between an ITO-glass electrode and a metallic mirror counterelectrode. This type of device (see Fig. 1.28) has no memory effect and requires a continuous passage of current since the coloured species can diffuse in the electrolyte, and erase the formed colour through electron transfer (inverse redox reaction). A similar dual-electrochromic system employing *N,N'*-di-*n*-heptyl-viologen perchlorate and *N,N,N',N'*-tetramethyl-*p*-phenylenediamine (TMPD) has been used to prepare a 3×3 matrix array device.¹⁹⁶

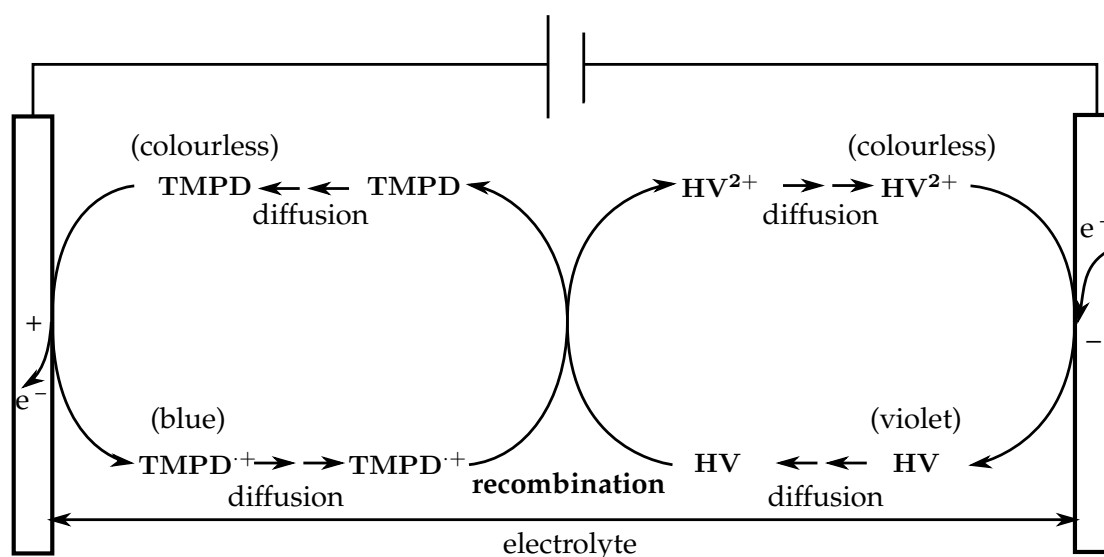


Figure 1.28 Working principle of the solution-phase heptyl viologen/TMPD ECD

More complex viologen based electrochromic systems make use of a surface modified electrode (using silanization)¹⁹⁷ or polyviologen systems. In the latter case, a preformed polymeric viologen system is prepared by reaction of 4,4'-bipyridyl and a difunctional haloalkane in a suitable solvent. The obtained product is usually deposited by spin-coating on the electrode surface.¹⁹⁸ Another deposition method employs polyviologen and PSS in an alternate layer-by-layer deposition procedure, to build a polyelectrolyte multilayer.^{199,200} A third approach, make use of viologens functionalized with electropolymerizable units (such as pyrrole,²⁰¹ thiophenes,^{202,203} EDOT²⁰⁴ etc.). These materials can be oxidatively polymerized to form conjugated polymers thin films embedding the viologen molecules. In these composite materials, both the viologen and the polymeric matrix are electroactive (and electrochromic). These polymers are likely to show an interesting multicolor electrochromism. Since this

kind of electrochromic polymeric system are better classified as "hybrid", they will be discussed in more detail in section 1.4.4.

A latter approach to viologen based ECDs make use of anchoring groups to adsorb the molecules on the surface of electrodes coated with nanostructured TiO_2 . This approach is similar to the one used for dye sensitized solar cells (DSSC) and the same type of electrodes is used²⁰⁵. In this way, a high colouration efficiency and a fast switching time can be obtained thanks to the high internal surface area and the surface confinement of the redox process.²⁰⁶ These characteristics have focused the interest of different groups on this technology.²⁰⁷⁻²¹³ Devices based on this technology are developed and commercialized by Ntera Limited as NanoChromics™ Ink System for the production of printed displays on flexible supports (Fig. 1.29c).²¹⁴ These devices (Fig. 1.29b) are based on a viologen molecule, carrying a phosphonic acid group (compound i) in Fig. 1.29a), chemisorbed on a $4\mu\text{m}$ thick TiO_2 layer deposited on an ITO/PET substrate. The counterelectrode is a $3\mu\text{m}$ thick film of high surface area $\text{SnO}_2:\text{Sb}$ on carbon/PET substrate. A ion-permeable TiO_2 layer can be placed between the electrodes to act as a diffuse reflector obtaining the effect of ink on white paper. In another configuration, phosphonated phenothiazine molecules (compound ii) in Fig. 1.29) can be absorbed on the counterelectrode obtaining a dual electrochromic device able to change from colourless to purple.^{215,216}

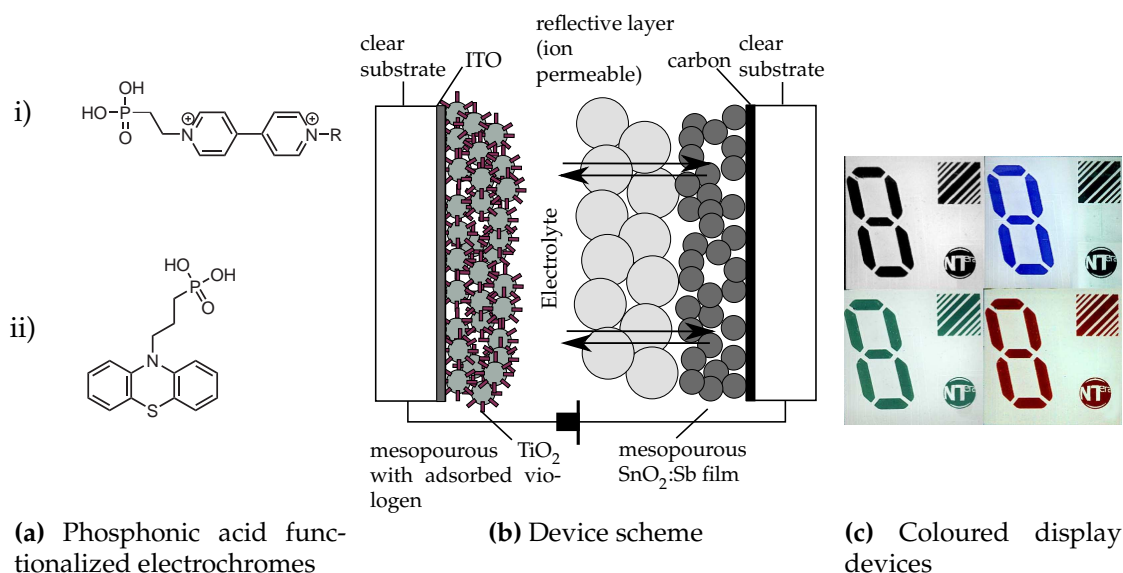


Figure 1.29 Scheme of a NanoChromics™ device^{214,215}

Phenothiazine, phenazine, phenoxathiin, thianthrene The title compounds cannot be clearly classified since they can be considered both Weitz type and

Wurster electrochromes. Phenothiazine derivatives are known to form very stable, red coloured radical cations, and have already been mentioned in paragraph 1.4.2.1 for their application in conjunction with viologens in electrochromic devices based on TiO₂-absorbed dyes. Application of phenothiazine alone in simple electrochromic devices has also been reported.²¹⁷

Arylene bisimides Compounds of this class have been extensively used as acceptors as a consequence of their low LUMO level, and hence they can easily form stable radical anions and dianions upon reduction at relatively high potentials.²¹⁸ They can be considered to be Wurster type viologens with the imide groups acting as redox centers. They show a two-step reversible reduction, with two reversible cathodic waves in CVs. The first peak can be attributed to the formation of the radical anion, while the second arise from the dianion formation. The peak separation is dependent on the size of the arylene core as an effect of the better delocalization of the radical anion and the lower coulombic repulsion in the dianion. As a consequence, the difference is higher for the smaller pyromellitic bisimides and naphthalene bisimides than for perylene ones. As an example di-n-amyl-pyromellitimide has its two reduction wave at -0.74 and -1.43 V (vs. SCE) (which correspond to $\sim -1.14/-1.82$ V vs. Fc/Fc⁺), di-sec-butyl-naphthalenebisimide at -1.14 and -1.56 V (vs. Fc/Fc⁺), while di-sec-butyl perylene bisimide has -1.08 and -1.27 V (vs. Fc/Fc⁺).^{218,219} Bisimides with very large cores, such as terrylene or quaterrylene, show a single two-electron reduction process.²²⁰ The electrochemical and spectroelectrochemical properties of thin films obtained from polymeric pyromellitic bisimides and naphthalene bisimides have been studied but no reports of their application in electrochromic devices is present in literature.^{219,221}

Aromatic dicarboxylic acids esters The electrochromic properties of these viologen redox systems (Wurster type) have been reported in 1987 by Nakamura *et al.*²²², but apparently no further developments followed their preliminary findings. The investigation on the electrochromism of these compounds was then reopened in 2004 by Kobayashi *et al.* who characterized the electrochemistry and spectroelectrochemistry of dimethyl terephthalate solutions in NMP.²²³ The compound is reduced at ~ -2.0 V vs. Ag/AgCl showing an increase in absorption at 530 nm. In a following paper, they built a solution phase 8×8 matrix ECD employing diacetylbenzene, dimethylterephthalate and biphenyl dicarboxylic acid diethyl ester cells using ferrocene as redox counterpart.²²⁴ At-

tempts to build flexible devices using PVB-based gel electrolyte has been conducted but the data for these devices show a very slow switching speed (around 100 s).²²⁵

The electrochromism of 5-substituted 1,3-isophthalates have been studied by Lee *et al.* who demonstrated the possibility to tune the colour of the reduced state changing the substituent.²²⁶

Biphenyl dicarboxylic acid diethyl ester show two-step reduction changing the colour of the solution from colorless to yellow and finally to red. An electrochemical cell using a solution of this compound and a NiO counterelectrode showed high colouration efficiency for the first reduction step ($377 \text{ cm}^2 \text{ C}^{-1}$) thanks to the adoption of a solid state counterelectrode material. Nevertheless, a 50% decay in contrast (ΔT) is observed after 1000 cycles.

Triphenylamine functionalized aromatic polyamides and polyimides Triphenylamine derivatives are widely used as hole-transport donor compounds in organic materials, TPD (*N,N'*-Bis(3-methylphenyl)-*N,N'*-diphenylbenzidine) being one of the most popular.²²⁷ The charged states in this material are stable highly delocalized radical cations with quinod character^{228,229}, hence it is no surprise that a closer look to its structure reveals it to be a Wurster type violene. According to Robin and Day²³⁰, systems of this type are classified as class III since a strong electronic coupling is present between the two redox centers.²³¹ Nonconjugated polymeric triphenylamine based systems, similar to these, have been extensively studied, since 2005, by Liou *et al.*^{232–238} They prepared and fully characterized a lot of different polyimides and polyamides with *N,N,N',N'*-tetraphenyl-1,4-phenylenediamine moieties and a variety of different aromatic and non-aromatic spacers in the main chain (see Fig. 1.4.2.1). The obtained polymers are soluble in most of the polar aprotic solvent (NMP, DMSO, DMAc, DMF, *m*-cresol) allowing them to prepare amorphous films by a drop-casting technique. These films are multichromic, showing a colorless \rightarrow green \rightarrow blue transition upon oxidation, and exhibit high contrast values (>60% in the visible region) and good cycling stabilities.²³² The introduction of methoxyl substituents on the electrochromic unit (b. in Fig. 1.4.2.1) in *p*-position lowered the oxidation potential and allowed to obtain more stable radical intermediates preventing dimerization reactions at these positions.²³⁵ These improved materials show contrasts values around 75% in the visible region and cycling stabilities up to 1000 cycles with a decay in colouration efficiencies of 5% for the colourless \rightleftharpoons green transition and 10% for colourless \rightleftharpoons blue one.

Switching times (colouring/bleaching) of these two transitions are 3.04s/1.87s

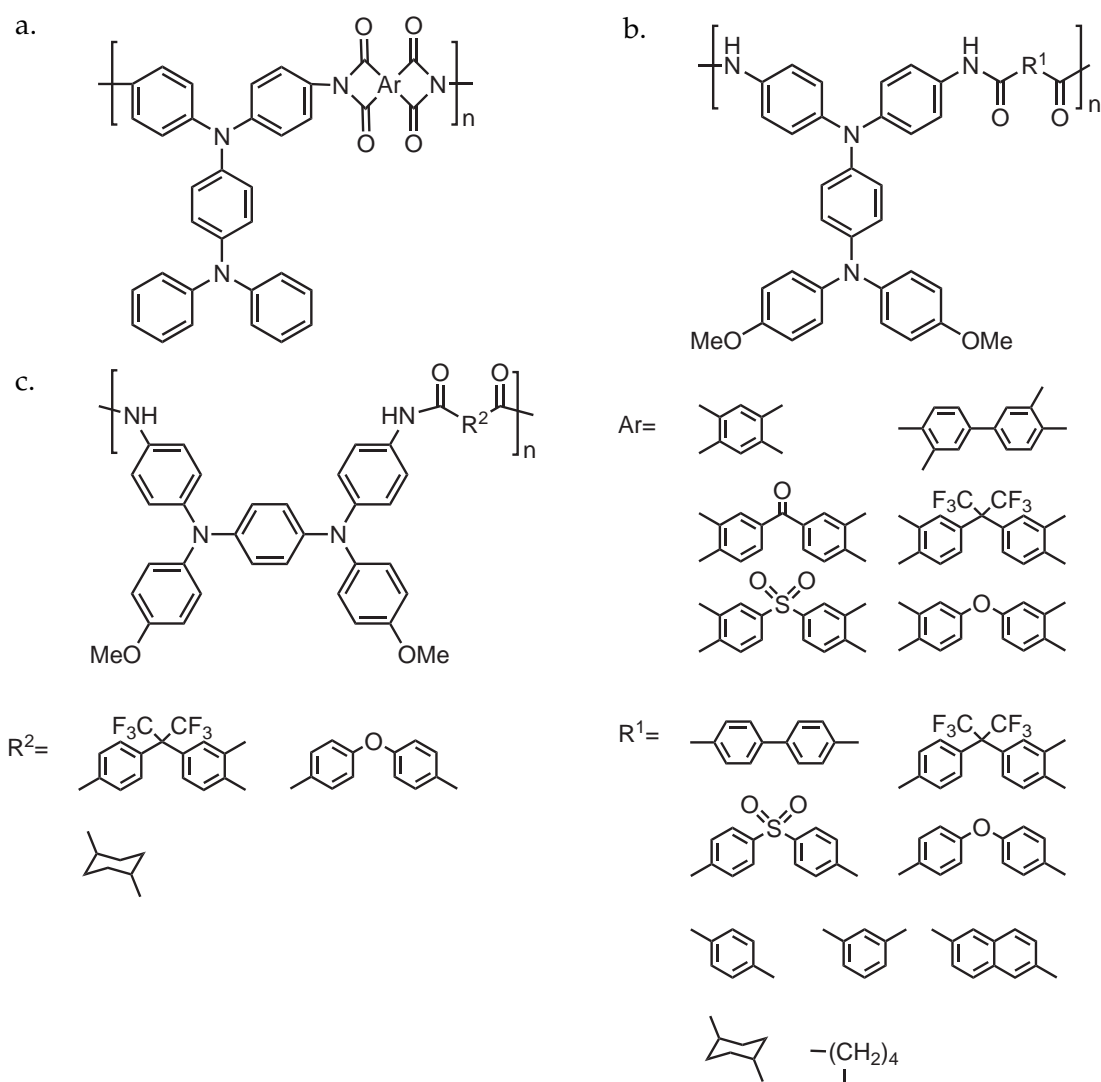


Figure 1.30 Examples of polyimides and polyamides incorporating *N,N,N',N'*-tetraphenyl-1,4-phenylenediamine moieties developed by Liou *et al.*

and 4.02s/2.02s respectively which are rather high values in comparison to those achieved with conjugated polymers (<0.5s).¹²⁶ A further improvement on the electrochromic properties of these polymers was obtained using *N,N'*-bis(4-aminophenyl)-*N,N'*-di(4-methoxyphenyl)-1,4-phenylenediamine as functional monomer (c. in Fig. 1.4.2.1).²³⁶ The obtained polymers retain 99% of their electroactivity after switching 10000 times between 0 and 0.70V (vs. Ag/AgCl) (colourless \rightleftharpoons green) with a decay in colouration efficiency of 4.89%. Similar good results are obtained switching to 1.10V (vs. Ag/AgCl) with a decay of 5.60% after 3000 cycles.

1.4.2.2 Violenes/Cyanine Hybrids

The violenes (see section 1.4.2.1) represent most of the known organic electrochromes. The main drawback of these system is the fact that the intensely coloured redox state (long wavelenght absorbing and high ϵ) is a radical ion. These open-shell states, even the most stable ones, have the tendency to be more reactive when compared to closed-shell ones. As a consequence, a similar redox system switching between closed-shell states is expected to be less prone to decomposition. In order to obtain reversible redox systems of this kind, with an highly coloured closed-shell state, a new general structure has been proposed by Hünig *et al.*²³⁹⁻²⁴¹ (see Fig. 1.31).

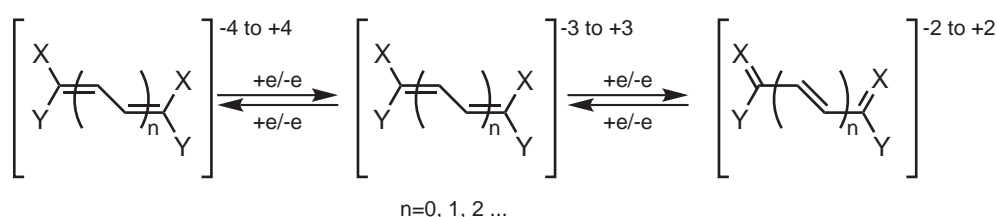


Figure 1.31 General structure for a Violenes/Cyanine redox system

This new general structure is clearly inspired by the violene one, but contains, as end groups, systems that in the reduced or oxidized form can be described as polymethine dyes (cyanines, oxonols and merocyanines; $X=C-Y$ in Fig. 1.31). Highly delocalized closed-shell systems of this class are known to possess strong thermodynamic stabilization. As a consequence, in such a system the fully reduced or fully oxidized states in the $RED \rightleftharpoons SEM \cdot \rightleftharpoons OX$ equilibrium are stabilized at the expense of the SEM radical species, with the result of a redox process that approaches a two-electron one. Furthermore, the cyaninic nature of one of the two accessible states make it strongly absorptive in the visible region ($\log \epsilon \simeq 5$). As an example, tetrakis(dimethylaminophenyl)ethene (TDAPE, compound b in Fig. 1.32), known since 1906²⁴², show a reversible $RED \rightarrow OX^{2+}$ two-electron redox process at $\simeq -0.30$ V (vs. Fc/Fc^+) in its cyclic voltammogram (Fig. 1.33a)²⁴⁰.

This process has been closely studied revealing a very small equilibrium concentration of $SEM^{\bullet+}$ species²⁴⁰. In contrast, the second oxidation wave at $\simeq -0.70$ V (vs. Fc/Fc^+), show a broadened peak with shoulders, and can be interpreted as closely spaced unresolved single electron processes. The spectroelectrochemistry of the $RED \rightarrow OX^{2+}$ transition, depicted in figure 1.33b, show the appearance of broad and intense absorption bands in the visible region. Although this complex spectrum cannot be simply described as derived

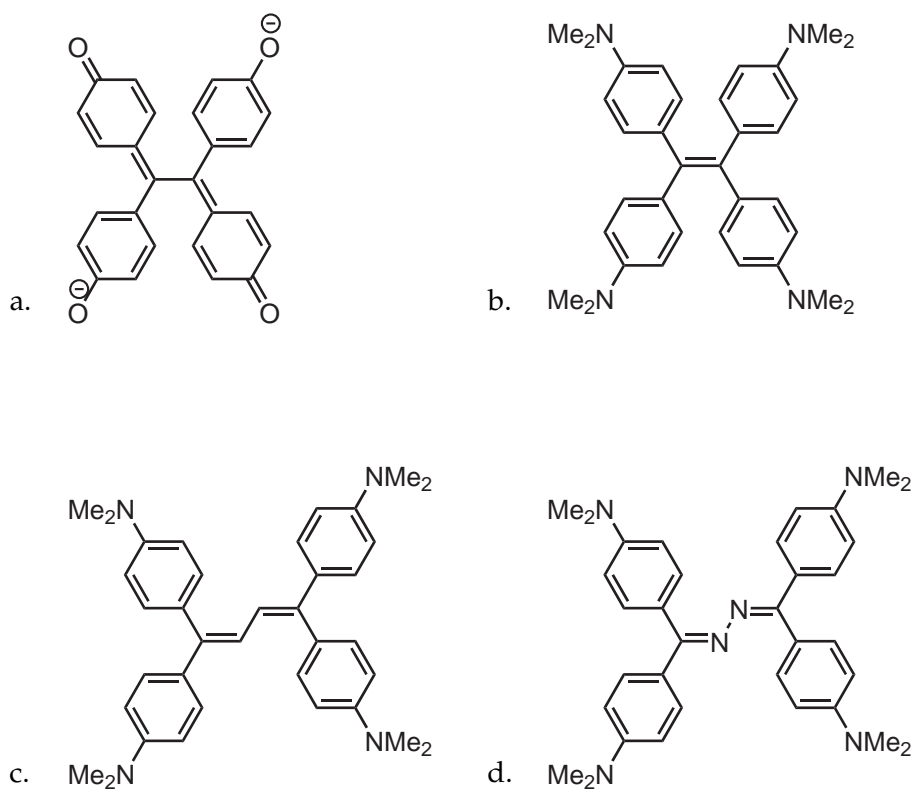
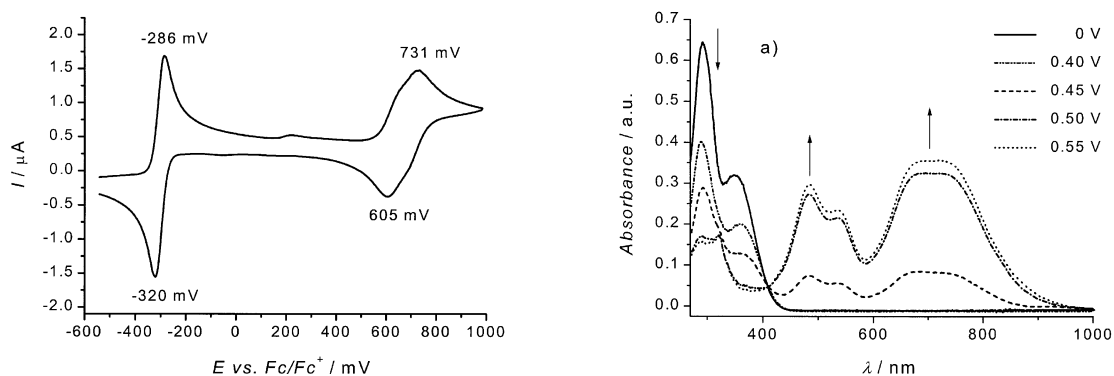


Figure 1.32 Examples of Violenes/Cyanine hybrids



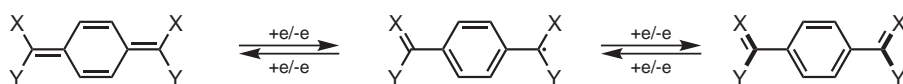
(a) Cyclic voltammogram of TDAPE in 0.1M $n\text{-Bu}_4\text{NPF}_6/\text{CH}_2\text{Cl}_2$; potentials vs. Fc/Fc^+ , scan rate 100mVs^{-1} .²⁴⁰

(b) Spectroelectrochromic (SEC) plot of $\text{RED} \rightarrow \text{OX}^{2+}$ oxidation step of TDAPE in 0.1M $n\text{-Bu}_4\text{NPF}_6/\text{CH}_3\text{CN}$; potentials vs. Ag/AgCl .

Figure 1.33

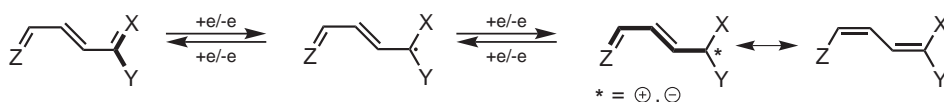
from the one of its cyaninic substructure (Michler's hydroxol blue), it demonstrates the possibility to obtain an highly coloured closed-shell state following the violene/cyanine approach. Further studies on these type of systems have been made by Ito *et al.* who developed more complex systems based on azulene moieties.²⁴³⁻²⁴⁷ Most of their structures do not fit in Hünig's simple violene/cyanine hybrid structure depicted in Fig. 1.31 and new types of hybrids were developed (Fig. 1.34). It can be noted that some of these systems posses

Inverse Wurster type Violene/Cyanine Hybrids

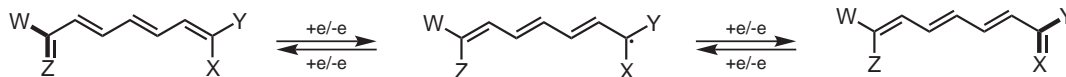


Cyanine-Cyanine Hybrids

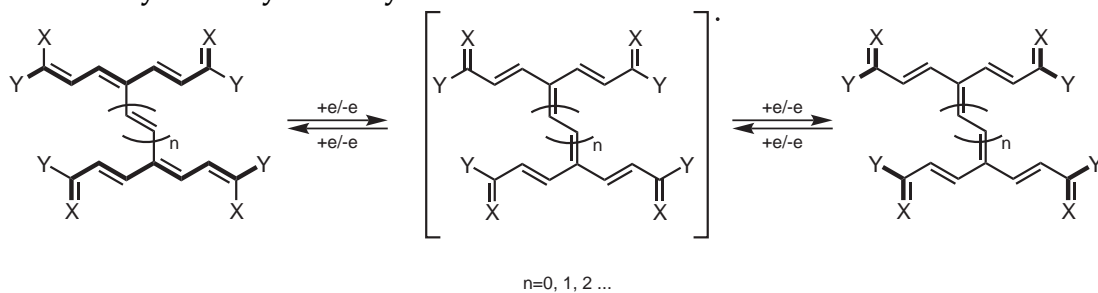
a) with two cyanine substructures



b) with two cyanine end groups



Violene-Cyanine-Cyanine Hybrids



Violene-Violene Hybrids

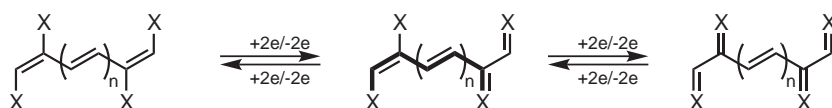


Figure 1.34 Examples of violene/cyanine hybrids structural motifs

more than one cyaninic oxidation state, giving them intriguing electrochromic properties (multichromic and highly absorptive). It is thus possible to specu-

late that more systems based on the violene/cyanine hybrid structures will be studied and some of them tested in ECDs.

1.4.2.3 Electrochromic systems based on intramolecular redox switching of bonds

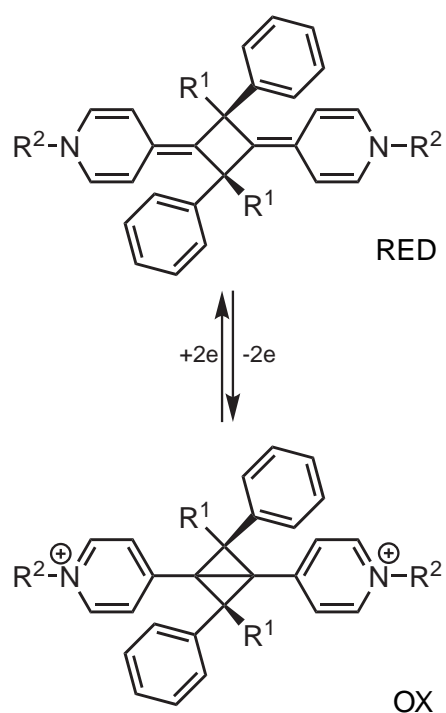
Although violene type and the related violene/cyanine hybrid systems account for most of the organic electrochromic compounds, a further class have to be considered. In contrast to violenes and similar systems, where reduction or oxidation are accompanied by a small conformational change and a modification in the bond lengths, in these systems the formation of new intramolecular bonds is observed as a consequence of valence tautomerization occurring during the electrochemical process. This is usually accomplished through a multistep process that involve an overall two-electron transfer and a bond formation/cleavage. The underlining mechanism is often of the ECE type (*electron transfer-chemical event-electron transfer*), where the valence tautomerization take place after the transfer of the first electron.

One of the first reported compound of this class was reported by Hünig *et al.* in 1977.^{248,249} In this case, compounds with a 1,3-dimethylenecyclobutane skeleton, show an homoconjugative interaction between the two chromophoric units, that lead to the formation of a bicyclo[1.1.0]butane skeleton upon oxidation to the dicationic forms (Fig. 1.35a). The overall chemical process is reversible since CV patterns are retained on multiscanning, but the electron transfer is irreversible as is apparent from the large separation between the oxidation and reduction waves (Fig. 1.35b). This characteristic is recurrent in this type of systems.

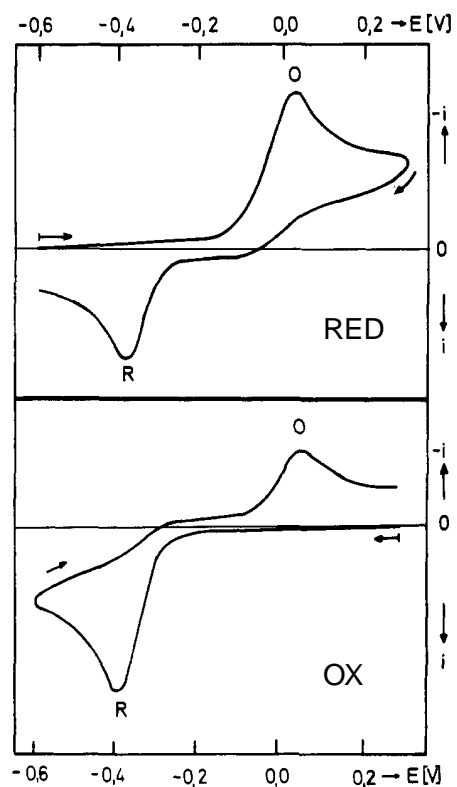
A series of systems of this type, based on a tetraaryldihydrophenanthrene skeleton, was published in 1997 by Suzuki *et al.*^{250,251} These molecules exploits the easy bond dissociation of hexaarylethane derivatives into trityl radicals to form a bistable redox active system that can be switched upon a two-electron transfer (with an ECE mechanism, see Fig. 1.36a). The cyclic voltammograms (Fig. 1.36b for Ar=4-Me₂NC₆H₄) show irreversible electron transfers but the presence of a reversible overall chemical process as in the previous case. The switching between the two forms is accompanied by drastic colour changes, with an oxidized form showing strong absorption bands in the visible region (λ_{max} (log ϵ): 661 nm (4.92), 604 nm (5.05); for Ar=4-Me₂NC₆H₄, Fig. 1.36c).

Similar systems, using cyanine radicals, were later studied by Hünig *et al.*^{253,254}, who proposed the two general structural motifs depicted in figure 1.37. In this

$R^1 = \text{H}, \text{CH}_3, R^2 = \text{CH}_3, \text{C}_5\text{H}_5\text{CH}_2$

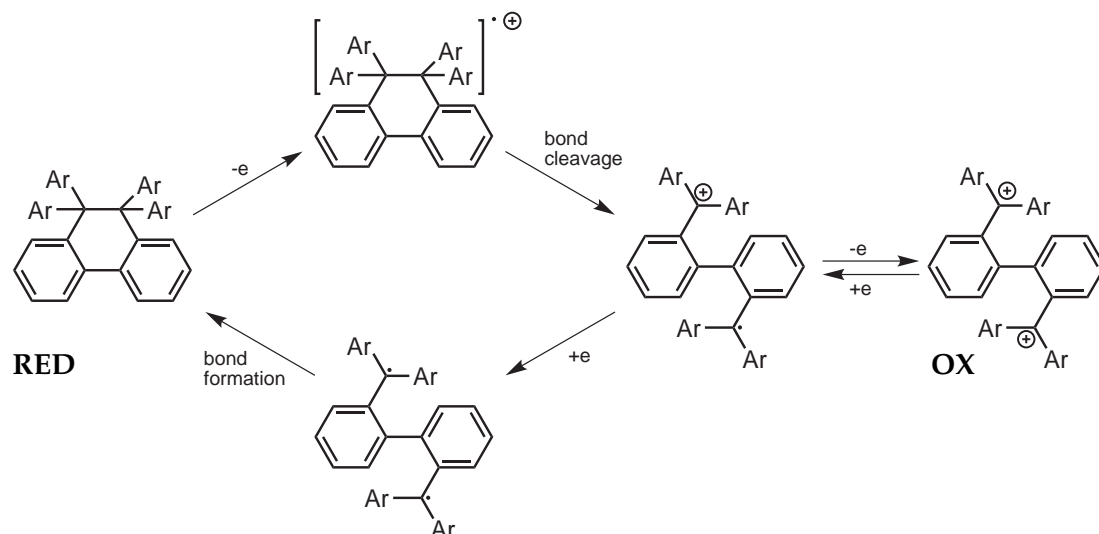


(a) Equilibrium between reduced (RED) and oxidized (OX) forms involving valence tautomerization



(b) Cyclic voltammogram of OX and RED forms with $R^1 = \text{H}$ and $R^2 = \text{CH}_3$ in 0.1 M $n\text{-Bu}_4\text{NBF}_4/\text{DMF}$; Pt vs Ag/AgCl/MeCN. Scan rate 200mVs^{-1} .²⁴⁹

Figure 1.35



(a) Interconversion of RED and OX forms in tetraaryldihydrophenanthrene systems (Ar=4-Me₂NC₆H₄, 4-MeOC₆H₄; Ar₂C⁺=9-xanthenylium) through an ECE type mechanism.²⁵²

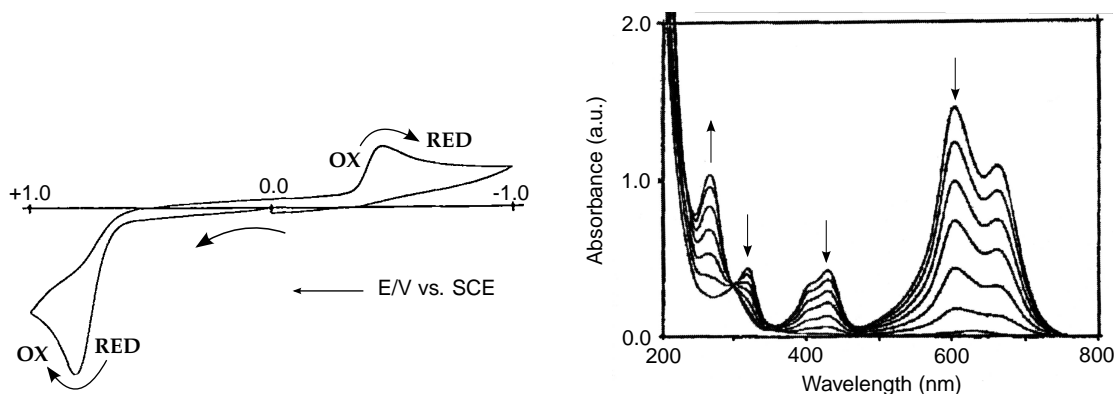


Figure 1.36

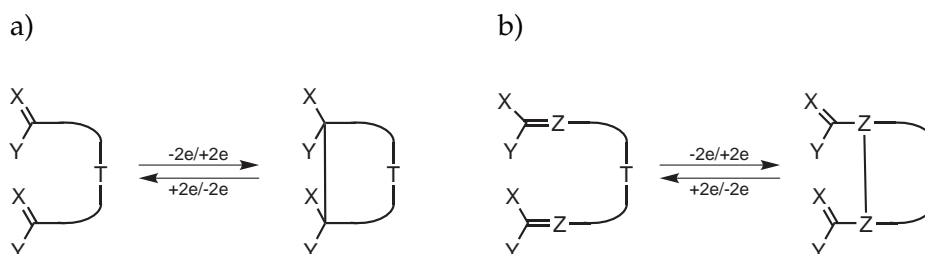


Figure 1.37 General structures of electrochromics based on single-bond redox switching.²⁵³

scheme the $X=C-Y$ system indicate a cyaninic type substructure that is able to stabilize the charge, T is a saturated or unsaturated tether and Z indicates N or C-R. Due to the presence of cyaninic substructures, these systems possess at least one strongly coloured, long wavelength absorbing state. In the case of a) type system, this corresponds with the open form, while the opposite is verified for the b) type system. By virtue of these characteristics, the electrochromic

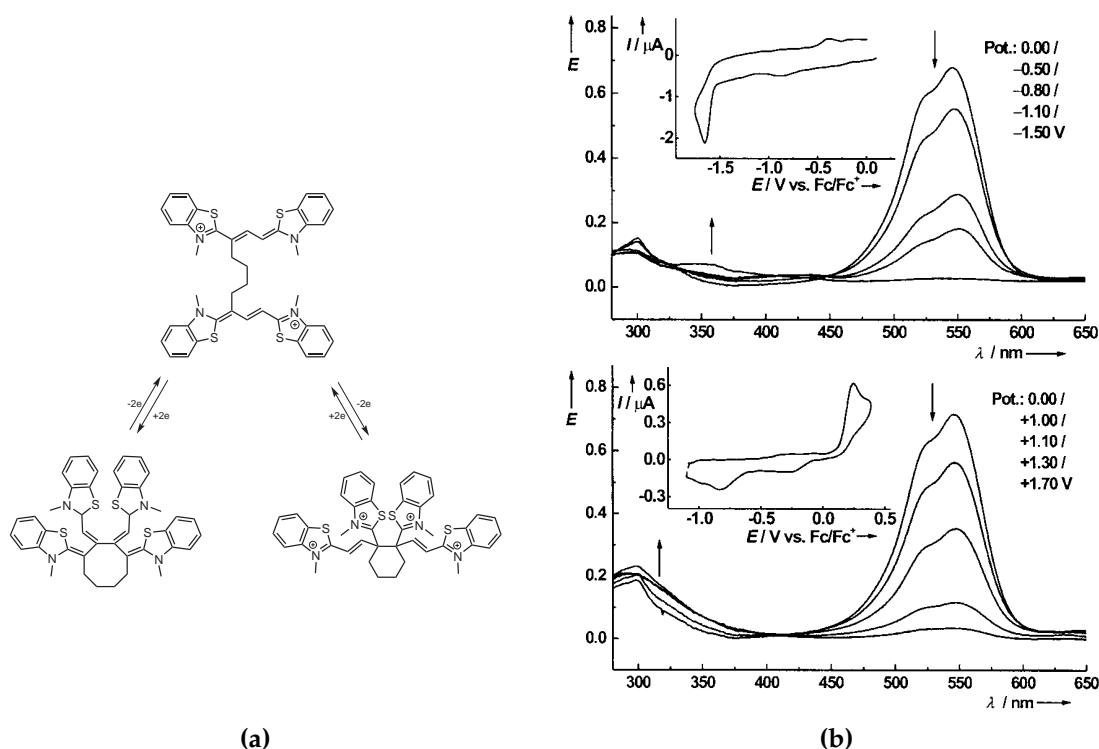


Figure 1.38 Cyclic voltammograms (vs. Fc/Fc^+ , $\nu=100\text{ mV s}^{-1}$, saturated solution) and spectroelectrograms (vs. $Ag/AgCl$) for reduction (up) and oxidation (down) of the cyanine based compound depicted on the left.²⁵³

properties of these closed-shell systems are very interesting since they can theoretically achieve very high contrast values in ECDs, but their application has not yet been reported.

1.4.3 Metal Coordination Complexes

Metal coordination complexes appear as promising electrochromic materials as a result of their intense colouration and redox activity combined with the possibility to modulate their properties through easy modification of the organic ligands.²⁵⁵ In this class of compounds, the transitions involved in the chromophoric properties are mainly: metal-to-ligand charge transfer (MLCT), in-

tervalence charge transfer and intra-ligand excitations; thus involving valence electrons. It follows that these transitions are altered or eliminated upon reduction or oxidation of the metal center, making these materials electrochromic. The incorporation of electrochromic metal coordination complexes in all-solid-state ECDs is of particular interest for applications but requires them to be prepared as thin-films or as polymers.

Polypyridyl Complexes

Polypyridyl ligands are known to form stable complexes with a variety of transition metals, and some of them show interesting electrochromic properties. An example is represented by the bipyridyl complexes $[M^{II}(\text{bipy})_3]^{2+}$ (M = iron, ruthenium, osmium; bipy = 2,2'-bipyridine) which appear as red, orange and green respectively as a consequence of the presence of a MLCT band which is suppressed on switching to the M^{III} redox state. Bipyridine based complexes in which ligands are functionalized with electron-withdrawing groups also show some ligand-based electrochemical processes, as an effect of the anodic shift of the redox potentials, that lead to multicolor electrochromism.^{256,257} The incorporation of polypyridyl complexes inside thin-films is usually accomplished through polymerization of properly functionalized ligands (carrying polymeric functionalities). Two approaches are found in literature: oxidative polymerization and reductive polymerization.

Reductive electropolymerization of $[M^{II}(\text{bipy})_3]^{2+}$ complexes is usually employed with vinyl-substituted pyridyl ligands and exploits the ligand-centered nature of the three sequential reduction shown by such ligands. Radical species generated upon reduction lead to oligomeric metallopolymers through C–C bond formation. The oligomeric species grow near the electrode surface and are deposited onto it once a critical size is reached (due to their insolubility).²⁵⁸

Electroactive thin-film formation by oxidative electropolymerization has been described for Fe^{II} and Ru^{II} complexes obtained from bipyridyl ligands substituted with amino²⁵⁹ moieties and aniline functionalized pendants²⁶⁰.

Recently, electrochromic films based on Os^{II} and Ru^{II} supramolecular assemblies prepared following a layer-by-layer deposition method have been reported. This approach uses polytopic vinyl-pyridyl based ligands to form metal complexes that are subsequently crosslinked on the surface using $\text{PdCl}_2(\text{PhCN})_2$ with an alternate deposition procedure, leading to porous metal-organic assemblies^{261,262}

Metallophthalocyanines and porphyrins

Metalloporphyrins are naturally occurring pigments containing a porphyrin ring chelating a metal ion. The most common examples are the hemes (found in hemoglobins, myoglobins, cytochromes, catalases, and peroxidases), chlorophylls, and bacteriochlorophylls. Synthetic approaches to the synthesis of a variety of different porphyrins have been developed. Excluding the case of highly non-symmetrical derivatives, in synthetic porphyrins substituents can be present on the β positions of the pyrroles (figure 1.39) and/or at the *meso* position between the pyrrolic rings (in this case R is usually an aromatic ring).²⁶³

Phthalocyanines (Pc) can be considered as tetraazatetrabenzo derivatives of



Figure 1.39 Common substitution patterns in synthetic porphyrins

porphyrins, which form coordination complexes with ions derived from more than 70 different elements of the periodic table. The metal ion in metallophthalocyanines is located either at the center of a single Pc ligand (Fig. 1.40a) or between two of them forming a sandwich-type complex (1.40b). The first type of complexes is common for transition metal ions while the latter is usually encountered with lanthanides. Metallophthalocyanines find industrial application as dyes and pigments (for inks, plastics and metal surfaces) while their water-soluble sulfonate derivatives are used as dyestuff for clothing. They find further applications as catalysts, liquid crystals, gas sensors, photosensitizers, NLO dyes and electrochromes. The colour of metallophthalocyanine derivatives is due to the presence of a very intense ($\epsilon > 10^5 \text{ Lmol}^{-1} \text{ cm}^{-1}$) absorption band located in the red region of the visible spectrum (around 670 nm), accompanied by weaker MLCT transitions in the region around 500 nm. These transitions make possible to modulate the resulting hue by changing the metal ion.

The first electrochromic phthalocyanine based thin-film was reported in 1970.²⁶⁴

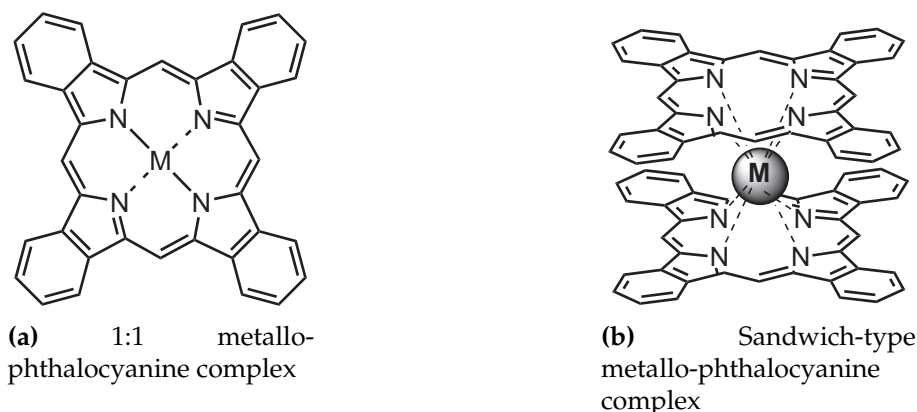
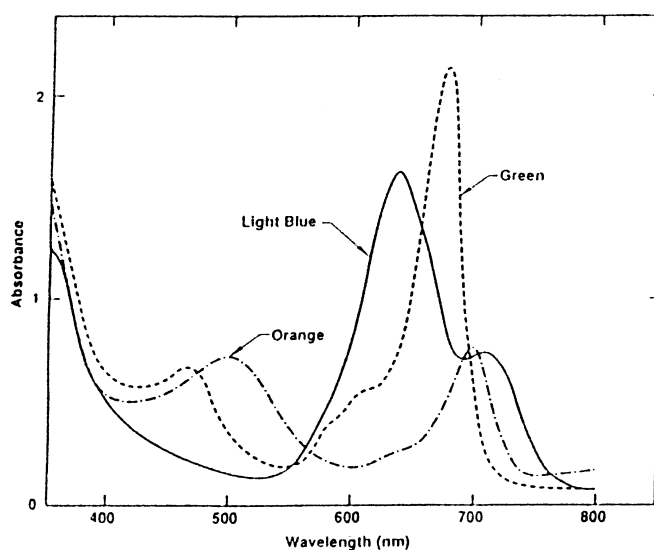


Figure 1.40

This material was obtained by vacuum sublimation of $[\text{Lu}(\text{Pc})_2]$ and was extensively studied in the following years. Films obtained in this way show a brilliant green color ($\lambda_{\text{max}}=605\text{nm}$) and possess a complex multicolor electrochromism (Eq. 1.33, 1.34, 1.35 and Fig. 1.43). Upon oxidation the film changes to a yellow-

Figure 1.41 Absorption spectra of $\text{Lu}(\text{Pc})_2$ in aqueous 1 M KCl.²⁶⁵

low/tan form (Eq. 1.33) and then to a red one of unknown composition,^{266–268} upon reduction it switches firstly to a blue form and then to a violet-blue one.²⁶⁹ Limiting the colour transition to yellow–tan \rightleftharpoons green, cycle lives greater than 5×10^5 cycles have been reported in suitable solvents with switching speeds $\simeq 40\text{ms}$, but the contrast between these two redox states is not very good.²⁷⁰ Devices containing Pc complexes also suffer from degradation problems correlated to the mechanical stress caused by the inward/outward motion of counterions in the electrochromic film during cycling. This factor, connected to the

colouration efficiency, ease of processing and hue modulability through functionalization. However, these latter characteristics appear to be rather limited if one looks at the literature examples. In particular, conjugated polymer based systems switching from a colourless highly transmissive state to one possessing a neutral hue (brown, grey, green) are still missing. The advent of the donor-acceptor approach solved the problem only in part since the known examples lack the highly transmissive state of the best PEDOT analogues. Furthermore, their coloured state exhibits pure hues that are unsuitable for application like smart windows or sunglasses since they lead to distortion in colour perception, as a consequence of uneven filtering of some spectral regions. The only exception is represented by the PProDOT based copolymer incorporating DA units developed by Reynolds *et al.* that shows a bluish-black to transmissive transition.²⁰ Nevertheless, the transmittance of the bleached form in the visible region ranges from 45% to 67% that are unacceptable values for the aforementioned applications. One possible solution to modify the colours of the existing electrochromic polymers is to incorporate a second, non-interacting, electrochrome inside their structure. Supposed that the two systems, the polymer and the embedded discrete electrochromic system, show independent redox behaviours, an easy way to colour tuning can be obtained. Furthermore, if both the polymer and the discrete electrochromic system (DES) possess a colourless state in the same potential range, a colourless to coloured transition could in principle be observed. There are few examples of this type of approach in literature.

In 1984, Bidan *et al.*²⁰¹ reported the electrooxidation of a pyrrole *N*-substituted with an aliphatic chain bearing a 4,4'-bipyridinium (viologen) on a Pt electrode. The cyclic voltammogram shows the presence of the polypyrrole redox process along with the two sharp redox waves of the viologen unit. Interestingly, a pre-peak superimposed to the poly(pyrrole) oxidation wave is also present. The authors state that the amount of charge attributed to this pre-peak is identical to the observed difference between the integrated charges for reduction and oxidation of the V^{2+} unit. This modified electrode appears to be not so stable, since a 15% charge drop in the viologen reduction peak was observed after 450 cycles (between 0 and $-0.9V$ vs. Ag/Ag^+). A similar system, in which the viologen unit was anchored to the 3-position of a thiophene unit through an alkyl tether, was prepared by Lee *et al.* in 2002.²⁰³ Even in this case the cyclic voltammograms of the polymers showed an additional peak superimposed to the polymer oxidation process. Quantitative consideration on the

charges involved in the redox waves, and additional experiments limiting the scan range, confirmed a similar behaviour to the one observed by Bidan *et al.* The authors explained this odd behaviour by the presence of a viologen mediated electron transfer process. Their hypothesis is that, upon reduction of the conjugated polymer backbone, charge trapping occurs, leaving residual charges. These species are then reduced at a lower potential through an electron transfer process mediated by $V^{\bullet+}$. Reoxidation occurs at the same potential as the rest of the polymeric chain. Nonetheless, the system appeared to have fairly good cycling stability, and spectroelectrograms of the system in its different oxidation states were recorded. Similar redox behaviors were reported with different redox active systems attached to conjugated polymers: viologen/poly(cyclopentadithiophene)²⁸³, viologen/polycarbazole²⁸⁴, titanocene/polypyrrole²⁸⁵, titanocene/PEDOT²⁸⁶, anthraquinone/PEDOT²⁸⁷. However, in most of these systems, the presence of pre-peaks is associated with a loss in the electroactivity of the attached redox-active unit. As an example, the cyclic voltammograms of the anthraquinone/PEDOT system studied by Otero *et al.*²⁸⁷, and the viologen/poly(cyclopentadithiophene) system studied by Lee *et al.*²⁸³ are reported in figure 1.42. Nevertheless, in 2004 Lee *et al.*²⁰⁴ reported the synthesis and elec-

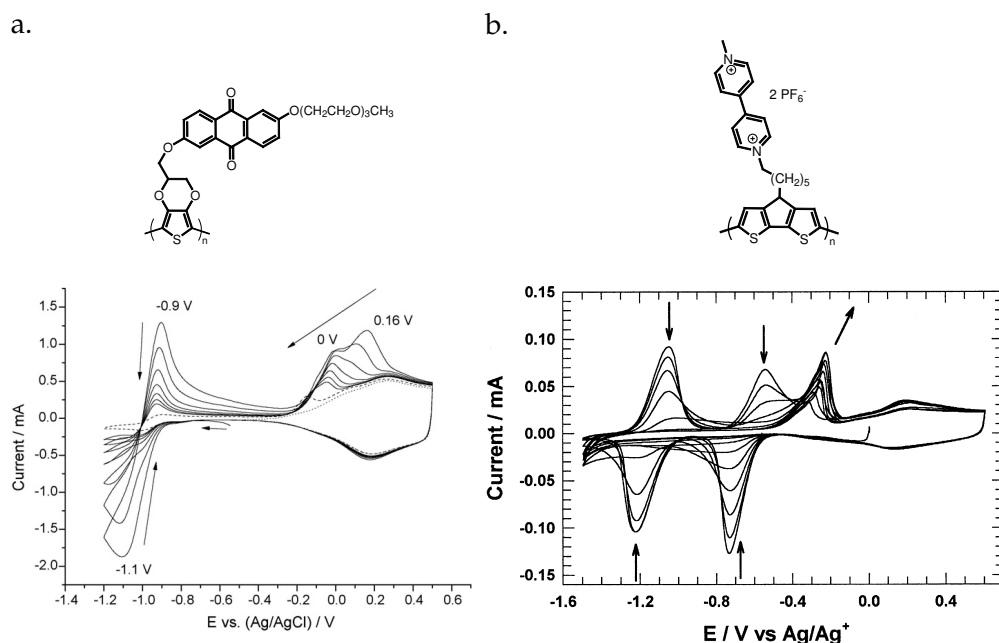


Figure 1.42 (a) CVs of p(AQ-EDOT) in monomer-free solution in 0.1 M Bu_4NPF_6 solution in CH_3CN , scan rate: 50 mV s^{-1} ;²⁸⁷ (b) CVs of P(CPDT- V^{2+} -Me) in a monomer-free 0.1 M Bu_4NPF_6 solution in $\text{CH}_3\text{CN}/\text{CH}_2\text{Cl}_2$ (1:3 by volume), scan rate: 50 mV s^{-1} .²⁸³

trochemical characterization of a stable PEDOT film incorporating a pendant vi-

ologen unit (Fig. 1.43). Interestingly, this system shows a stable electrochemical behaviour, as opposed to the almost identical system published the same year by Czardybon *et al.*²⁸⁸, the only difference between the two being a butyl chain on one of the viologen nitrogen atoms instead of a methyl group. The spectroelectrochromogram of Lee's polymer clearly shows a contrast enhancement and slight modification of the hue of reduced PEDOT to a darker one, as a consequence of the absorption of of $V^{\cdot+}$ species, after half-reduction of the viologen.

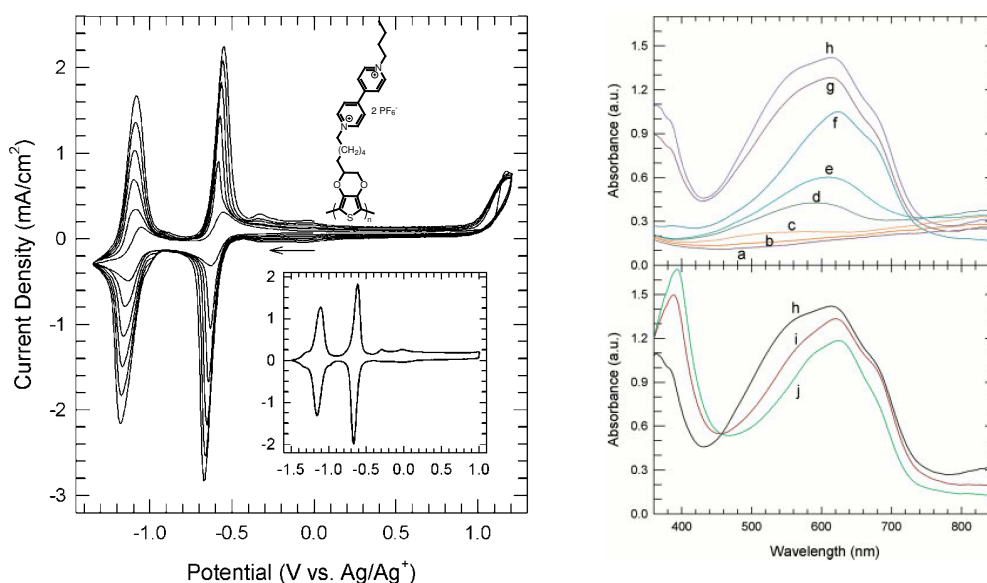


Figure 1.43 Cyclic voltammograms of the electropolymerization of a 2mM EDOT- V^{2+} solution in 0.1M Bu₄NPF₆ in MeCN/CH₂Cl₂ 1:5, scan rate 50mV s⁻¹, inset shows the CV of the obtained polymer in monomer-free solution (0.1M Bu₄NPF₆ in MeCN, 50mV s⁻¹) (left); and spectroelectrochemistry of a p(EDOT- V^{2+}) on ITO/glass at various potentials: a) 0.5, b) 0.2, c) 0.0, d) -0.2, e) -0.4, f) -0.6, g) -0.7, h) -0.8 to -1.0, i) -1.2 and j) -1.4 to -1.6V vs. Ag/Ag⁺ (right).²⁰⁴

Conjugated polymers incorporating arylenebisimides²⁸⁹⁻²⁹³ and TTF²⁹⁴ and tetracyanoanthraquinodimethane²⁹¹ have also been reported. The different approaches to the incorporation of discrete electrochromic systems in conjugated polymers include post-functionalization of polymeric films via click-reaction²⁹⁵ and the use of functionalized polyelectrolytes²⁹⁶. Using this latter approach Palmore *et al.* prepared a PEDOT film doped with poly(3-methyl-2-[3-(4-vinyl-benzyl)--3H-benzothiazol-2-ylidene]-hydrazono-2,3-dihydro-benzothiazole-6-sulfonic) acid showing an interesting multichromic behaviour.

Chapter 2

Two step reversible discrete electrochromes switching from coloured to highly transmissive

2.1 Introduction

Organic electrochromic materials represent a well established alternative to the inorganic ones, currently used in most of the devices. An overview of the different classes have been presented in section 1.4 in the introduction. One of their most intriguing properties is the possibility to tailor the hue of their coloured states trough functionalization. This allows to expand, almost endlessly, the colour palette of the existing electrochromes.

Among the different organic electrochromic systems, conjugated polymers have certainly received much more attention, and most of the research efforts have been focused on the development of new ones. This can be easily explained considering their superior electrochromic performances and extended cycle lives, combined with good processability. Applications like smart windows, rearview mirrors or sunglasses require the material to posses an highly transmissive state and a coloured one with a panchromatic absorption with a resultant neutral hue. Currently available polymeric electrochromes are still far from reaching these targets. The application in sunglasses, for example, would require a final device with transmittance close to 90% in the bleached state and <20% over the

whole spectrum in the coloured one. The best example in literature²⁰ shows a transmittance of the colourless state ranging from 45% to 67% and an uneven absorbing reduced state. This example attests the limitations of this class of compounds. Firstly, it is intrinsically difficult to obtain a colourless state with very high transmissivity as a result of the tailing of the polaron band in the visible region. This effect can be reduced by modification of the monomer and optimization of the parameters involved in the polymerization process.²⁹⁷ Moreover, the use of the donor-acceptor approach to modify the hue of the reduced form is not satisfactory in this respect, and complicates the bleaching process as a consequence of the presence of localized levels on the acceptor. This considerations rise the interest in the development of different types of electrochromic materials. As discussed in the introduction, several other classes exists. Violenes, in particular, possess very good electrochromic properties, and could allow to access a wide spectrum of different colours.

2.2 Concepts of molecular design of violenes

Despite the huge number of different violene type molecules studied, just few of them received some kind of development or device application: viologens, *N,N,N',N'*-tetraphenyl-1,4-phenylenediamine, 2,2'-Azo-3,3'-dialkylbis(benzothiazol-3-ium) and phenothiazine. The first, in particular, have been the most studied, with a huge variety of different functionalizations in order to modulate their solubility and colour, and have found application in solution-based devices. Nevertheless, as already pointed out by Hünig *et al.*²⁴⁰, their coloured state is a radicalic open-shell structure. Structures of this type have the tendency to be more reactive than the corresponding closed-shell ones, and hence more prone to decomposition reactions that reduce the cycle life. On the other side, the neutral direduced form of the viologen has very little absorption in the visible region since its transition is not so intense and centred in the UV region. As a consequence, a new electrochromic system should fulfill the following requirements:

1. switch reversibly between a coloured and a colourless form;
2. both forms should have a closed-shell structure;
3. further functionalizable to allow an easy tuning of the properties;
4. posses chemical and photochemical stability (at least to visible radiation);

5. be easily synthetically accessible, starting from cheap precursors.

The first of these can be easily fulfilled by a large number of violene type compounds. The second one is far more difficult to achieve since most of the violene type structures have a two step redox behavior with a wide stability range of the intermediate radicalic form. This characteristic is usually evaluated from the difference in potential between the two redox waves that characterize this type of systems as follows:²⁹⁸

$$K_{sem} = e^{\frac{(E_2-E_1)F}{RT}} \stackrel{298\text{K}}{=} 10^{\frac{(E_2-E_1)}{0.059\text{V}}} = \frac{[\text{SEM}]^2}{[\text{RED}][\text{OX}]} \quad (2.1)$$

Looking at the large library developed by Hünig *et al.*¹⁷⁸ it is possible to pick few suitable structural types. Interestingly, in their review¹⁷⁷ the authors noted that increasing the number of vinylene groups in violene systems has the effect of reducing the K_{sem} . As an example, while the methyl viologen radical has a reported stability constant of 2.5×10^7 , those of the vinylogous systems have stability constants of: 2.5×10^3 (n=1), 1.3 (n=2) and 4.8×10^{-2} (n=3) (Fig. 2.1).

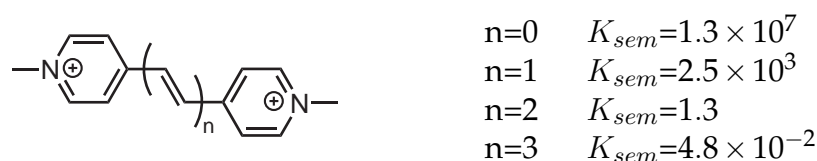


Figure 2.1 Thermodynamic stability constraints K_{sem} of the vinylogous of methyl viologen.¹⁷⁷

This trend has been associated, at least for nitrogen containing violenes, to a variation in the Coulomb repulsion integral, and hence to the separation of positive charges.²⁹⁹ Further reduction in the stability of the radical intermediate have been correlated to the lack of planarity between the terminal heteroaromatic rings. An example of this effect is offered by the huge difference in K_{sem} observed between *N,N'*-dimethyl-4-4'-bipyridyl ($K_{sem}=1.3 \times 10^7$) and *N,N'*-dimethyl-2-2'-bipyridyl ($K_{sem}=20$), which is believed to be a consequence of the twisted conformation adopted by the latter.^{300,301} For the same reason, a shift of the reduction potential to more negative values is also observed in the latter system. Benzocondensation has also proved to have an effect on both potentials and K_{sem} . This can be noted by comparison of the aforementioned bipyridine vinylogous series to the one obtained from quinoline (Fig. 2.2).¹⁷⁷ It can be noted, from the examples, that weitz type violenes systems that exhibit bielectronic transitions between the two forms can be obtained by exten-

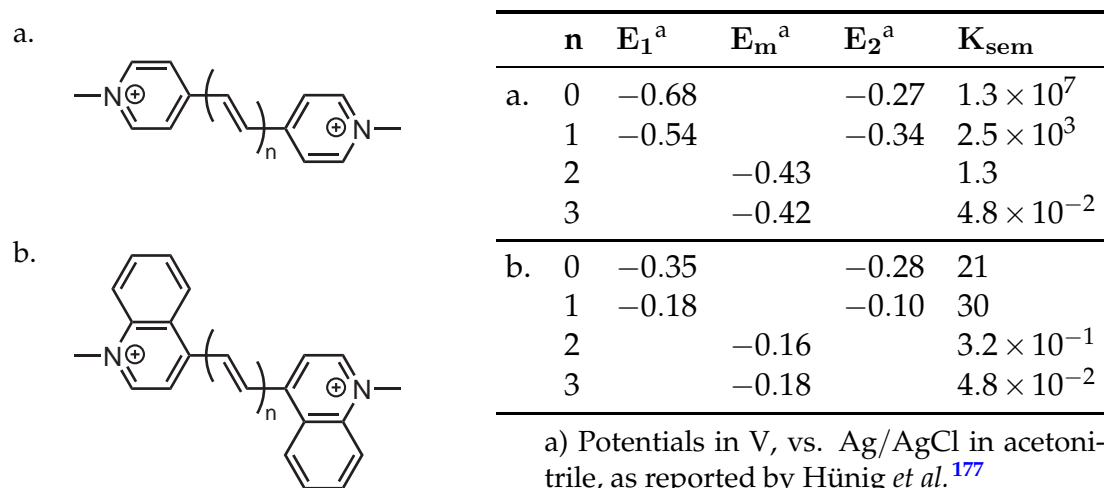


Figure 2.2 Effect of benzocondensation on K_{sem} in the series of vinylologous diazininium compounds on the left.

sion of the viologen structure. Although it has been demonstrated that similar bielectronic behaviour is achievable abandoning the violene structural motif, in favour of the so called "violene-cyanine hybrid", the higher complexity of these systems make their synthesis and further functionalization challenging.^{239,240} The extended viologens are expected to provide a red shifted absorption band in the reduced form as a consequence of extended conjugation. This has been confirmed by Muramatsu *et al.*³⁰² measuring the properties of 1,2-bis(1-methylpyridin-4(1*H*)-ylidene)ethane obtained by chemical reduction with sodium amalgam of (*E*)-4,4'-(ethene-1,2-diyl)bis(1-methylpyridinium) tetrafluoroborate. In light of these considerations, these compounds can be considered good candidates for electrochromic applications, and certainly deserve further development.

In this contribution, the synthesis of a library of different diazium ethenes is described, along with the characterization of their electrochemical and spectroelectrochemical properties. In particular, the effect of:

- nature of the end groups (heteroaromatic azines);
- connectivity between the end groups;
- presence of substituents;

are detailed. These observations are exploited to develop the optimal strategy to achieve colour modulation in this class of compounds. It is demonstrated how colour modulation can be achieved by simple synthetic modifications of

the general structure. Moreover, our approach uses versatile synthetic protocols that make use of cheap starting materials, and can be easily upscaled to multigram quantities.

2.3 Novel electrochromes based on heteroaromatic diazinium ethenes

As outlined in section 2.2, azinium ethenes possess a series of favourable electrochemical properties, and it is worth to expand the library of known compounds in order to understand the structure-properties relationships that affect them. At first, a more rough investigation was accomplished, switching in a second time to a more systematic approach directed to a fine tune of the electrochromic properties.

In the section 2.2 we mentioned that, in the series of diazinium ethenes developed by Hünig *et al.*, an effect related to benzocondensation emerges, resulting in a shift of the reduction potentials to less negative values. This can be attributed to the strongly π -acceptor capabilities of quinoline ring with respect to pyridine (lower LUMO and lower HOMO) and to the aromatic stabilization of the reduced form. It has to be considered, in fact, that an aromatic to quinoid transition takes place upon reduction to the fully reduced form. Benzocondensation allows to retain a certain grade of aromatic stabilization, as illustrated in picture 2.3, according to the fact that one of the two rings in the terminal group gains full benzenoid aromaticity upon reduction. In

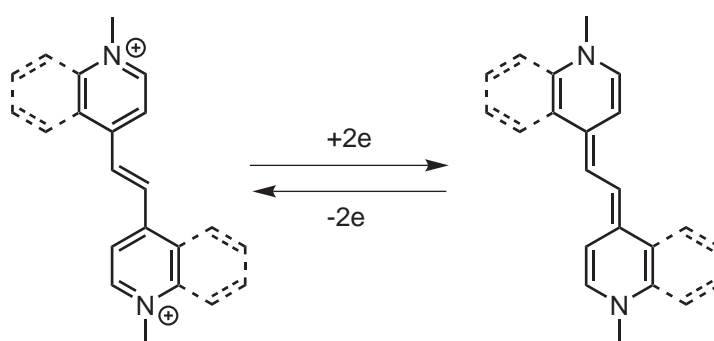


Figure 2.3 Stabilizing effect of benzocondensation on the reduced form of diazinium ethenes.

order to investigate this effect, we extended further the benzocondensation and prepared 1,2-bis(10-methylacridin-9(10*H*)-ylidene)ethane ($\mathbf{1}^{\text{red}}$), representing the reduced form of (*E*)-9,9'-(ethene-1,2-diyl)bis(10-methylacridinium) di-

cation. This novel compound, isolated in its stable reduced form, have already proved to be applicable as a donor for modification of the work function of metal surfaces in a recent publication by our group.³⁰³ It has to be noted that, in this case, a clear-cut classification of the system in the Weitz or Wurster types cannot be made since most of the aromaticity is retained upon switching (see section 1.4.2.1). We also prepared compound **2** in order to have a reference to evaluate the performances and stabilities of our molecules. This molecule represent just a little modification of the known (*E*)-4,4'-(ethene-1,2-diyl)-bis(1-methylpyridinium) dication. The longer alkyl chain on one of the two nitrogen atoms is intended to enhance the solubility of this derivative, extending the range of possible applications in comparison to the parent compound. In addition, the asymmetric substitution on the terminal nitrogen atoms can improve the write erase efficiency of the system³⁰⁴, and illustrates the possibility of monofunctionalization attained.

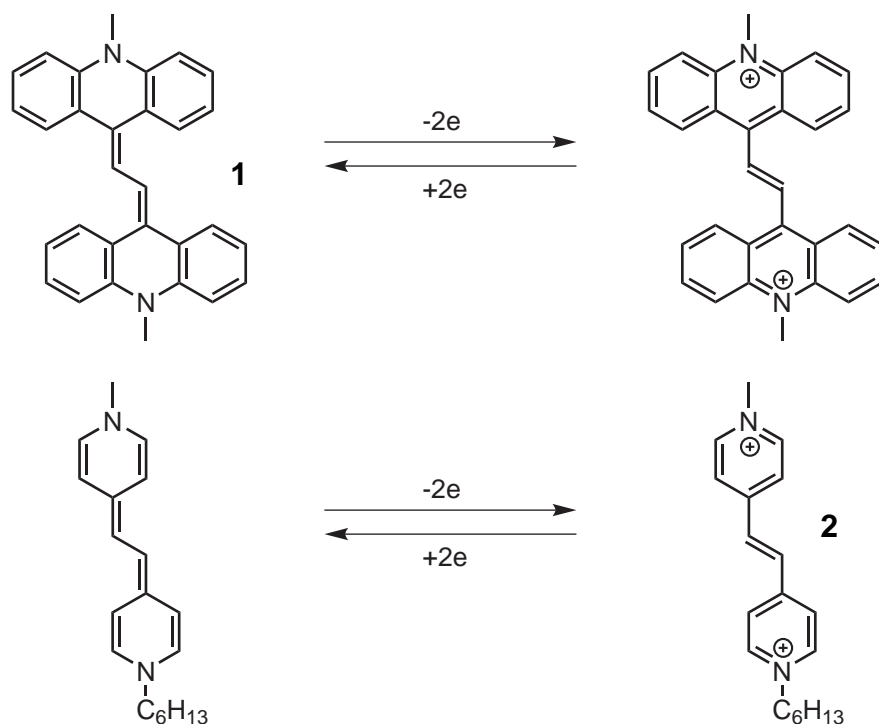
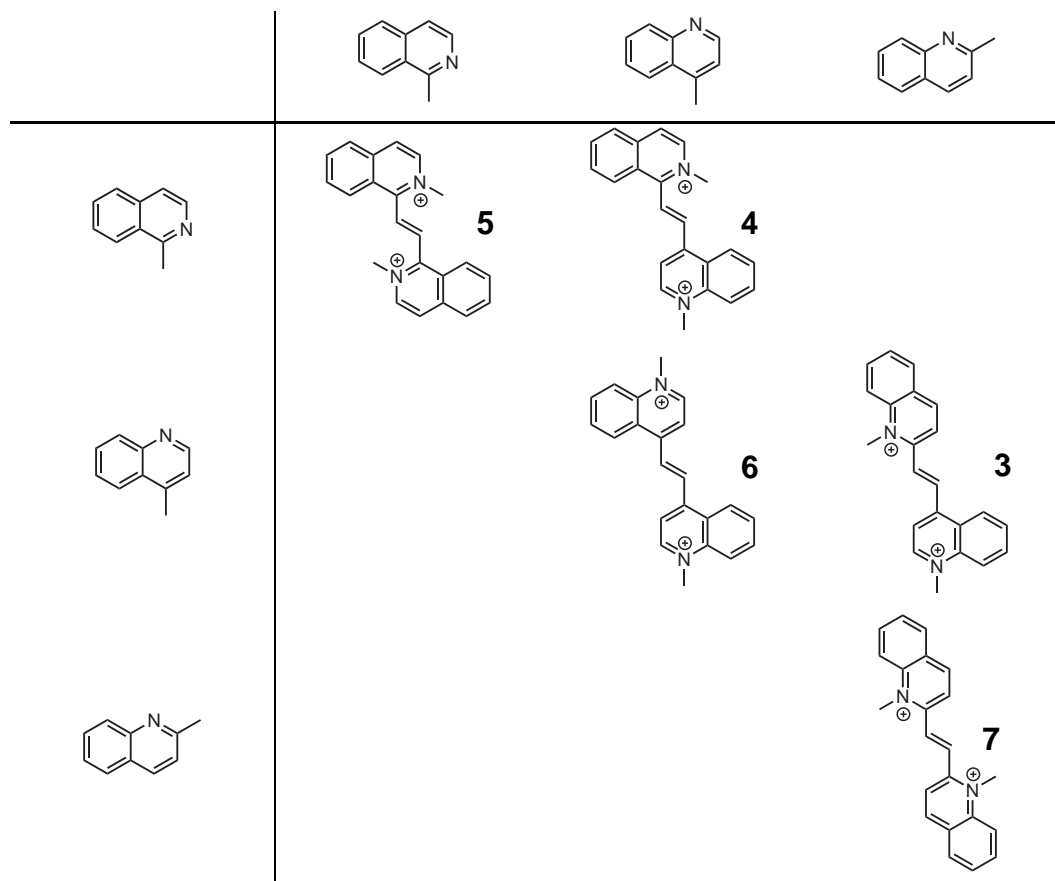


Figure 2.4 Redox equilibria in compound **2** and its benzocondensed analogous **1**.

The other class of compounds is represented by 1,2-diazinium-ethenes with quinolinium end groups. This class of compounds was extended to comprise isoquinolinium end groups and most of the possible combinations of these structural units. In particular, all the non-symmetrical isomers of this class were unknown in literature (**3**, **4**) along with the symmetric derivative **5** (ta-

ble 2.1). In this way we tested the effect of the different connection patterns on the reduction potentials and on the stability of the intermediate radical cationic state. Most of these compounds can be obtained with different substituents on

Table 2.1 Quinolinium and isoquinolinium substituted ethenes studied in this work.



the nitrogen atoms. This allows both to enhance solubility and to attain monofunctionalization. This latter possibility is very important in view of further development of these electrochromic compounds. An example of monofunctionalization will be described in chapter 3.

Among these compounds, derivative 4 was selected as the most promising for our purposes as a consequence of its good electrochromic properties and easy synthetic access. The effect of the presence of different substituents on the electrochemical and spectroelectrochemical properties of this compound were tested with the aim of developing the optimal strategy to tune the colour of its reduced state. For this purpose, derivatives 8, 9, 10 and 11 were prepared. In order to maximise the effect of substitution, the halogen groups in derivatives 8, 9 and 10 were placed in the *p*-position with respect to the position of

the ethylene bridge. The choice of the tetrahydroacridine end group to explore the effect of alkyl donating groups, in compound **11**, was dictated by synthetic convenience. On substitution with electron withdrawing groups, a little shift of

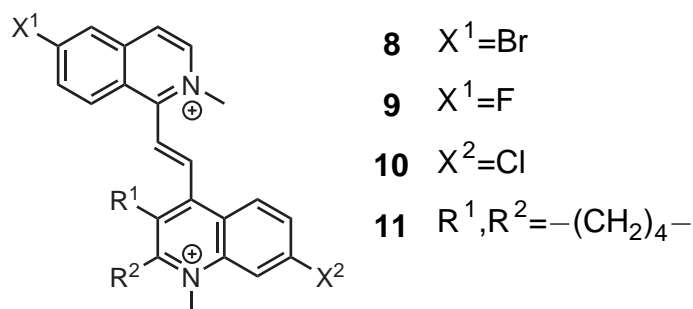
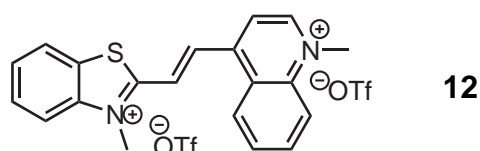


Figure 2.5 Substituted derivatives of compound 4.

the redox wave to higher potential values is expected. On the other hand, the effect on the electrochromic properties is difficult to predict *a priori*, justifying such an empirical approach.

Despite the huge number of Weitz type violene systems studied by Hünig *et al.*, for some reason, they always limited their investigation to symmetric systems, even in those cases where asymmetric derivatives were synthetically accessible. In this respect our study clearly prove the possibility to mix different heterocycles with similar redox potentials. In order to offer a further example in this direction, we prepared the asymmetric compound **12**, formally derived by substitution of one quinolinium moiety with a benzothiazolium one.

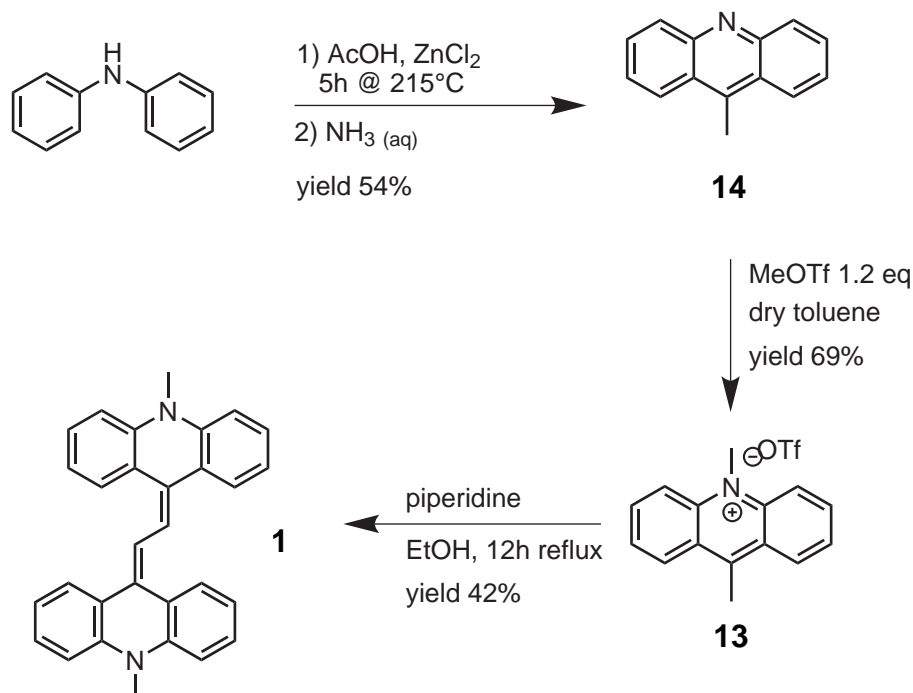


2.3.1 Synthesis of the electrochromes

2.3.1.1 1,2-bis(10-methylacridin-9(10H)-ylidene)ethane

The synthetic protocol for the synthesis of the acridinyl based derivative **1** is illustrated in scheme 2.1. The last synthetic step involves the dimerization of the 9,10-dimethylacridinium salt **13** in refluxing ethanol in presence of piperidine as a base. This peculiar synthesis was discovered by chance in our laboratory trying to condense the 9,10-dimethylacridinium salt **13** with an aldehyde under base catalysis. The mechanism of the reaction is still under investigation

and the reported yield is based on the assumption of a simple 2:1 stoichiometry. Intermediate **14** was prepared using Bernthsen reaction³⁰⁵ by modification



Scheme 2.1 Synthetic scheme for the preparation of derivative **1**

of a literature synthetic protocol³⁰⁶. In particular, the chromatographic purification step was replaced by multiple crystallization from EtOH/H₂O mixture obtaining pure **14** as yellow needles. Subsequent *N*-alkylation with methyl trifluoromethanesulfonate in dry toluene yielded **13**. The moderate yield of this step, can be attributed to the low nucleophilicity of the acridine nitrogen.

2.3.1.2 Quinolinium/isoquinolinium substituted ethenes

Synthesis via base catalysed condensation We developed different synthetic strategies for the synthesis of this class of compounds, as a consequence of their different reactivities and the availability of the starting materials. Most of them can be obtained following scheme **2.2**. This synthetic strategy involves the condensation of the quinolinium or isoquinolinium methyl iodide with the proper aldehyde in MeOH, using piperidine as a catalyst, to yield a monoalkylated intermediate. The solubility of the product has proved to play an important role in determining the yield of this step. Early attempts with quinolinium and isoquinolinium triflates, instead of iodides, were unsuccessful. We believe this to be a consequence of the higher solubility of the triflate derivatives. Prolonged

heating was found to produce a complex mixture of decomposition products, hampering the isolation of the desired ones.

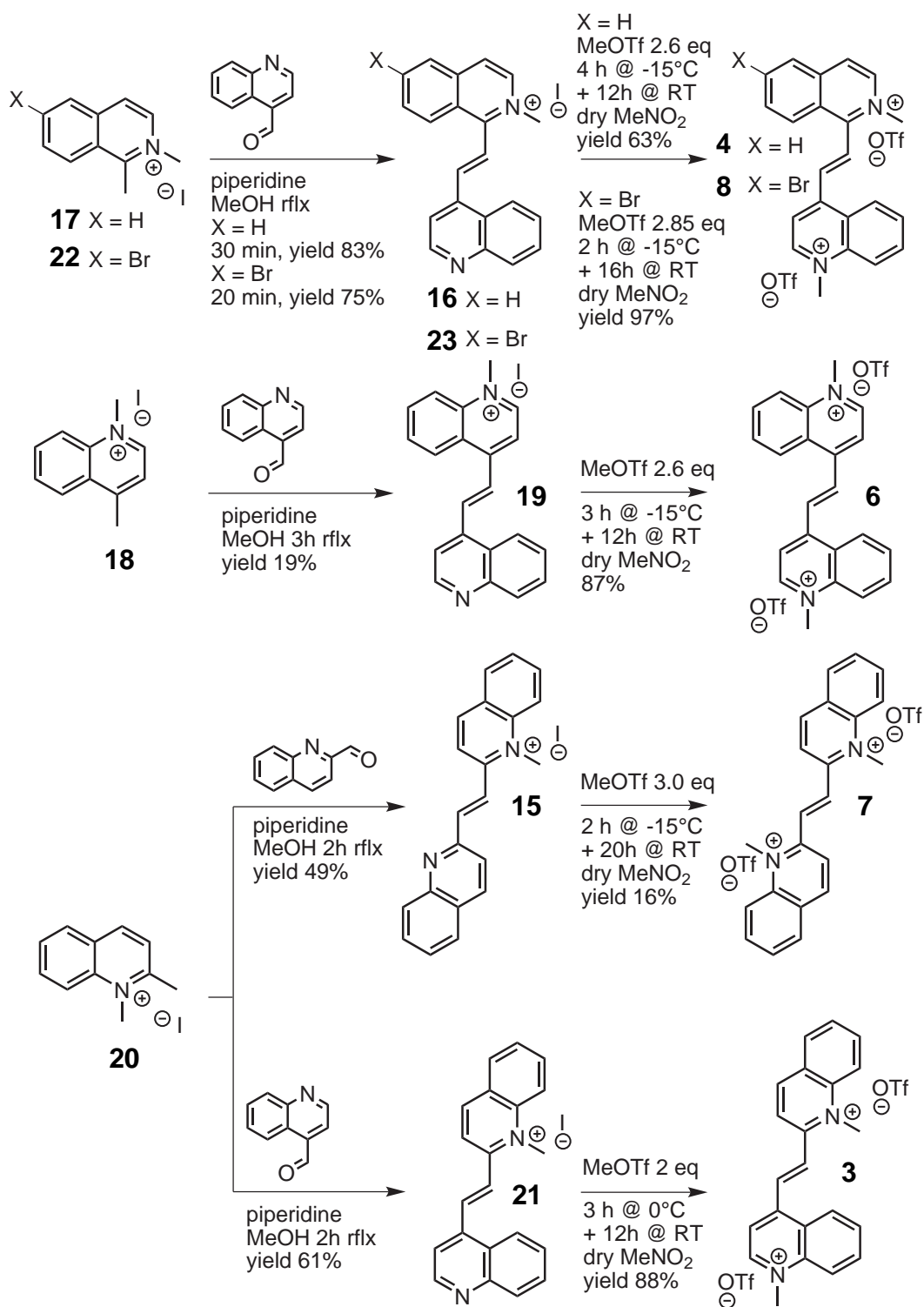
The alkylation of the second nitrogen atom was then performed with an excess of the strong alkylating agent MeOTf in cold dry MeNO₂. More than twofold excess of MeOTf is required in this second step, since a Finkelstein³⁰⁷ type reaction take place between the nucleophilic counterion (iodide) and MeOTf. This last alkylation step has proved to be more problematic for **15**, as consequence of the lower reactivity of the hindered quinoline nitrogen. A similar effect has been observed in the alkylation of the isomer of **16** carrying the methyl group on the other nitrogen atom*.

The starting quinolinium and isoquinolinium methyl iodides were prepared by reaction of 2- and 4-methyl quinolines and 1-methyl isoquinoline with methyl iodide. In order to overcome their low reactivity, these reaction were performed either without solvent or in a very concentrated acetone solution (~1 M) at 95 °C under pressure in a microwave reaction apparatus. Thanks to this technique short reaction times (<10 min) and high yields have been achieved.

Although commercially available, 1-methyl-isoquinoline (**26**) was prepared following two distinct literature procedures: Bischler-Napieralski³⁰⁸ reaction, starting from β -phenethylamine, and the Schittler-Müller³⁰⁹ modification of the Pomeranz-Fritsch^{310,311} reaction, starting from α -phenethylamine (scheme 2.3). The former involves a dehydrogenation of the intermediate 1-methyl-3,4-dihydroisoquinoline (**25**). This leads to the formation of a small quantity of 1-methyl-5,6,7,8-tetrahydroisoquinoline as subproduct. As a consequence, the latter proved to be superior for our scope since a purer product can be obtained without any complex purification step. In order to overcome the lower reactivity of the bromine substituted aldimine in the electrophilic cyclization step leading to 6-bromo-1-methylisoquinoline (**28**), a modified procedure³¹², using P₂O₅/H₂SO₄ as a solvent instead of H₂SO₄ alone, was adopted. Using this latter reaction conditions satisfactory yields of the desired product were obtained.

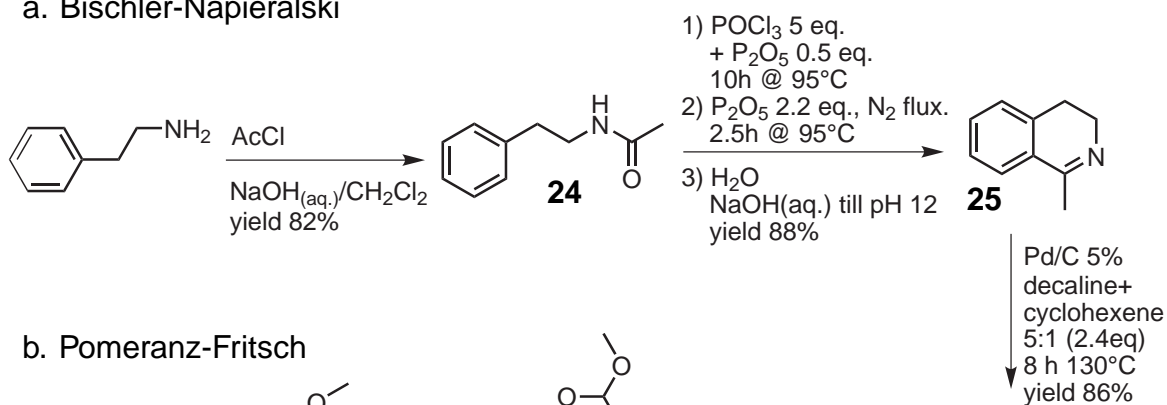
The benzothiazolium/quinolinium substituted ethene **12** was prepared following a base catalysed condensation under similar conditions to those illustrated. The synthetic approach involves the condensation of 2,3-dimethylbenzothiazolium iodide (**30**) with quinoline-4-carbaldehyde under basic catalysis to produce a monoalkylated derivative **31** that is subsequently alkylated on the quinoline nitrogen with an excess of methyl trifluoromethanesulfonate in nitromethane obtaining **12** (scheme 2.4). Nevertheless, in this case the piperi-

*the synthesis of this compound has not been reported

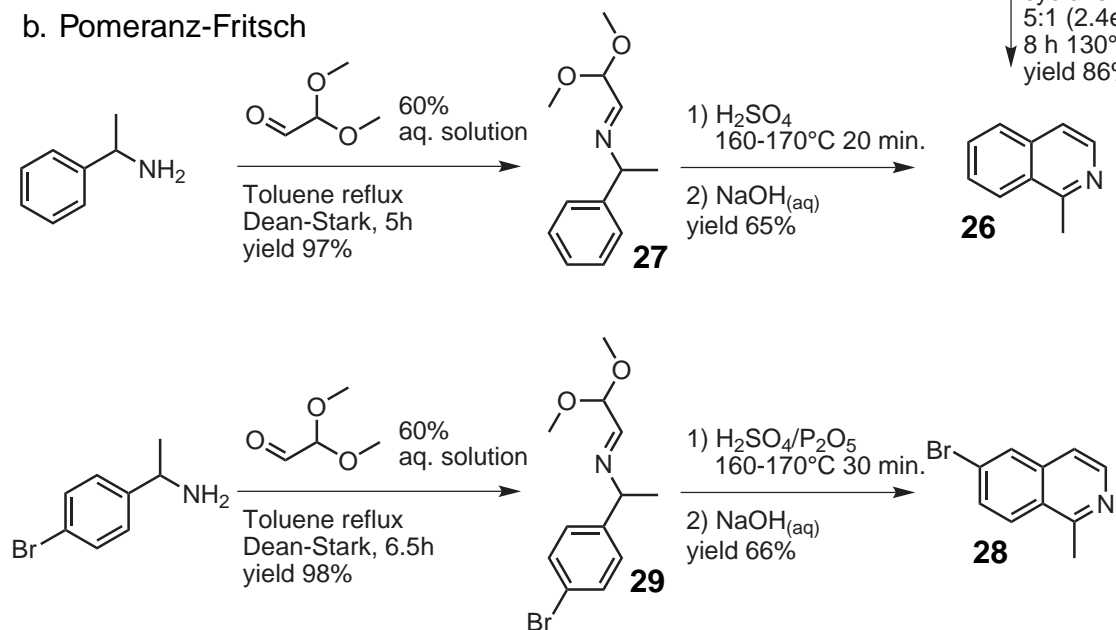


Scheme 2.2

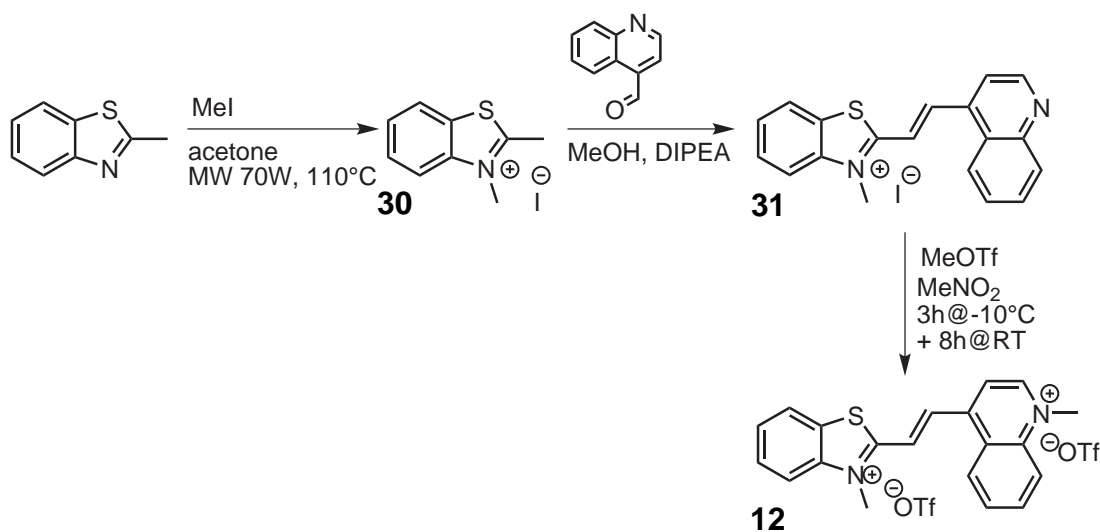
a. Bischler-Napieralski



b. Pomeranz-Fritsch



Scheme 2.3



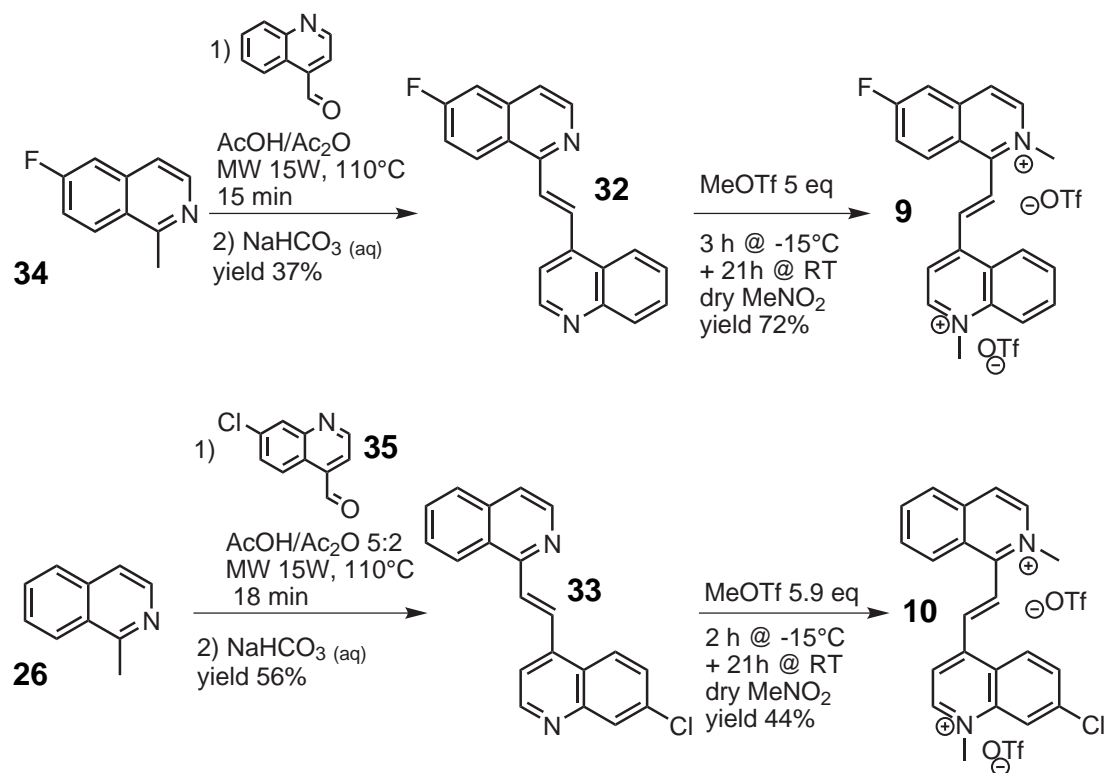
Scheme 2.4

dine catalysed condensation proved to be unsatisfactory, leading to a complex mixture of products. Using *N,N*-diisopropylethylamine (DIPEA), as a non-nucleophilic base, the desired product was isolated, although in low yield.

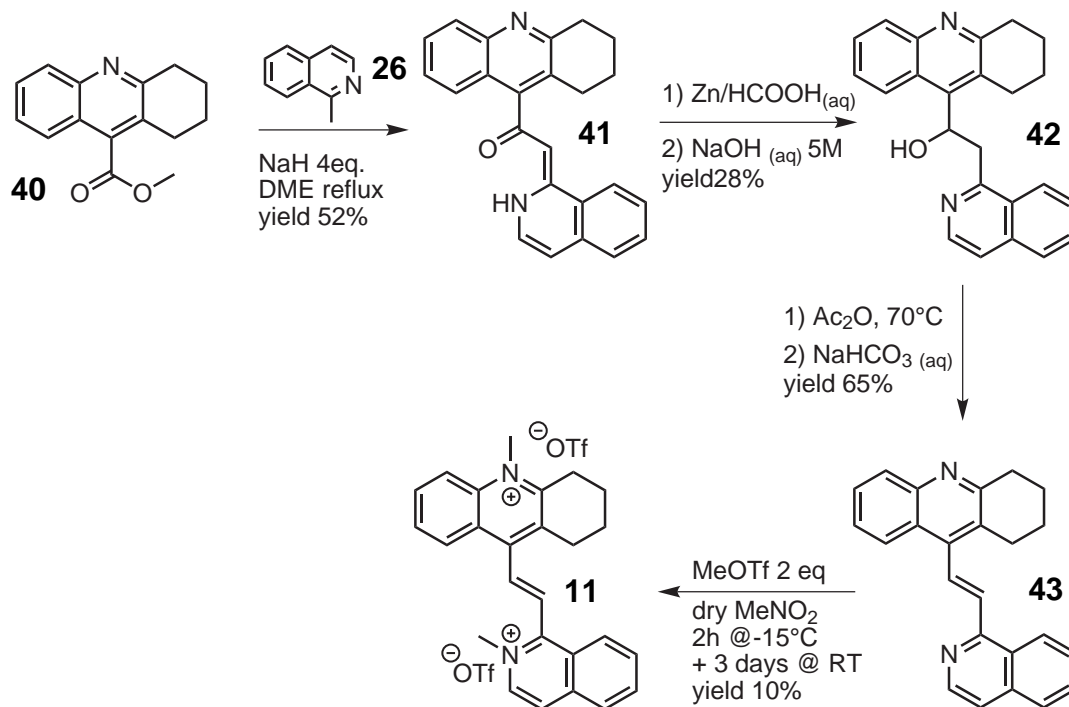
Synthesis via acid catalyzed condensation A different reaction sequence (scheme 2.5) was adopted for the preparation of the chlorine functionalized derivative **10** and the fluorine functionalized one **9**. In the former case the choice was motivated by an higher overall yield, while in the latter the base catalyzed condensation was proved not to be applicable. In fact, the fluorine atom in 1,2-dimethyl-6-fluoroisoquinolinium iodide is easily displaced upon treatment with piperidine or other bases of comparable nucleophilicity. Attempts with non-nucleophilic bases such as *N,N*-diisopropylethylamine also failed. The alternative reaction sequence involves the acid catalyzed condensation between 1-methylisoquinoline (**26**) and the proper 4-quinoline carboxyaldehyde in a mixture of acetic anhydride and acetic acid under microwave irradiation.^{313,314} The product of this reaction is isolated as an adduct with acetic acid, which is subsequently removed by treatment with aqueous NaHCO₃. The obtained compounds (**32** and **33**) were then doubly alkylated with MeOTf in conditions analogous to those described for the monoalkylated derivatives. The 7-chloroquinoline-4-carbaldehyde (**35**) was prepared, starting from the cheap 4,7-dichloroquinoline, following a literature procedure³¹⁵ to obtain the 7-chloro-4-iodoquinoline (**36**), that was subsequently converted in **35** with a Bouveault aldehyde synthesis³¹⁶. The 6-fluoro-1-methylisoquinoline was obtained from the commercially available 1-(4-fluorophenyl)ethanamine (**37**), following the already mentioned Schittler-Müller modified Pomeranz-Fritsch reaction, and isolated from the reaction mixture by steam distillation.

Synthesis via enaminones As a consequence of the initial difficulties we encountered in the synthesis of 1,2,3,4-tetrahydroacridine-9-carbaldehyde (**38**), and the very low yield of the basic catalyzed condensation between compound **17** and isoquinoline-1-carboxyaldehyde (prepared by reduction of the corresponding ester (**39**) with DIBAL-H), we adopted a different synthetic protocol for the synthesis of compounds **11** (scheme 2.6) and **5** (scheme 2.7).

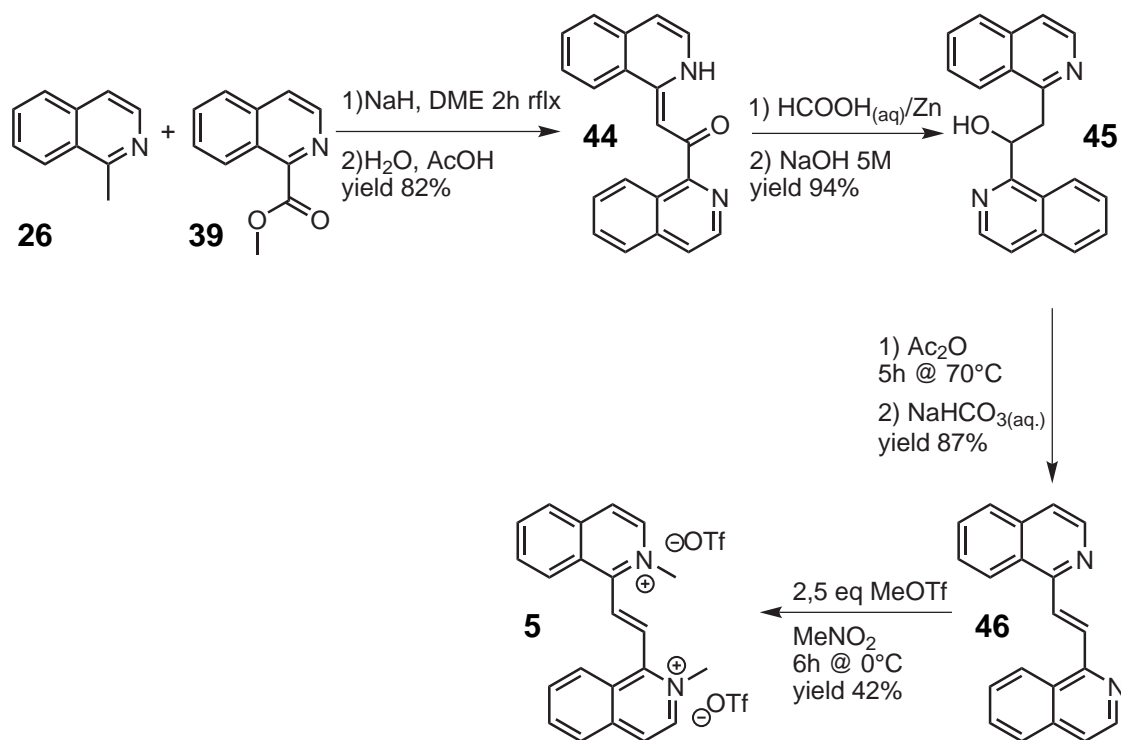
In these reaction schemes the methyl 1,2,3,4-tetrahydroacridine-9-carboxylate (**40**), or methyl 1-isoquinoline carboxylate (**39**) were reacted with isoquinoline in dimethoxyethane, under inert atmosphere and using NaH as a base, obtaining the desired condensation products as their enaminone tautomers (**41**



Scheme 2.5



Scheme 2.6

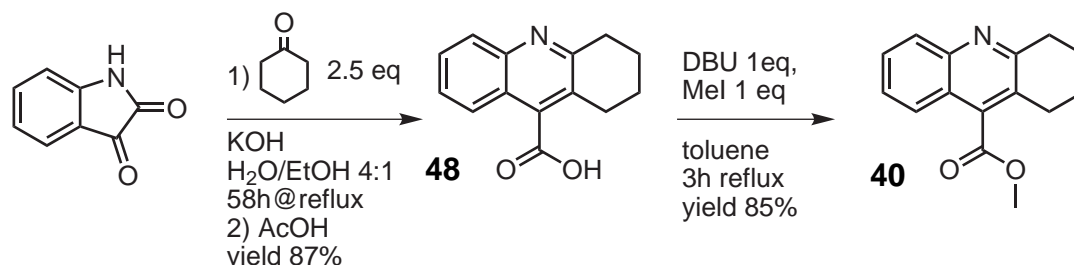


Scheme 2.7

and **44**). These intermediates were then reduced with zinc dust in aqueous formic acid to the aldols **42** and **45**. A subsequent dehydration step with acetic anhydride at 70°C yields the desired ethenes (**43** and **46**). A higher reaction temperature in this last step was found to promote the retro-aldol reaction. A similar behaviour has been reported for 2-, and 4-(2-Hydroxy-2-arylethyl)pyridines.³¹⁷ To the best of our knowledge, the first part of this sequence was first developed by Andrews *et al.*³¹³ for the synthesis of 1,2-di-2'-quinolyl-ethanol, 1-4'-quinolyl-2-2'-quinolyl-ethanol and 1-2'-quinolyl-2-1'-isoquinolyl-ethanol. The authors erroneously reported the structure of the condensation products in their ketonic tautomeric form. The assignment was made following literature NMR data.³¹⁸ The freebases **43** and **46** were subsequently alkylated with MeOTf in MeNO_2 similarly to **32** and **33** described in section 2.3.1.2. The low yield observed in the alkylation of **46** can be attributed to steric hindrance around the nitrogen atom.

The two esters **39** and **40**, used as starting material, were prepared from the corresponding acids **47** and **48**. The isoquinoline ester can be prepared by classic acid catalyzed esterification with MeOH, either at reflux temperature or under pressure (faster). Nevertheless, the esterification of acid **48** does not proceed under these conditions, but can be carried out smoothly by nucleophilic es-

terification. Both DBU/MeI and DBU/dimethylcarbonate proved to be useful in this respect. The 1,2,3,4-tetrahydroacridine-9-carboxylic acid (**48**) was prepared by Pfitzinger reaction^{319,320} between isatin and cyclohexanone (scheme 2.8), while **47** is commercially available.



Scheme 2.8

2.3.2 Electrochemical and Spectroelectrochemical Properties

The properties of the new violene type redox systems were tested through electrochemical measurements. In particular, cyclic voltammetry (CV) experiments were conducted in order to identify the half wave potentials of the redox processes involved. For most of the compounds spectroelectrochemical measurements in solution were also performed, hence fully characterizing the electrochromism of these systems.

2.3.2.1 (E)-1-hexyl-4-(2-(1-methylpyridinium-4-yl)vinyl)pyridinium iodide trifluoromethanesulfonate

As explained in section 2.3, compound **2** was prepared and characterized in order to have a reference for the further development of diazinium substituted ethenes. Its cyclic voltammogram, depicted in figure 2.6, displays two mono-electronic redox waves at -840mV and -1047mV vs. Fc/Fc^+ with peak separations of 59mV and 69mV respectively. These data demonstrate the presence of a rather stable radical cation intermediate for this compound, and a stability constant (K_{sem}) of 3.2×10^3 can be calculated.

2.3.2.2 1,2-bis(10-methylacridin-9(10H)-ylidene)ethane

The cyclic voltammograms of **1** (Fig. 2.7) display a single reversible redox wave corresponding to the oxidation at both acridine end groups. The higher current density obtained with the glassy carbon (GC) disc compared to the gold

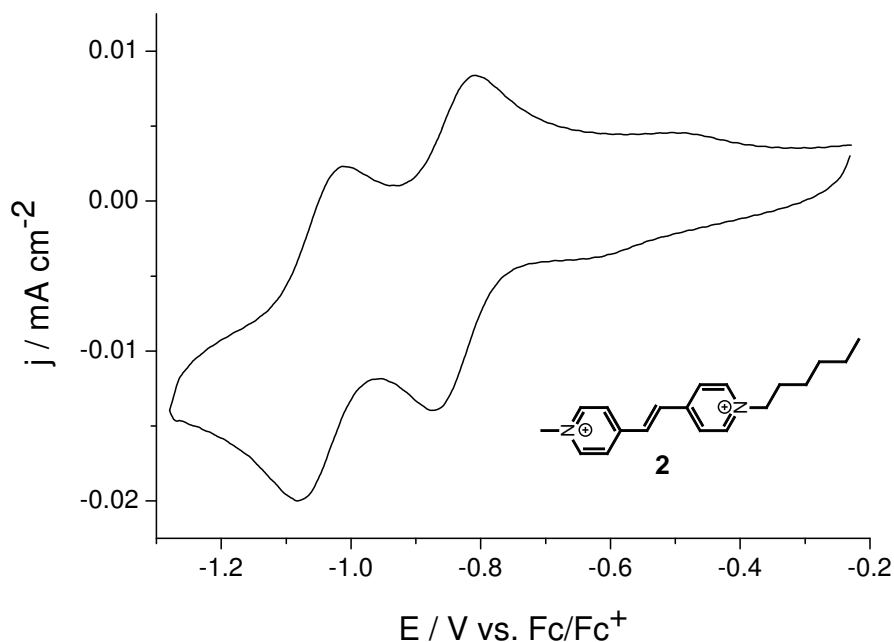


Figure 2.6 Cyclic voltammograms of a 10^{-4}M solution of **2** in 0.1M $\text{LiClO}_4/\text{MeCN}$ (scan rate 50mV s^{-1}) on gold pin electrode. Reference electrode: Ag/AgCl wire calibrated with 0.1mM Fc solution in the electrolyte.

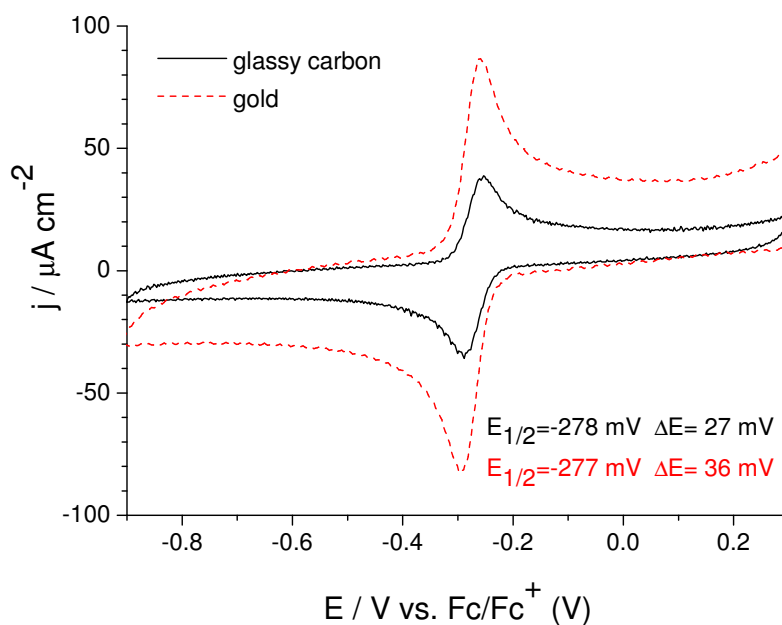


Figure 2.7 Cyclic voltammograms of a 10^{-4}M solution of **1** in 0.1M $\text{Bu}_4\text{NPF}_6/\text{MeCN}$ (scan rate 100mV s^{-1}) on gold pin (red dashed line) and glassy carbon (black solid line) electrodes.

disc is most probably due to the higher molecular coverage on the gold electrode surface. In fact, the difference in potential between the oxidation and reduction peaks is about 30 mV, proving the simultaneous bi-electronic character of the electrochemical reaction. The oxidation potentials, referred to the ferrocene (Fc/Fc⁺) redox couple, are the same for the two electrode materials (*i.e.* -0.28 V). When reported versus the absolute vacuum scale³²¹ the corresponding highest occupied molecular level of **1** is at -4.9 eV. Figure 2.8 shows the *in situ* spectroelectrogram of a 10⁻⁴ M solution of **1** on stepwise oxidation. The first absorption maximum of **1**, centred at 471 nm ($\epsilon=30700 \text{ L mol}^{-1} \text{ cm}^{-1}$), is shifted to 448 nm upon oxidation and a second absorption maximum appears at 363 nm. This electrochromic behavior couples with the red to yellow transition of a solution of **1**, observed upon chemical oxidation of a CH₂Cl₂ solution with SbCl₅. Since the absorption of this derivative in the 400-550 nm range is

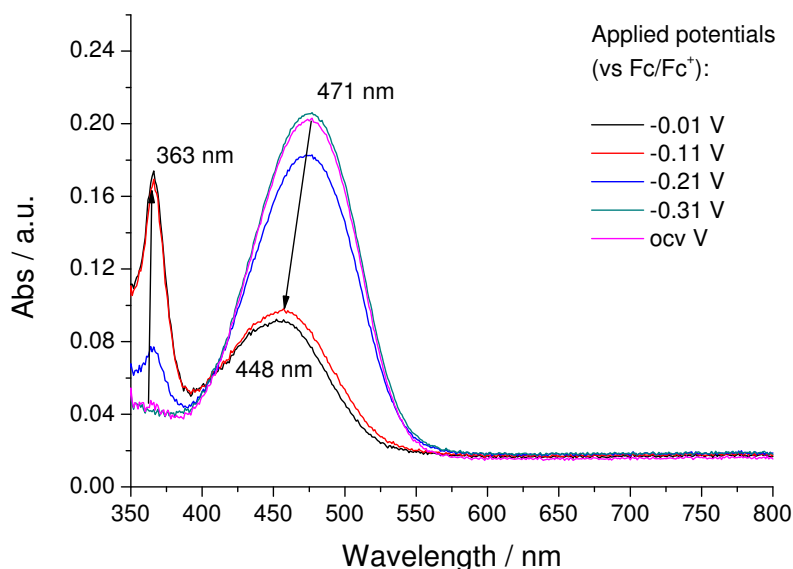


Figure 2.8 Spectroelectrogram of a 10⁻³ M solution of **1** in 0.1 M Bu₄NPF₆/MeCN on stepwise oxidation.

not completely bleached upon oxidation, its possible application to ECDs is quite limited. Nevertheless, its completely reversible two-electron redox process located at easily accessible potentials place this molecules among the most interesting redox active organic molecules. The instability of the radical cationic intermediate, when compared to the fully oxidized and fully reduced forms, is likely to be a consequence of the lack of planarity between the two acridine rings, that prevents an efficient delocalization to exist in the intermediate form.

The oxidized form 1_{ox}^{2+} have been isolated by chemical oxidation with $Fe(OTs)_3$ confirming its structure by NMR analysis.

2.3.2.3 Quinolinium/isoquinolinium substituted ethenes

The electrochemical properties of this class of compounds were also tested by cyclic voltammetry measurements. The obtained voltammograms are depicted in figure 2.9. It can be noted that all systems exhibit reversible redox processes centred around $-0.7V$ vs. Fc/Fc^+ . In particular, the presence of two separate redox waves is evident in compound 3 and 7 with a separation of $\sim 100mV$. A similar behaviour is likely to exist in 6, although the two processes cannot be clearly resolved from the voltammogram. On the contrary, a highly reversible two-electron transfer process is involved in 5 as testified by the low peak separation observed ($\Delta E=38mV$) in the sharply peaked redox wave. Similar behavior is observed in the asymmetric compound 4. In this case, the measured peak separation is somewhat larger ($\Delta E=62mV$) but another measure (not shown) with a different electrolyte ($0.1M Bu_4NClO_4/MeCN$) provided a value of $40mV$, thus confirming the involvement of a two-electron transfer process. Peak data for all derivatives is summarized in table 2.9f.

These two latter compounds (4, 5), along with compound 7 were further characterized by *in situ* spectroelectrochemical measurements using a $10^{-4}M$ solution of the compounds in a thin layer cell (Fig. 2.10). In the case of compound 4, a lowering of the UV centred ($\simeq 350nm$) absorption band of the oxidized form and the appearance of a strong absorption band, centred at $493nm$, are observed upon reduction. A weak absorption centred at $603nm$ is also present at intermediate potentials, but is subsequently bleached, although not completely, on further reduction. A similar behavior is observed with compound 5. In this case, the absorption band of the reduced form is shifted to lower wavelengths ($456nm$), and an almost complete bleaching of the weak band centred at $593nm$ take place. The spectra of the oxidized forms are recovered upon reoxidation, by switching back to the initial potentials, although not completely. As can be noted from the spectroelectrogram of compound 4, a broad weak absorption from 400 to $700nm$ can be detected in the visible region, along with an incomplete recovery of the UV centred band. A similar phenomenon is observed in the spectroelectrogram of compound 7. However, in this case, it is far more evident since no variations of the spectrum can be observed after switching back to oxidative potentials. Moreover, the typical absorption band of the reduced form of this class of derivatives, can hardly be

2.3 - Novel electrochromes based on heteroaromatic diazinium ethenes

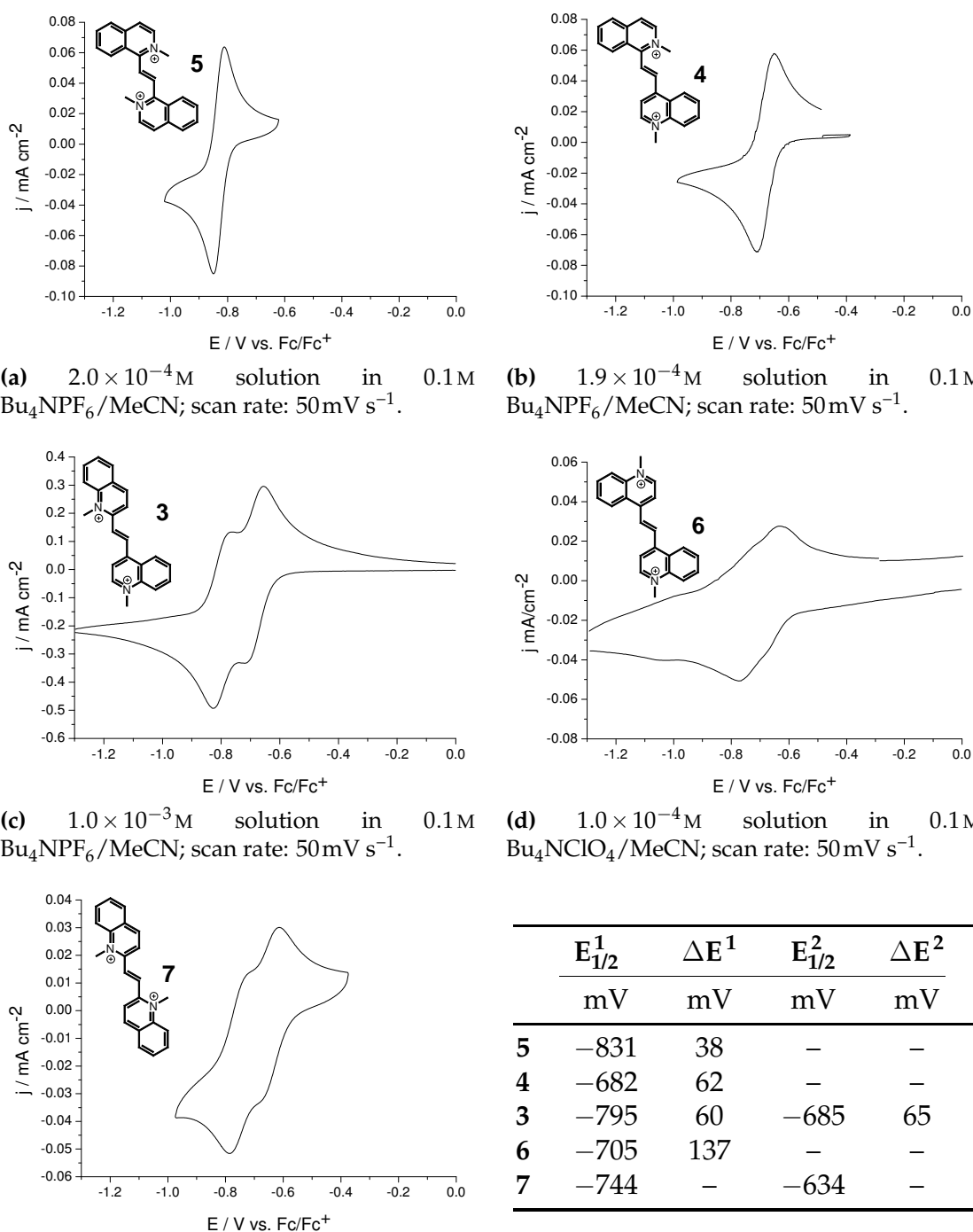
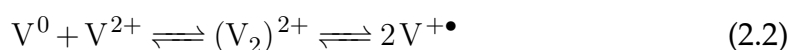


Figure 2.9 Cyclic voltammograms of quinolinium/isoquinolinium ethenes. Table (f) summarise peak data. Peak potentials for 7 are obtained from a DPV measure (scan rate 10 mV s^{-1}).

recognized at ~ 465 nm in the spectrum recorded at an intermediate potential. A reason for this kind of behaviour cannot be clearly identified. Nevertheless, a possible explanation can be the formation of stable intermolecular aggregates or dimers. A similar phenomenon has been observed for viologens during studies directed to solve ageing problems of ECDs comprising them as electrochromic materials.¹ The possible causes have been related to the deposition of radical-cation salt on the electrode surface, containing spin-paired radical-cation dimers with sandwich type structure, and their reorientation into a ordered phase during open-circuit periods.^{322,323} Further investigation on deposited heptyl viologens radicals ($HV^{+\bullet}$), revealed the presence of a contribution from dimerization of radical cations in solution.³²⁴ A second mechanism for dimer formation can involve a comproportionation reaction between the neutral viologen and the oxidized form (Eq. 2.2).^{325,326}



The dimer has diminished electroactivity, as a consequence of its very slow oxidation rate,³²⁷ and a lowering of the write-erase efficiency of the system is thus observed.³²⁸ It has been demonstrated that the use of redox-mediators can have beneficial effects,¹⁹⁴ as the functionalization of the nitrogen atoms or the bipyridine core.^{304,329,330}

In our case, we suppose that a similar aggregation or dimerization process can take place in solution during spectroelectrochemical measures, resulting in loss of electroactivity and deviation of the observed spectrum from the one expected from the reduced form. The symmetric structure and the higher stability of the intermediate radical cation in **7** can both have a contribution in making this effect more evident in this derivative.

In view of its good electrochemical and spectroelectrochemical behavior, **4** was selected for further derivatization with different substituents. Compound **5** was not further developed, despite its good properties, as a consequence of its more difficult and less versatile synthetic access. Derivatives of **4** carrying halogen substituents on the 6-position of the isoquinoline ring (F (**9**), Br (**8**)) or on the 7-position of the quinoline ring (Cl (**10**)) and one with a tetramethylene tether connecting the 2- and 3- positions of quinoline ring (**11**) were prepared (see section 2.3.1.2). The cyclic voltammograms of these derivatives are depicted in figure 2.11. All the derivatives show a two-electron reversible electron transfer process around -0.75 V vs. Fc/Fc^+ , with low peak separation (~ 40 mV). The

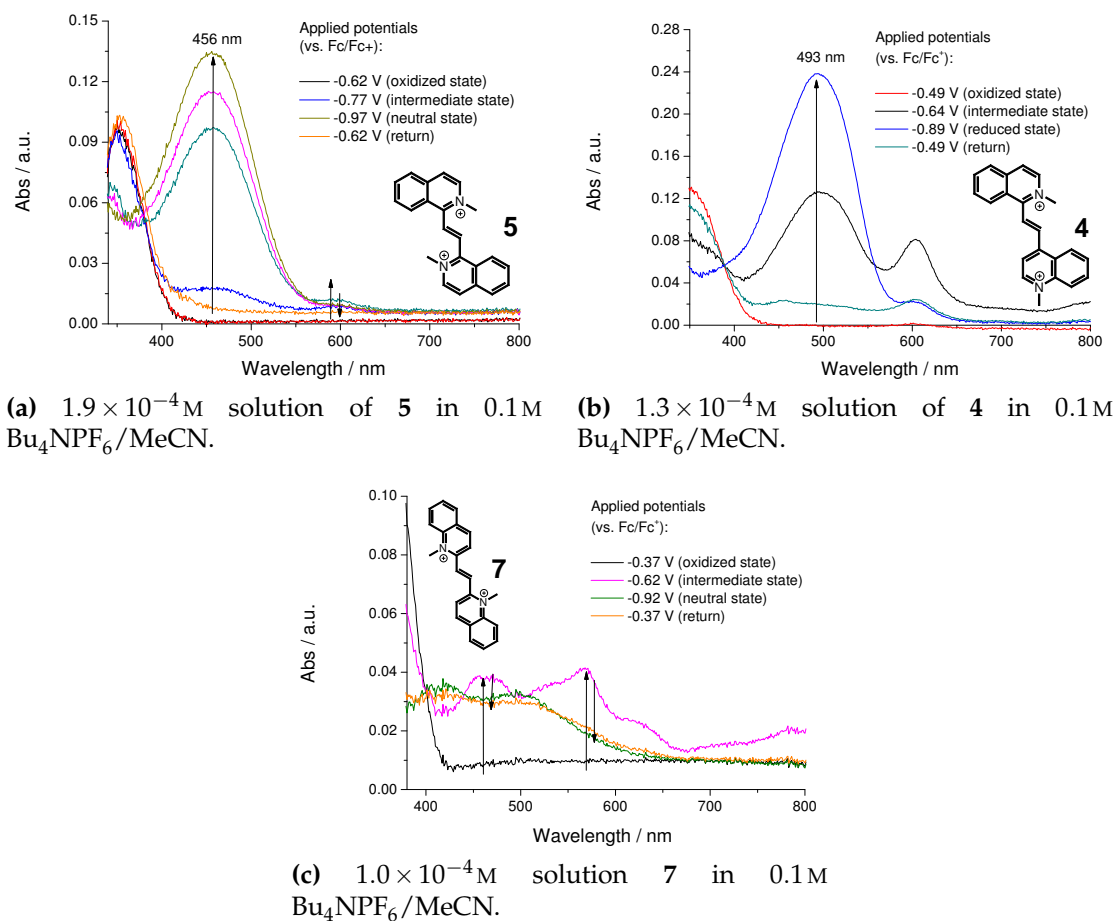


Figure 2.10 Spectroelectrograms of compounds **5**, **4** and **7**.

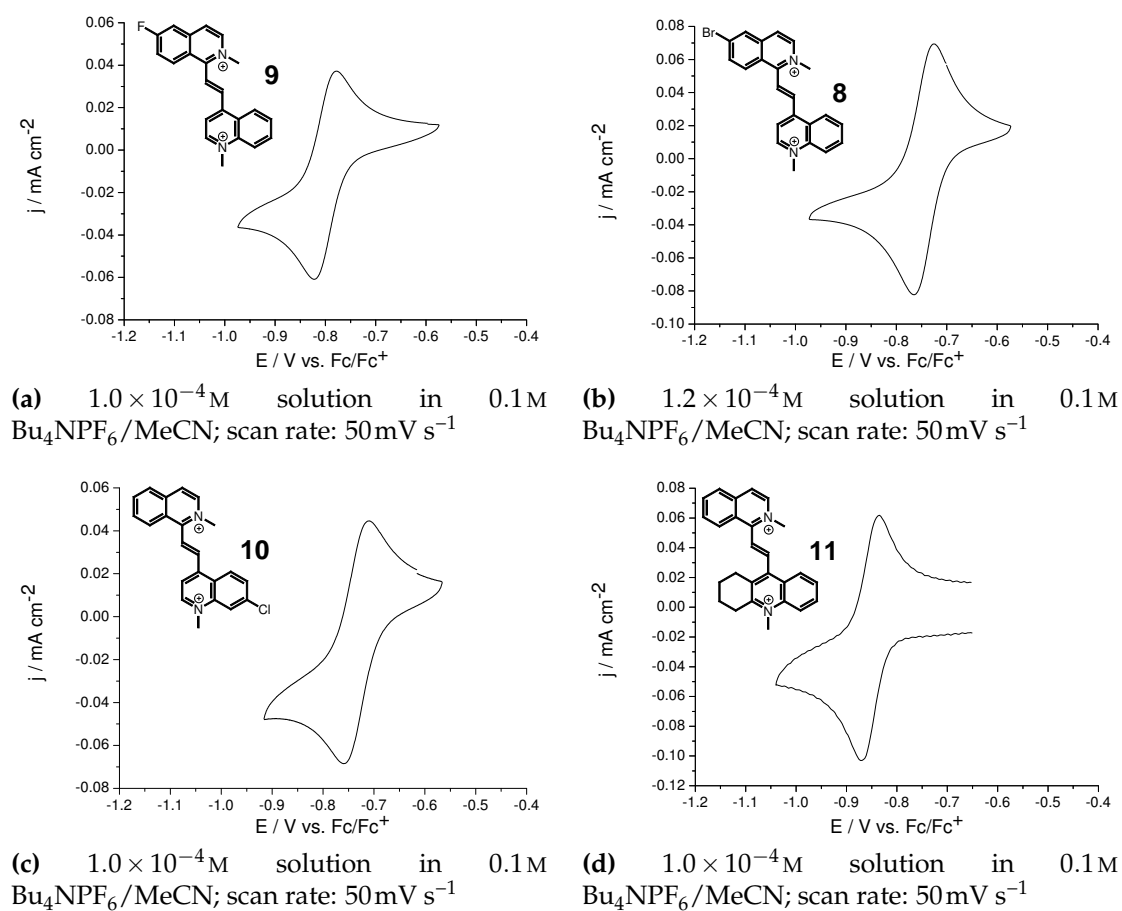


Figure 2.11 Cyclic voltammograms of substituted derivatives of 4.

Cl- and Br- substituted derivatives do not show a significant deviation from the reduction potential measured on the parent compound **4**. The difference is a little more pronounced in the case of compound **9** and **11** in the direction of lower reduction potentials. This can be explained, at least in the case of **11**, as the effect of the electron donating alkyl groups on LUMO energy. In this particular derivative, one can also speculate that the presence of a substituents induced deviation from planarity in the reduced form play a role.

Table 2.2 Electrochemical and spectroelectrochemical data for substituted derivatives of **4**.

	$E_{1/2}$	ΔE	$\lambda_{\max}^{\text{RED}}$
	mV	mV	nm
9	-800	44	490
8	-745	39	503
10	-735	48	506
11	-852	34	467

Table 2.2 shows electrochemical data of the compounds derived from cyclic voltammograms (Fig. 2.12), along with the position of the absorption maxima of the reduced forms. In derivatives **8** and **10** the absorption bands of the reduced form are centred at 503nm and 506nm respectively, thus being a little red shifted in comparison with the parent compound. An opposite behaviour is observed for compounds **9** (490nm) and **11** (467nm). In this case, in fact, a blue shift of the band is observed. The effect is more intense in derivative **11** demonstrating that substituents on the 2- or 3- positions of the quinoline ring can strongly alter the electrochemical and optical properties of the compound. A closer look at the spectroelectrograms of compounds **9** and **10**, reveal that the reduction process is associated to the formation of a third species absorbing around 455-460nm. The extra absorption is not bleached upon reoxidation; a behaviour similar to the one previously observed for compound **7**. As we already discussed before, this phenomenon can be ascribed to the formation in solution of radical cation dimers with low electroactivity.

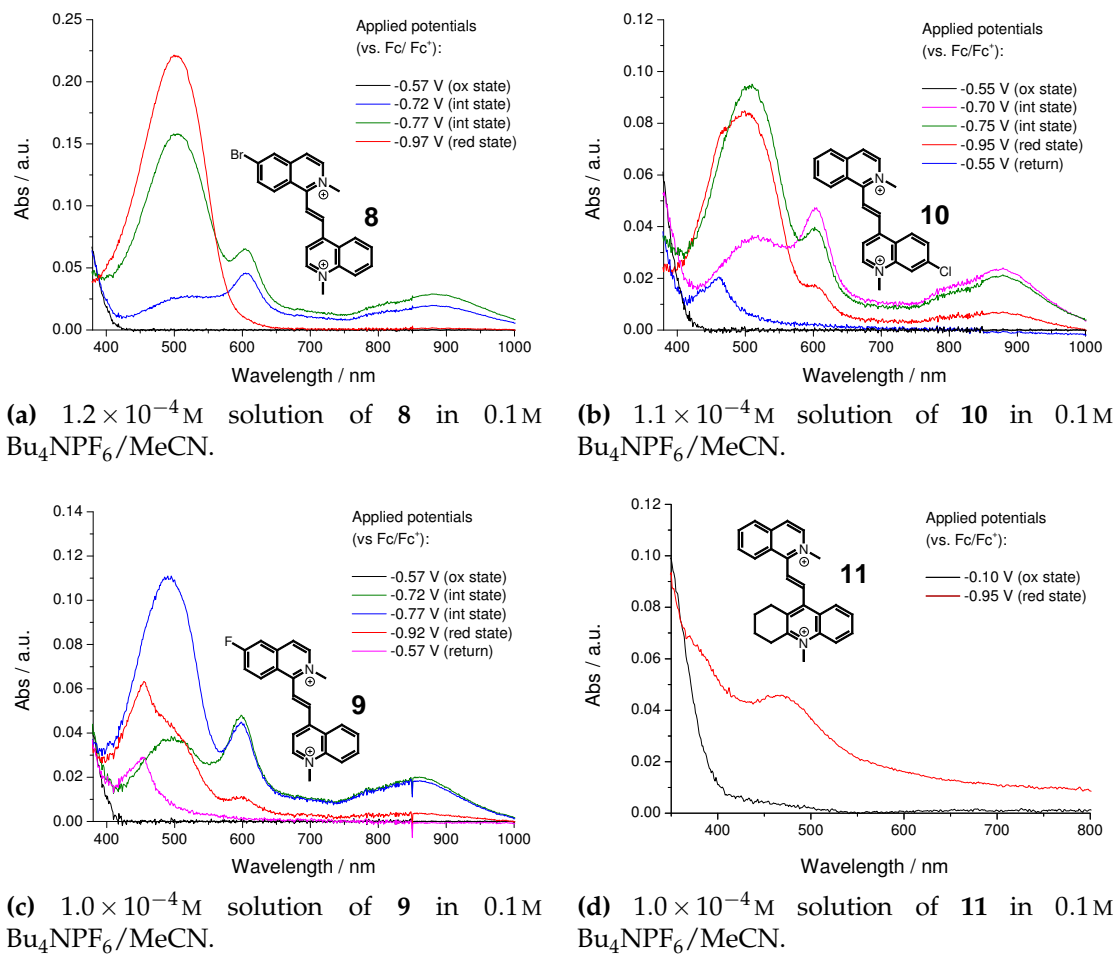


Figure 2.12 Spectroelectrograms of substituted derivatives of 4.

2.3.2.4 (*E*)-3-methyl-2-(2-(1-methylquinolinium-4-yl)vinyl)benzo[*d*]thiazol-3-ium trifluoromethanesulfonate

The cyclic voltammogram of the benzothiazolium/quinolinium substituted ethene **12** clearly displays two reversible monoelectronic redox waves at -465 and -625 mV with peak separations of 56 mV and 58 mV respectively. The presence of two completely reversible electron transfer process clearly demonstrates that the violen general structure can be extended to unsymmetrical systems. The observed redox potentials are higher than those of the quinolinium ethenes. In contrast, the stability of the intermediate radical cation is higher ($K_{sem}=5.2 \times 10^2$) when compared to diquinolinium ethenes, but lower if a comparison with a 2,2'-dimethylbenzothiazolium ethene is made ($K_{sem}=4 \times 10^4$)¹⁷⁷.

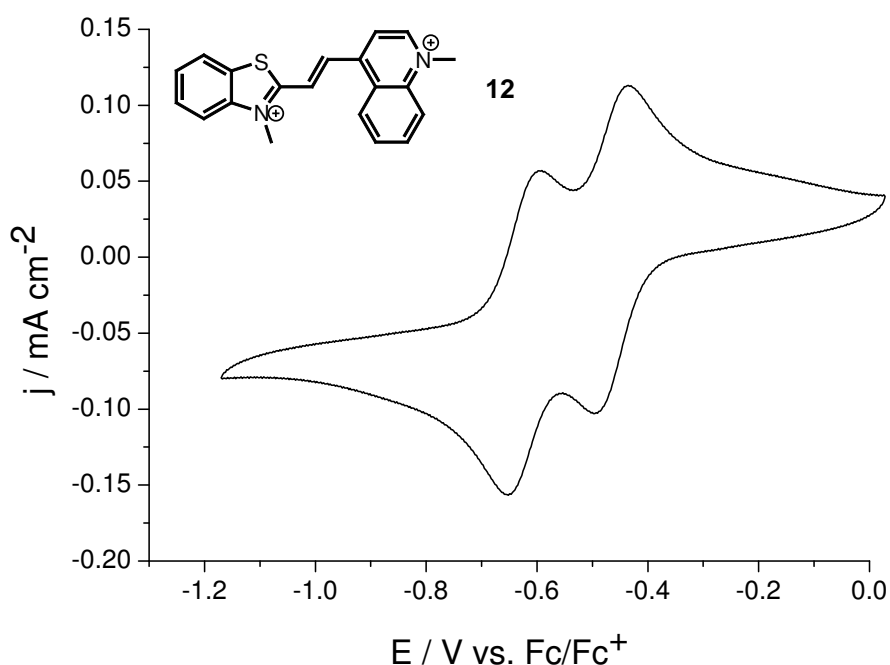


Figure 2.13 Cyclic voltammogram of compound **12** (5×10^{-4} M) in 0.1 M $\text{Bu}_4\text{NPF}_6/\text{MeCN}$. Scan rate 50 mV s^{-1} .

2.4 Conclusions

In this chapter, we have described the design, synthesis and characterization of new discrete electrochromic systems of the Weitz type. We demonstrated that systems showing two-electron redox processes and switching between two stable closed-shell structures, can be obtained using simple diazinium ethenes with the proper end-groups. The new isoquinolinium/quinolinium ethenes

were investigated further in order to understand the effect of substitution on the switching potential and the colour of the reduced form. Our findings reveal that halogen substitution on the 6-position of the isoquinoline ring or on the 7-position of the quinoline ring has little effect on the position of the low-energy absorption band of the reduced form, while substitution on the 2- and 3-positions of the quinoline ring with alkyl groups promotes a consistent blue shift of this band. Spectroelectrochemical measures showed that substitution has an unpredictable effect on the reversibility of the electrochemical process in solution. The observed phenomenon was attributed to the formation of stable radical cation dimers or other stable intermolecular aggregates under open circuit conditions.

However, our novel synthetically accessible electrochromes possess very interesting electrochromic properties, showing a colorless to red transition with absorption centred around 500 nm. This characteristic, combined with their unique redox properties and the possibility to tune the absorption spectrum through functionalization, make these new derivatives an important acquisition for this class of electrochromic compounds. Moreover, the versatile synthetic approach can allow to easily extend their functionality, and incorporate them in solid state electrochromic systems, overcoming the limitations of current materials.

Chapter 3

Novel EDOT functionalized diaziniium ethenes (ISOx) and polymers thereof

3.1 Introduction to multichromophoric polymeric systems

As discussed in section 1.4.4 in the introduction, although conjugated polymers represent the state-of-the-art in organic electrochromic systems, some limitations emerge when considering their practical application in ECDs that require an highly transmissive to absorptive transition. These can be summarized as:

- low transmissivity in the transmissive state
- uneven absorption throughout the visible spectrum in the dark state.

As an example, in ophthalmic applications these limitations are clearly apparent looking at figure 3.1 that compares the performances of the best panchromatic absorptive electrochromic polymer to the state-of-the-art of photochromic lenses (Transition VITM by Essilor). It is evident that the absorptive reduced state of this DA conjugated polymer presents a little too low absorption around 450nm, while the transmissive state appears to be very absorptive. A comparison with a ProDOTEt₂ derivative (also shown in figure 3.1) highlights the reduction in transmissivity "paid" in order to obtain the panchromatic absorption

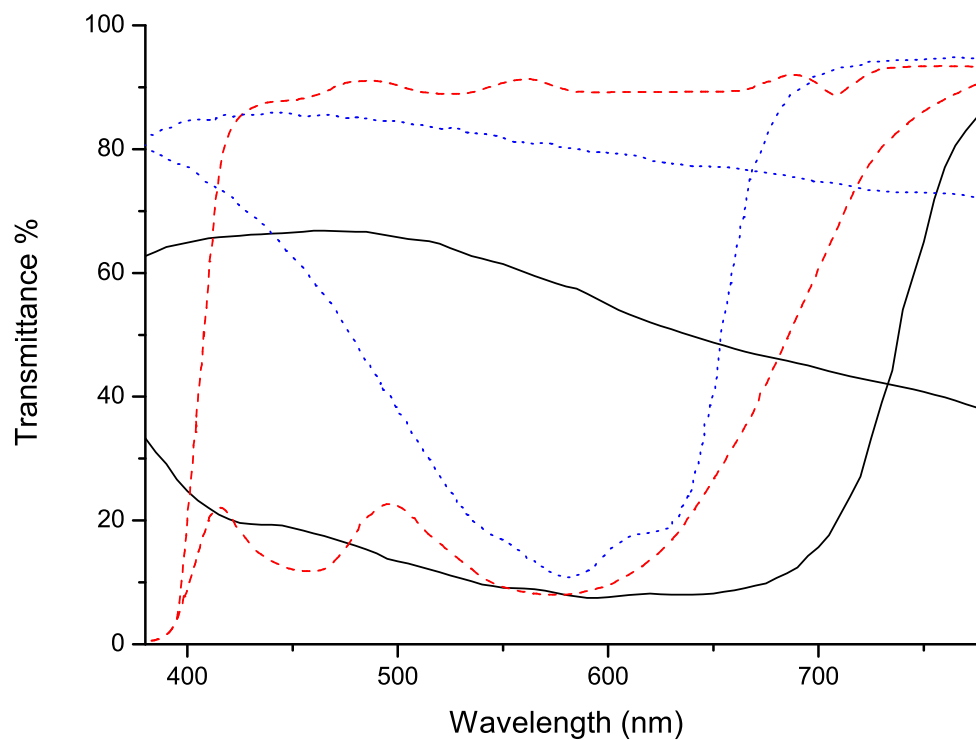


Figure 3.1 Comparison of the best known panchromatic absorptive electrochromic polymer, developed by Reynolds *et al.*²⁰ (black solid lines), with Transition VITM photochromic lenses (dashed red lines) and a p(ProDOTEt₂) derivative¹²⁶ (dotted blue lines).

in the reduced state. In performing this comparisons, it has to be considered that photochromics, despite their excellent contrast, still have the drawback of very low switching times ($\tau_{dark} \sim 1$ min, $\tau_{bleach} \sim 10$ min) when compared to electrochromics. Nevertheless, a strong motivation in finding an alternative to the donor-acceptor approach in the development of transmissive to panchromatic absorptive electrochromics emerges. One of the possible alternatives is represented by the adoption of multichromophoric polymeric systems. As explained in section 1.4.4, in these systems a second electrochrome is incorporated in the polymeric matrix. The underlying idea is that the conjugated polymer and the discrete electrochrome (hereafter DE) remain electrochemically independent, and the resulting absorption spectrum is given by the sum of the spectra of the single components (conjugated polymer and DE). In light of these considerations, and looking again at figure 3.1, one can speculate that a DE absorbing in the 450-500nm can modify the colour of the reduced state of a PEDOT-like polymer obtaining the desired neutral hue. The best example in this direction is represented by the viologen functionalized PEDOT by Lee *et al.*²⁰⁴ However, in this system the absorption of the $V^{\bullet+}$ species is too red shifted (around 600 nm) to attain the desired effect.

3.2 Incorporation of violenes in a PEDOT matrix

Few different strategies to incorporate redox active molecules in a conjugated polymer can be imagined. The first one is to simply dissolve the compound in the polymeric matrix. This approach is not feasible, especially in the case violenes, for many reasons. It has to be considered that most of the violene systems posses low solubility and even after functionalization with solubilizing alkyl chains, they still retain a tendency for phase segregation. These characteristics favour the formation of separated phases that lead to a drastic reduction of the fraction of redox active compound inside the film and/or to poor optical properties (hazy films). Furthermore, the DE can diffuse away from the electrode on prolonged cycling, leading to a drastic reduction in the performance. An alternative approach, demonstrated by Palmore *et al.*²⁹⁶, uses a properly functionalized eletrochrome to form a polyelectrolyte that, acting as a counterions for PEDOT chains, is incorporated in the polymeric matrix.

A more general approach uses modified EDOT monomers functionalized, through a tether, with the desired discrete electrochromic system. Monomers of this kind can be electrochemically polymerized to obtain thin films of the modified

PEDOT. This appears to be the better strategy since it avoids the aforementioned problems. However, the electrochemical polymerization of electroactive monomers carrying bulky substituents has proved to be more difficult, as a consequence of lower reactivity and slow diffusion. To circumvent this problem pulsed techniques and copolymerization have been applied.³³¹ A last strategy relies on post-functionalization of a formed polymer layer. As an example, Segura *et al.*²⁹⁵ polymerized an azide functionalized EDOT monomer, and exploited the azide-alkyne Huisgen cycloaddition to incorporate redox active compounds in the polymeric layer.

3.3 Novel poly(ISOx) electrochromic polymers

In view of the good electrochemical and spectroelectrochemical properties of the novel violene type systems we developed (chapter 2), we decided to incorporate them in PEDOT layers. This choice was motivated by the possibility to obtain a polymeric PEDOT based system with a strong enhancement of electrochromic contrast in the 450-550nm region and a resulting modification in the colour of the reduced state. In order to achieve this ambitious target, we selected the best performing of our library of violene systems, and developed it further to allow its incorporation in the PEDOT matrix. In particular, we selected compound 4 since it combines:

- highly reversible two-electron process;
- blue shifted absorption in the oxidized state with minimal tailing in the visible region;
- reduced state with absorption centered at 494nm;
- simple synthetic access;
- non-symmetric functionalizability on the two *N*-positions.

In order to incorporate our molecules, we adopted the strategy of direct functionalization of the EDOT monomer and subsequent polymerization of the same either electrochemically or chemically (using Fe(OTs)₃ as an oxidant). We thus prepared the series of monomers depicted in figure 3.2. An acronym (ISOx) has been attributed to each monomer to allow faster referencing. Different variations on the basic chromophoric unit have been attempted in order to modulate

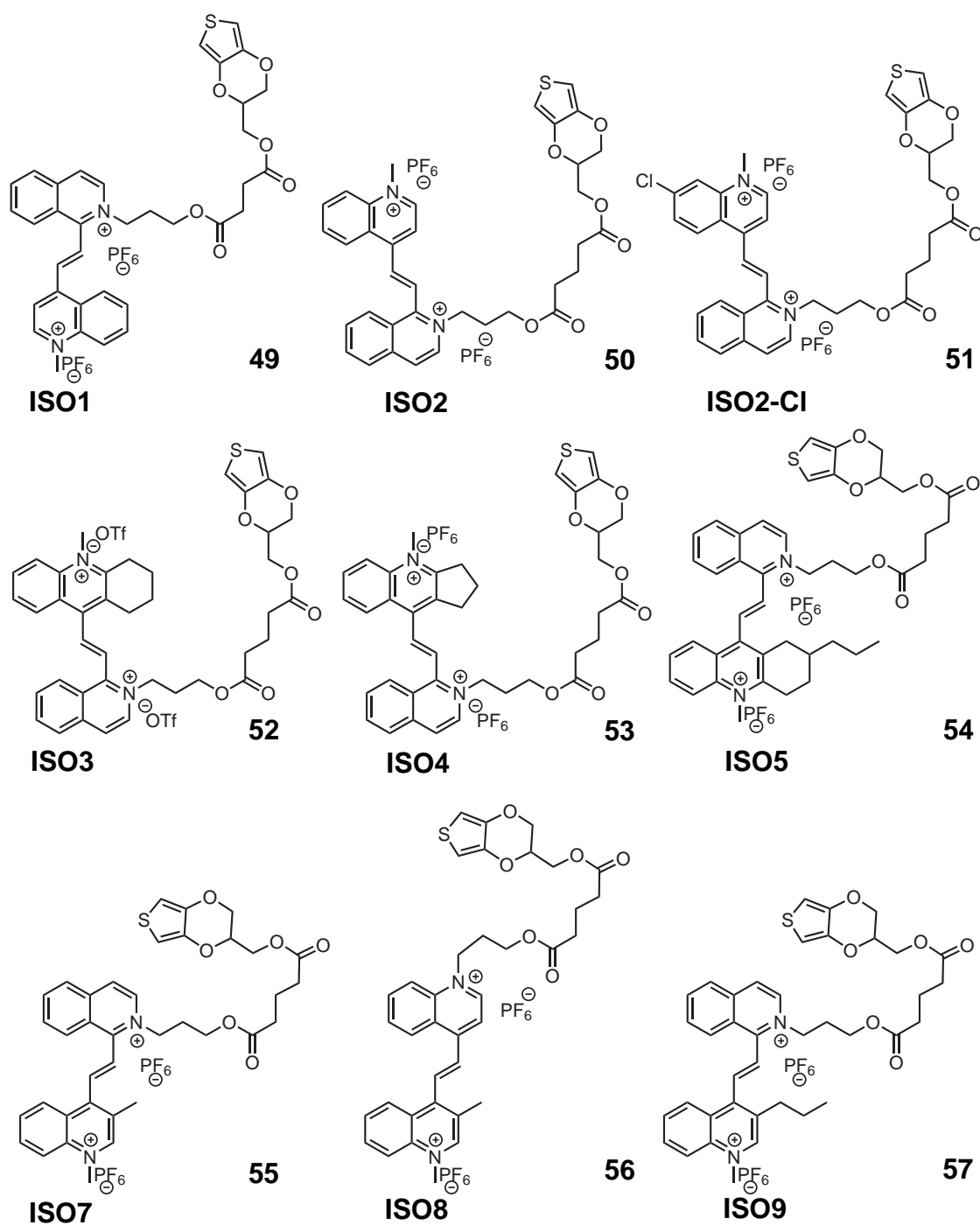


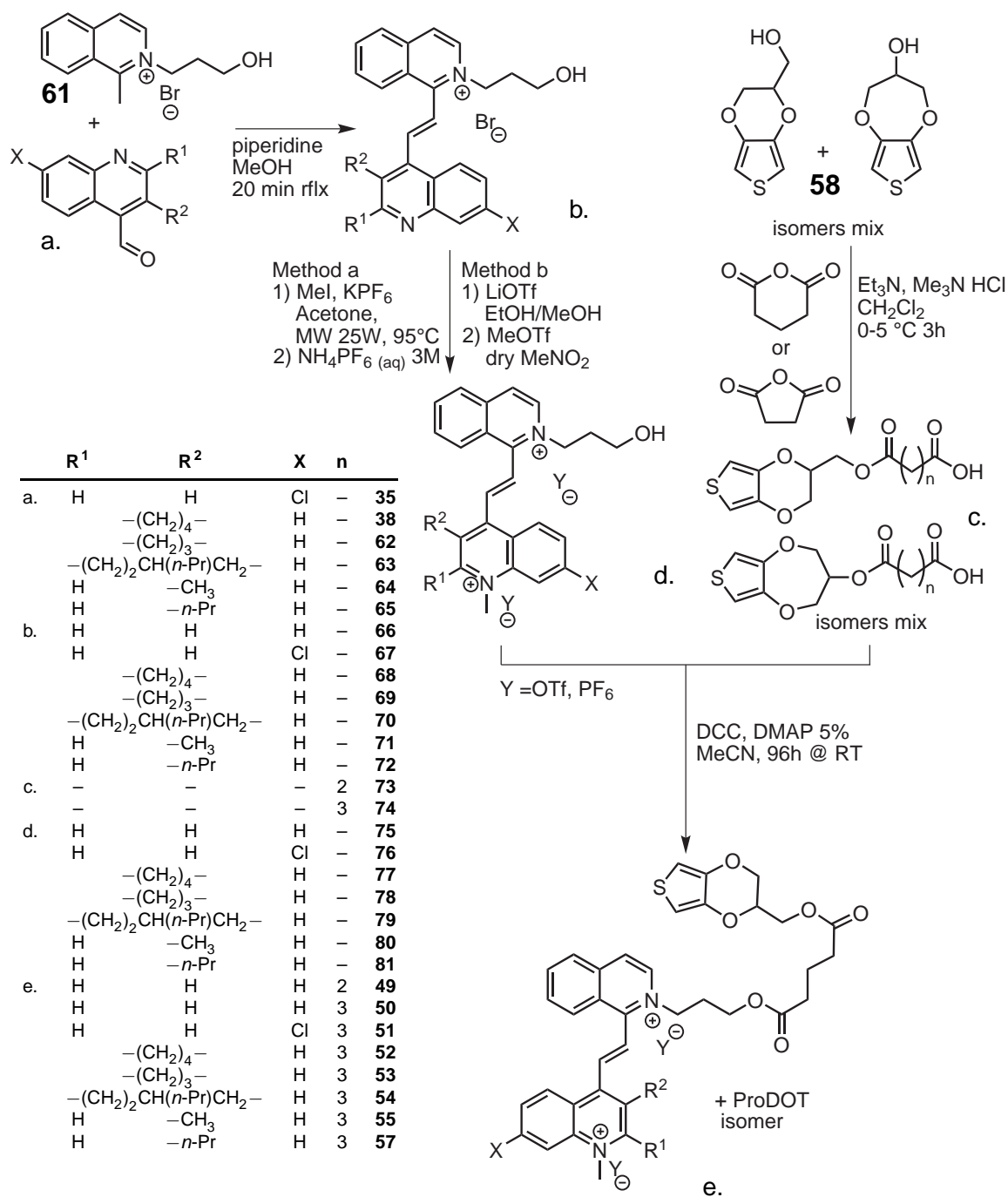
Figure 3.2 Novel viosene functionalized EDOT monomers (ISOx).

the electrochemical and spectral properties of the resulting polymers. In particular, modifications with different alkyl substituents on the isoquinoline ring have been performed since, as we demonstrated in chapter 2, this proved to be the most effective way to blue shift the absorbance of the reduced form. An example with a derivative of compound 6 was also prepared (ISO8 (56)) to further expand the library. The aim of this approach was the develop a composite system that can effectively cover the 450-550nm region compensating for the lack of absorption exhibited by reduced PEDOT in this spectral region.

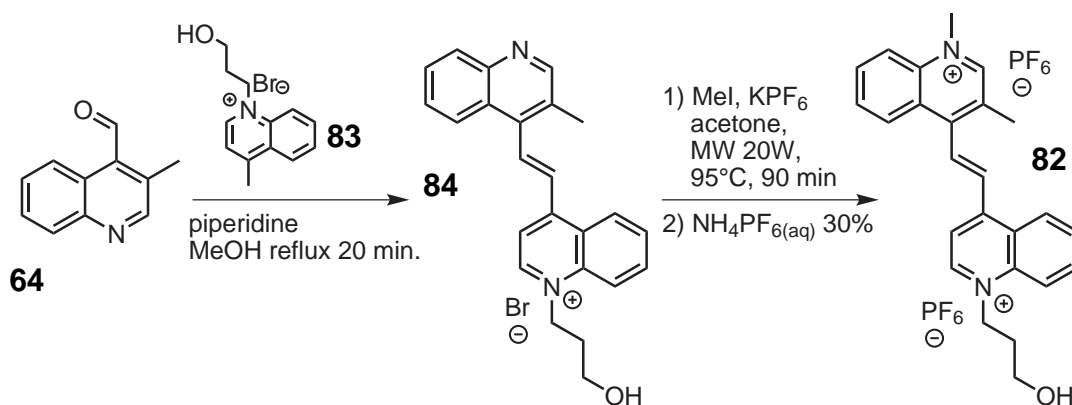
3.3.1 Synthesis of the monomers (ISOx)

For the synthesis of the ISOx monomers, we adopted the convergent synthetic strategy illustrated in scheme 3.1. Although commercially available, the EDOT starting material 58 was provided by COC - Centrum Organicé Chemie s.r.o. as a mixture of ProDOT-OH and EDOT-MeOH isomers in a 1:4 ratio, unless differently specified. This mixture was converted, by esterification with succinic and glutaric anhydrides, in the corresponding mixtures 59 and 60. The EDOT isomer of 59 was already known in literature, although prepared in slightly different conditions.^{332,333}

The alcohol functionalized discrete electrochromes 75, 80, 81, 76 and 79 were obtained by the same general synthetic protocol, while a little modification was necessary in the case of derivatives 77 and 78. The synthesis of compound 82 followed the same strategy, but for reasons of clarity is reported in scheme 3.2. The process is rather similar to the one employed for the synthesis of the dimethyl derivative 4 with some notable differences. In this case, an isoquinolinium salt carrying an alcohol functionality is obtained by alkylation of 1-methyl-isoquinoline with 3-bromopropanol, and subsequently condensed with the proper aldehyde in refluxing methanol with piperidine as a catalyst. The successive alkylation of the quinolinic nitrogen proved to be the most difficult synthetic step, as a consequence of the low solubility of the reagents and their low reactivity. Moreover, the highly polar nature of these systems ruled out the possibility of a chromatographic purification of the raw products, especially on a large scale. We coped with these problems using two different solutions. The first one, that proved to work with most of our derivatives, consisted in performing the alkylation with MeI in acetone under pressure in presence of 2 eq. of KPF₆. The presence of the KPF₆ generates the more soluble hexafluorophosphate derivative *in situ* as a result of ion metathesis, and let the reaction

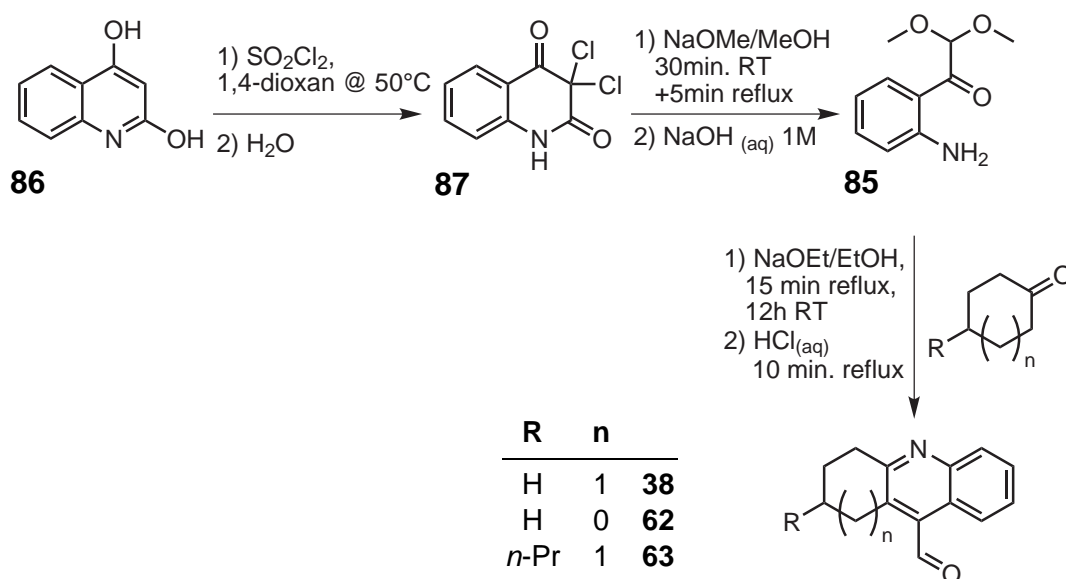


Scheme 3.1



Scheme 3.2

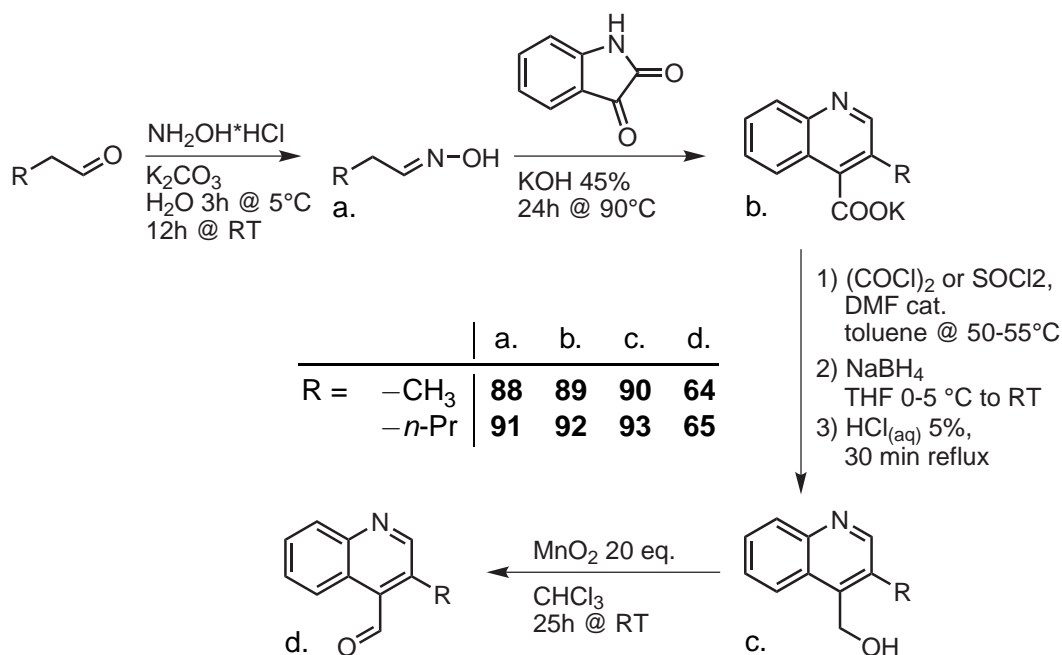
proceed faster. The second solution, applied in the synthesis of compound 77 and 78, consisted in performing the ion exchange with LiOTf, followed by the alkylation with MeOTf. In this latter case, careful controlled conditions and a low excess of alkylating agent had to be adopted. In fact, with large excess of MeOTf we observed loss of selectivity and *O*-alkylation on the alcoholic group. The substituted quinoline-4-carboxyaldehydes used as starting materials for this synthesis (a. in scheme 3.1) were prepared by three different routes. The first one, adopted for derivatives 38, 62 and 63 uses the modified Friedländer synthesis developed by Ziegler *et al.*^{334–336} In this case, a ketone is reacted under strongly basic conditions with *o*-aminophenylglyoxal dimethoxyacetal (85) to obtain the acetal intermediate that gives the desired aldehyde after acid hydrolysis (scheme 3.3). The second route, adopted for aldehydes 64 and 65, re-



Scheme 3.3

3.3 - Novel poly(ISOx) electrochromic polymers

lies on the reduction of the corresponding acids, easily prepared from isatin and the proper aldoxime using Pfitzinger reaction.^{319,320,337} This reduction is



Scheme 3.4

performed in multiple steps: at first the acids are converted in the corresponding acyl chlorides (using SOCl_2 or oxalyl chloride), then reduced to alcohol by NaBH_4 in THF,³³⁸ and finally selectively reoxidised to aldehydes with activated MnO_2 .³³⁹ Purification can be conveniently performed by crystallization on the high melting alcohol derivatives **90** and **93**.

The obtained alcohol functionalized violene systems were coupled to the acid functionalized EDOTs through esterification (scheme 3.1). In this step, a Steglich esterification protocol, using *N,N*-dicyclohexylcarbodiimide (DCC) and 4-dimethylamino-pyridine (DMAP) in MeCN, was adopted.³⁴⁰ This mild esterification method allowed to obtain the desired products in good yields and with a relatively easy workup procedure. After elimination of the insoluble dicyclohexylurea and solvent evaporation, in fact, pure product is recovered after prolonged washing with solvents (Et_2O and EtOH). Pure ISOx monomers appear as light brown powders, although impurities, undetectable by NMR, can give them a greenish colour. This colouration can be removed with extended washing in EtOH or treating with activated charcoal a solution in MeCN/ H_2O . ISOx are very soluble in polar aprotic solvents like MeCN, DMAc, DMF, DMSO, PC or in MeNO_2 . In contrast, they exhibit low to very low solubility in alcohols, ketones and chlorinated solvents. A slightly different behaviour is observed with

compounds bearing trifluoromethanesulfonate counterions, resulting in higher solubility in alcoholic solvents. As a result of their structure, they possess both the reactivity of EDOT and quinolinium salts, being sensitive to acidic conditions and strong nucleophiles. Nevertheless, they appear to possess very good stability to environmental conditions. Samples stored in closed dark glass containers do not show any noticeable sign of degradation after a two year period.

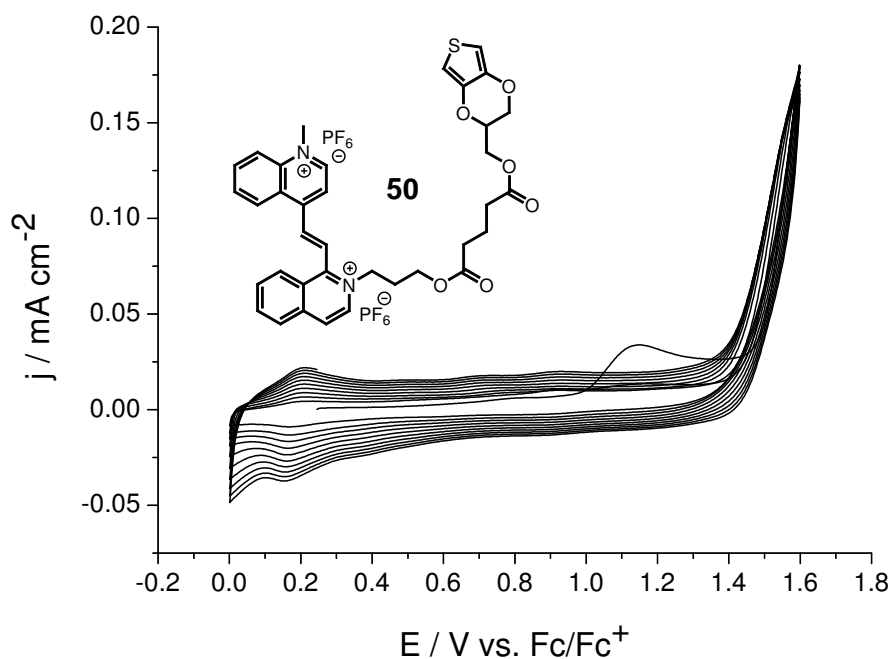
3.3.2 Electrochemical characterization of ISOx and p(ISOx) compounds

In order to obtain polymeric films, ISOx derivatives were polymerized both electrochemically and chemically on transparent electrodes (OTEs). The obtained polymeric layers were subsequently characterized by cyclic voltammetry experiments and spectroelectrochemical measurements. A long optimization procedure allowed to delineate the ideal conditions for the obtainment of homogeneous and electrochemically stable films with good cycle life. Some of the most relevant results will be reported in the upcoming section.

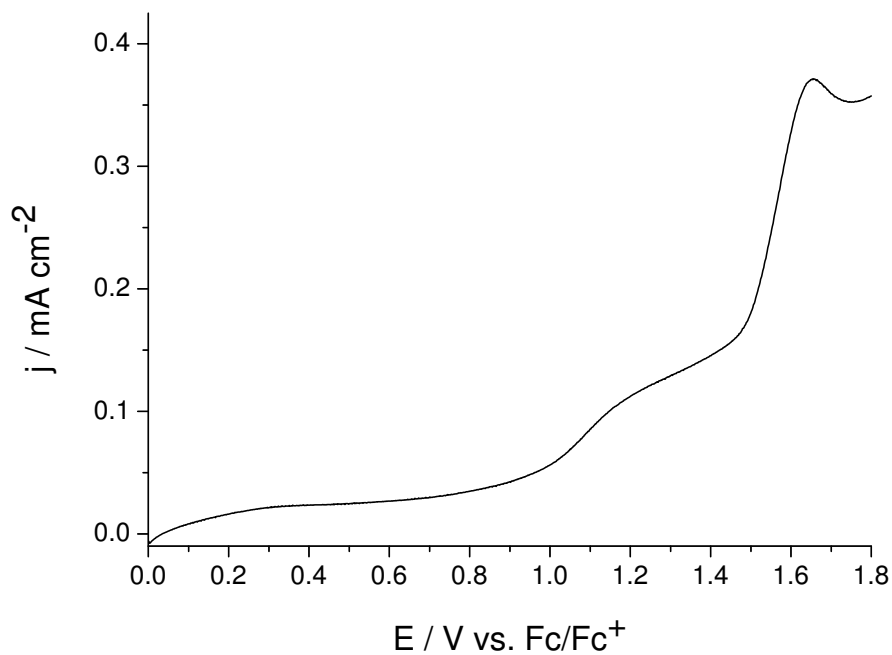
3.3.2.1 Electrochemical polymerization

The members of the ISOx class possess many common features and they also have very similar electrochemical behaviour. In the following, these characteristics will be explained with the aid of some examples without listing all the huge amount of data collected. However, some notable differences in the behaviour of the obtained polymers will be highlighted where needed.

A cyclic voltammogram of a solution of **50** in nitrobenzene is shown in figure 3.3. An oxidative process at 1.13 V (vs. Fc/Fc⁺) is present on the first cycle, followed by the onset of the oxidative polymerization at 1.44 V. Polymer growth is confirmed by the increase of anodic and cathodic currents in the region between 0 and 1.44 V upon cycling. The choice of nitrobenzene as the solvent was dictated by the failure of first attempts with other solvents that ended with the formation of polymeric layers having very poor cycle life. The cyclic voltammogram of the polymeric film in a monomer-free solution clearly shows the presence of a redox wave centered at -0.704 V with a peak separation of 31 mV (figure 3.4). This process can be attributed to the electrochemistry of the violenene core **4**. A comparison with the cyclic voltammogram of **4** reveals a minimal deviation in the half-wave potential with substantial broadening of both the cathodic and anodic waves. This broadening is expected, as a consequence of in-



(a) Cyclic voltammogram of a 10^{-3}M solution of **50** in $0.1\text{M Bu}_4\text{NPF}_6/\text{PhNO}_2$. Working electrode: FTO/glass; scan rate: 100mV s^{-1} ; 10 cycles.



(b) Linear scan voltammogram of a 10^{-3}M solution of **50** in $0.1\text{M Bu}_4\text{NPF}_6/\text{PhNO}_2$. Working electrode: FTO/glass; scan rate: 50mV s^{-1} .

Figure 3.3

homogeneities in the polymeric matrix and hindered diffusion of counterions. In the region above -0.48V the doping/dedoping process of the PEDOT chain

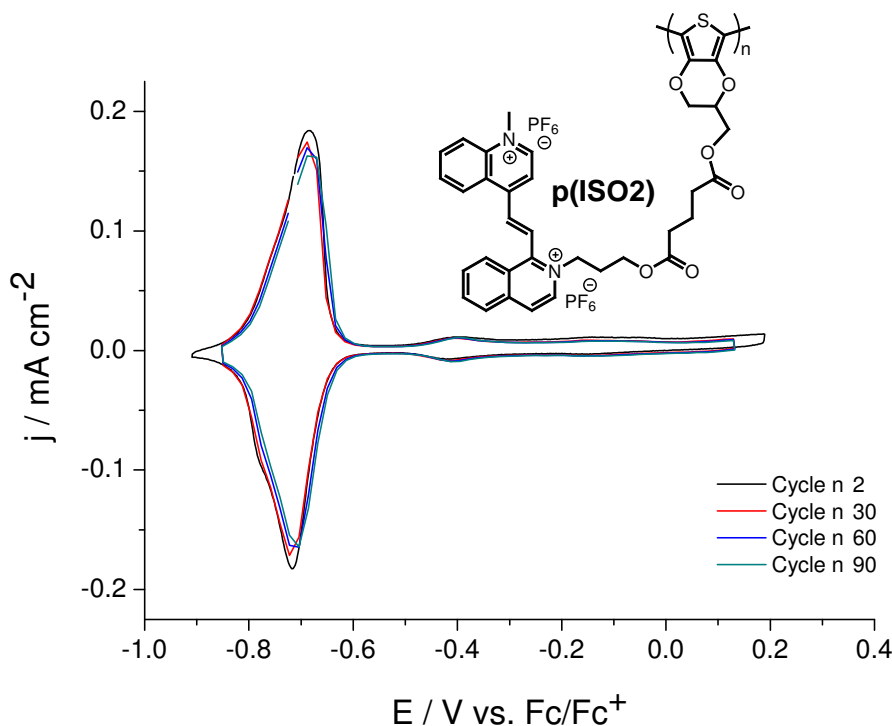
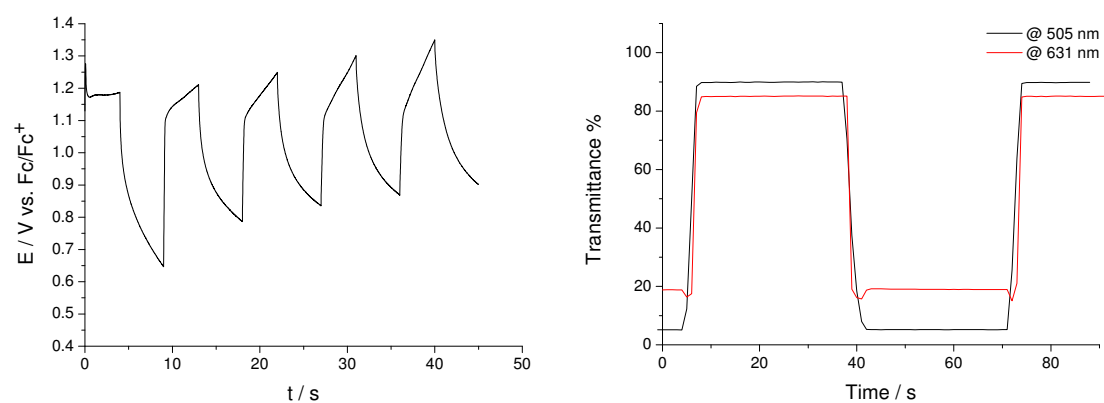


Figure 3.4 Cyclic voltammogram of a poly(ISO2) layer on FTO/glass in 0.1M $\text{Bu}_4\text{PF}_6/\text{MeCN}$ monomer-free solution; scan rate 25mV s^{-1} . Polymer was prepared by cyclic voltammetry $0\text{-}1.6\text{V}$ vs. Fc/Fc^+ , 10 cycles.

takes place. The polymer possesses a rather stable electrochemical behavior with a slight decrease in the charge associated to the viologen redox process upon cycling. The material exhibits a remarkable multichromic behaviour, switching from a colourless fully oxidized state to a blue one in the region between -0.50V and -0.65V , and finally a very dark violet-red colour. The spectroelectrochemical properties of poly(ISO2) and the other poly(ISOx) polymers will be discussed in more detail in section 3.3.2.3.

The adoption of pulsed techniques for the electrochemical deposition of p(ISOx) films proved to be beneficial for the cycle life of the resulting materials. As already mentioned, these techniques have been successfully used in literature to circumvent the problems connected with diffusion-limited mass transport to the electrode surface experienced with bulky monomers.³³¹ The resting periods between the pulses permit to replenish the diffusion layer, reestablishing the bulk monomer concentration in front of the electrode. When using these techniques, a subtraction of the charging current of the electrochemical double-layer has to be performed in order to evaluate the Faradaic current. A pulsed

galvanostatic deposition of p(ISO2) is depicted in figure 3.5a. Chronoabsorptometric measures were also performed on the obtained films showing acceptable switching times. Data obtained from a rather thick film, deposited with a total deposition current of ~ 15 mC, demonstrate switching times of 3.0/3.7 s and 3.3/1.9 s for colouration/bleaching processes, at 505 nm and 631 nm respectively, to attain 95% of the final ΔT (Fig. 3.5b). Films of p(ISO2) were also

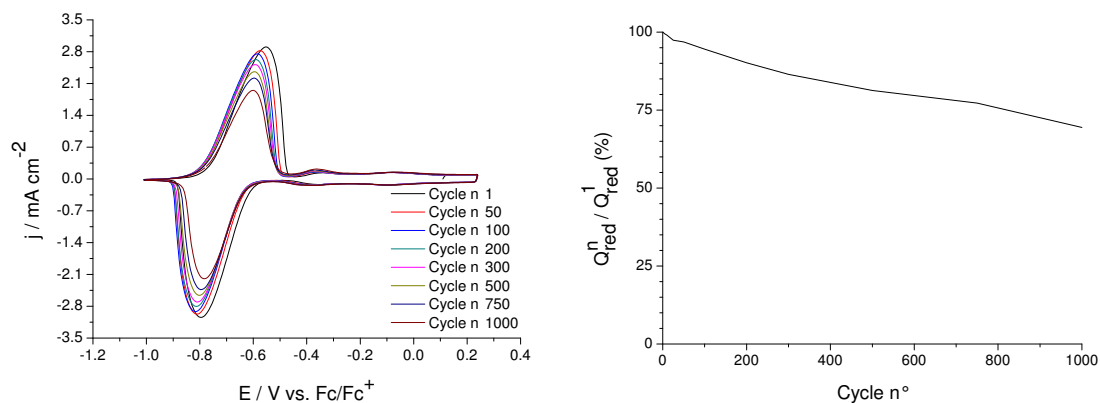


(a) Pulsed galvanostatic deposition of poly(ISO2) from a 5×10^{-3} M solution of compound **50** (ISO2) in 0.1 M $\text{Bu}_4\text{NClO}_4/\text{MeCN}$. Pulse: 4 s @ 0.75 mA + 5 s @ 0 mA.

(b) Chronoabsorptometric data of a p(ISO2) layer in monomer-free 0.1 M $\text{Bu}_4\text{NClO}_4/\text{MeCN}$. Potential steps between -1.15 and 0.25 V vs. Fc/Fc^+ . Polymer was deposited on FTO/glass substrate with pulsed galvanostatic technique (5 pulses, ~ 15 mC of deposition charge).

Figure 3.5

subjected to extended cycling tests and the obtained data is presented in figure 3.6. The polymer possesses moderately good cycling stability, retaining 70% of the initial reduction charge after 1000 cycles. It can be noted that the loss of electrochemical activity involves mainly the viologene redox process. As we discussed in section 1.4.4, this is a common feature of viologen functionalized polymers. The electrochemical irreversibility of p(ISOx) films gets higher when other derivatives are considered. In particular, some p(ISOx)s derivatives ($x=3, 4, 5, 9$) presented a rather high instability and very low cycle life, despite the very good spectroelectrochemical properties. As an example, the cyclic voltammogram of a p(ISO3) film is depicted in figure 3.8b. The cyclic voltammogram is irreversible with the redox process associated with the attached redox active unit gradually decreasing upon cycling. A concomitant gradual displacement of the potentials of the anodic and cathodic waves from the middle point in opposite directions is also observed. Nevertheless, the electrochemical activity of the PEDOT chains is retained, and the voltammetric charge associated



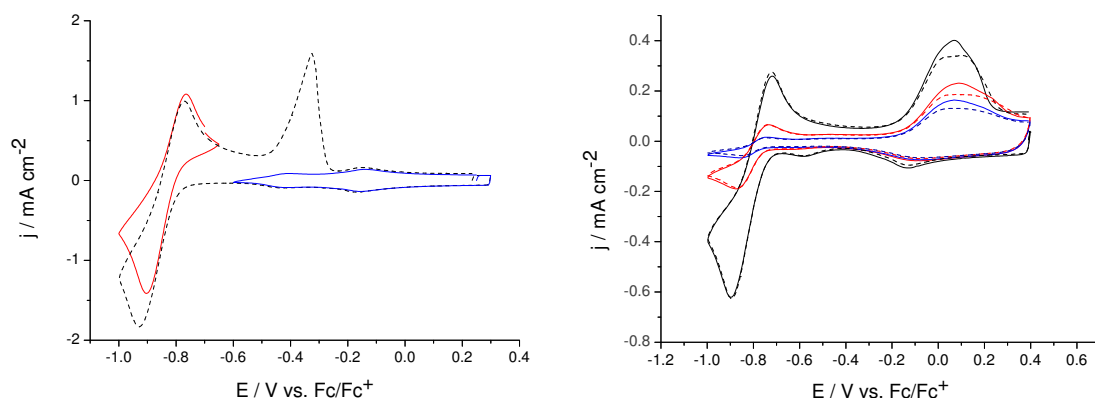
(a) Cyclic voltammograms in 0.1 M $\text{Bu}_4\text{NBF}_4/\text{MeCN}$. Scan rate 50 mV s^{-1} .

(b) Ratio of the cathodic charge for cycle n to the cathodic charge of the first cycle.

Figure 3.6 Decay of the electrochemical activity of a poly(ISO2) film cycled in 0.1 M $\text{Bu}_4\text{NBF}_4/\text{MeCN}$. Film was obtained by pulsed galvanostatic deposition (see fig. 3.5a) (8 pulses).

with their redox process is not affected by cycling. Another interesting feature is the appearance of an irreversible steep anodic peak in the lower end of PEDOT oxidation, with an onset around $-0.47 \text{ V vs. Fc/Fc}^+$. However, when the film is cycled in the -0.6 - 0.3 V range, the aforementioned peak is not present (fig. 3.7a). It's worth noting that the observed loss in redox activity is partially recovered upon thermal treatment as depicted in figure 3.7b. The cured film experiences the same decay trend observed on the pristine film.

This somewhat surprising behaviour closely resemble the one of similar systems in which a redox active unit is incorporated in a conjugated polymer matrix. We partially discussed this phenomenon in section 1.4.4 with two examples taken from the literature.^{283,287} As a consequence of the complexity of the system, a definitive explanation of the phenomenon is difficult to find. Nonetheless, on the basis of our evidences and those from literature, it is apparent that, while scanning cathodically, the formation of some stable species takes place during the reduction process at -0.84 V . These species then require an high anodic overpotential to be reoxidized, giving rise to the pre-peak observed on the cathodic scan, but cannot be reduced again, resulting in a loss in electroactivity. However, the underlying mechanism is still an open question. Different hypothesis exist but none is able to completely answer the question. A first one considers the involvement of the variation of film conductivity. In fact, after the complete reduction of the PEDOT chains, a drop in film conductivity is expected, and the charge conduction is driven by a hopping process between the redox-active centres. As a result, if stable species having an higher



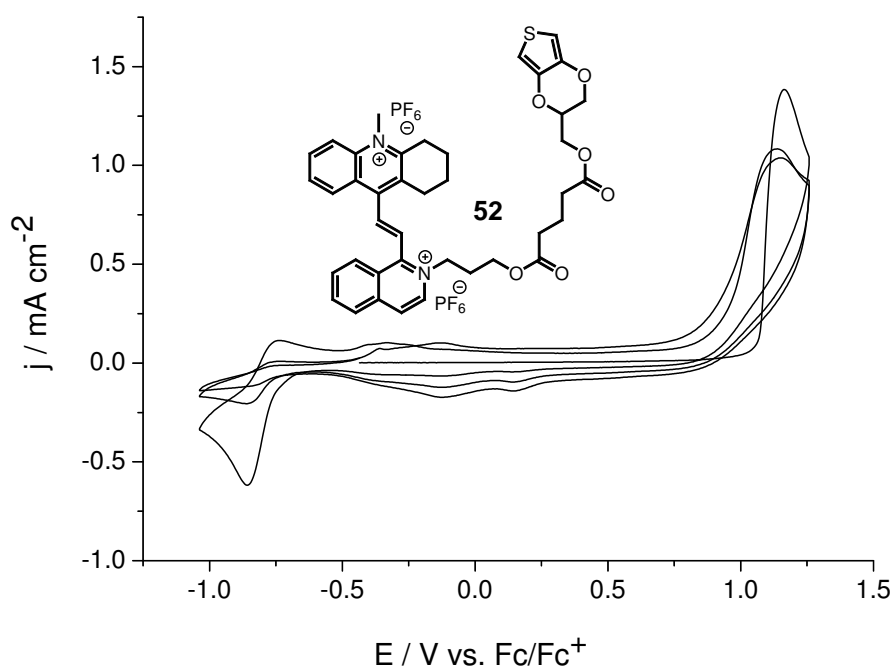
(a) Cyclic voltammograms of an electrochemically deposited poly(ISO3) film on FTO/glass in 0.1M LiClO₄/MeCN monomer-free solution. The potential was cycled in the -1.0 - 0.23 V range (black dashed line), in the -1.0 - -0.65 V range (red solid line) and in the -0.6 - 0.3 V range (blue solid line). Scan rate 50mV s^{-1} .

(b) Cyclic voltammograms of chemically deposited poly(ISO3) films on ITO/PET substrates in 1M LiTFSI/PC solution after 1, 10 and 25 cycles. Scan rate 50mV s^{-1} . Dashed lines represent voltammograms of the same sample obtained after thermal curing at 120°C for 30 min.

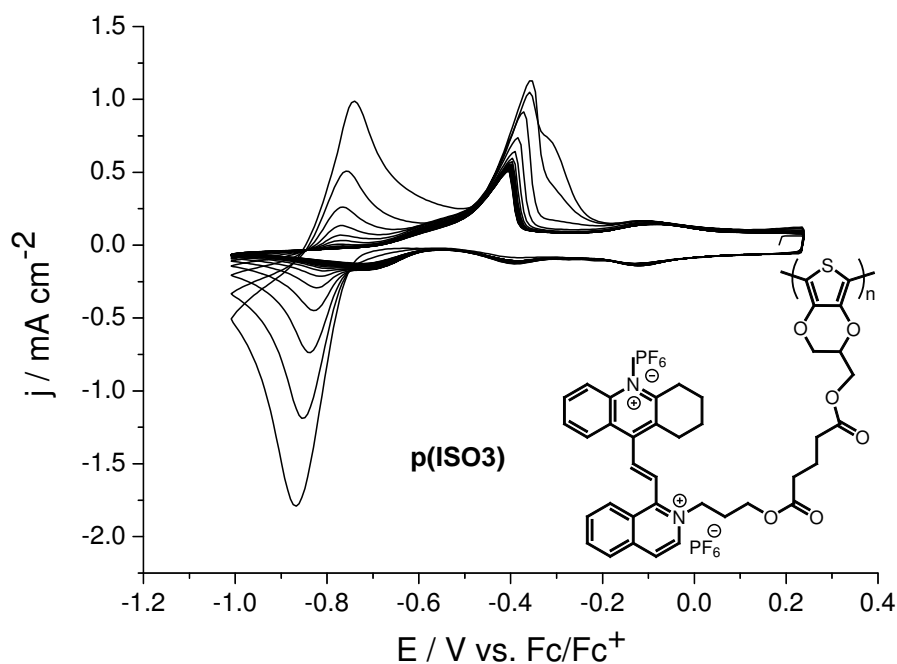
Figure 3.7

oxidation potential are formed during the cathodic scan, their oxidation cannot take place until a sufficient conductivity of the film is attained. This leads to a shift of the oxidation wave of these species to higher potentials, where a good conductivity of the matrix is obtained as a consequence of PEDOT oxidation. This effect can explain the high overpotential that originates the pre-peak. A similar effect can also be the result of film inhomogeneities that lead to trapping of some of the reduced viologene molecules in insulating regions where they cannot be reoxidized. Another possible contribution involves the evolution of the polymer structure during cycling. In fact, during reduction, the polymeric matrix experiences a modification of its structure and morphology as a consequence of the change in bond length alternation in both PEDOT chains and viologene moieties and the outward motion of counterions. On reoxidation, the recovery of the initial situation can give rise to hysteresis phenomena. In this framework, the observed pre-peak can result from a variation of film capacity that accompanies the structural reorganization.

A last effect to be considered is related to the irreversible spectroelectrochemical behaviour exhibited by some of our systems in solution (see section 2.3.2). We attributed that effect to the instability of the reduced form under open circuit conditions that results in the formation of stable intermolecular aggregates or dimers. A similar behaviour could be present even in the solid state,



(a) Cyclic voltammogram of a $5 \times 10^{-3} \text{ M}$ solution of **52** in 0.1 M $\text{Bu}_4\text{NClO}_4/\text{MeCN}$. Working electrode: FTO/glass; scan rate: 50 mV s^{-1} ; 3 cycles.



(b) Cyclic voltammogram of a poly(ISO3) layer on FTO/glass in 0.1 M $\text{Bu}_4\text{BF}_4/\text{MeCN}$ monomer-free solution; scan rate 50 mV s^{-1} . Polymer was prepared by pulsed galvanostatic deposition: $7 \times (5 \text{ s @ } 0.75 \text{ mA} + 5 \text{ s @ OCV})$ from a $5 \times 10^{-3} \text{ M}$ solution of **52** in 0.1 M $\text{Bu}_4\text{ClO}_4/\text{MeCN}$.

Figure 3.8

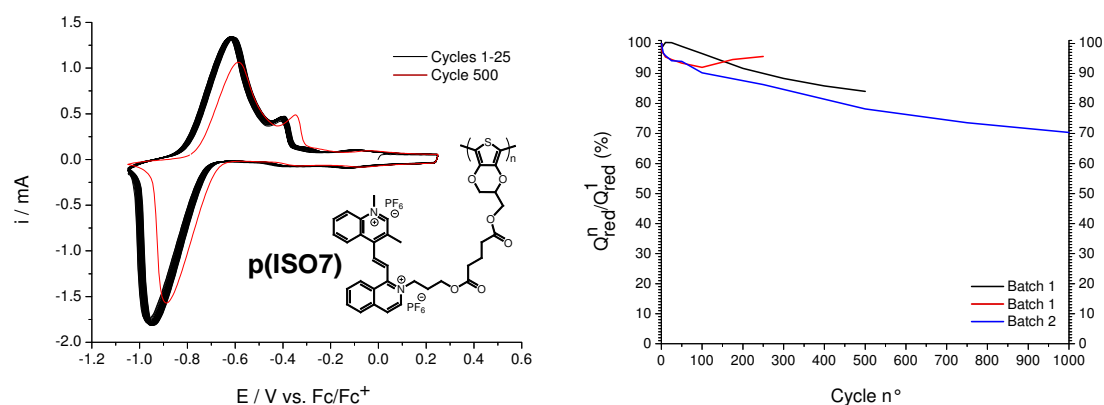
thanks to the close proximity of the redox centres.

However, a clear evidence, is the striking dependence of the phenomenon on minimal structural variations on the monomer. Examples of such surprising behaviour were already present in literature. A comparison of the viologen substituted PEDOTs published by Czardybon *et al.*²⁸⁸ and by Lee *et al.*²⁰⁴ testifies this effect. In this case, the substitution of a methyl group with a butyl chain on one of the two *N*-positions apparently solved the problems of electrochemical instability exhibited by the polymer prepared by the former authors. In view of these considerations, we tested many different functionalizations in order to find the ideal trade-off between stability and colorimetric properties.

3.3.2.2 *In situ* chemical polymerization of ISOx derivatives

To the best of our knowledge, there are no reported attempts of *in situ* chemical polymerizations on EDOT monomers functionalized with redox active units. The reason probably is a combination of the fact that this approach consumes larger amounts of monomers than the electrochemical one, and the lack of knowledge on the proper conditions to adopt. In fact, as a consequence of the large differences in solubility and chemical behaviour between the common alkyl functionalized EDOT monomers and these high molecular weight charged derivatives, the usual procedures adopted with the former fails with the latter. Nevertheless, *in situ* chemical polymerization is a key technological achievement since it allows the depositions of films with larger surface area when compared to the electrochemical methods. Moreover, the obtained films are highly uniform. The possibility to fine tune the formulation with addition of plasticizers, adhesion promoters or other additives, and the variation of deposition procedure or thermal treatment can allow to enhance both the electrochemical stability and the optical properties. The drawback is that the huge amount of variables to control make their optimization a difficult task. After several trials with different formulations and treatment conditions we adopted the general procedure described in the experimental section. Our formulation make use of the same oxidant solution used for the *in situ* polymerization of PEDOT, namely a 40% solution of Fe(OTs)₃ in *n*-butanol. Nevertheless, this oxidant solution is modified by the addition of PEG-*ran*-PPG since it proved to inhibit the crystallization of the oxidant and the monomer during solvent evaporation, leading to better films.¹⁶⁵ This modified solution is then added to a solution of the monomer. In this case, a complex solvent mixture was adopted, comprising 1-methoxy-2-propanol, nitromethane and a small amount of propylene

carbonate. The adoption of nitromethane was dictated by the good solubility of the monomer in this solvent combined with its not so high evaporation rate. The addition of 1-methoxy-2-propanol, a solvent commonly used as thinner for paints, strongly enhance the film forming properties of the mixture. Finally, the presence of a high boiling solvent, like propylene carbonate, prevents crystallization to occur during solvent evaporation keeping the monomers in solution till polymerization take place. As an example, electrochemical data on long term cycling stability of a poly(ISO7) film obtained by *in situ* chemical polymerization are depicted in figure 3.9.



(a) Cyclic voltammogram of a poly(ISO7) layer deposited by *in situ* chemical polymerization on FTO/glass in 0.1 M $\text{Bu}_4\text{ClO}_4/\text{MeCN}$ monomer-free solution; scan rate 50 mV s^{-1} .

(b) Ratio of the cathodic charge for cycle n to the cathodic charge of the first cycle

Figure 3.9 Electrochemical data of a chemically polymerized poly(ISO7) thin film on FTO/glass substrate.

3.3.2.3 Electrochromic properties of polyISOx polymers

Poly(ISOx) polymers possess a very interesting multichromic electrochromism. As an example, figure 3.10 shows the spectroelectrogram of an electrochemically deposited p(ISO2) layer cycled in a monomer-free solution. A broad absorption band, centred at 632 nm, gradually appears on cathodic scanning at potentials below 0.3 V vs Fc/Fc^+ . This absorption is attributed to the reduction of the PEDOT chains. During this process the film colour changes from colourless to blue. On further cathodic scanning, another redox process takes place at potentials between -0.65 and -0.9 V. This process leads to the appearance of a new absorption band, centered at 519 nm, that changes the colour of the film to violet-red. Figure 3.11 shows, as an example, the absorption spectra of the re-

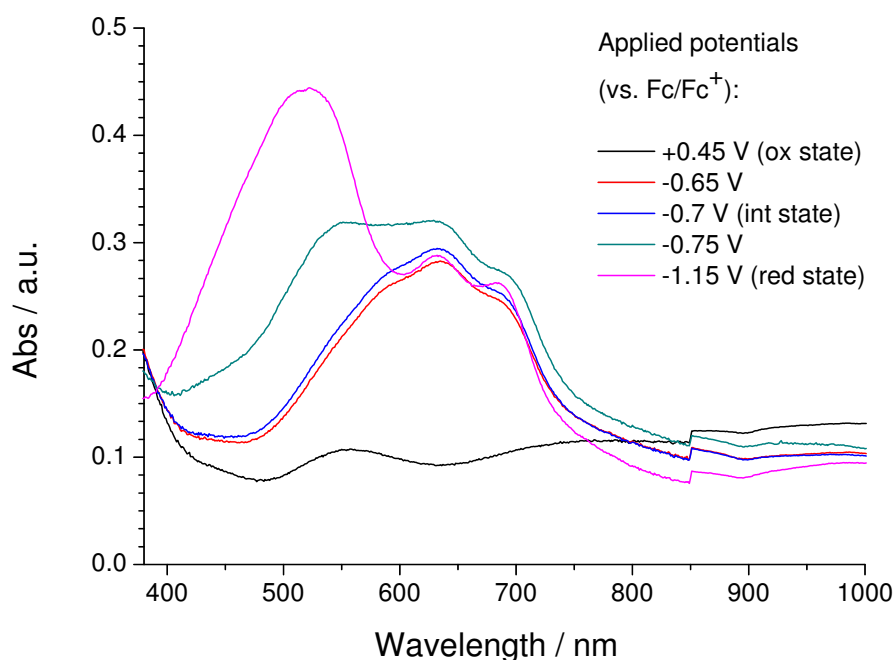


Figure 3.10 Spectroelectrogram of a p(ISO2) layer in 0.1 M $\text{Bu}_4\text{ClO}_4/\text{MeCN}$ monomer-free solution. Polymer was deposited by LSV on FTO/glass substrate.

duced and oxidized states of a poly(ISO2) layer on a transmittance scale, along with the contrast (calculated as ΔT). This graph clearly testifies the impressive enhancement of contrast achieved with our approach. In particular, a ΔT up to 82% has been obtained in the region around 490 nm. As a term of comparison, p(ProDOT-Et₂), depicted in figure 3.1 at the beginning of this chapter, has a contrast of 42% at this wavelength. Moreover, the oxidized state preserves a very high transmissivity with an average transmittance in the visible (400-800 nm) of 77% that compares to the 54% exhibited by the polymer published by Reynolds *et al.*²⁰

The normalized absorption spectra of the different poly(ISOx) derivatives are displayed in figure 3.12. These graphs demonstrate the control over the absorption spectrum (and hence the hue) that has been obtained through functionalization of the monomers. In particular, most of the alkyl substituted derivatives (p(ISO3), p(ISO5), p(ISO7) and p(ISO9)) show a blue shifted absorption spectrum, with an absorption maximum around 490 nm. This 15 nm shift (with respect to the p(ISO2)) is enough to modify the resultant hue giving rise to desirable neutral tints (grey and brown). Although initially this achievement was accompanied by the electrochemical instability of the resultant polymeric layers (see section 3.3.2.1), a careful control of the substituents allowed to find

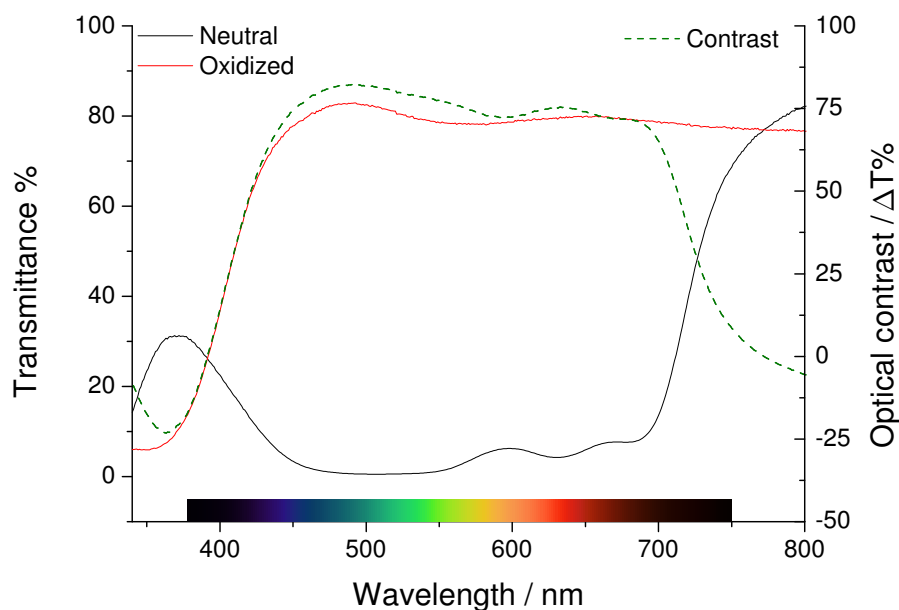


Figure 3.11 Absorption spectrum of the neutral (black solid line) and oxidized (red solid line) states of a poly(ISO2) layer obtained by galvanostatic pulsed deposition. Deposition charge $\sim 30 \text{ mC cm}^{-2}$. Optical contrast is represented by a dashed green line.

the ideal trade-off in poly(ISO7). The latter combines very interesting spectral properties with a promising electrochemical stability (fig. 3.9). The CIE 1931 colour coordinates of the reduced and oxidized states of p(ISO2) and p(ISO7) layers were calculated from their UV/Vis spectra and plotted in figure 3.13.²⁴ It is worth noting how the colour of the reduced state in p(ISO7) is very close to the white point (or grey), indicating the achievement of a neutral hue with this derivative. Both oxidized states have high luminance values ($L^*=91.39$ for p(ISO2) and 93.74 for p(ISO7) layer) that is drastically reduced upon switching to the reduced form ($L^*=19.46$ for p(ISO2) and 58.50 for p(ISO7) layer). The higher luminance of the reduced state measured for p(ISO7) can be attributed to the much lower thickness of this layer and an improvement is expected using thicker ones. The value of luminance variation (contrast) for p(ISO2) film is very high ($\Delta L^*=71.9\%$), especially if compared to the one reported by Reynolds *et al.* for their panchromatic absorbing DA polymer ($\Delta L^*=52\%$).²⁰

In contrast, a red shifted absorption has been obtained with poly(ISO8). In this case, a large absorption band having two maxima of almost equal intensity at 525 and 554 nm is obtained. This results in a saturated purple reduced state and an highly transmissive oxidized state. Nevertheless, its blue shifted absorption make it an interesting candidate for copolymerizations, in order to enhance contrast in the 550 nm region and fine tune the hue. Pictures showing

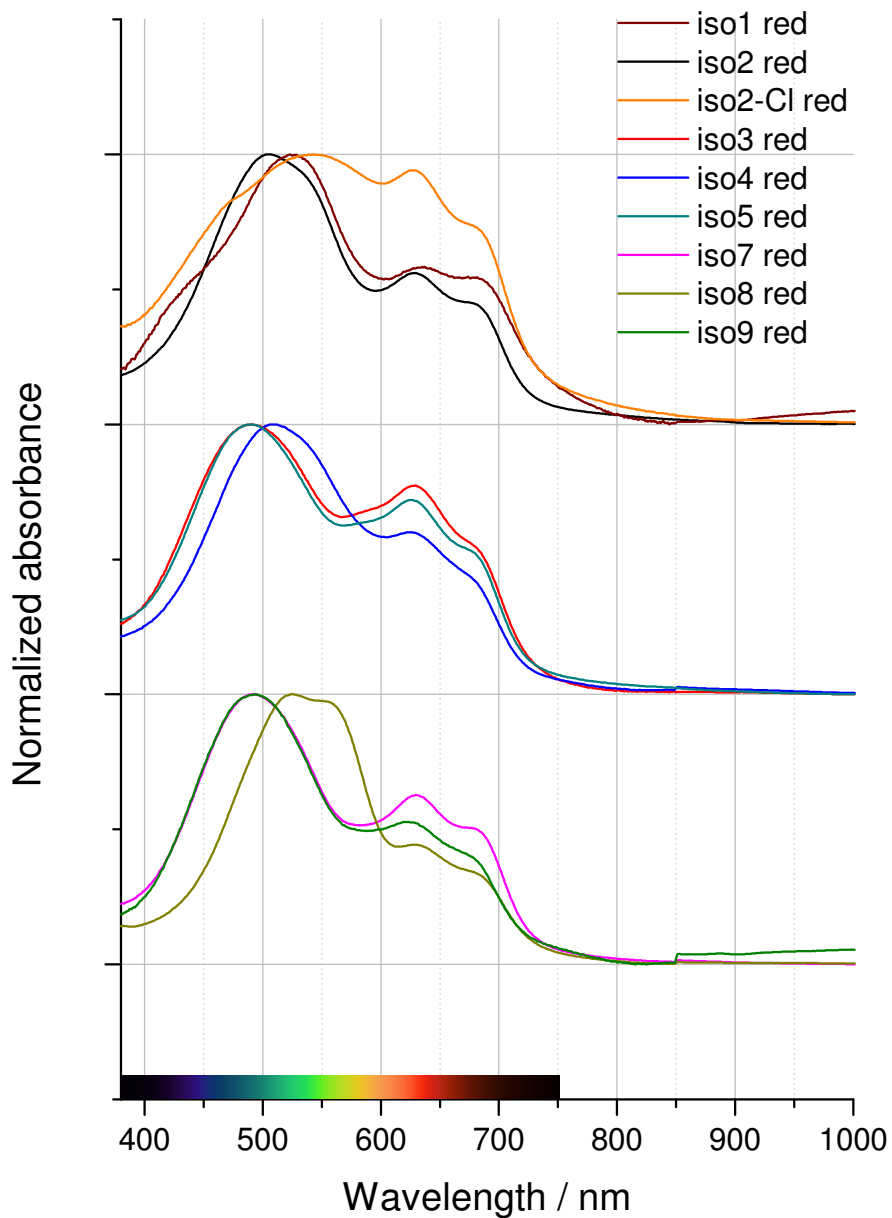


Figure 3.12 Normalized spectra of the reduced forms of poly(ISOX) derivatives.

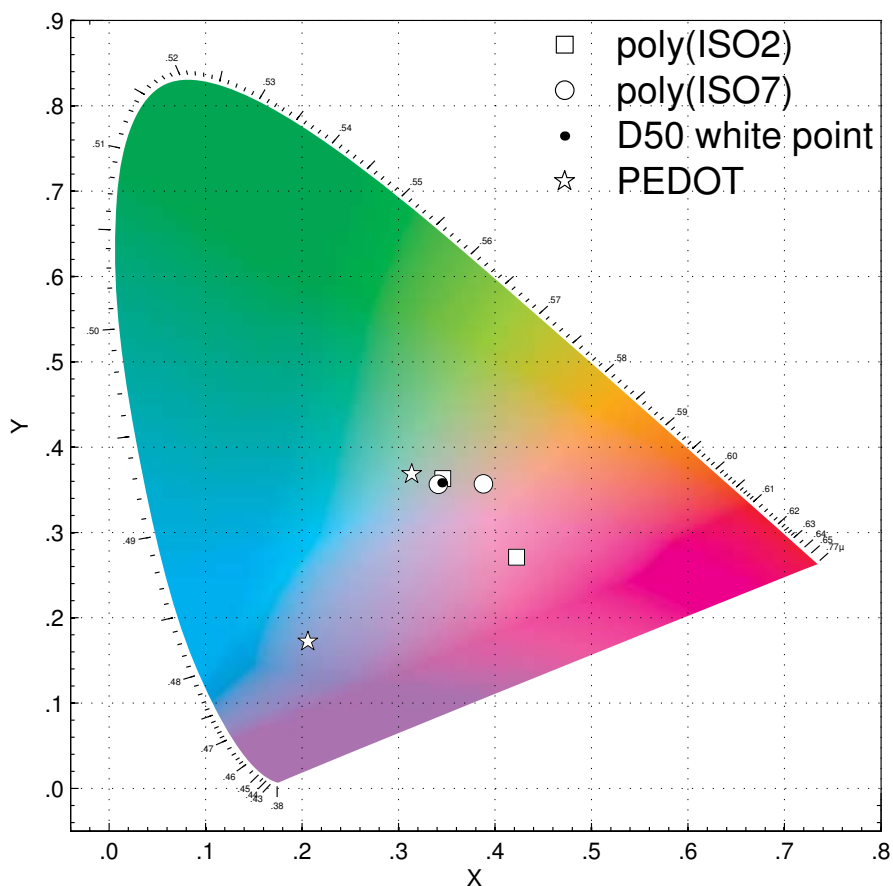


Figure 3.13 Colour coordinates on the CIE 1931 chromaticity diagram for poly(ISO2) (squares) and poly(ISO7) (circles) reduced (p(ISO2): $x = 0.422$ $y = 0.271$; p(ISO7): $x = 0.388$ $y = 0.356$) and oxidized forms (p(ISO2): $x = 0.346$ $y = 0.363$; p(ISO7): $x = 0.341$ $y = 0.356$). Values were calculated from the recorded transmittance spectrum.²⁴ Values for PEDOT ($x = 0.314$ $y = 0.368$ ox; $x = 0.206$ $y = 0.172$ red) are also indicated for comparison.¹⁸ A D50 illuminant was used in the calculations and its white point is indicated on the graph.


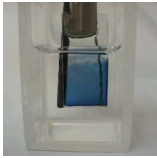





















the colours of the reduced, intermediate and oxidized states of poly(ISOx) electrochromic polymers are displayed in table 3.1. As can be noted, an interesting colour palette has been obtained through structural modification of the starting monomer. This comprises violet-red, grey and brown hues.

3.4 Conclusions

In this chapter we have described the design, synthesis and characterization of a new type of conjugated electrochromic polymers. These are part of the class of multichromophoric polymeric systems, composed of a conjugated polymer backbone with pendant redox-active units. In particular, functionalization of EDOT moieties with pendant electrochromic units is known to allow the obtainment of electrochromic polymers with a desirable colourless oxidized state and enhanced contrast in the reduced form.²⁰⁴

In doing this we exploited the remarkable electrochemical and electrochromic properties of the new diazinium ethenes Weitz type violenes described in chapter 2. These new electrochromes, in fact, show a reversible two-electron reduction process that leads to a coloured form absorbing in the region around 500nm. The developed convergent synthetic strategy, allowed to prepare multi-gram quantities of monomers comprising an EDOT unit connected by a tether to the new quinolinium/isoquinolinium ethenes. These new monomers were polymerized both chemically and electrochemically obtaining electrochromic layers with state-of-the-art electrochromic properties. Substitution on the violene core proved to have an effect on both colour and electrochemical stability of the polymers. In particular, despite the unsatisfactory cyclability shown by some of our polymers, we demonstrated the possibility to obtain stable electrochromic layers through careful optimization of the monomer structure and polymerization conditions. In this way, we obtained stable polymers possessing a colourless highly transmissive oxidized form and an absorptive reduced one with a variety of different colours (violet-red, purple, brown). These systems possess very high contrast in the visible region, thank to their panchromatic absorption, with a luminance variation between the two states up to 72%. Moreover, one of our systems (p(ISO7)) possesses a neutral tint, with colour coordinates in its reduced state close to the white point. This latter characteristic is of central importance for applications in light filtering ECDs like sunglasses, rearview mirrors or smart windows, where colour distortion has to be avoided. All these features, make our new monomers an important step forward for or-

Table 3.1 Pictures of the reduced, intermediate and oxidized states of poly(ISOX) polymeric layers.

	Oxidized state	Intermediate state	Reduced state
ISO1			
ISO2			
ISO3		—	
ISO4			
ISO5			
ISO7			
ISO8			
ISO9			

ganic electrochromic materials, redefining many aspect of the state-of-the-art in this field.

Chapter 4

emEDOT: a versatile new entry in EDOT chemistry

4.1 Introduction

As we discussed in the introduction (section 1.4.1.5), PEDOT and its derivatives represent the most important class of electrochromic conjugated polymers. This reflects the unique combination of thermal, electrochemical and environmental stability, processability and optical properties that characterize this class of polythiophene derivatives. Furthermore, the stability of the monomer under ambient conditions has allowed the preparation of a variety of derivatives. From the point of view of electrochromic materials, it has been demonstrated that even the simple derivatization with alkyl chains of different length, can affect the polymer band gap and its absorption spectrum.⁵³ Moreover, derivatives with long alkyl chains possess higher cyclability and shorter switching time, as a consequence of the facilitated inward/outward motion of counterions.¹¹⁶ Longer alkyl chains allow the obtainment of polymers that are soluble in their reduced form with obvious improvements from the point of view of processability.

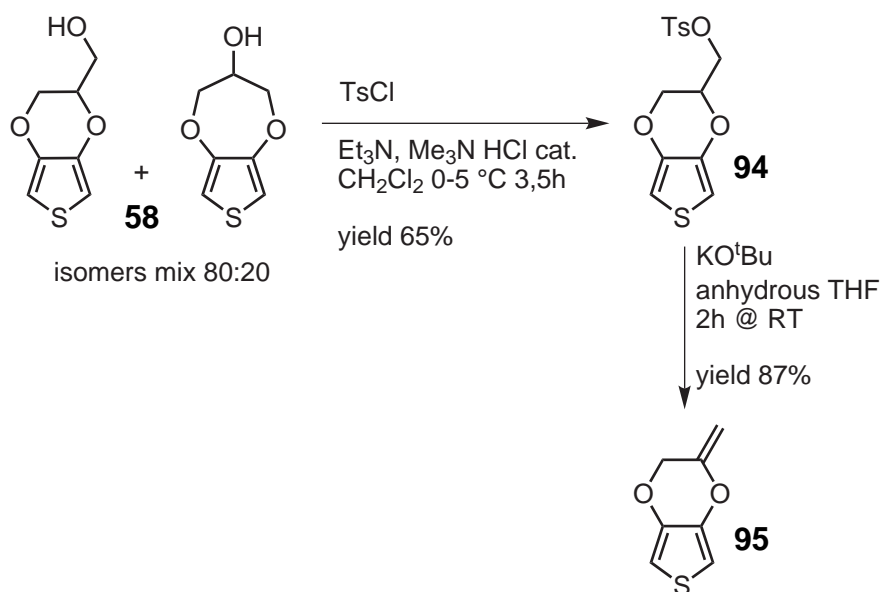
Beside electrochromics, the interest in combining the characteristics of PEDOT with various additional properties has driven the research efforts toward the development of new derivatives and new synthetic approaches.^{112,341} The attainment of EDOT derivatives that maintain the structural unit of the parent

monomer implies a derivatization on the ethylenedioxy bridge. The most used intermediate for the development of this kind of derivatives is EDOT-MeOH. This versatile building block can be obtained through a well established synthetic scheme and is now also commercially available. This derivative can be further functionalized through esterification,¹¹⁸ Williamson ether synthesis^{116,342} or reaction with isocyanates³⁴³. In order to overcome some limitations imposed by the chemistry of EDOT-MeOH, opening the way to new EDOT derivatives, EDOT-CH₂Cl was synthesized. This derivative can undergo nucleophilic substitution reactions with displacement of the chlorine atom.^{290,291,344,345} Another interesting synthon is azidomethyl-EDOT that can easily undergo 1,3-dipolar cycloadditions (click chemistry) with alkynes, even in a post-functionalization approach.²⁹⁵

In view of these considerations, the development of a new versatile intermediate for the preparation of EDOT derivatives, is of great interest since it would allow to access new classes of functional compounds. In this contribution, we describe the synthesis of a new EDOT derivative, *exo*-methylene-EDOT (emEDOT). The chemistry of this compound makes it the ideal synthon for the preparation of a new class of EDOT derivatives.

4.2 Synthesis of exomethylene-EDOT (emEDOT)

The title compound can be easily prepared following the scheme depicted in scheme 4.1. The starting material for this preparation is the commercially available EDOT-MeOH. This starting material can be easily prepared following a well established synthetic protocol.³⁴⁶ However, this synthetic scheme leads to an isomeric mixture of EDOT-MeOH and ProDOT-OH that is difficult to separate. It is worth noting that our synthetic protocol bypass this step performing the separation by simple crystallization of the isomeric mixture of the tosylate esters from methanol. These are obtained from the isomeric mixture of EDOT-MeOH and ProDOT-OH by esterification with *p*-toluenesulfonyl chloride in CH₂Cl₂ using a mixture of Et₃N and Me₃N·HCl as catalysts.³⁴⁷ The obtained pure EDOT-MeOH tosylate **94**, hereafter EDOT-MeOTs, is then dissolved in THF at room temperature and treated with KO*t*-Bu under N₂ atmosphere. Under this conditions it readily undergoes elimination to yield the desired exomethylene-EDOT in high yield as a colourless liquid. The reactivity of compound **95** was subsequently tested. In particular the ability of its vinyl ether functionality to undergo acid catalyzed addition of alcohols and radicalic



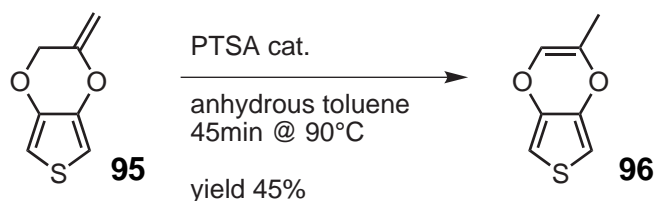
Scheme 4.1

addition of thiols were explored.

4.3 Reactivity of the *exo*-methylene group

4.3.1 Acid catalyzed isomerization

Product **95** undergoes a fast acid catalyzed isomerization (scheme 4.2) to give compound **96**, upon treatment of a toluene solution of the same with anhydrous *p*-toluenesulfonic acid at 90 °C. This interesting compound is a methyl substituted derivative of 3,4-vinylendioxythiophene (VDOT). The latter represented a long-sought derivative, and was finally reported by Roncali *et al.*³⁴⁸ in 2005. The interest in this compound was dictated by the planarization of the six-membered ring induced by the double bond.^{349,350} This effect deeply alter the electrochemical properties of the monomer resulting in an unsuccessful electropolymerization. In our case, the observed isomerization was attributed to the higher thermodynamic stability of compound **96**. This can be a simple consequence of the higher substitution of the double bond (Saytzeff's rule) but a contribution from the electronic effects on the thiophene ring cannot be excluded.



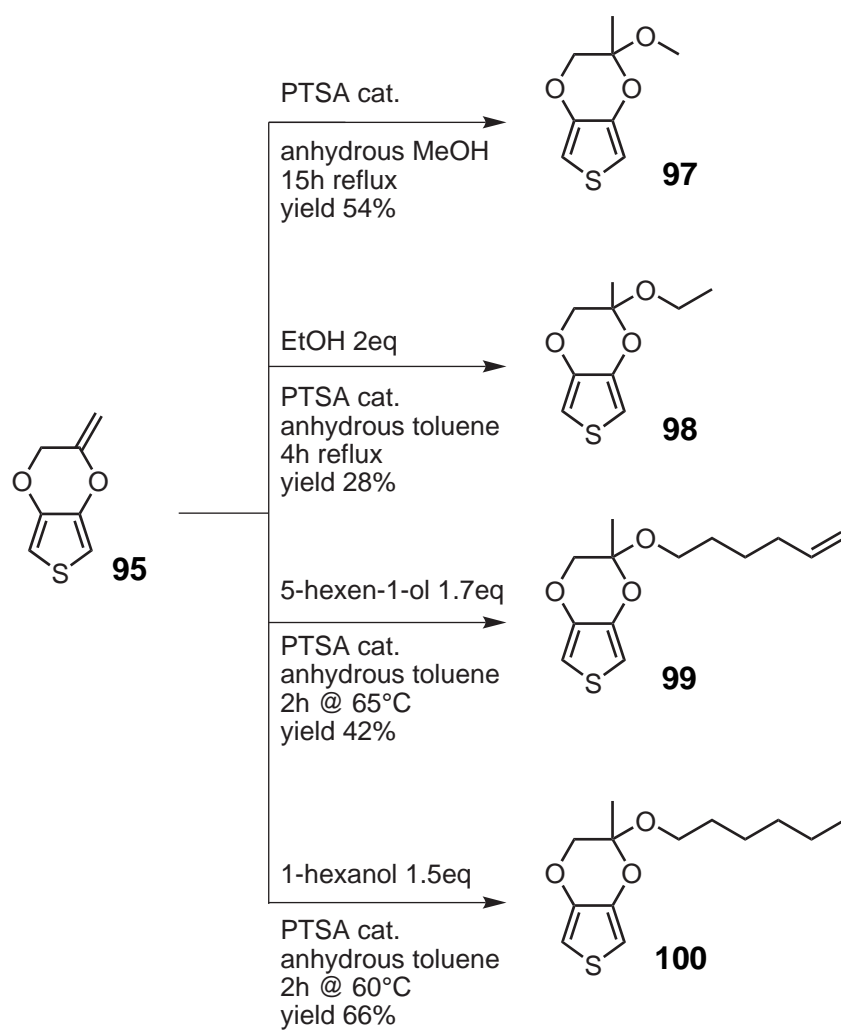
Scheme 4.2

4.3.2 Acid catalyzed addition of alcohols

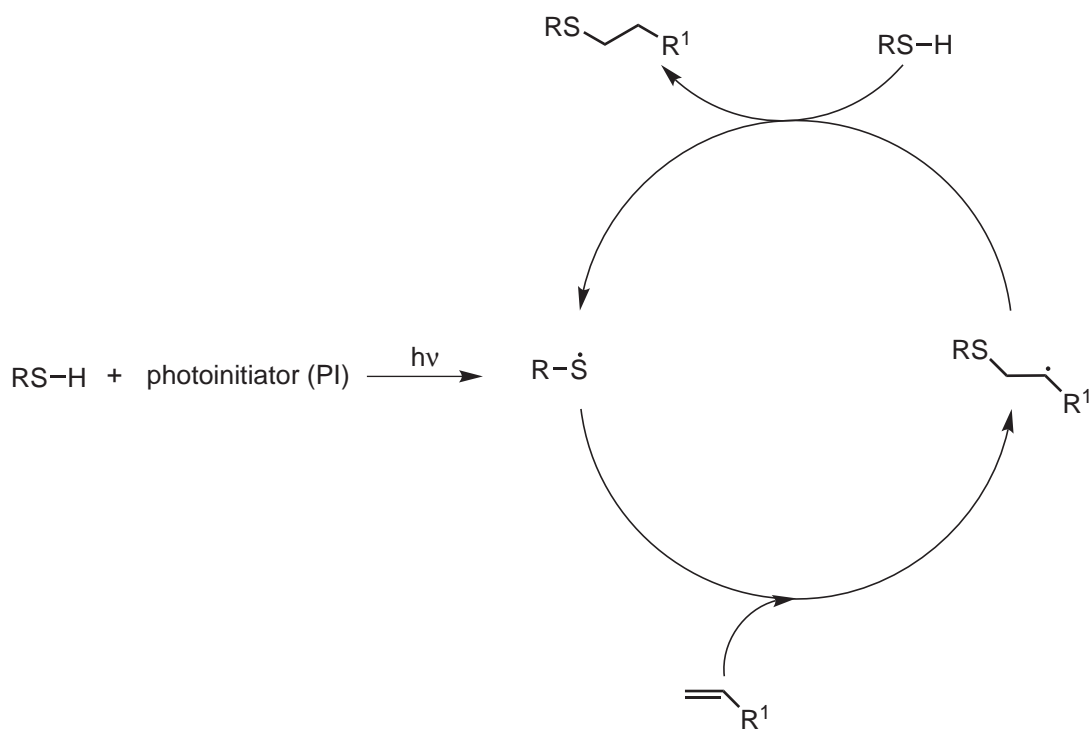
Under similar conditions, but using lower temperatures and in the presence of alcohols, an acid catalysed addition to the double bond is observed (scheme 4.3). This reaction can be performed both using solutions of the reagents in an inert solvent (anhydrous toluene), or without solvent, with excess of alcohol. A careful control of the reaction temperature proved to allow attainment of the desired products in good yields. The alcohol addition proceeds, as expected, on the more substituted position of the double bond, supporting an underlying carbocationic mechanism (Markovnikov's rule). The electrochemical properties of these new and easily prepared compounds have been tested. These products possess a ketal functionality that might exhibit an equilibrium with the corresponding emiketal and ketone under the proper conditions. However, this reactivity has not been explored yet.

4.3.3 Radical addition of thiols

Although thiols can add to double bonds via a carbocationic mechanism giving the Markovnikov product, in presence of radical initiators or photochemically, a radicalic mechanism leading to the anti-Markovnikov product takes place. This latter pathway is also known as the thiol-ene reaction and has been the subject of a number of recent reviews.³⁵¹⁻³⁵⁵ This hydrothiolation reaction has been known for 100 years³⁵⁶, but has recently received a renovated interest from the scientific community as a consequence of its unconventional characteristics. These include an high versatility that make it applicable to a wide range of different alkenes and thiols, extreme rapidity (can go to complete conversion in a matter of seconds), regioselectivity and high yields. Furthermore, it is very tolerant to the presence of oxygen and moisture. All these features made this reaction to be considered part of the so-called "click" reactions, following the criteria defined by Sharpless.³⁵⁷ The mechanism of the reaction is depicted in scheme 4.4.



Scheme 4.3



Scheme 4.4 Radicalic mechanism of the thiol-ene reaction.

Despite its general applicability, different substrates have different reactivities in the thiol-ene reaction. Nevertheless, general trends have been identified during studies in the field of polymer chemistry.^{358,359} In particular, the reactivity of the alkene under radicalic conditions is known to follow the order: norbornene > vinyl ether > propenyl > alkene \simeq vinyl ester > *N*-vinylamide > allyl ether \simeq allyl triazine \simeq allyl isocyanurate > acrylate > *N*-substituted maleimide > acrylonitrile \simeq methacrylate > styrene > conjugated diene. Furthermore, the reactivity of terminal alkenes is known to be higher compared to internal ones. In light of this consideration, compound **95** is expected to be a perfect candidate to exploit this reaction.

In order to test the reactivity of compound **95** in the thiol-ene reaction, we performed a test reaction with 11-mercaptoundecanoic acid in CD₃OD, following the same by NMR. In absence of any initiator, under UV irradiation at 365 nm from an handheld UV lamp, the reaction proceeds slowly. As demonstrated by the NMR spectra in figure 4.1, after 3 days of irradiation the reagents are still present in the mixture, and a 63% conversion is attained. Under otherwise identical conditions, the presence of a catalytic amount of 2,2-dimethoxy-2-phenylacetophenone (DMPA) as photoinitiator drives the reaction to a 91.7% conversion in 90 min (figure 4.2). Interestingly, a closer look at the spectrum reveals

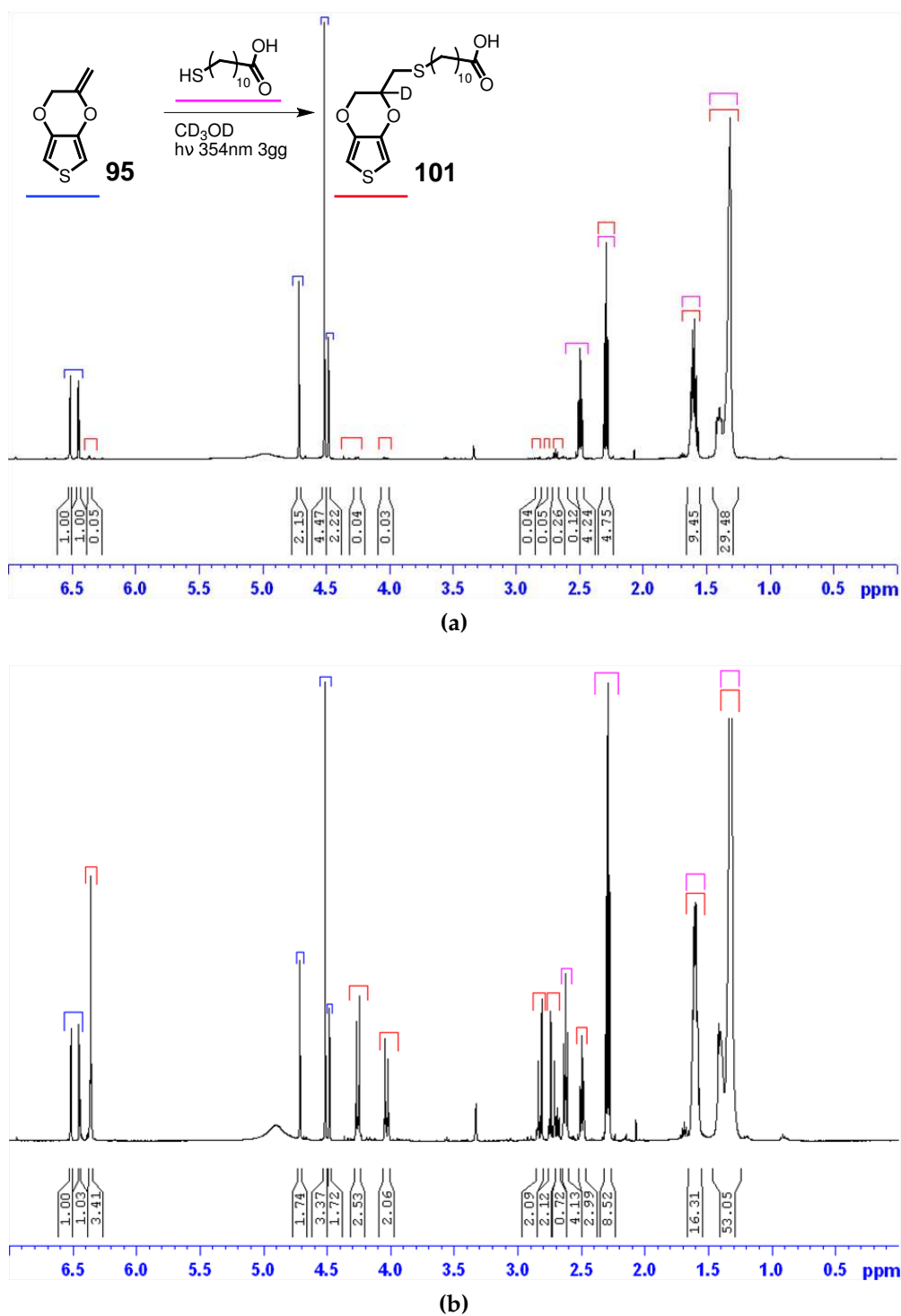


Figure 4.1 Photocatalyzed thiol-ene reaction between **95** (0.43 mmol) and 11-mercaptoundecanoic acid (0.43 mmol in CD₃OD (0.7 ml) under irradiation at 365 nm in an NMR tube. a) before irradiation; b) after 3 days of irradiation.

the absence of the signal of the proton on the tertiary carbon on the ethylene-dioxy bridge of **101**, along with the couplings between this proton and the two diastereoisomeric proton couples close to it. This phenomenon is due to the deuteration of this position during the reaction as a consequence of a transfer of the radical to the solvent. This hypothesis was confirmed performing the same reaction in nondeuterated methanol. The excellent conversion achieved

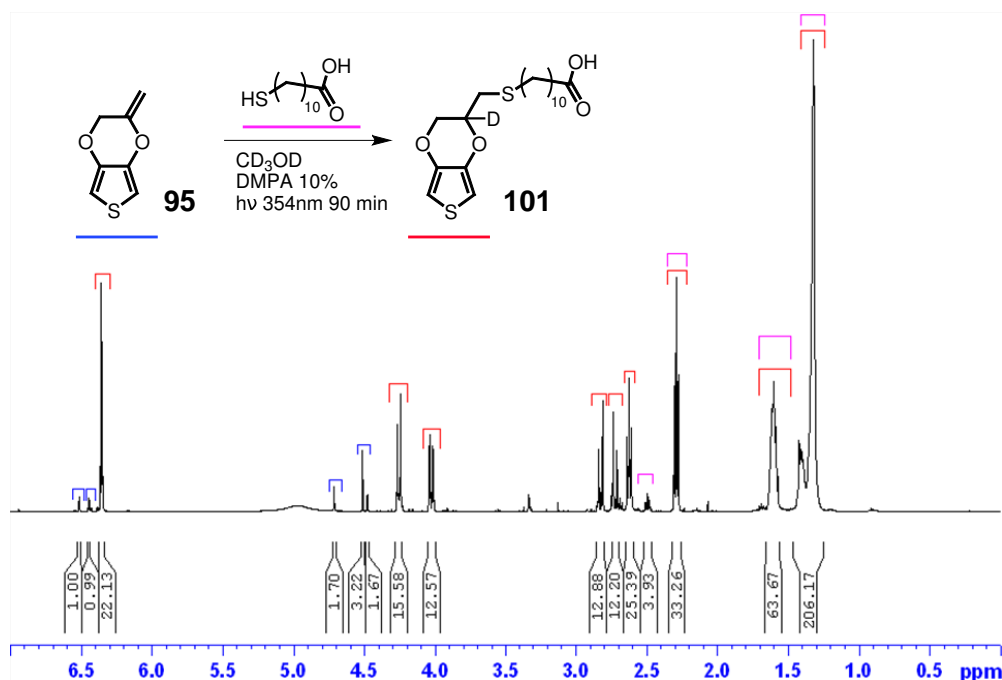


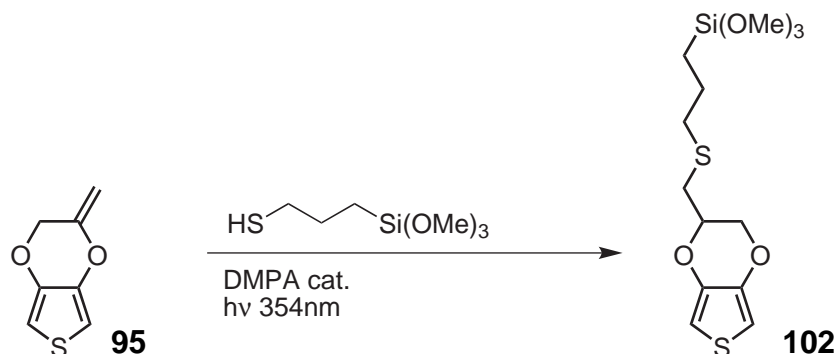
Figure 4.2 Photocatalyzed thiol-ene reaction between **95** (0.42 mmol) and 11-mercaptoundecanoic acid (0.42 mmol in CD₃OD (0.7 ml)) under irradiation at 365 nm in the presence of 10% of photoinitiator (DMPA), in an NMR tube. Spectrum was recorded after 90 min of irradiation.

testifies the applicability of the thiol-ene reaction on compound **95**. Moreover, it demonstrates the possibility to prepare the entire family of thioether derivatives easily and in high yields under very mild conditions. A comparison with known synthetic access to this class of derivatives clearly demonstrates the superiority of this protocol.³⁶⁰

As a further example in this direction, we prepared the trimethoxysilane functionalized EDOT derivative **102** by reaction of **95** with the commercially available 3-mercaptopropyltrimethoxysilane (MPTMS) without solvent in presence of 1% of DMPA as a catalyst. Under these conditions the reaction proceeds to completeness in less than 3 min of irradiation* and the obtained product can be used without further purification. To the best of our knowledge, there are

*monitored by ATR-IR spectroscopy

no reported examples of EDOT monomers which possess an alkyl tether tied to a trialkoxysilane moiety. Nonetheless, examples of this kind exist for pyrrole^{361,362} and thiophene³⁶³ monomers.



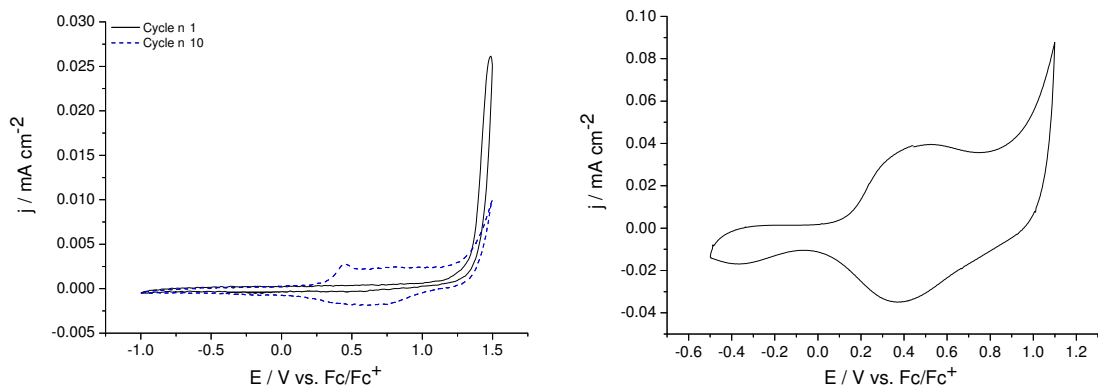
Scheme 4.5 Synthesis of the trialkoxysilane functionalized derivative **102**.

4.4 Electrochemical characterization of the derivatives

4.4.1 emEDOT and methyl-VDOT

The cyclic voltammogram of compound **95**, depicted in figure 4.3a, shows the onset of an oxidative process at 1.2V. On further cycling current peaks in the region between 0.3 and 0.8V appear as a consequence of the deposition of electroactive oligomers and polymers on the electrode surface. However, the current in this region rises very slowly with the number of cycles, and a very thin film of material is obtained. Moreover, the deposited material possesses low reversibility as testified by the difference in anodic and cathodic charges in the cyclic voltammogram in figure 4.3b. These results demonstrate that **95** exhibits a very inefficient polymerization process. The reason for this behaviour might be related to a low reactivity of the cation radical as a consequence of the presence of the double bond.

A similar behavior is observed for the isomer **96**. Despite the presence of an oxidation process with an onset around 0.6V, the cyclic voltammogram of this compound (Fig. 4.4) does not show any increase in current upon repetitive cycling. This clearly indicates that, in this case, polymerization is completely hindered. This confirms the observations of Roncali *et al.* on the parent compound VDOT.³⁴⁸



(a) Cyclic voltammogram of a 10^{-2} M solution of **95** in 0.1 M $\text{Bu}_4\text{NPF}_6/\text{CH}_2\text{Cl}_2$; scan rate 50 mV s^{-1} , WE gold pin.

(b) Cyclic voltammogram of poly(**95**) in 0.1 M $\text{Bu}_4\text{NPF}_6/\text{CH}_2\text{Cl}_2$ monomer-free solution; scan rate 50 mV s^{-1} . Polymer was deposited by LSV on glass/FTO.

Figure 4.3 Electrochemical characterization of compound **95**.

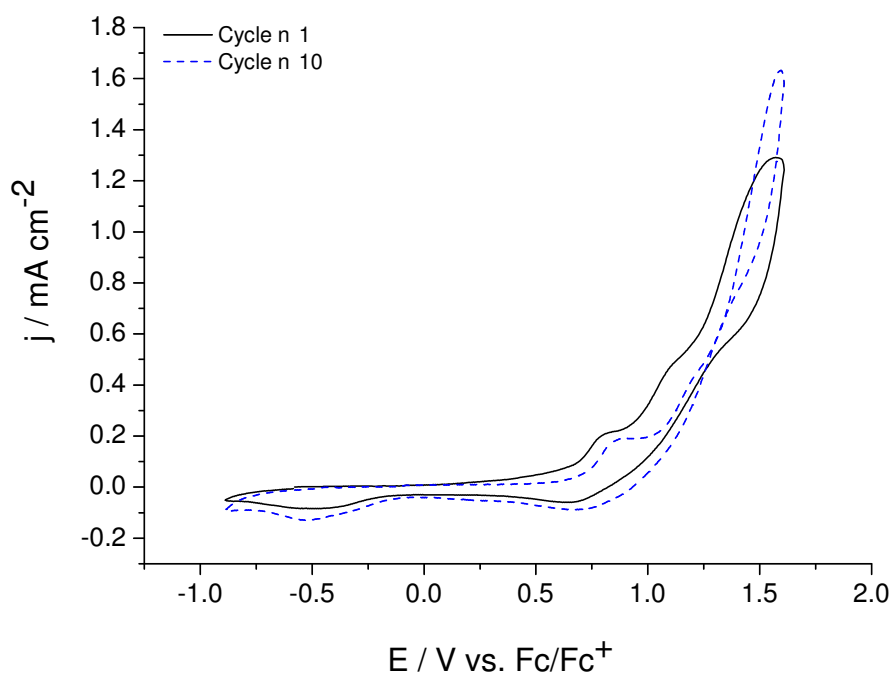
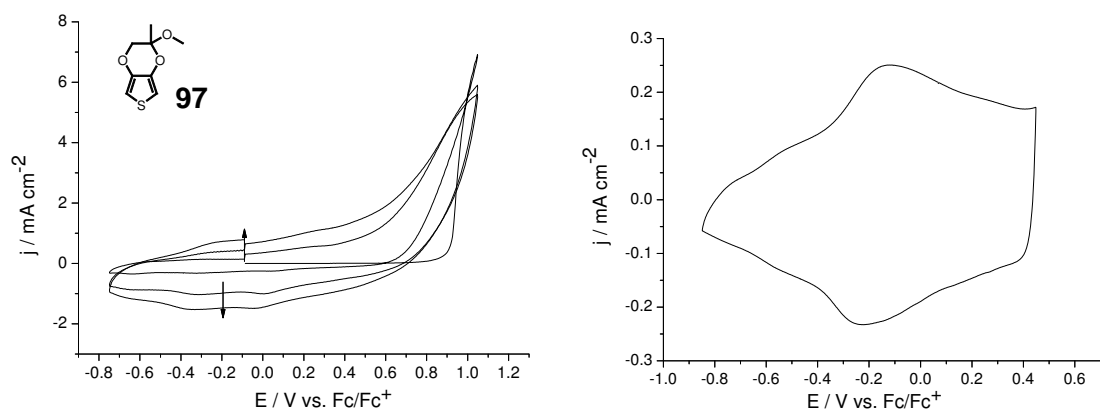


Figure 4.4 Cyclic voltammogram of a 10^{-2} M solution of **96** in 0.1 M $\text{Bu}_4\text{NClO}_4/\text{CH}_2\text{Cl}_2$; scan rate 50 mV s^{-1} , WE gold pin.

4.4.2 2-alkoxy-2-methyl-2,3-dihydrothieno[3,4-*b*][1,4]dioxines

The title compounds, obtained by acid catalyzed additions of alcohols to the exomethylene moiety, show a markedly different electrochemical behaviour from their precursor. The cyclic voltammogram of **97** (Fig. 4.5a) shows the presence of an oxidation process with an onset at 0.94 V vs. Fc/Fc⁺ in the first cycle, and a typical nucleation loop on the reverse scan. This features, combined with the observed increment of current intensities upon cycling, clearly demonstrate that a polymerization takes place with concomitant deposition of electroactive material on the electrode surface. The cyclic voltammogram of the obtained poly(**97**) in a monomer-free solution (Fig. 4.5b) displays a reversible redox process between -0.8 and 0.4 V that is unchanged upon cycling. The spectroelec-



(a) Cyclic voltammogram of a 8×10^{-3} M solution of **95** in 0.1 M $\text{Bu}_4\text{NClO}_4/\text{MeCN}$; scan rate 50 mV s^{-1} .

(b) Cyclic voltammogram of poly(**97**) in 0.1 M $\text{Bu}_4\text{NClO}_4/\text{MeCN}$ monomer-free solution; scan rate 50 mV s^{-1} . Polymer was deposited galvanostatically at 2.5 mA cm^{-2} with a total charge of 15 mC cm^{-2} on FTO/glass.

Figure 4.5

trogram of poly(**97**), depicted in figure 4.6, shows the emergence of a broad absorption band centred at 572 nm on the cathodic scan. This transition is accompanied by a change in the colour of the film from light blueish-grey to indigo. The spectrum of the oxidized film shows the presence of a very broad NIR centered band that tails in the visible region. However, this band does not seem to decay smoothly, as in other EDOT derivatives, but presents many distinguishable shoulders. A similar feature can be noted also in the band of the reduced form. In light of these observation, we suspect the presence of oligomers in the deposited material, as a consequence of an inefficient polymerization process. Polymerization proved to become more difficult on elongation of the alkyl chains. In particular derivative **98**, although still polymerizable, leads to a ma-

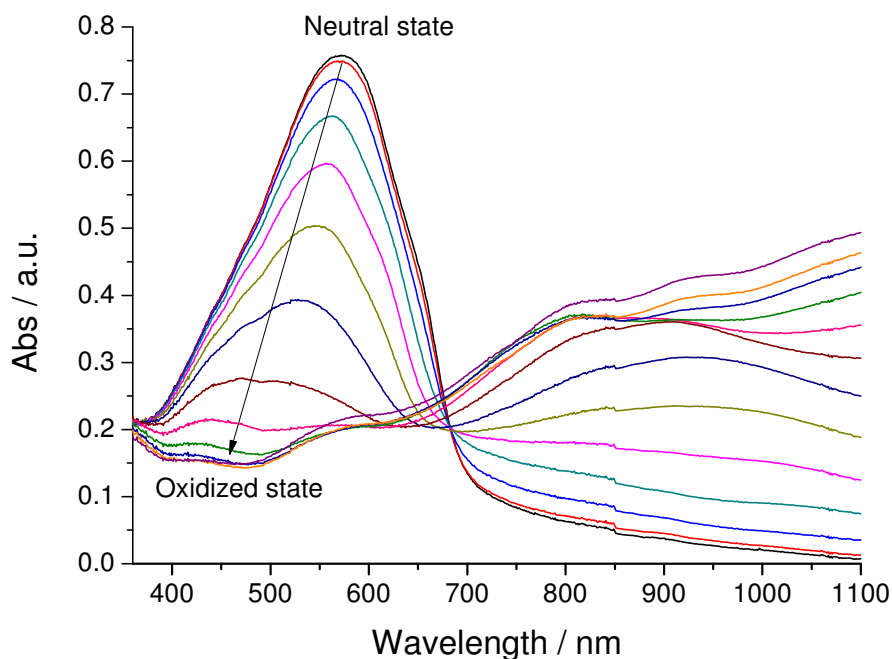
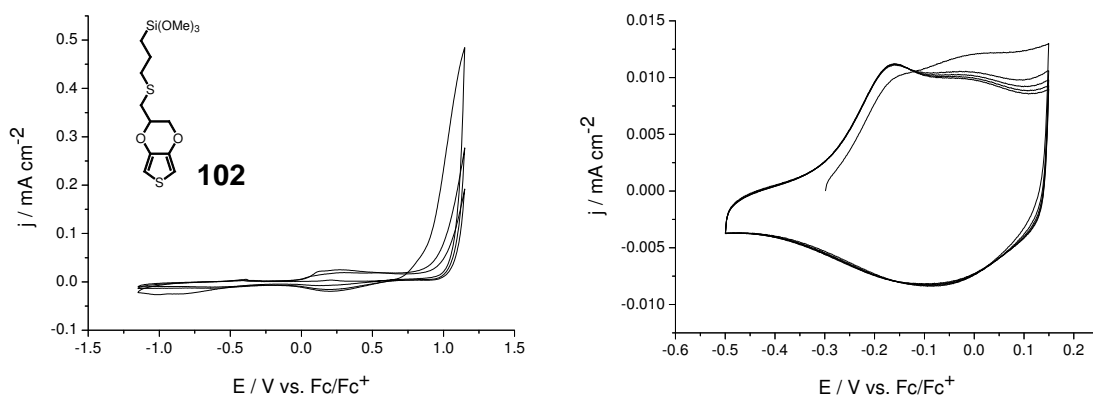


Figure 4.6 Spectroelectrogram of poly(97) in 0.1 M $\text{Bu}_4\text{NClO}_4/\text{MeCN}$ monomer-free solution; scan rate 50 mV s^{-1} . Polymer was deposited galvanostatically at 2.5 mA cm^{-2} with a total charge of 15 mA cm^{-2} .

terial with lower electrochemical reversibility. Its spectroelectrogram presents a strongly absorptive, broad and featureless oxidized state resulting from the presence of oligomers of different lengths and a broad blue shifted band in the reduced state with very low contrast. Attempts to polymerize derivatives **99** and **100** lead to passivation of the working electrode due to inhomogeneous growth of insulating material.

4.4.3 EDOT-(methyl)(3-(trimethoxysilyl)propyl)sulfide

As we will discuss in more detail in the forthcoming section, the title compound **102** represent a fascinating EDOT derivative. The trialkoxysilane functionality can in principle strongly enhance the adhesion of the deposited material to the metal oxide substrates and impart rigidity to the matrix through crosslinking of the PEDOT chains. Our preliminary tests demonstrate that this derivative can be successfully electrochemically polymerized obtaining stable polymeric layers. The cyclic voltammogram of **102** (Fig. 4.7a), in fact, shows an oxidation process with an onset at $0.92 \text{ V vs. Fc/Fc}^+$. This process is accompanied by an increase in current in the $0.0\text{-}0.6 \text{ V}$ potential window that testifies the deposition of electroactive material on the electrode surface. Moreover, the cyclic voltammogram of the polymeric layer, cycled in monomer-free electrolytic solution,



(a) Cyclic voltammogram of a 1.0×10^{-2} M solution of **102** in 0.1 M Bu₄NClO₄/MeCN; scan rate 50 mV s⁻¹.

(b) Spectroelectrogram of poly(**102**) in 0.1 M Bu₄NClO₄/MeCN monomer-free solution; scan rate 50 mV s⁻¹. Polymer was deposited by LSV on an FTO/glass electrode from a 10⁻² M solution of the monomer.

Figure 4.7

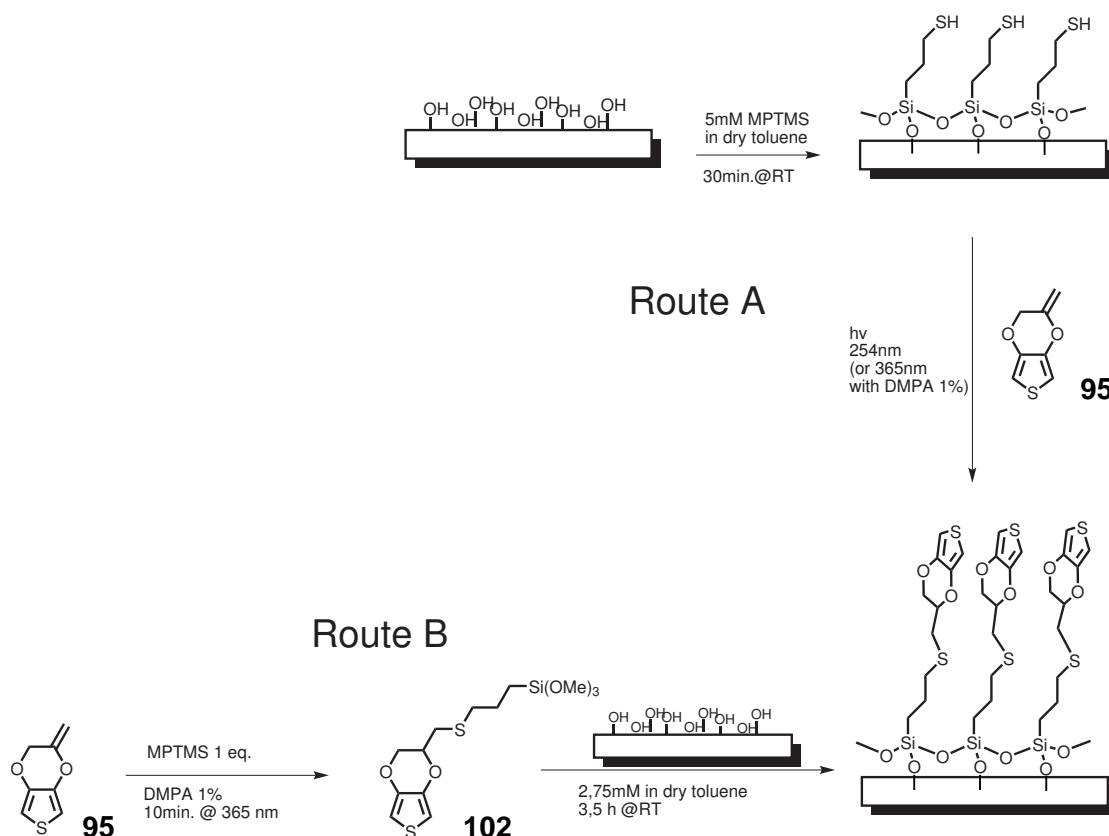
shows the presence of a reversible redox process that is stable upon repetitive cycling. This redox activity is confined in a rather narrow potential window (-0.35-0.15 V) with respect to common EDOT derivatives. This effect may be due to the presence of low molecular weight oligomers rather than long polymeric chains. Nevertheless, the observed cycling stability demonstrates the robust attachment of these species to the electrode surface.

4.5 Surface functionalizations

One of the main problems encountered in the deposition of conjugated polymers on silicon or metal oxides is connected with the adhesion of the organic semiconductor to the substrate. This represents a key factor in determining the long-term operation of devices, including electrochromic ones. As we mentioned in section 1.4.1.8, adhesion is usually assured by deposition of a so-called adhesion promoter, usually composed by a very thin film of PEDOT:PSS or silane coupling agent. In the latter case, γ -glycidoxypropyltrimethoxysilane is usually employed. Coupling layers of this type allow to obtain stronger adhesion forces between the polymeric chains and the substrate, thus making delamination of the film more difficult to occur. It is easy to understand that a covalent linkage between the polymer chains and the substrate would represent the best possible solution to the adhesion problems. This latter consideration motivated the efforts of different groups in this direction. In particular, silane

functionalized pyrrole moieties have been tested as adhesion promoters by different groups and their beneficial effect on the adhesion of polypyrrole films to the underlying substrate was demonstrated.^{361,362,364-366} Examples of this kind have not been reported for EDOT based polymers, probably as a consequence of the more difficult derivatization of this monomer. In light of these considerations, our easily prepared trialkoxysilane functionalized EDOT (**102**) may represent a valuable adhesion promoter for EDOT layers. In section 4.4.3 we showed that **102** can be electrochemically polymerized on an electrode surface to give a strongly adherent polymeric film. We will now illustrate two different approaches to surface functionalization with ultrathin layers of covalently attached EDOT monomers.

In order to obtain surface functionalization, two different routes, illustrated in scheme 4.6, were tested. The first one (route A) takes advantage of an *in situ* thiol-ene reaction between surface attached thiol groups and compound **95**, while the second (route B) consists in a solution deposition of the preformed silane **102** on clean substrates. In the first case, thiol layers are prepared by



Scheme 4.6 Synthetic strategies for surface functionalization with EDOT monomers. Route A: *in situ* thiol-ene reaction. Route B: deposition of a layer of **102** from solution.

treatment of piranha cleaned substrates (quartz and silicon) with a 5 mM solution of commercially available 3-mercaptopropyltrimetoxysilane (MPTMS) in anhydrous toluene following a procedure similar to the one described by Hu *et al.*³⁶⁷ The obtained layers were characterized by ellipsometry, synchrotron XRR and AFM. The first technique gave a thickness of 8.0 Å for the deposited layer, while the second reported a value of 8.9 Å with a roughness of 5 Å. The obtained data was further confirmed by the AFM images that show the presence of big polymeric agglomerates on an otherwise smooth surface (Fig. 4.5). Prior to utilization, the layers were treated with a 100 mM dithiothreitol solu-

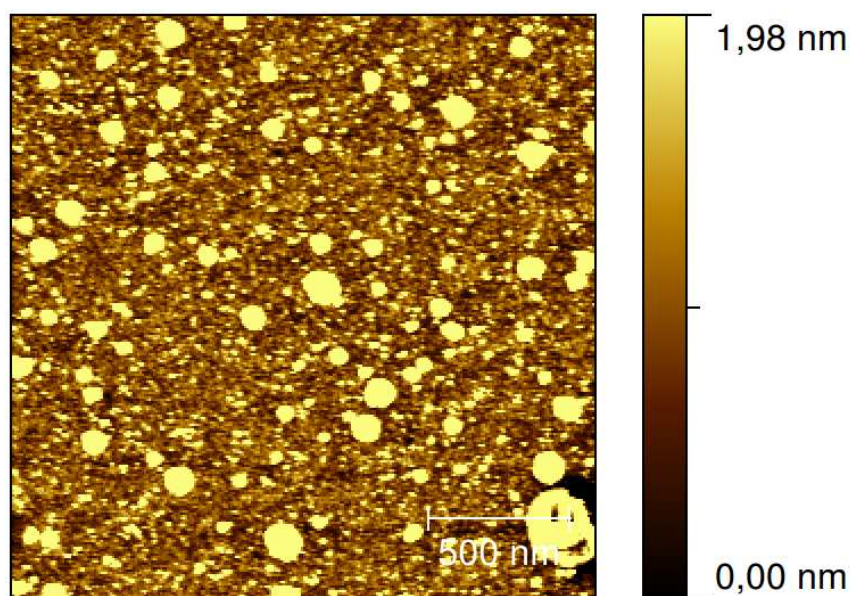


Figure 4.8 AFM image of a Si:100 surface functionalized with MPTMS by treatment with a 5 mM solution of the same.

tion in 10 mM sodium phosphate buffer to reduce the S–S bonds eventually formed.³⁶⁸ The thiol functionalized substrates were finally covered with a film of **95** and exposed to UV radiation from an handheld UV lamp. A 254 nm radiation was used in absence of initiator while a 365 nm one was adopted with the addition of 1% DMPA to the deposited **95**.

In contrast, the second procedure (route B) involved a simple solution deposition of **102** by treatment of the clean substrates (quartz and silicon) with a 2.75 mM solution of the same in anhydrous toluene. XRR data for the obtained samples show a layer thickness of 6.7 Å with a roughness of 3.6 Å. We suppose that this low thickness value, combined with the high roughness, is the result of low coverage of the substrate and the presence of disordered SAM with the

molecules bent over toward the surface The UV/Vis spectra of the quartz sub-

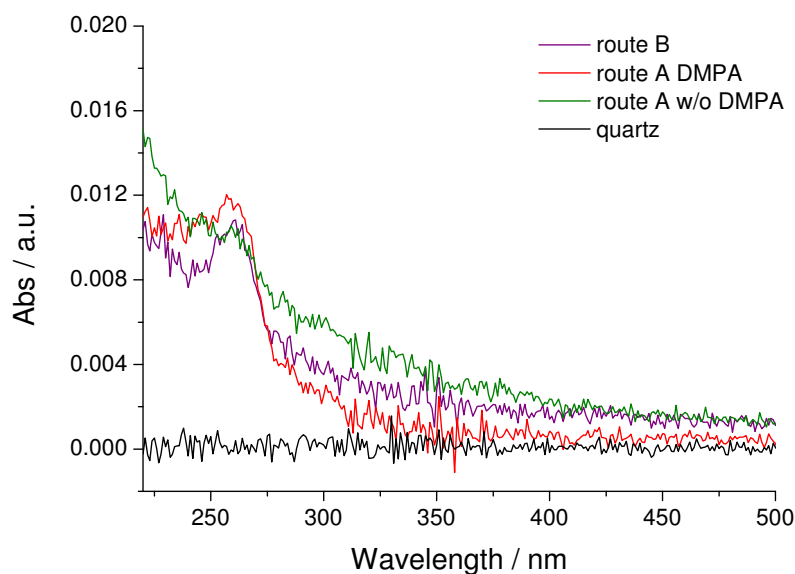


Figure 4.9

strates (Fig. 4.9) show, after functionalization, the presence of a UV centred absorption band around 258nm that does not decrease in intensity after rubbing the surface with paper tissue. This evidence further confirms the attained covalent anchoring of EDOT monomers on the surfaces.

4.6 Conclusions

In this chapter, we have described the synthesis of the new EDOT derivative **95** and discussed its potential application as a versatile synthon for EDOT derivatization. Derivative **95**, in fact, easily undergoes addition reactions with alcohols under acid catalysis at moderate temperatures. We thus prepared four different derivatives: **97**, **98**, **99** and **100**. Unfortunately, these compounds do not efficiently electropolymerize. Electrochemically stable polymeric layers were obtained only from derivatives **97** and **98** but a careful analysis revealed the presence of oligomeric species. Nevertheless, these compounds represent an important addition to the chemistry of EDOT derivatives and certainly deserve further investigation.

On the other hand, the thiol-ene reaction of **95** with thiols represents a versatile synthetic approach to a large class of EDOT derivatives with general structure EDOT-CH₂SR, some of which have been described by Sallé *et al.*³⁶⁰ As

an example, the reaction of **95** with 11-mercaptoundecanoic acid was tested obtaining a high yield in a short reaction time. Moreover, we exploited further this reactivity synthesizing the trimethoxysilane functionalized EDOT derivative **102**. This new interesting derivative proved to be electropolymerizable forming a stable adherent layer on the electrode.

We also demonstrated the possibility to obtain surfaces covalently functionalized with EDOT moieties by taking advantage of the reactivity of the trimethoxysilane group. A similar functionalization proved to be obtainable even performing an *in situ* thiol-ene reaction between a thiol functionalized surface and compound **95**. This kind of EDOT functionalized surfaces can, in principle, outperform the existing silane based coupling layers currently used in the deposition of EDOT based conjugated polymers.

References

1. R. M. Paul Monk, D. Rosseinsky, *Electrochromism and Electrochromic Devices*, Cambridge University Press, **2007**, DOI [10.1017/CBO9780511550959](https://doi.org/10.1017/CBO9780511550959).
2. R. J. Mortimer, *Chem. Soc. Rev.* **1997**, *26*, 147–156, DOI [10.1039/CS9972600147](https://doi.org/10.1039/CS9972600147).
3. R. J. Mortimer, A. L. Dyer, J. R. Reynolds, *Displays* **2006**, *27*, 2–18, DOI [10.1016/j.displa.2005.03.003](https://doi.org/10.1016/j.displa.2005.03.003).
4. K. Bange, T. Gambke, *Advanced Materials* **1990**, *2*, 10–16, DOI [10.1002/adma.19900020103](https://doi.org/10.1002/adma.19900020103).
5. R. M. Paul Monk, D. Rosseinsky, *Electrochromism: Fundamentals and Applications*, Wiley VCH, **1995**.
6. J. Y. Lim, H. C. Ko, H. Lee, *Synthetic Metals* **2005**, *155*, 595–598, DOI [10.1016/j.synthmet.2005.09.040](https://doi.org/10.1016/j.synthmet.2005.09.040).
7. J. Padilla, V. Seshadri, G. Sotzing, T. Otero, *Electrochemistry Communications* **2007**, *9*, 1931–1935, DOI [10.1016/j.elecom.2007.05.004](https://doi.org/10.1016/j.elecom.2007.05.004).
8. T. Pauporte, *Journal of The Electrochemical Society* **2002**, *149*, C539–C545, DOI [10.1149/1.1509070](https://doi.org/10.1149/1.1509070).
9. M. Deepa, A. Srivastava, S. Singh, S. Agnihotry, *Journal of Materials Research* **2004**, *19*, 2576–2585, DOI [10.1557/JMR.2004.0336](https://doi.org/10.1557/JMR.2004.0336).
10. A. Bessi re, J. C. Badot, M. Certiat, J. Livage, V. Lucas, N. Baffier, *Electrochimica Acta* **2001**, *46*, 2251–2256, DOI [10.1016/S0013-4686\(01\)00383-8](https://doi.org/10.1016/S0013-4686(01)00383-8).
11. L. D. Kadam, P. S. Patil, *Solar Energy Materials and Solar Cells* **2001**, *69*, 361–369, DOI [10.1016/S0927-0248\(00\)00403-7](https://doi.org/10.1016/S0927-0248(00)00403-7).
12. F. J. Green, *The Sigma-Aldrich Handbook of Stains, Dyes and Indicators*, Aldrich Chem Co Library, **1990**.
13. C. L. Gaupp, D. M. Welsh, R. D. Rauh, J. R. Reynolds, *Chemistry of Materials* **2002**, *14*, 3964–3970, DOI [10.1021/cm020433w](https://doi.org/10.1021/cm020433w).
14. J. P. Lock, J. L. Lutkenhaus, N. S. Zacharia, S. G. Im, P. T. Hammond, K. K. Gleason, *Synthetic Metals* **2007**, *157*, 894–898, DOI [10.1016/j.synthmet.2007.08.022](https://doi.org/10.1016/j.synthmet.2007.08.022).
15. R. Mortimer, J. Reynolds, *J. Mater. Chem.* **2005**, *15*, 2226–2233, DOI [10.1039/B418771G](https://doi.org/10.1039/B418771G).

16. *Colorimetry: Understanding the CIE System*, (Ed.: J. Schanda), Wiley-Interscience, 2007.
17. D. L. Macadam, *J. Opt. Soc. Am.* **1942**, 32, 247–273, DOI 10.1364/JOSA.32.000247.
18. B. C. Thompson, P. Schottland, K. Zong, J. R. Reynolds, *Chemistry of Materials* **2000**, 12, 1563–1571, DOI 10.1021/cm000097o.
19. G. Sonmez, C. K. F. Shen, Y. Rubin, F. Wudl, *Angewandte Chemie International Edition* **2004**, 43, 1498–1502, DOI 10.1002/anie.200352910.
20. P. M. Beaujuge, S. Ellinger, J. R. Reynolds, *Nat Mater* **2008**, 7, 795–799, DOI 10.1038/nmat2272.
21. P. Shi, C. M. Amb, E. P. Knott, E. J. Thompson, D. Y. Liu, J. Mei, A. L. Dyer, J. R. Reynolds, *Advanced Materials* **2010**, 22, 4949–4953, DOI 10.1002/adma.201002234.
22. A. S. for Testing Materials, E308-08. *Standard Method for Computing the Colors of Objects by Using the CIE system*, 2008, DOI 10.1520/E0308-08.
23. R. J. Mortimer, T. S. Varley, *Displays* **2011**, 32, 35–44, DOI 10.1016/j.displa.2010.10.001.
24. B. J. Lindbloom, *Spectral Calculator Spreadsheets*, <http://www.brucelindbloom.com/index.html?SpectCalcSpreadsheets.html>, 2011.
25. C. M. Amb, A. L. Dyer, J. R. Reynolds, *Chemistry of Materials* **2011**, 23, 397–415, DOI 10.1021/cm1021245.
26. G. Sonmez, H. B. Sonmez, C. K. F. Shen, R. W. Jost, Y. Rubin, F. Wudl, *Macromolecules* **2005**, 38, 669–675, DOI 10.1021/ma0484173.
27. C. M. Amb, J. A. Kerszulis, E. J. Thompson, A. L. Dyer, J. R. Reynolds, *Polym. Chem.* **2011**, 2, 812–814, DOI 10.1039/C0PY00405G.
28. R. J. Mortimer, *Annual Review of Materials Research* **2011**, 41, 1–28, DOI 10.1146/annurev-matsci-062910-100344.
29. J. Berzelius, *Afh. Fys. Kemi Miner.* **1815**, 4, 293.
30. N. Kobosew, N. Nekrassow, *Z. Elektrochem.* **1930**, 36, 529.
31. S. K. Deb, *Solar Energy Materials and Solar Cells* **2008**, 92, 245–258, DOI 10.1016/j.solmat.2007.01.026.
32. Gmelin, *Handbuch der Anorganischen Chemie*, Vol. 59, Eisen B, Frankfurt am Main, Deutsche Chemische Gesellschaft, 1930, p. 671.
33. M. B. Robin, *Inorganic Chemistry* **1962**, 1, 337–342, DOI 10.1021/ic50002a028.
34. V. D. Neff, *Journal of The Electrochemical Society* **1978**, 125, 886–887, DOI 10.1149/1.2131575.
35. R. J. Mortimer, D. R. Rosseinsky, A. Glidle, *Solar Energy Materials and Solar Cells* **1992**, 25, 211–223, DOI 10.1016/0927-0248(92)90069-2.

-
36. R. J. Mortimer, D. R. Rosseinsky, *J. Chem. Soc. Dalton Trans.* **1984**, 2059–2062, DOI [10.1039/DT9840002059](https://doi.org/10.1039/DT9840002059).
 37. K. Itaya, K. Shibayama, H. Akahoshi, S. Toshima, *Journal of Applied Physics* **1982**, 53, 804–805, DOI [10.1063/1.329997](https://doi.org/10.1063/1.329997).
 38. M. K. Carpenter, R. S. Conell, *Journal of The Electrochemical Society* **1990**, 137, 2464–2467, DOI [10.1149/1.2086962](https://doi.org/10.1149/1.2086962).
 39. M. A. Habib, S. P. Maheswari, M. K. Carpenter, *Journal of Applied Electrochemistry* **1991**, 21, 203–207, DOI [10.1007/BF01052571](https://doi.org/10.1007/BF01052571).
 40. J.-G. Béraud, D. Deroo, *Solar Energy Materials and Solar Cells* **1993**, 31, 263–275.
 41. K.-C. Ho, *Electrochimica Acta* **1999**, 44, 3227–3235, DOI [10.1016/S0013-4686\(99\)00041-9](https://doi.org/10.1016/S0013-4686(99)00041-9).
 42. E. A. R. Duek, M.-A. De Paoli, M. Mastragostino, *Advanced Materials* **1992**, 4, 287–291, DOI [10.1002/adma.19920040410](https://doi.org/10.1002/adma.19920040410).
 43. E. A. R. Duek, M.-A. De Paoli, M. Mastragostino, *Advanced Materials* **1993**, 5, 650–652, DOI [10.1002/adma.19930050912](https://doi.org/10.1002/adma.19930050912).
 44. N. Leventis, Y. C. Chung, *Journal of The Electrochemical Society* **1990**, 137, 3321–3322, DOI [10.1149/1.2086215](https://doi.org/10.1149/1.2086215).
 45. T.-S. Tung, K.-C. Ho, *Solar Energy Materials and Solar Cells* **2006**, 90, 521–537, DOI [10.1016/j.solmat.2005.02.018](https://doi.org/10.1016/j.solmat.2005.02.018).
 46. K.-C. Chen, C.-Y. Hsu, C.-W. Hu, K.-C. Ho, *Solar Energy Materials and Solar Cells* **2011**, *In Press, Corrected Proof*, –, DOI [10.1016/j.solmat.2011.03.029](https://doi.org/10.1016/j.solmat.2011.03.029).
 47. I. F. Chang, B. L. Gilbert, T. I. Sun, *Journal of The Electrochemical Society* **1975**, 122, 955–962, DOI [10.1149/1.2134377](https://doi.org/10.1149/1.2134377).
 48. H. Shirakawa, E. J. Louis, A. G. MacDiarmid, C. K. Chiang, A. J. Heeger, *J. Chem. Soc. Chem. Commun.* **1977**, 578–580, DOI [10.1039/C39770000578](https://doi.org/10.1039/C39770000578).
 49. C. K. Chiang, M. A. Druy, S. C. Gau, A. J. Heeger, E. J. Louis, A. G. MacDiarmid, Y. W. Park, H. Shirakawa, *Journal of the American Chemical Society* **1978**, 100, 1013–1015, DOI [10.1021/ja00471a081](https://doi.org/10.1021/ja00471a081).
 50. C. K. Chiang, C. R. Fincher, Y. W. Park, A. J. Heeger, H. Shirakawa, E. J. Louis, S. C. Gau, A. G. MacDiarmid, *Phys. Rev. Lett.* **1977**, 39, 1098–1101, DOI [10.1103/PhysRevLett.39.1098](https://doi.org/10.1103/PhysRevLett.39.1098).
 51. A. J. Heeger, S. Kivelson, J. R. Schrieffer, W. P. Su, *Rev. Mod. Phys.* **1988**, 60, 781–850, DOI [10.1103/RevModPhys.60.781](https://doi.org/10.1103/RevModPhys.60.781).
 52. J. L. Bredas, G. B. Street, *Accounts of Chemical Research* **1985**, 18, 309–315, DOI [10.1021/ar00118a005](https://doi.org/10.1021/ar00118a005).
 53. P. M. Beaujuge, J. R. Reynolds, *Chemical Reviews* **2010**, 110, 268–320, DOI [10.1021/cr900129a](https://doi.org/10.1021/cr900129a).
 54. H. Letheby, *J. Chem. Soc.* **1862**, 15, 161–163, DOI [10.1039/JS8621500161](https://doi.org/10.1039/JS8621500161).
-

-
55. T. Kobayashi, H. Yoneyama, H. Tamura, *Journal of Electroanalytical Chemistry* **1984**, *161*, 419–423, DOI [http://dx.doi.org/10.1016/0022-0728\(84\)80229-6](http://dx.doi.org/10.1016/0022-0728(84)80229-6).
 56. T. Kobayashi, H. Yoneyama, H. Tamura, *Journal of Electroanalytical Chemistry and Interfacial Electrochemistry* **1984**, *177*, 281–291, DOI [10.1016/0022-0728\(84\)80229-6](https://doi.org/10.1016/0022-0728(84)80229-6).
 57. A. MacDiarmid, L. Yang, W. Huang, B. Humphrey, *Synthetic Metals* **1987**, *18*, 393–398, DOI [10.1016/0379-6779\(87\)90911-8](https://doi.org/10.1016/0379-6779(87)90911-8).
 58. R. J. Mortimer, *J. Mater. Chem.* **1995**, *5*, 969–973, DOI [10.1039/JM9950500969](https://doi.org/10.1039/JM9950500969).
 59. S. Ramirez, A. R. Hillman, *Journal of The Electrochemical Society* **1998**, *145*, 2640–6247, DOI [10.1149/1.1838693](https://doi.org/10.1149/1.1838693).
 60. G. D'Aprano, M. Leclerc, G. Zotti, *Journal of Electroanalytical Chemistry* **1993**, *351*, 145–158, DOI [10.1016/0022-0728\(93\)80230-F](https://doi.org/10.1016/0022-0728(93)80230-F).
 61. M. K. Ram, E. Maccioni, C. Nicolini, *Thin Solid Films* **1997**, *303*, 27–33, DOI [10.1016/S0040-6090\(97\)00068-0](https://doi.org/10.1016/S0040-6090(97)00068-0).
 62. W. Gazotti, R. Faez, M.-A. D. Paoli, *Journal of Electroanalytical Chemistry* **1996**, *415*, 107–113, DOI [10.1016/S0022-0728\(96\)04712-2](https://doi.org/10.1016/S0022-0728(96)04712-2).
 63. S. Shreepathi, R. Holze, *Chemistry of Materials* **2005**, *17*, 4078–4085, DOI [10.1021/cm050117s](https://doi.org/10.1021/cm050117s).
 64. J. Jang, J. Ha, J. Cho, *Advanced Materials* **2007**, *19*, 1772–1775, DOI [10.1002/adma.200602127](https://doi.org/10.1002/adma.200602127).
 65. S. J. Yoo, J. Cho, J. W. Lim, S. H. Park, J. Jang, Y.-E. Sung, *Electrochemistry Communications* **2010**, *12*, 164–167, DOI [10.1016/j.elecom.2009.11.014](https://doi.org/10.1016/j.elecom.2009.11.014).
 66. B. P. Jelle, G. Hagen, *Solar Energy Materials and Solar Cells* **1999**, *58*, 277–286, DOI [10.1016/S0927-0248\(99\)00009-4](https://doi.org/10.1016/S0927-0248(99)00009-4).
 67. M. M. Verghese, M. K. Ram, H. Vardhan, B. D. Malhotra, S. M. Ashraf, *Polymer* **1997**, *38*, 1625–1629, DOI [10.1016/S0032-3861\(96\)00655-6](https://doi.org/10.1016/S0032-3861(96)00655-6).
 68. A. Siove, D. Ades, E. N'gbilo, C. Chevrot, *Synthetic Metals* **1990**, *38*, 331–340, DOI [10.1016/0379-6779\(90\)90086-Z](https://doi.org/10.1016/0379-6779(90)90086-Z).
 69. C. Chevrot, E. Ngbilo, K. Kham, S. Sadki, *Synthetic Metals* **1996**, *81*, 201–204, DOI [10.1016/S0379-6779\(96\)03752-6](https://doi.org/10.1016/S0379-6779(96)03752-6).
 70. Y.-J. Qiu, J. R. Reynolds, *Journal of The Electrochemical Society* **1990**, *137*, 900–904, DOI [10.1149/1.2086575](https://doi.org/10.1149/1.2086575).
 71. B. Bezgin, A. Cihaner, A. M. Önal, *Thin Solid Films* **2008**, *516*, 7329–7334, DOI [10.1016/j.tsf.2008.02.003](https://doi.org/10.1016/j.tsf.2008.02.003).
 72. S. Kuwabata, H. Yoneyama, H. Tamura, *Bulletin of the Chemical Society of Japan* **1984**, *57*, 2247–2253, DOI [10.1246/bcsj.57.2247](https://doi.org/10.1246/bcsj.57.2247).
 73. M. A. De Paoli, S. Panero, P. Prospero, B. Scrosati, *Electrochimica Acta* **1990**, *35*, 1145–1148, DOI [10.1016/0013-4686\(90\)80030-R](https://doi.org/10.1016/0013-4686(90)80030-R).
-

-
74. M.-A. De Paoli, S. Panero, S. Paserini, B. Scrosati, *Advanced Materials* **1990**, *2*, 480–482, DOI 10.1002/adma.19900021007.
75. A. Diaz, J. Castillo, K. Kanazawa, J. Logan, M. Salmon, O. Fajardo, *Journal of Electroanalytical Chemistry and Interfacial Electrochemistry* **1982**, *133*, 233–239, DOI 10.1016/0368-1874(82)85140-X.
76. W. A. Gazotti, M. A. D. Paoli, G. Casalbore Miceli, A. Geri, G. Zotti, *Journal of Applied Electrochemistry* **1999**, *29*, 757–761, DOI 10.1023/A:1003585201464.
77. C. Gatti, G. Frigerio, T. Benincori, E. Brenna, F. Sannicoló, G. Zotti, S. Zecchin, G. Schiavon, *Chemistry of Materials* **2000**, *12*, 1490–1499, DOI 10.1021/cm000092r.
78. T. Benincori, E. Brenna, F. Sannicoló, G. Zotti, S. Zecchin, G. Schiavon, C. Gatti, G. Frigerio, *Chemistry of Materials* **2000**, *12*, 1480–1489, DOI 10.1021/cm000087n.
79. A. Zelikin, V. R. Shastri, R. Langer, *The Journal of Organic Chemistry* **1999**, *64*, 3379–3380, DOI 10.1021/jo9823339.
80. I. Burley, B. Bilic, A. T. Hewson, J. R. A. Newton, *Tetrahedron Letters* **2000**, *41*, 8969–8972, DOI 10.1016/S0040-4039(00)01591-4.
81. J. Freitas, L. Abrantes, T. Darbre, *Helvetica Chimica Acta* **2005**, *88*, 2470–2478, DOI 10.1002/hlca.200590183.
82. J. Roncali, *Chemical Reviews* **1992**, *92*, 711–738, DOI 10.1021/cr00012a009.
83. M. Gazard, J. C. Dubois, M. Champagne, F. Garnier, G. Tourillon, *J. Phys. Colloques* **1983**, *44*, C3–537–C3–542, DOI 10.1051/jphyscol:19833108.
84. F. Garnier, G. Tourillon, M. Gazard, J. C. Dubois, *Journal of Electroanalytical Chemistry and Interfacial Electrochemistry* **1983**, *148*, 299 – 303, DOI 10.1016/S0022-0728(83)80406-9.
85. M. A. Druy, R. J. Seymour, *J. Phys. Colloques* **1983**, *44*, C3–595–C3–598, DOI 10.1051/jphyscol:19833119.
86. M. Mastragostino, C. Arbizzani, A. Bongini, G. Barbarella, M. Zambianchi, *Electrochimica Acta* **1993**, *38*, 135–140, DOI 10.1016/0013-4686(93)80020-Z.
87. R. Elsenbaumer, K. Jen, G. Miller, L. Shacklette, *Synthetic Metals* **1987**, *18*, 277–282, DOI 10.1016/0379-6779(87)90892-7.
88. I. Osaka, R. D. McCullough, *Accounts of Chemical Research* **2008**, *41*, 1202–1214, DOI 10.1021/ar800130s.
89. J.-P. Léré-Porte, J. Moreau, C. Torrellas, *European Journal of Organic Chemistry* **2001**, *2001*, 1249–1258, DOI 10.1002/1099-0690(200104)2001:7<1249::AID-EJOC1249>3.0.CO;2-F.
90. C. Arbizzani, A. Bongini, M. Mastragostino, A. Zanelli, G. Barbarella, M. Zambianchi, *Advanced Materials* **1995**, *7*, 571–574, DOI 10.1002/adma.19950070614.
91. S. Alkan, C. Cutler, J. Reynolds, *Adv. Funct. Mater.* **2003**, *13*, 331–336, DOI 10.1002/adfm.200304307.
-

-
92. S. K. Ritter, R. E. Noffle, A. E. Ward, *Chemistry of Materials* **1993**, *5*, 752–754, DOI [10.1021/cm00030a004](https://doi.org/10.1021/cm00030a004).
 93. C. Lee, K. J. Kim, S. B. Rhee, *Synthetic Metals* **1995**, *69*, 295–296, DOI [10.1016/0379-6779\(94\)02456-9](https://doi.org/10.1016/0379-6779(94)02456-9).
 94. P. Camurlu, A. Cirpan, L. Toppare, *Materials Chemistry and Physics* **2005**, *92*, 413–418, DOI [10.1016/j.matchemphys.2005.01.040](https://doi.org/10.1016/j.matchemphys.2005.01.040).
 95. M. Giglioti, F. Trivinho-Strixino, J. T. Matsushima, L. O. S. Bulhões, E. C. Pereira, *Solar Energy Materials and Solar Cells* **2004**, *82*, 413–420, DOI [10.1016/j.solmat.2004.02.001](https://doi.org/10.1016/j.solmat.2004.02.001).
 96. J. C. Gustafsson-Carlberg, O. Inganäs, M. R. Andersson, C. Booth, A. Azens, C. G. Granqvist, *Electrochimica Acta* **1995**, *40*, 2233–2235, DOI [10.1016/0013-4686\(95\)00169-F](https://doi.org/10.1016/0013-4686(95)00169-F).
 97. A. Iraqi, J. A. Crayston, J. C. Walton, *J. Mater. Chem.* **1995**, *5*, 1831–1836, DOI [10.1039/JM9950501831](https://doi.org/10.1039/JM9950501831).
 98. A. S. Ribeiro, V. C. Nogueira, P. F. dos Santos Filho, M. A. D. Paoli, *Electrochimica Acta* **2004**, *49*, 2237–2242, DOI [10.1016/j.electacta.2003.12.044](https://doi.org/10.1016/j.electacta.2003.12.044).
 99. J. L. Bredas, A. J. Heeger, F. Wudl, *The Journal of Chemical Physics* **1986**, *85*, 4673–4678, DOI [10.1063/1.451741](https://doi.org/10.1063/1.451741).
 100. F. Wudl, M. Kobayashi, A. J. Heeger, *The Journal of Organic Chemistry* **1984**, *49*, 3382–3384, DOI [10.1021/jo00192a027](https://doi.org/10.1021/jo00192a027).
 101. J. Roncali, *Chemical Reviews* **1997**, *97*, 173–206, DOI [10.1021/cr950257t](https://doi.org/10.1021/cr950257t).
 102. C.-G. Wu, M.-I. Lu, S.-J. Chang, C.-S. Wei, *Advanced Functional Materials* **2007**, *17*, 1063–1070, DOI [10.1002/adfm.200600381](https://doi.org/10.1002/adfm.200600381).
 103. F. Jonas, G. Heywang, W. Schmidtberg, J. Heinze, M. Dietrich, *U.S. Patent*, US 4959430, **1990**.
 104. N. Billingham, P. Calvert in *Conducting Polymers/Molecular Recognition*, Vol. 90, Springer Berlin / Heidelberg, **1989**, pp. 1–104, DOI [10.1007/3-540-51096-6_1](https://doi.org/10.1007/3-540-51096-6_1).
 105. M. Feldhues, T. Mecklenburg, P. Wegener, G. Kämpf, *EU Patent*, EP 0257573 B1, **1994**.
 106. G. Kämpf, M. Feldhues, *EU Patent*, EP 0292905 B1, **1993**.
 107. D. Kämpf, Günther, D. Feldhues, Michael, *EU Patent*, EP 0328981 B1, **1993**.
 108. M. Feldhues, G. Kämpf, H. Litterer, T. Mecklenburg, P. Wegener, *Synthetic Metals* **1989**, *28*, 487–493, DOI [10.1016/0379-6779\(89\)90563-8](https://doi.org/10.1016/0379-6779(89)90563-8).
 109. G. Daoust, M. Leclerc, *Macromolecules* **1991**, *24*, 455–459, DOI [10.1021/ma00002a018](https://doi.org/10.1021/ma00002a018).
 110. T. Hagiwara, M. Yamaura, K. Sato, M. Hirasaka, K. Iwata, *Synthetic Metals* **1989**, *32*, 367–379, DOI [10.1016/0379-6779\(89\)90778-9](https://doi.org/10.1016/0379-6779(89)90778-9).
-

-
111. T. Yamamoto, A. Kashiwazaki, K. Kato, *Die Makromolekulare Chemie* **1989**, *190*, 1649–1654, DOI 10.1002/macp.1989.021900716.
112. A. Elschner, S. Kirchmeyer, W. Lövenich, U. Merker, R. Knud, *PEDOT: Principles and Applications of an Intrinsically Conductive Polymer*, CRC Press, **2010**.
113. E. E. Havinga, C. M. J. Mutsaers, L. W. Jenneskens, *Chemistry of Materials* **1996**, *8*, 769–776, DOI 10.1021/cm9504551.
114. S. A. Sapp, G. A. Sotzing, J. R. Reynolds, *Chemistry of Materials* **1998**, *10*, 2101–2108, DOI 10.1021/cm9801237.
115. A. Kumar, J. R. Reynolds, *Macromolecules* **1996**, *29*, 7629–7630, DOI 10.1021/ma960879w.
116. B. Sankaran, J. R. Reynolds, *Macromolecules* **1997**, *30*, 2582–2588, DOI 10.1021/ma961607w.
117. D. M. Welsh, A. Kumar, M. C. Morvant, J. R. Reynolds, *Synthetic Metals* **1999**, *102*, 967–968, DOI 10.1016/S0379-6779(98)01014-5.
118. I. Schwendeman, C. Gaupp, J. Hancock, L. Groenendaal, J. Reynolds, *Advanced Functional Materials* **2003**, *13*, 541–547, DOI 10.1002/adfm.200304372.
119. E. Ventosa, A. Colina, A. Heras, A. Martínez, O. Orcajo, V. Ruiz, J. López-Palacios, *Electrochimica Acta* **2008**, *53*, 4219–4227, DOI 10.1016/j.electacta.2007.12.064.
120. E. Aqad, M. V. Lakshmikantham, M. P. Cava, *Organic Letters* **2001**, *3*, 4283–4285, DOI 10.1021/ol0169473.
121. A. Patra, Y. H. Wijsboom, S. S. Zade, M. Li, Y. Sheynin, G. Leituss, M. Bendikov, *Journal of the American Chemical Society* **2008**, *130*, 6734–6736, DOI 10.1021/ja8018675.
122. M. Li, Y. Sheynin, A. Patra, M. Bendikov, *Chemistry of Materials* **2009**, *21*, 2482–2488, DOI 10.1021/cm9003596.
123. M. Li, A. Patra, Y. Sheynin, M. Bendikov, *Advanced Materials* **2009**, *21*, 1707–1711, DOI 10.1002/adma.200802259.
124. A. Kumar, D. M. Welsh, M. C. Morvant, F. Piroux, K. A. Abboud, J. R. Reynolds, *Chemistry of Materials* **1998**, *10*, 896–902, DOI 10.1021/cm9706614.
125. D. M. Welsh, A. Kumar, E. W. Meijer, J. R. Reynolds, *Advanced Materials* **1999**, *11*, 1379–1382, DOI 10.1002/(SICI)1521-4095(199911)11:16<1379::AID-ADMA1379>3.0.CO;2-Q.
126. C. L. Gaupp, D. M. Welsh, J. R. Reynolds, *Macromolecular Rapid Communications* **2002**, *23*, 885–889, DOI 10.1002/1521-3927(20021001)23:15<885::AID-MARC885>3.0.CO;2-X.
127. D. M. Welsh, L. J. Kloeppner, L. Madrigal, M. R. Pinto, B. C. Thompson, K. S. Schanze, K. A. Abboud, D. Powell, J. R. Reynolds, *Macromolecules* **2002**, *35*, 6517–6525, DOI 10.1021/ma0120409.
-

-
128. B. D. Reeves, C. R. G. Grenier, A. A. Argun, A. Cirpan, T. D. McCarley, J. R. Reynolds, *Macromolecules* **2004**, *37*, 7559–7569, DOI [10.1021/ma049222y](https://doi.org/10.1021/ma049222y).
129. R. Walczak, J. Reynolds, *Advanced Materials* **2006**, *18*, 1121–1131, DOI [10.1002/adma.200502312](https://doi.org/10.1002/adma.200502312).
130. P. Schottland, K. Zong, C. L. Gaupp, B. C. Thompson, C. A. Thomas, I. Giurgiu, R. Hickman, K. A. Abboud, J. R. Reynolds, *Macromolecules* **2000**, *33*, 7051–7061, DOI [10.1021/ma000490f](https://doi.org/10.1021/ma000490f).
131. C. L. Gaupp, K. Zong, P. Schottland, B. C. Thompson, C. A. Thomas, J. R. Reynolds, *Macromolecules* **2000**, *33*, 1132–1133, DOI [10.1021/ma9916180](https://doi.org/10.1021/ma9916180).
132. K. Zong, J. R. Reynolds, *The Journal of Organic Chemistry* **2001**, *66*, 6873–6882, DOI [10.1021/jo001620l](https://doi.org/10.1021/jo001620l).
133. G. Sönmez, I. Schwendeman, P. Schottland, K. Zong, J. R. Reynolds, *Macromolecules* **2003**, *36*, 639–647, DOI [10.1021/ma021108x](https://doi.org/10.1021/ma021108x).
134. R. M. Walczak, J.-H. Jung, J. S. Cowart, J. R. Reynolds, *Macromolecules* **2007**, *40*, 7777–7785, DOI [10.1021/ma071478r](https://doi.org/10.1021/ma071478r).
135. E. Havinga, W. ten Hoeve, H. Wynberg, *Synthetic Metals* **1993**, *55*, 299–306, DOI [10.1016/0379-6779\(93\)90949-W](https://doi.org/10.1016/0379-6779(93)90949-W).
136. U. Salzner, *Synthetic Metals* **2001**, *119*, 215–216, DOI [10.1016/S0379-6779\(00\)01411-9](https://doi.org/10.1016/S0379-6779(00)01411-9).
137. U. Salzner, M. E. Köse, *The Journal of Physical Chemistry B* **2002**, *106*, 9221–9226, DOI [10.1021/jp020142a](https://doi.org/10.1021/jp020142a).
138. U. Salzner, *The Journal of Physical Chemistry B* **2002**, *106*, 9214–9220, DOI [10.1021/jp020141i](https://doi.org/10.1021/jp020141i).
139. J.-M. Raimundo, P. Blanchard, H. Brisset, S. Akoudad, J. Roncali, *Chem. Commun.* **2000**, 939–940, DOI [10.1039/B002369H](https://doi.org/10.1039/B002369H).
140. P. Blanchard, J.-M. Raimundo, J. Roncali, *Synthetic Metals* **2001**, *119*, 527–528, DOI [10.1016/S0379-6779\(00\)00956-5](https://doi.org/10.1016/S0379-6779(00)00956-5).
141. D. Aldakov, M. A. Palacios, P. Anzenbacher, *Chemistry of Materials* **2005**, *17*, 5238–5241, DOI [10.1021/cm050985p](https://doi.org/10.1021/cm050985p).
142. A. Durmus, G. E. Gunbas, P. Camurlu, L. Toppare, *Chem. Commun.* **2007**, 3246–3248, DOI [10.1039/B704936F](https://doi.org/10.1039/B704936F).
143. A. Durmus, G. E. Gunbas, L. Toppare, *Chemistry of Materials* **2007**, *19*, 6247–6251, DOI [10.1021/cm702143c](https://doi.org/10.1021/cm702143c).
144. G. Gunbas, A. Durmus, L. Toppare, *Advanced Materials* **2008**, *20*, 691–695, DOI [10.1002/adma.200701979](https://doi.org/10.1002/adma.200701979).
145. G. E. Gunbas, A. Durmus, L. Toppare, *Advanced Functional Materials* **2008**, *18*, 2026–2030, DOI [10.1002/adfm.200701386](https://doi.org/10.1002/adfm.200701386).
-

-
146. P. M. Beaujuge, S. Ellinger, J. R. Reynolds, *Advanced Materials* **2008**, *20*, 2772–2776, DOI 10.1002/adma.200800280.
147. J. Heinze, B. A. Frontana-Uribe, S. Ludwigs, *Chemical Reviews* **2010**, *110*, 4724–4771, DOI 10.1021/cr900226k.
148. A. Diaz, J. I. Castillo, J. Logan, W.-Y. Lee, *Journal of Electroanalytical Chemistry and Interfacial Electrochemistry* **1981**, *129*, 115–132, DOI 10.1016/S0022-0728(81)80008-3.
149. E. Genies, G. Bidan, A. Diaz, *Journal of Electroanalytical Chemistry and Interfacial Electrochemistry* **1983**, *149*, 101–113, DOI 10.1016/S0022-0728(83)80561-0.
150. S. Asavapiriyant, G. Chandler, G. Gunawardena, D. Pletcher, *Journal of Electroanalytical Chemistry and Interfacial Electrochemistry* **1984**, *177*, 229–244, DOI 10.1016/0022-0728(84)80225-9.
151. H. Randriamahazaka, G. Sini, F. Tran Van, *The Journal of Physical Chemistry C* **2007**, *111*, 4553–4560, DOI 10.1021/jp068525m.
152. G.-D. Wolf, F. Jonas, R. Schomäcker, *EU Patent*, EP 0707440 B1, **2001**.
153. S. Kirchmeyer, F. Jonas, *U.S. Patent*, WO 2000/045625 A2.
154. R. Corradi, S. Armes, *Synthetic Metals* **1997**, *84*, 453–454, DOI 10.1016/S0379-6779(97)80828-4.
155. S. G. Im, D. Kusters, W. Choi, S. H. Baxamusa, M. C. M. van de Sanden, K. K. Gleason, *ACS Nano* **2008**, *2*, 1959–1967, DOI 10.1021/nm800380e.
156. S. L. McFarlane, B. A. Deore, N. Svenda, M. S. Freund, *Macromolecules* **2010**, *43*, 10241–10245, DOI 10.1021/ma102257a.
157. F. Jonas, G. Heywang, W. Schmidtberg, J. Heinze, M. Dietrich, *EU Patent*, EP 0339340 B1, **1999**.
158. D. de Leeuw, P. Kraakman, P. Bongaerts, C. Mutsaers, D. Klaassen, *Synthetic Metals* **1994**, *66*, 263–273, DOI 10.1016/0379-6779(94)90076-0.
159. C. M. J. Mutsaers, D. M. De Leeuw, M. M. J. Simenon, *EU Patent*, EP 0615256 B1, **1998**.
160. B. Winther-Jensen, D. W. Breiby, K. West, *Synthetic Metals* **2005**, *152*, 1–4, DOI 10.1016/j.synthmet.2005.07.085.
161. S. Kirchmeyer, K. Reuter, *J. Mater. Chem.* **2005**, *15*, 2077–2088, DOI 10.1039/B417803N.
162. S. Kirchmeyer, F. Jonas, *U.S. Patent*, US 2003/0161941 A1, **2003**.
163. T. S. Hansen, K. West, O. Hassager, N. B. Larsen, *Synthetic Metals* **2006**, *156*, 1203–1207, DOI 10.1016/j.synthmet.2006.08.009.
164. Y.-H. Ha, N. Nikolov, S. Pollack, J. Mastrangelo, B. Martin, R. Shashidhar, *Advanced Functional Materials* **2004**, *14*, 615–622, DOI 10.1002/adfm.200305059.
-

-
165. K. Zuber, M. Fabretto, C. Hall, P. Murphy, *Macromolecular Rapid Communications* **2008**, *29*, 1503–1508, DOI 10.1002/marc.200800325.
166. H. Meng, D. F. Perepichka, F. Wudl, *Angewandte Chemie International Edition* **2003**, *42*, 658–661, DOI 10.1002/anie.200390181.
167. H. Meng, D. F. Perepichka, M. Bendikov, F. Wudl, G. Z. Pan, W. Yu, W. Dong, S. Brown, *Journal of the American Chemical Society* **2003**, *125*, 15151–15162, DOI 10.1021/ja037115y.
168. T. Yamamoto, M. Abla, *Synthetic Metals* **1999**, *100*, 237–239, DOI 10.1016/S0379-6779(99)00005-3.
169. T. Yamamoto, K. Shiraishi, M. Abla, I. Yamaguchi, L. Groenendaal, *Polymer* **2002**, *43*, 711–719, DOI 10.1016/S0032-3861(01)00644-9.
170. F. Tran-Van, S. Garreau, G. Louarn, G. Froyer, C. Chevrot, *J. Mater. Chem.* **2001**, *11*, 1378–1382.
171. F. Tran-Van, S. Garreau, G. Louarn, G. Froyer, C. Chevrot, *Synthetic Metals* **2001**, *119*, 381–382, DOI 10.1016/S0379-6779(00)01045-6.
172. C. Wurster, R. Sendtner, *Berichte der deutschen chemischen Gesellschaft* **1879**, *12*, 1803–1807, DOI 10.1002/cber.187901202155.
173. C. Wurster, E. Schobig, *Berichte der deutschen chemischen Gesellschaft* **1879**, *12*, 1807–1813, DOI 10.1002/cber.187901202156.
174. C. Wurster, *Berichte der deutschen chemischen Gesellschaft* **1879**, *12*, 528–530, DOI 10.1002/cber.187901201150.
175. E. Weitz, *Angewandte Chemie* **1954**, *66*, 658–677, DOI 10.1002/ange.19540662103.
176. L. Michaelis, M. P. Schubert, R. K. Reber, J. A. Kuck, S. Granick, *Journal of the American Chemical Society* **1938**, *60*, 1678–1683, DOI 10.1021/ja01274a042.
177. S. Hünig, H. Berneth in *Organic Chemistry, Vol. 92*, Springer Berlin / Heidelberg, **1980**, pp. 1–44, DOI 10.1007/BFb0034356.
178. K. Deuchert, S. Hünig, *Angewandte Chemie International Edition in English* **1978**, *17*, 875–886, DOI 10.1002/anie.197808753.
179. R. W. Baldock, P. Hudson, A. R. Katritzky, F. Soti, *J. Chem. Soc. Perkin Trans. 1* **1974**, 1422–1427, DOI 10.1039/P19740001422.
180. J. R. Kirtley, J. Mannhart, *Nat Mater* **2008**, *7*, 520–521, DOI 10.1038/nmat2211.
181. M. B. Nielsen, C. Lomholt, J. Becher, *Chem. Soc. Rev.* **2000**, *29*, 153–164, DOI 10.1039/A803992E.
182. M. R. Bryce, *Advanced Materials* **1999**, *11*, 11–23, DOI 10.1002/(SICI)1521-4095(199901)11:1<11::AID-ADMA11>3.0.CO;2-3.
183. P. M. S. Monk, *The Viologens: Physicochemical Properties, Synthesis and Applications of the Salts of 4,4'-Bipyridine*, Wiley VCH, **1998**.
-

-
184. L. Michaelis, E. S. Hill, *The Journal of General Physiology* **1933**, *16*, 859–873, DOI [10.1085/jgp.16.6.859](https://doi.org/10.1085/jgp.16.6.859).
185. J. D. Badjić, V. Balzani, A. Credi, S. Silvi, J. F. Stoddart, *Science* **2004**, *303*, 1845–1849, DOI [10.1126/science.1094791](https://doi.org/10.1126/science.1094791).
186. R. A. Bissell, E. Cordova, A. E. Kaifer, J. F. Stoddart, *Nature* **1994**, *369*, 133–137, DOI [10.1038/369133a0](https://doi.org/10.1038/369133a0).
187. C. G. Claessens, J. F. Stoddart, *Journal of Physical Organic Chemistry* **1997**, *10*, 254–272, DOI [10.1002/\(SICI\)1099-1395\(199705\)10:5<254::AID-POC875>3.0.CO;2-3](https://doi.org/10.1002/(SICI)1099-1395(199705)10:5<254::AID-POC875>3.0.CO;2-3).
188. E. H. Yonemoto, R. L. Riley, Y. I. Kim, S. J. Atherton, R. H. Schmehl, T. E. Mallouk, *Journal of the American Chemical Society* **1992**, *114*, 8081–8087, DOI [10.1021/ja00047a017](https://doi.org/10.1021/ja00047a017).
189. R. J. Mortimer, *Electrochimica Acta* **1999**, *44*, 2971–2981, DOI [10.1016/S0013-4686\(99\)00046-8](https://doi.org/10.1016/S0013-4686(99)00046-8).
190. C. L. Bird, A. T. Kuhn, *Chem. Soc. Rev.* **1981**, *10*, 49–82, DOI [10.1039/CS9811000049](https://doi.org/10.1039/CS9811000049).
191. C. J. Schoot, J. J. Ponjee, H. T. van Dam, R. A. van Doorn, P. T. Bolwijn, *Applied Physics Letters* **1973**, *23*, 64–65, DOI [10.1063/1.1654808](https://doi.org/10.1063/1.1654808).
192. R. J. Jasinski, *Journal of The Electrochemical Society* **1978**, *125*, 1619–1623, DOI [10.1149/1.2131256](https://doi.org/10.1149/1.2131256).
193. A. Yasuda, H. Mori, Y. Takehana, A. Ohkoshi, N. Kamiya, *Journal of Applied Electrochemistry* **1984**, *14*, 323–327, DOI [10.1007/BF01269932](https://doi.org/10.1007/BF01269932).
194. P. M. Monk, *Journal of Electroanalytical Chemistry* **1997**, *432*, 175–179, DOI [10.1016/S0022-0728\(97\)00078-8](https://doi.org/10.1016/S0022-0728(97)00078-8).
195. H. J. Byker, M. I. Holland, *U.S. Patent*, US 4902108, **1990**.
196. N. Leventis, M. Chen, A. I. Liapis, J. W. Johnson, A. Jain, *Journal of The Electrochemical Society* **1998**, *145*, L55–L58, DOI [10.1149/1.1838413](https://doi.org/10.1149/1.1838413).
197. R. N. Dominey, T. J. Lewis, M. S. Wrighton, *The Journal of Physical Chemistry* **1983**, *87*, 5345–5354, DOI [10.1021/j150644a008](https://doi.org/10.1021/j150644a008).
198. H. Akahoshi, S. Toshima, K. Itaya, *The Journal of Physical Chemistry* **1981**, *85*, 818–822, DOI [10.1021/j150607a018](https://doi.org/10.1021/j150607a018).
199. J. Stepp, J. B. Schlenoff, *Journal of The Electrochemical Society* **1997**, *144*, L155–L158, DOI [10.1149/1.1837709](https://doi.org/10.1149/1.1837709).
200. G. Decher, *Science* **1997**, *277*, 1232–1237, DOI [10.1126/science.277.5330.1232](https://doi.org/10.1126/science.277.5330.1232).
201. G. Bidan, A. Deronzier, J.-C. Moutet, *J. Chem. Soc. Chem. Commun.* **1984**, 1185–1186, DOI [10.1039/C39840001185](https://doi.org/10.1039/C39840001185).
202. P. Bäuerle, K.-U. Gaudl, *Advanced Materials* **1990**, *2*, 185–188, DOI [10.1002/adma.19900020407](https://doi.org/10.1002/adma.19900020407).
-

-
203. H. C. Ko, S. ah Park, W. kie Paik, H. Lee, *Synthetic Metals* **2002**, *132*, 15–20, DOI [10.1016/S0379-6779\(02\)00217-5](https://doi.org/10.1016/S0379-6779(02)00217-5).
204. H. C. Ko, M. Kang, B. Moon, H. Lee, *Advanced Materials* **2004**, *16*, 1712–1716, DOI [10.1002/adma.200400218](https://doi.org/10.1002/adma.200400218).
205. B. O'Regan, M. Gratzel, *Nature* **1991**, *353*, 737–740, DOI [10.1038/353737a0](https://doi.org/10.1038/353737a0).
206. X. Marguerettaz, R. O'Neill, D. Fitzmaurice, *Journal of the American Chemical Society* **1994**, *116*, 2629–2630, DOI [10.1021/ja00085a057](https://doi.org/10.1021/ja00085a057).
207. R. Cinnsealach, G. Boschloo, S. N. Rao, D. Fitzmaurice, *Solar Energy Materials and Solar Cells* **1998**, *55*, 215–223, DOI [10.1016/S0927-0248\(98\)00096-8](https://doi.org/10.1016/S0927-0248(98)00096-8).
208. R. Cinnsealach, G. Boschloo, S. N. Rao, D. Fitzmaurice, *Solar Energy Materials and Solar Cells* **1999**, *57*, 107–125, DOI [10.1016/S0927-0248\(98\)00156-1](https://doi.org/10.1016/S0927-0248(98)00156-1).
209. P. Bonhôte, E. Gogniat, F. Campus, L. Walder, M. Grätzel, *Displays* **1999**, *20*, 137–144, DOI [10.1016/S0141-9382\(99\)00015-3](https://doi.org/10.1016/S0141-9382(99)00015-3).
210. M. O. M. Edwards, G. Boschloo, T. Gruszecki, H. Pettersson, R. Sohlberg, A. Hagfeldt, *Electrochimica Acta* **2001**, *46*, 2187–2193, DOI [10.1016/S0013-4686\(01\)00398-X](https://doi.org/10.1016/S0013-4686(01)00398-X).
211. M. Edwards, M. Andersson, T. Gruszecki, H. Pettersson, R. Thunman, G. Thuraingham, L. Vestling, A. Hagfeldt, *Journal of Electroanalytical Chemistry* **2004**, *565*, 175–184, DOI [10.1016/j.jelechem.2003.10.006](https://doi.org/10.1016/j.jelechem.2003.10.006).
212. P. Periyat, N. Leyland, D. E. McCormack, J. Colreavy, D. Corr, S. C. Pillai, *J. Mater. Chem.* **2010**, *20*, 3650–3655, DOI [10.1039/B924341K](https://doi.org/10.1039/B924341K).
213. M. Freitag, E. Galoppini, *Langmuir* **2010**, *26*, 8262–8269, DOI [10.1021/la904671w](https://doi.org/10.1021/la904671w).
214. D. Corr, U. Bach, D. Fay, M. Kinsella, C. McAtamney, F. O'Reilly, S. N. Rao, N. Stobie, *Solid State Ionics* **2003**, *165*, 315–321, DOI [10.1016/j.ssi.2003.08.054](https://doi.org/10.1016/j.ssi.2003.08.054).
215. D. Cummins, G. Boschloo, M. Ryan, D. Corr, S. N. Rao, D. Fitzmaurice, *The Journal of Physical Chemistry B* **2000**, *104*, 11449–11459, DOI [10.1021/jp001763b](https://doi.org/10.1021/jp001763b).
216. M. Gratzel, *Nature* **2001**, *409*, 575–576, DOI [10.1038/35054655](https://doi.org/10.1038/35054655).
217. X. Tu, X. Fu, Q. Jiang, *Displays* **2010**, *31*, 150–154, DOI [10.1016/j.displa.2010.05.001](https://doi.org/10.1016/j.displa.2010.05.001).
218. P. Gawrys, D. Boudinet, M. Zagorska, D. Djurado, J.-M. Verilhac, G. Horowitz, J. Pécaud, S. Pouget, A. Pron, *Synthetic Metals* **2009**, *159*, 1478–1485, DOI [10.1016/j.synthmet.2009.04.003](https://doi.org/10.1016/j.synthmet.2009.04.003).
219. S. Mazur, P. S. Lugg, C. Yarnitzky, *Journal of The Electrochemical Society* **1987**, *134*, 346–353, DOI [10.1149/1.2100458](https://doi.org/10.1149/1.2100458).
220. S. K. Lee, Y. Zu, A. Herrmann, Y. Geerts, K. Müllen, A. J. Bard, *Journal of the American Chemical Society* **1999**, *121*, 3513–3520, DOI [10.1021/ja984188m](https://doi.org/10.1021/ja984188m).
221. P. Gawrys, G. Louarn, M. Zagorska, A. Pron, *Electrochimica Acta* **2011**, *56*, 3429–3435, DOI [10.1016/j.electacta.2010.09.070](https://doi.org/10.1016/j.electacta.2010.09.070).
-

-
222. K. Nakamura, Y. Oda, T. Sekikawa, M. Sugimoto, *Japanese Journal of Applied Physics* **1987**, *26*, 931–935, DOI 10.1143/JJAP.26.931.
223. H. Urano, S. Sunohara, H. Ohtomo, N. Kobayashi, *J. Mater. Chem.* **2004**, *14*, 2366–2368, DOI 10.1039/B406093H.
224. N. Kobayashi, S. Miura, M. Nishimura, H. Urano, *Solar Energy Materials and Solar Cells* **2008**, *92*, 136–139, DOI 10.1016/j.solmat.2007.02.027.
225. N. Kobayashi, S. Miura, M. Nishimura, Y. Goh, *Electrochimica Acta* **2007**, *53*, 1643–1647, DOI 10.1016/j.electacta.2007.05.073.
226. W. Sharmoukh, K. C. Ko, J. H. Ko, H. J. Nam, D.-Y. Jung, C. Noh, J. Y. Lee, S. U. Son, *J. Mater. Chem.* **2008**, *18*, 4408–4413, DOI 10.1039/B808638A.
227. U. Mitschke, P. Bauerle, *J. Mater. Chem.* **2000**, *10*, 1471–1507, DOI 10.1039/A908713C.
228. M. Malagoli, J. L. Brédas, *Chemical Physics Letters* **2000**, *327*, 13–17, DOI 10.1016/S0009-2614(00)00757-0.
229. P. J. Low, M. A. J. Paterson, H. Puschmann, A. E. Goeta, J. A. K. Howard, C. Lambert, J. C. Cherryman, D. R. Tackley, S. Leeming, B. Brown, *Chemistry – A European Journal* **2004**, *10*, 83–91, DOI 10.1002/chem.200305200.
230. M. B. Robin, P. Day in *Advances in Inorganic Chemistry, Vol. 10* (Eds.: H. Emeléus, A. Sharpe), Academic Press, **1968**, pp. 247 – 422, DOI 10.1016/S0065-2792(08)60179-X.
231. A. V. Szeghalmi, M. Erdmann, V. Engel, M. Schmitt, S. Amthor, V. Kriegisch, G. Nöll, R. Stahl, C. Lambert, D. Leusser, D. Stalke, M. Zabel, J. Popp, *Journal of the American Chemical Society* **2004**, *126*, 7834–7845, DOI 10.1021/ja0395386.
232. S.-H. Cheng, S.-H. Hsiao, T.-H. Su, G.-S. Liou, *Macromolecules* **2005**, *38*, 307–316, DOI 10.1021/ma048774d.
233. C.-W. Chang, G.-S. Liou, S.-H. Hsiao, *J. Mater. Chem.* **2007**, *17*, 1007–1015, DOI 10.1039/B613140A.
234. S.-H. Hsiao, G.-S. Liou, Y.-C. Kung, H.-J. Yen, *Macromolecules* **2008**, *41*, 2800–2808, DOI 10.1021/ma702426z.
235. G.-S. Liou, C.-W. Chang, *Macromolecules* **2008**, *41*, 1667–1674, DOI 10.1021/ma702146h.
236. H.-J. Yen, G.-S. Liou, *Chemistry of Materials* **2009**, *21*, 4062–4070, DOI 10.1021/cm9015222.
237. H.-J. Yen, G.-S. Liou, *J. Mater. Chem.* **2010**, *20*, 9886–9894, DOI 10.1039/C0JM01889A.
238. H.-J. Yen, H.-Y. Lin, G.-S. Liou, *Chemistry of Materials* **2011**, *23*, 1874–1882, DOI 10.1021/cm103552k.
239. S. Hünig, M. Kemmer, H. Wenner, I. F. Perepichka, P. Bäuerle, A. Emge,

- G. Gescheid, *Chemistry – A European Journal* **1999**, *5*, 1969–1973,
DOI 10.1002/(SICI)1521-3765(19990702)5:7<1969::AID-CHEM1969>3.0.CO;2-5.
240. S. Hünig, M. Kemmer, H. Wenner, F. Barbosa, G. Gescheidt, I. F. Perepichka, P. Bäuerle, A. Emge, K. Peters, *Chemistry – A European Journal* **2000**, *6*, 2618–2632,
DOI 10.1002/1521-3765(20000717)6:14<2618::AID-CHEM2618>3.0.CO;2-W.
241. S. Hünig, I. F. Perepichka, M. Kemmer, H. Wenner, P. Bäuerle, A. Emge, *Tetrahedron* **2000**, *56*, 4203–4211, DOI 10.1016/S0040-4020(00)00345-8.
242. R. Willstätter, M. Goldmann, *Berichte der deutschen chemischen Gesellschaft* **1906**, *39*, 3765–3776, DOI 10.1002/cber.19060390443.
243. S. Ito, S. Kikuchi, T. Okujima, N. Morita, T. Asao, *The Journal of Organic Chemistry* **2001**, *66*, 2470–2479, DOI 10.1021/jo001709r.
244. S. Ito, A. Nomura, N. Morita, C. Kabuto, H. Kobayashi, S. Maejima, K. Fujimori, M. Yasunami, *The Journal of Organic Chemistry* **2002**, *67*, 7295–7302,
DOI 10.1021/jo020381u.
245. S. Ito, H. Inabe, N. Morita, K. Ohta, T. Kitamura, K. Imafuku, *Journal of the American Chemical Society* **2003**, *125*, 1669–1680, DOI 10.1021/ja0209262.
246. S. Ito, N. Morita, *European Journal of Organic Chemistry* **2009**, *2009*, 4567–4579,
DOI 10.1002/ejoc.200900393.
247. T. Shoji, J. Higashi, S. Ito, T. Okujima, N. Morita, *European Journal of Organic Chemistry* **2011**, *2011*, 584–592, DOI 10.1002/ejoc.201001212.
248. M. Horner, S. Huenig, *Journal of the American Chemical Society* **1977**, *99*, 6120–6122,
DOI 10.1021/ja00460a057.
249. M. Horner, S. Huenig, *Journal of the American Chemical Society* **1977**, *99*, 6122–6124,
DOI 10.1021/ja00460a058.
250. T. Suzuki, J.-i. Nishida, T. Tsuji, *Angewandte Chemie International Edition in English* **1997**, *36*, 1329–1331, DOI 10.1002/anie.199713291.
251. T. Suzuki, J.-i. Nishida, T. Tsuji, *Chem. Commun.* **1998**, 2193–2194,
DOI 10.1039/A806037A.
252. T. Suzuki, E. Ohta, H. Kawai, K. Fujiwara, T. Fukushima, *Synlett* **2007**, *2007*, 0851–0869, DOI 10.1055/s-2007-973887.
253. S. Hünig, C. A. Briehn, P. Bäuerle, A. Emge, *Chemistry – A European Journal* **2001**, *7*, 2745–2757,
DOI 10.1002/1521-3765(20010702)7:13<2745::AID-CHEM2745>3.0.CO;2-C.
254. S. Hünig, S. Aldenkortt, P. Bäuerle, C. Briehn, M. Schäferling, I. Perepichka, D. Stalke, B. Walfort, *European Journal of Organic Chemistry* **2002**, *2002*, 1603–1613,
DOI 10.1002/1099-0690(200205)2002:10<1603::AID-EJOC1603>3.0.CO;2-9.
255. R. Mortimer, N. Rowley in *Comprehensive Coordination Chemistry II: From Biology to Nanotechnology*, Vol. 9 (Ed.: M. Ward), Elsevier Pergamon, Oxford, UK, **2003**, pp. 581–619.

-
256. C. M. Elliott, J. G. Redepenning, *Journal of Electroanalytical Chemistry and Interfacial Electrochemistry* **1986**, *197*, 219–232, DOI 10.1016/0022-0728(86)80151-6.
257. F. Pichot, J. H. Beck, C. M. Elliott, *The Journal of Physical Chemistry A* **1999**, *103*, 6263–6267, DOI 10.1021/jp991196w.
258. H. D. Abruna, P. Denisevich, M. Umana, T. J. Meyer, R. W. Murray, *Journal of the American Chemical Society* **1981**, *103*, 1–5, DOI 10.1021/ja00391a001.
259. C. D. Ellis, L. D. Margerum, R. W. Murray, T. J. Meyer, *Inorganic Chemistry* **1983**, *22*, 1283–1291, DOI 10.1021/ic00151a005.
260. C. P. Horwitz, Q. Zuo, *Inorganic Chemistry* **1992**, *31*, 1607–1613, DOI 10.1021/ic00035a017.
261. L. Motiei, M. Lahav, A. Gulino, M. A. Iron, M. E. van der Boom, *The Journal of Physical Chemistry B* **2010**, *114*, 14283–14286, DOI 10.1021/jp910898f.
262. L. Motiei, M. Lahav, D. Freeman, M. E. van der Boom, *Journal of the American Chemical Society* **2009**, *131*, 3468–3469, DOI 10.1021/ja900507c.
263. K. Smith in *Comprehensive Coordination Chemistry II: From Biology to Nanotechnology*, Vol. 1 (Ed.: M. Ward), Elsevier Pergamon, Oxford, UK, **2003**, pp. 419–506.
264. P. Moskalev, I. Kirin, *Opt. Spectros.* **1970**, *29*, 220.
265. P. Moskalev, I. Kirin, *Opt. Spectros.* **1970**, *29*, 414.
266. M. M. Nicholson, F. A. Pizzarello, *Journal of The Electrochemical Society* **1980**, *127*, 2617–2620, DOI 10.1149/1.2129531.
267. M. M. Nicholson, F. A. Pizzarello, *Journal of The Electrochemical Society* **1980**, *127*, 821–827, DOI 10.1149/1.2129764.
268. M. M. Nicholson, F. A. Pizzarello, *Journal of The Electrochemical Society* **1979**, *126*, 1490–1495, DOI 10.1149/1.2129313.
269. M. M. Nicholson, F. A. Pizzarello, *Journal of The Electrochemical Society* **1981**, *128*, 1740–1743, DOI 10.1149/1.2127722.
270. G. C. S. Collins, D. J. Schiffrin, *Journal of The Electrochemical Society* **1985**, *132*, 1835–1842, DOI 10.1149/1.2114227.
271. F. A. Pizzarello, M. M. Nicholson, *Journal of The Electrochemical Society* **1981**, *128*, 1288–1290, DOI 10.1149/1.2127608.
272. G. Collins, D. Schiffrin, *Journal of Electroanalytical Chemistry and Interfacial Electrochemistry* **1982**, *139*, 335–369, DOI 10.1016/0022-0728(82)85133-4.
273. P. R. Somani, S. Radhakrishnan, *Materials Chemistry and Physics* **2003**, *77*, 117–133, DOI 10.1016/S0254-0584(01)00575-2.
274. M. L. Rodriguez-Mendez, R. Aroca, J. A. DeSaja, *Chemistry of Materials* **1993**, *5*, 933–937, DOI 10.1021/cm00031a010.
-

-
275. M. L. Rodriguez-Mendez, R. Aroca, J. A. DeSaja, *Chemistry of Materials* **1992**, *4*, 1017–1020, DOI 10.1021/cm00023a018.
276. C. Granito, L. M. Goldenberg, M. R. Bryce, A. P. Monkman, L. Troisi, L. Pasimeni, M. C. Petty, *Langmuir* **1996**, *12*, 472–476, DOI 10.1021/la950490m.
277. M. L. Rodriguez-Mendez, J. Souto, J. A. de Saja, R. Aroca, *J. Mater. Chem.* **1995**, *5*, 639–642, DOI 10.1039/JM9950500639.
278. H. Li, T. F. Guarr, *Journal of Electroanalytical Chemistry and Interfacial Electrochemistry* **1991**, *297*, 169–183, DOI 10.1016/0022-0728(91)85366-W.
279. D. J. Moore, T. F. Guarr, *Journal of Electroanalytical Chemistry and Interfacial Electrochemistry* **1991**, *314*, 313–321, DOI 10.1016/0022-0728(91)85445-U.
280. N. Trombach, O. Hild, D. Schlettwein, D. Wohrle, *J. Mater. Chem.* **2002**, *12*, 879–885, DOI 10.1039/B109283A.
281. J. W. Dodd, N. S. Hush, *J. Chem. Soc.* **1964**, 4607–4612, DOI 10.1039/JR9640004607.
282. G. L. Closs, L. E. Closs, *Journal of the American Chemical Society* **1963**, *85*, 818–819, DOI 10.1021/ja00889a038.
283. H. C. Ko, J. Yom, B. Moon, H. Lee, *Electrochimica Acta* **2003**, *48*, 4127–4135, DOI 10.1016/S0013-4686(03)00580-2.
284. J. Y. Lim, H. C. Ko, H. Lee, *Synthetic Metals* **2006**, *156*, 695–698, DOI 10.1016/j.synthmet.2006.03.008.
285. M. Vorotyntsev, M. Casalta, E. Pousson, L. Roullier, G. Boni, C. Moise, *Electrochimica Acta* **2001**, *46*, 4017–4033, DOI 10.1016/S0013-4686(01)00717-4.
286. M. Skompska, M. A. Vorotyntsev, M. Refczynska, J. Goux, E. Lesniewska, G. Boni, C. Moise, *Electrochimica Acta* **2006**, *51*, 2108–2119, DOI 10.1016/j.electacta.2005.01.066.
287. J. Arias-Pardilla, T. Otero, R. Blanco, J. Segura, *Electrochimica Acta* **2010**, *55*, 1535–1542, DOI 10.1016/j.electacta.2009.10.011.
288. A. Czardybon, J. Żak, M. Łapkowski, *Polish Journal of Chemistry* **2004**, *Vol. 78 / nr 9*, 1533–1541.
289. W. Choi, H. C. Ko, B. Moon, H. Lee, *Journal of The Electrochemical Society* **2004**, *151*, E80–E83, DOI 10.1149/1.1640629.
290. J. L. Segura, R. Gómez, E. Reinold, P. Bäuerle, *Organic Letters* **2005**, *7*, 2345–2348, DOI 10.1021/ol050573m.
291. J. L. Segura, R. Gómez, R. Blanco, E. Reinold, P. Bäuerle, *Chemistry of Materials* **2006**, *18*, 2834–2847, DOI 10.1021/cm0602085.
292. N. C. Tansil, E. A. B. Kantchev, Z. Gao, H.-h. Yu, *Chem. Commun.* **2011**, *47*, 1533–1535.
293. H.-H. Yu, J. Y. Ying, E. A. B. Kantchev, *U.S. Patent*, WO 2008/057054 A1, **2008**.
-

-
294. L. Huchet, S. Akoudad, E. Levillain, J. Roncali, A. Emge, P. Bäuerle, *The Journal of Physical Chemistry B* **1998**, *102*, 7776–7781, DOI 10.1021/jp982593u.
295. H.-B. Bu, G. Götz, E. Reinold, A. Vogt, S. Schmid, J. L. Segura, R. Blanco, R. Gómez, P. Peter Bäuerle, *Tetrahedron* **2011**, *67*, 1114–1125, DOI 10.1016/j.tet.2010.12.022.
296. J. Fei, K. G. Lim, G. T. R. Palmore, *Chemistry of Materials* **2008**, *20*, 3832–3839, DOI 10.1021/cm7022983.
297. A. Celik, U. Posset, G. Schottner, G. Pagani, R. Ruffo, L. Beverina, C. M. Mari, G. Patriarca, A. Abboto, *U.S. Patent*, WO 2008/064878 A1, **2008**.
298. L. Michaelis, *Chemical Reviews* **1935**, *16*, 243–286, DOI 10.1021/cr60054a004.
299. R. Zahradnik, S. Huenig, D. Scheutzow, P. Carsky, *The Journal of Physical Chemistry* **1971**, *75*, 335–339, DOI 10.1021/j100673a007.
300. R. F. Homer, G. C. Mees, T. E. Tomlinson, *Journal of the Science of Food and Agriculture* **1960**, *11*, 309–315, DOI 10.1002/jsfa.2740110604.
301. S. Hünig, J. Groß, W. Schenk, *Justus Liebigs Annalen der Chemie* **1973**, *1973*, 324–338, DOI 10.1002/jlac.197319730220.
302. T. Muramatsu, A. Toyota, Y. Ikegami, *The Journal of Organic Chemistry* **1995**, *60*, 4925–4927, DOI 10.1021/jo00120a043.
303. B. Bröker, R.-P. Blum, L. Beverina, O. T. Hofmann, M. Sassi, R. Ruffo, G. A. Pagani, G. Heimel, A. Vollmer, J. Frisch, J. P. Rabe, E. Zojer, N. Koch, *ChemPhysChem* **2009**, *10*, 2947–2954, DOI 10.1002/cphc.200900472.
304. G. G. Barna, J. G. Fish, *Journal of The Electrochemical Society* **1981**, *128*, 1290–1292, DOI 10.1149/1.2127609.
305. A. Bernthsen, *Justus Liebigs Annalen der Chemie* **1884**, *224*, 1–56, DOI 10.1002/jlac.18842240102.
306. H. Suzuki, Y. Tanaka, *The Journal of Organic Chemistry* **2001**, *66*, 2227–2231, DOI 10.1021/jo001334+.
307. H. Finkelstein, *Berichte der deutschen chemischen Gesellschaft* **1910**, *43*, 1528–1532, DOI 10.1002/cber.19100430257.
308. A. Bischler, B. Napieralski, *Berichte der deutschen chemischen Gesellschaft* **1893**, *26*, 1903–1908, DOI 10.1002/cber.189302602143.
309. E. Schlittler, J. Müller, *Helvetica Chimica Acta* **1948**, *31*, 914–924, DOI 10.1002/hlca.19480310332.
310. C. Pomeranz, *Monatshefte für Chemie / Chemical Monthly* **1893**, *14*, 116–119, DOI 10.1007/BF01517862.
311. P. Fritsch, *Berichte der deutschen chemischen Gesellschaft* **1893**, *26*, 419–422, DOI 10.1002/cber.18930260191.
-

-
312. E. V. Brown, *The Journal of Organic Chemistry* **1977**, *42*, 3208–3209, DOI 10.1021/jo00439a025.
313. H. Andrews, S. Skidmore, H. Suschitzky, *J. Chem. Soc.* **1962**, 2370–2374, DOI 10.1039/JR9620002370.
314. H. Kaplan, H. G. Lindwall, *Journal of the American Chemical Society* **1943**, *65*, 927–928, DOI 10.1021/ja01245a043.
315. A. C. Bissember, M. G. Banwell, *The Journal of Organic Chemistry* **2009**, *74*, 4893–4895, DOI 10.1021/jo9008386.
316. J. J. Li, J. J. Li in *Name Reactions*, Springer Berlin Heidelberg, **2009**, pp. 64–64, DOI 10.1007/978-3-642-01053-8_31.
317. Y. Houminer, D. L. Williams, *The Journal of Organic Chemistry* **1983**, *48*, 2622–2625, DOI 10.1021/jo00163a046.
318. R. A. M. O’Ferrall, B. A. Murray, *J. Chem. Soc. Perkin Trans. 2* **1994**, 2461–2470, DOI 10.1039/P29940002461.
319. W. Pfitzinger, *Journal für Praktische Chemie* **1886**, *33*, 100–100, DOI 10.1002/prac.18850330110.
320. M.-A. Shvekhgeimer, *Chemistry of Heterocyclic Compounds* **2004**, *40*, 257–294, DOI 10.1023/B:COHC.0000028623.41308.e5.
321. A. Bard, L. Faulkner, *Electrochemical methods: fundamentals and applications*, Alibaazar, **2006**.
322. G. G. Barna, *Journal of The Electrochemical Society* **1980**, *127*, 1317–1319, DOI 10.1149/1.2129880.
323. R. G. Compton, A. M. Waller, P. M. S. Monk, D. R. Rosseinsky, *J. Chem. Soc. Faraday Trans.* **1990**, *86*, 2583–2586, DOI 10.1039/FT9908602583.
324. A. Goldon, J. Przulski, *Electrochimica Acta* **1985**, *30*, 1231–1235, DOI 10.1016/0013-4686(95)80019-0.
325. P. M. S. Monk, R. D. Fairweather, M. D. Ingram, J. A. Duffy, *J. Chem. Soc. Perkin Trans. 2* **1992**, 2039–2041, DOI 10.1039/P29920002039.
326. P. M. Monk, N. M. Hodgkinson, S. A. Ramzan, *Dyes and Pigments* **1999**, *43*, 207–217, DOI 10.1016/S0143-7208(99)00054-6.
327. D. R. Rosseinsky, P. M. S. Monk, *J. Chem. Soc. Faraday Trans.* **1990**, *86*, 3597–3601, DOI 10.1039/FT9908603597.
328. O. Poizat, C. Sourisseau, J. Corset, *Journal of Molecular Structure* **1986**, *143*, 203–206, DOI 10.1016/0022-2860(86)85238-3.
329. J. Bruinink, C. G. A. Kregting, J. J. Ponjee, *Journal of The Electrochemical Society* **1977**, *124*, 1854–1858, DOI 10.1149/1.2133175.
330. J. A. Barltrop, A. C. Jackson, *J. Chem. Soc. Perkin Trans. 2* **1984**, 367–371, DOI 10.1039/P29840000367.
-

-
331. W. Schuhmann, C. Kranz, H. Wohlschläger, J. Strohmeier, *Biosensors and Bioelectronics* **1997**, *12*, 1157–1167, DOI 10.1016/S0956-5663(97)00086-9.
332. S.-C. Luo, E. Mohamed Ali, N. C. Tansil, H.-h. Yu, S. Gao, E. A. B. Kantchev, J. Y. Ying, *Langmuir* **2008**, *24*, 8071–8077, DOI 10.1021/la800333g.
333. E. M. Ali, E. A. B. Kantchev, H.-h. Yu, J. Y. Ying, *Macromolecules* **2007**, *40*, 6025–6027, DOI 10.1021/ma0708949.
334. E. Ziegler, R. Salvador, T. Kappe, *Monatshefte für Chemie / Chemical Monthly* **1962**, *93*, 1376–1382, DOI 10.1007/BF00909961.
335. E. Ziegler, T. Kappe, *Monatshefte für Chemie / Chemical Monthly* **1965**, *96*, 889–895, DOI 10.1007/BF00919162.
336. E. Ziegler, T. Kappe, H. G. Foraita, *Monatshefte für Chemie / Chemical Monthly* **1966**, *97*, 409–416, DOI 10.1007/BF00905258.
337. G. Ornstein, *Berichte der deutschen chemischen Gesellschaft* **1907**, *40*, 1088–1095, DOI 10.1002/cber.190704001163.
338. I. Chujo, Y. Masuda, K. Fujino, S. Kato, T. Ogasa, S. ichiro Mohri, M. Kasai, *Bioorganic & Medicinal Chemistry* **2001**, *9*, 3273–3286, DOI 10.1016/S0968-0896(01)00238-3.
339. J. Attenburrow, A. F. B. Cameron, J. H. Chapman, R. M. Evans, B. A. Hems, A. B. A. Jansen, T. Walker, *J. Chem. Soc.* **1952**, 1094–1111, DOI 10.1039/JR9520001094.
340. B. Neises, W. Steglich, *Angewandte Chemie International Edition in English* **1978**, *17*, 522–524, DOI 10.1002/anie.197805221.
341. L. Groenendaal, F. Jonas, D. Freitag, H. Pielartzik, J. R. Reynolds, *Advanced Materials* **2000**, *12*, 481–494, DOI 10.1002/(SICI)1521-4095(200004)12:7<481::AID-ADMA481>3.0.CO;2-C.
342. P. Schottland, O. Stéphan, P.-Y. Le Gall, C. Chevrot, *J. Chim. Phys.* **1998**, *95*, 1258–1261, DOI 10.1051/jcp:1998260.
343. K. Reuter, *EU Patent*, EP 1352918 B1, **2006**.
344. S. Yeislay, C. J. J. Dubois, C.-H. Hsu, S. W. Shuey, Y. Shen, H. Skulason, *U.S. Patent*, WO 2006/073968 A2, **2006**.
345. S. J. Higgins, F. Mouffouk, *U.S. Patent*, WO 2006/018643 A2, **2006**.
346. M. Blohm, J. Pickett, P. VanDort, *U.S. Patent*, US 5,111,327, **1992**.
347. Y. Yoshida, Y. Sakakura, N. Aso, S. Okada, Y. Tanabe, *Tetrahedron* **1999**, *55*, 2183–2192, DOI 10.1016/S0040-4020(99)00002-2.
348. P. Leriche, P. Blanchard, P. Frere, E. Levillain, G. Mabon, J. Roncali, *Chem. Commun.* **2006**, 275–277, DOI 10.1039/B513923F.
349. S. Hong, *Bull. Korean Chem. Soc.* **2003**, *24*, 961–966.
-

-
350. G. Brocks, *The Journal of Physical Chemistry* **1996**, *100*, 17327–17333, DOI [10.1021/jp962106f](https://doi.org/10.1021/jp962106f).
351. C. Hoyle, C. Bowman, *Angewandte Chemie International Edition* **2010**, *49*, 1540–1573, DOI [10.1002/anie.200903924](https://doi.org/10.1002/anie.200903924).
352. A. B. Lowe, *Polym. Chem.* **2010**, *1*, 17–36, DOI [10.1039/B9PY00216B](https://doi.org/10.1039/B9PY00216B).
353. M. J. Kade, D. J. Burke, C. J. Hawker, *Journal of Polymer Science Part A: Polymer Chemistry* **2010**, *48*, 743–750, DOI [10.1002/pola.23824](https://doi.org/10.1002/pola.23824).
354. C. Becer, R. Hoogenboom, U. Schubert, *Angewandte Chemie International Edition* **2009**, *48*, 4900–4908, DOI [10.1002/anie.200900755](https://doi.org/10.1002/anie.200900755).
355. A. Dondoni, *Angewandte Chemie International Edition* **2008**, *47*, 8995–8997, DOI [10.1002/anie.200802516](https://doi.org/10.1002/anie.200802516).
356. T. Posner, *Berichte der deutschen chemischen Gesellschaft* **1905**, *38*, 646–657, DOI [10.1002/cber.190503801106](https://doi.org/10.1002/cber.190503801106).
357. H. C. Kolb, M. G. Finn, K. B. Sharpless, *Angewandte Chemie International Edition* **2001**, *40*, 2004–2021, DOI [10.1002/1521-3773\(20010601\)40:11<2004::AID-ANIE2004>3.0.CO;2-5](https://doi.org/10.1002/1521-3773(20010601)40:11<2004::AID-ANIE2004>3.0.CO;2-5).
358. C. E. Hoyle, T. Y. Lee, T. Roper, *Journal of Polymer Science Part A: Polymer Chemistry* **2004**, *42*, 5301–5338, DOI [10.1002/pola.20366](https://doi.org/10.1002/pola.20366).
359. C. R. Morgan, F. Magnotta, A. D. Ketley, *Journal of Polymer Science: Polymer Chemistry Edition* **1977**, *15*, 627–645, DOI [10.1002/pol.1977.170150311](https://doi.org/10.1002/pol.1977.170150311).
360. M. Balog, H. Rayah, F. Le Derf, M. Salle, *New J. Chem.* **2008**, *32*, 1183–1188, DOI [10.1039/B715568A](https://doi.org/10.1039/B715568A).
361. X. Cai, E. Jaehne, H.-J. Adler, W. Guo, *Chinese Journal of Chemistry* **2010**, *28*, 1272–1278, DOI [10.1002/cjoc.201090220](https://doi.org/10.1002/cjoc.201090220).
362. R. A. Simon, A. J. Ricco, M. S. Wrighton, *Journal of the American Chemical Society* **1982**, *104*, 2031–2034, DOI [10.1021/ja00371a045](https://doi.org/10.1021/ja00371a045).
363. S. Inaoka, D. M. Collard, *Langmuir* **1999**, *15*, 3752–3758, DOI [10.1021/la981330o](https://doi.org/10.1021/la981330o).
364. F. Faverolle, A. J. Attias, B. Bloch, P. Audebert, C. P. Andrieux, *Chemistry of Materials* **1998**, *10*, 740–752, DOI [10.1021/cm970466p](https://doi.org/10.1021/cm970466p).
365. D. Cossement, F. Plumier, J. Delhalle, L. Hevesi, Z. Mekhalif, *Synthetic Metals* **2003**, *138*, 529–536, DOI [10.1016/S0379-6779\(02\)01260-2](https://doi.org/10.1016/S0379-6779(02)01260-2).
366. C.-G. Wu, C.-Y. Chen, *J. Mater. Chem.* **1997**, *7*, 1409–1413, DOI [10.1039/A608365J](https://doi.org/10.1039/A608365J).
367. M. Hu, S. Noda, T. Okubo, Y. Yamaguchi, H. Komiyama, *Applied Surface Science* **2001**, *181*, 307–316, DOI [10.1016/S0169-4332\(01\)00399-3](https://doi.org/10.1016/S0169-4332(01)00399-3).
368. U. Jonsson, M. Malmqvist, I. Ronnberg, *Biochem. J* **1985**, *227*, 363–371.
-

Appendix A

Experimental procedures

General notes

Synthesis of derivatives

After synthesis, ^1H and ^{13}C NMR spectra were recorded using a Bruker AMX-500 spectrometer operating at 500 and 125.70 MHz, respectively.

All chemicals were purchased from Aldrich and used without purification. Melting points were determined using an OPTIMELT MV-160 apparatus and are uncorrected. Chromatographic purifications were performed using Merck 9385 silica gel, pore size 60 Å, (230-400 mesh).

Electrochemical measures

Electrochemical measures were carried out using a PARSTAT2273 potentiostat in a single chamber three electrodes electrochemical cell, in a glove box filled with Argon ($[\text{O}_2] \leq 1$ ppm). Glassy Carbon (GC) and gold discs were used as working electrodes. The counter and pseudo-reference electrodes were a Pt flag and a Ag/AgCl wire, respectively. Both GC and gold pins were well polished with alumina 0.1 μm suspension, sonicated for 15 min in acetone and washed with 2-propanol before use. The Ag/AgCl pseudo-reference electrode was calibrated before and after each measurement using a 1 mM ferrocene solution in the electrolyte; no more than 5 mV difference was observed between two successive calibrations.

Optical absorption spectroscopy was performed using a Jasco V570 spectrophotometer. Spectroelectrochemical measures of solutions were performed using a thin layer quartz cell with 0.5 or 1 mm optical path lengths (Als Co. Ltd; Japan), and using gold mesh, Pt wire and Ag/AgCl as working, counter and reference electrodes respectively.

Surface functionalizations

Toluene was dried using an M. Braun solvent purification system and degassed before being introduced into an M. Braun glovebox. MPTMS and DTT were purchased from Aldrich and used without purification. All glassware and Teflon holders for film formation were cleaned by immersion in a piranha solution (7:3 v/v H_2SO_4 /30% H_2O_2) for 10 min and then DI water. Single-crystal silicon (100) substrates, purchased from Wafernet (San Jose, CA), were cleaned by sonication for 8 min sequentially in n-hexane, acetone, and ethanol and then dried

A.1 - General procedure for *in situ* chemical polymerization of ISOx monomers

under a stream of N₂. Subsequently, the slides were treated with a UVOCS cleaning system (Montgomery, PA), washed with isopropanol, dried under a stream of N₂, and heated overnight at 130 °C in an oven. Quartz slides (Chem-glass, Inc.), were rinsed with DI water and cleaned by immersion in a piranha solution for 1 h. The substrates were then rinsed with DI water followed by the RCA cleaning protocol (1:5:1 (v/v) solution of aqueous NH₃ (33%)/H₂O/30% H₂O₂ at room temperature for 1 h). The substrates were subsequently washed with DI water and isopropanol, dried under a N₂ stream, and heated overnight at 130 °C. UV/Vis spectra were recorded on glass slides with a Cary 100 spectrophotometer in the double beam mode. Atomic force microscopy (AFM) images were recorded using a Solver P47 (NT-MDT, Russia) instrument operated in the semicontact/tapping scanning mode. Film thicknesses were estimated on silicon using a J.A.Woollam (Lincoln, NB) model M-2000 V variable angle spectroscopic ellipsometer with the VASE32 software. XRR measurements were performed at Beamline X6B of the National Synchrotron Light Source, Brookhaven (Upton, NY) using a four-circle Huber diffractometer in the specular reflection mode (i.e., incident angle \hat{I} was equal to the exit angle). X-rays with an energy of $E = 10.0 \text{ keV}$ ($\lambda = 1.240 \text{ \AA}$) were used. The beam size was 0.30 mm vertically and 0.50 mm horizontally. The samples were held under a helium atmosphere during the measurements to reduce radiation damage and background scattering from the ambient gas. The off-specular background was measured and subtracted from the specular count.

A.1 General procedure for *in situ* chemical polymerization of ISOx monomers

A solution of the monomer (ISO2) was prepared adding to 150 mg of the pure compound: propylene carbonate (90 mg), nitromethane (678 mg) and 1-methoxy-2-propanol (1044 mg) in the stated order. An oxidant solution (426 mg) of Fe(OTs)₃ (36%) and PEG-*ran*-PPG (9%) in 1-butanol was added to the aforementioned one under stirring at room temperature. The mixture was heated at 70 °C in a water bath for 5 min, and then kept at room temperature for 4 h. The obtained green solution was microfiltered through a 0.45 μm PTFE filter and deposited by spin coating on clean substrates (deposition @ 0 rpm + 30 s @ 600 rpm + 10 s @ 1200 rpm). After 5 min at room temperature, the substrates were cured in an oven at 115 °C for 30 min. Once cooled, the polymerized layers were rinsed in

EtOH for 2 min and blown dried with compressed air.

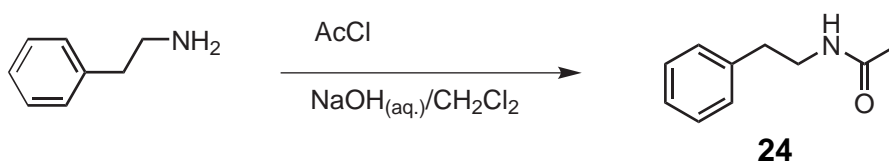
A.2 Procedures for surface functionalizations

Route A: A 5 mM solution of 3-mercaptopropyl-trimethoxysilane (MPTMS) in toluene (150 ml) was prepared under N₂ in a glove box. The cleaned substrates (quartz and silicon) were immersed in the solution for 30 min and subsequently rinsed twice with 150 ml of anhydrous toluene. The substrates were taken out of the box and successively sonicated in toluene, acetone and ethanol, and finally dried under a stream of N₂. Prior to utilization the substrates were immersed for 30 min in a 100 mM solution of dithiothreitol (DTT) in 10 mM sodium phosphate buffer. The substrates were subsequently washed in the same buffer followed by DI water and ethanol, and finally dried under a stream of N₂. A drop of **95** was deposited on each substrate. They were subsequently covered with a quartz slide forming a uniform thin film of liquid **95** between the two surfaces. The slides were irradiated for 15 min with an handheld UV/lamp from a distance of $\simeq 10$ cm using a 254 nm wavelength. In a second trial, 1% molar of 2,2-Dimethoxy-2-phenylacetophenone (DMPA) was dissolved in the monomer, and the samples were irradiated at 365 nm. The samples were then washed with THF, followed by acetone and ethanol, and finally dried under a stream of N₂.

Route B: A 2.75 mM solution of **102** in toluene (150 ml) was prepared under N₂ in a glove box. The cleaned substrates (quartz and silicon) were immersed in the solution for 3.5 h and subsequently rinsed twice with 150 ml of anhydrous toluene. The substrates were taken out of the box and successively sonicated in toluene, acetone and ethanol, and finally dried under a stream of N₂.

A.3 Synthetic procedures

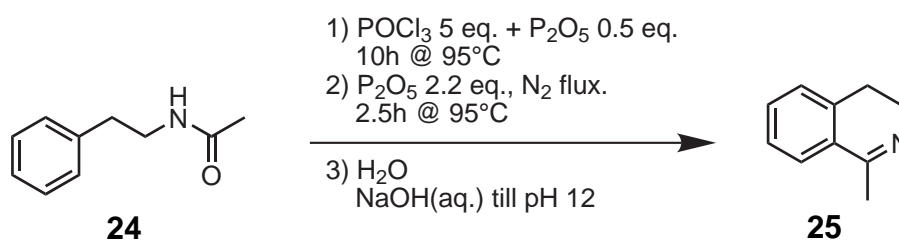
Synthesis of *N*-phenethylacetamide (**24**)



To a mixture of 2-phenylethanamine (103.9 g, 0.857 mol), CH₂Cl₂ (100 ml) and water (30 ml); acetyl chloride (73.6 g, 0.943 mol) and a 30% aqueous NaOH solution (40.0 g, 1.00 mol) were simultaneously added over 1 h, cooling the flask with an ice/water bath. The mixture was stirred for further 30 min then 150 ml of CH₂Cl₂ and 80 ml of water were added. The organic phase was collected and the aqueous one was extracted with further 2 × 30 ml of CH₂Cl₂. The solution was washed with 2 × 40 ml of HCl_(aq) 5%, 40 ml of saturated NaHCO₃ aqueous solution and with 50 ml of brine. The organic phase was dried over Na₂SO₄ overnight, and the solvent was evaporated under reduced pressure obtaining product as a white solid (115.11 g, 0.705 mol, m.p.=51.5-52.1 °C, yield 82%).

¹H NMR (500 MHz, CDCl₃) δ [ppm]: 7.32 (t, *J*=7.3 Hz, 2H), 7.26-7.23 (m, 1H), 7.21 (d, *J*=7.1 Hz, 2H), 5.78 (s, 1H), 3.52 (q, *J*=6.1 Hz, 2H), 2.83 (t, *J*=7.0 Hz, 2H), 1.95 (s, 3H).

Synthesis of 1-methyl-3,4-dihydroisoquinoline (25)



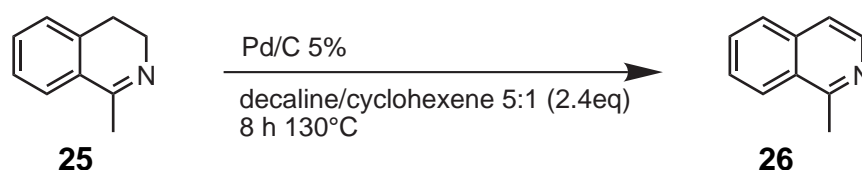
To a mixture of **24** (104.36 g, 0.639 mol) and P₂O₅ (53.0 g, 0.374 mol), under nitrogen atmosphere, POCl₃ was added (300 ml, 502.5 g, 3.28 mol). The mixture was heated to 95 °C for 10 h. Reaction seemed to reach equilibrium and imidoyl chlorides (uncyclized intermediates) spot was still present on TLC*. Reaction was cooled to RT. A further amount of P₂O₅ (200 g, 1.41 mol) was added, and nitrogen was fluxed through the mixture. Reaction was heated to 95 °C for 2.5 h. Imidoyl chlorides spot disappeared from TLC, and complete conversion was achieved. The mixture was cooled to RT and slowly poured in crushed ice (1.5 kg) cooling with an ice bath. After 2 h NaOH pellets were slowly added to the mixture till pH 12 cooling with an ice-water bath. An amber coloured oil with rose-like smell separated from the solution. Diethyl ether (200 ml) was added to the stirred mixture, and the organic layer was collected. A large amount of crystalline Na₃PO₄ · 12 H₂O precipitated from the aqueous

*reaction was monitored by TLC (eluent Et₂O/MeOH 20:1) treating a sample of the mixture with basic water and extracting with Et₂O

phase (over the weekend). The solid was filtered out and washed on the filter with Et₂O (70 ml). The filtrate was extracted with 2 × 70 ml of Et₂O. All the organic phases were collected, washed with 5 × 70 ml of brine, and dried over Na₂SO₄. Solvent was evaporated under reduced pressure obtaining product **25** as a yellow oil (81.27 g, 0.56 mol, yield 88%).

¹H NMR (500 MHz, DMSO-d₆) δ [ppm]: 7.54 (d, *J*=7.6 Hz, 1H), 7.39 (td, *J*=7.4 Hz, *J*=1.3 Hz, 1H), 7.33 (t, *J*=7.5 Hz, 1H), 7.24 (d, *J*=7.3 Hz, 1H), 3.52 (m, 2H), 2.63 (t, *J*=7.8 Hz, 2H), 2.30 (t, *J*=1.5 Hz, 3H).

Synthesis of 1-methylisoquinoline (26)

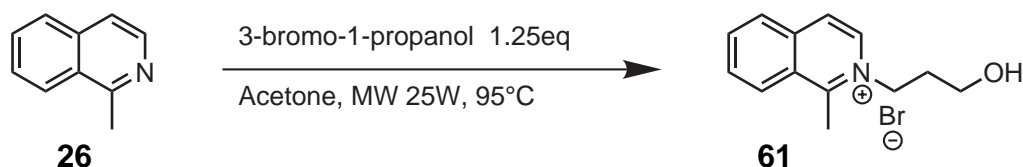


Acetic acid (2 ml) was added to 4.00 g of Pd/C 5%. After 10 min cyclohexene (135 ml, 1.33 mol), decalin (500 ml) and **25** (81.27 g, 0.56 mol) were added. The mixture was refluxed for 8 h (reflux temperature was 130 °C). The mixture was cooled to RT, and the catalyst was filtered out and recovered. An aqueous solution of HCl (3 M) was added to the mixture till pH 1. The aqueous phase was collected, and the organic one was extracted with further 2 × 50 ml of HCl_(aq) 3 M collecting the aqueous phase. The aqueous solution was washed with 5 × 40 ml of CH₂Cl₂, and then Na₂CO₃ was added till pH 10. A yellow oil separated, and the mixture was extracted with 100 ml + 5 × 40 ml of Et₂O. The organic phase was dried overnight over Na₂SO₄ then the solvent was evaporated under reduced pressure (1 mmHg) obtaining product as a yellow oil (68.617 g, 0.479 mol, yield 86%).

¹H NMR (500 MHz, CDCl₃) δ [ppm]: 8.38 (d, *J*=5.8 Hz, 1H), 8.08 (d, *J*=8.4 Hz, 1H), 7.77 (d, *J*=8.2 Hz, 1H), 7.64 (t, *J*=7.5 Hz, 1H), 7.56 (t, *J*=8.2 Hz, 1H), 7.48 (d, *J*=5.8 Hz, 1H), 2.94 (s, 3H).

Synthesis of 2-(3-hydroxypropyl)-1-methylisoquinolinium bromide (61)

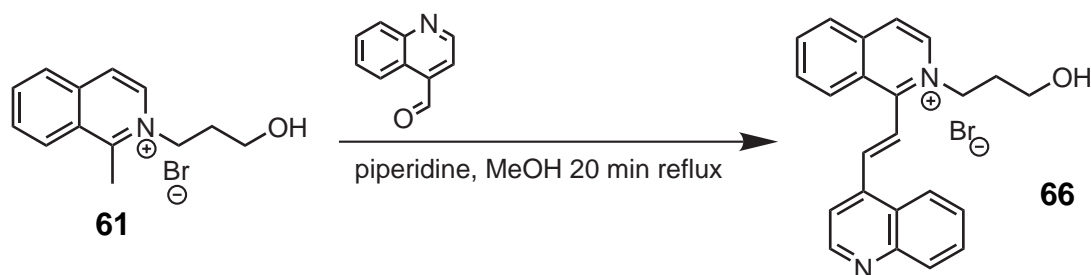
A mixture of **26** (4.00 g, 27.9 mmol), 3-bromo-1-propanol (4.84 g, 34.8 mmol) and 10 ml of acetone was heated in a CEM Discover microwave reactor for 2.5 h (*P*_{max}=25 W, 95 °C, cooling off, 35 ml vessel), and cooled to RT. The vessel was



kept at -18°C overnight; the white solid was filtered on a Büchner funnel, washed with acetone and then with Et_2O . Residual solvent was evaporated under reduced pressure (0.4 torr) at 40°C (5.186 g, 18.37 mmol, yield 66%, m.p.: $176-177^\circ\text{C}$). Product can be further purified by crystallization from *i*-PrOH.

^1H NMR (200 MHz, $\text{DMSO}-d_6$) δ [ppm]: 8.79-8.73 (m, 2H), 8.44 (d, $J=6.9$ Hz, 1H), 8.31 (d, $J=7.8$ Hz, 1H), 8.20 (t, $J=6.9$ Hz, 1H), 8.03 (t, $J=7.8$ Hz, 1H), 4.84 (t, $J=7.3$ Hz, 2H), 3.54 (t, $J=5.7$ Hz, 2H), 3.31 (s, 3H), 2.10 (qui, $J=6.3$ Hz, 2H); Anal. Calcd for $\text{C}_{13}\text{H}_{16}\text{BrNO}$: C, 55.33; H, 5.72; N, 4.96. Found: C, 54.96; H, 6.05; N, 4.87.

Synthesis of (*E*)-2-(3-hydroxypropyl)-1-(2-(quinolin-4-yl)vinyl)-isoquinolinium bromide (66)

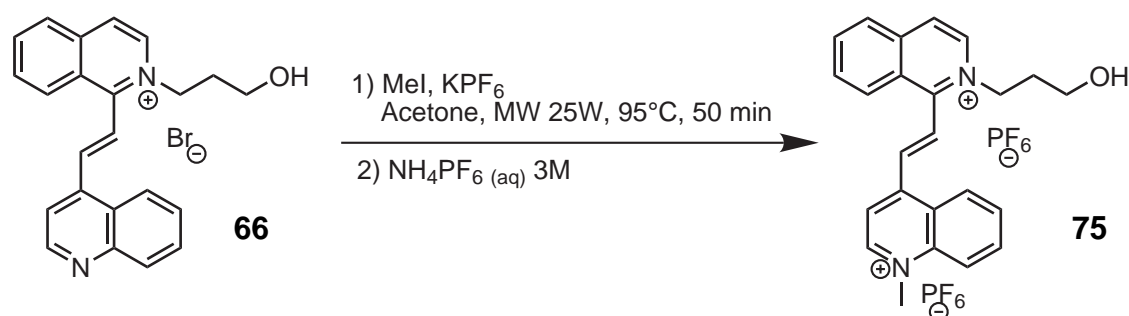


To a mixture of **61** (10.341 g, 36.64 mmol) and quinoline-4-carboxaldehyde (6.507 g, 41.40 mmol), a solution of piperidine (1.0 ml, 862 mg, 10.12 mmol) in 10 ml of MeOH was added. The mixture was heated to reflux for 20 min obtaining a red homogeneous solution. The solution was let cool to room temperature and product was left to crystallize overnight. The crystalline solid was filtered on a Büchner funnel and washed with 10 ml of acetone and 30 ml of Et_2O . Residual solvent was removed under reduced pressure at 50°C . Product was recovered as a yellow solid (13.199 g, 31.3 mmol, yield 86%, m.p.: 191°C (dec.)).

^1H NMR (500 MHz, $\text{DMSO}-d_6$) δ [ppm]: 9.10 (d, $J=4.5$ Hz, 1H), 8.95 (d, $J=6.9$ Hz, 1H), 8.66-8.63 (m, 2H), 8.44 (d, $J=8.1$ Hz, 1H), 8.32-8.27 (m, 3H), 8.20 (d, $J=4.5$ Hz, 1H), 8.16-8.13 (m, 2H), 8.08 (t, $J=7.75$ Hz, 1H), 7.85 (t, $J=6.7$ Hz, 1H), 7.70 (t,

$J=8.0\text{Hz}$, 1H), 4.94 (t, $J=7.4\text{Hz}$, 2H), 4.85 (t, $J=4.9\text{Hz}$, 1H), 3.53 (q, $J=5.3\text{Hz}$, 2H), 2.17 (qui, $J=6.7\text{Hz}$, 2H); ^{13}C NMR (125.7MHz, $\text{DMSO}-d_6$) δ [ppm]: 157.11, 150.98, 148.73, 140.16, 140.05, 137.93, 136.73, 136.32, 131.84, 130.54, 130.34, 130.17, 128.20, 127.89, 127.87, 126.04, 125.49, 124.33, 123.34, 119.03, 57.77, 56.78, 32.99; Anal. Calcd for $\text{C}_{23}\text{H}_{21}\text{BrN}_2\text{O} \cdot 0.5\text{CH}_3\text{OH} \cdot 0.25\text{H}_2\text{O}$: C, 63.88; H, 5.36; N, 6.34. Found: C, 63.72; H, 5.52; N, 6.40.

Synthesis of (*E*)-4-(2-(2-(3-hydroxypropyl)isoquinolinium-1-yl)-vinyl)-1-methylquinolinium hexafluorophosphate (75)



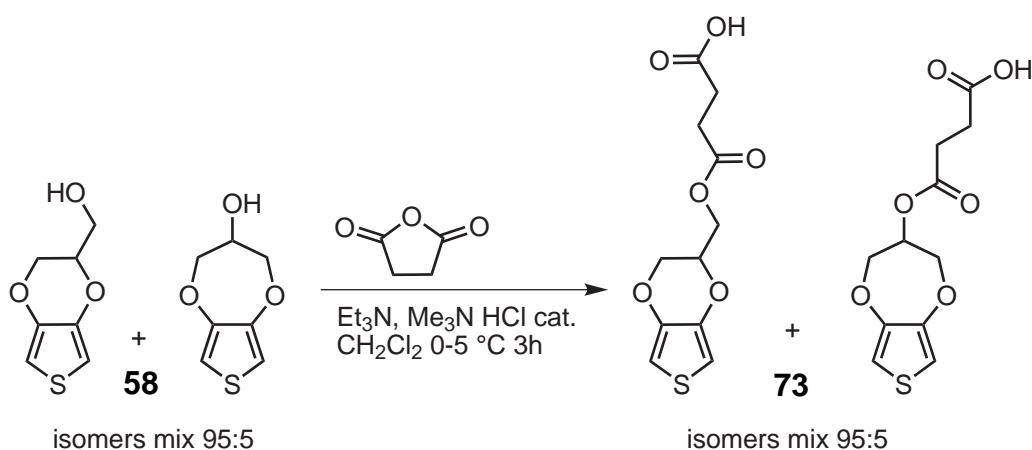
A suspension of **66** (3.00 g, 7.12 mmol), KPF_6 (3.100 g, 16.84 mmol) in 10.5 ml of acetone was stirred at room temperature for 20 min, and MeI was subsequently added (1.65 g, 11.62 mmol). The mixture was heated in a CEM Discover microwave reactor for 50 min ($P_{\text{max}}=25\text{W}$, 95°C , cooling off, 35 ml closed vessel), cooled to RT and left to precipitate overnight.* The solid was filtered on a Büchner funnel and washed with few ml of acetone and then with Et_2O . The solid was suspended in 18 ml of $\text{NH}_4\text{PF}_6(\text{aq})$ 30% and stirred for 3 days. The product was filtered and washed with few ml of HPLC grade water and few ml of EtOH. Residual solvent was evaporated under reduced pressure (0.4 torr) at 40°C obtaining product as a pale yellow solid (3.77 g, 5.83 mmol, yield 82%, m.p.: $199\text{-}201^\circ\text{C}$).

^1H NMR (500MHz, $\text{DMSO}-d_6$) δ [ppm]: 9.67 (d, $J=6.2\text{Hz}$, 1H), 8.93 (d, $J=6.8\text{Hz}$, 1H), 8.77 (d, $J=6.1\text{Hz}$, 1H), 8.7-8.65 (m, 3H), 8.62 (d, $J=8.9\text{Hz}$, 1H), 8.50 (d, $J=16.3\text{Hz}$, 1H), 8.45 (d, $J=8.2\text{Hz}$, 1H), 8.41 (d, $J=16.3\text{Hz}$, 1H), 8.38-8.31 (m, 2H), 8.14-8.08 (m, 2H), 4.91 (t, $J=7.2\text{Hz}$, 2H), 3.52 (t, $J=5.7\text{Hz}$, 2H), 2.16 (qui, $J=6.4\text{Hz}$, 2H); ^{13}C NMR (125.7MHz, $\text{DMSO}-d_6$) δ [ppm]: 155.92, 150.24, 149.95, 139.20, 137.98, 137.39, 137.00, 136.44, 135.92, 131.98; 130.79, 130.42, 129.20, 128.26,

*reaction was checked by TLC (eluent: $\text{MeOH}/\text{MeNO}_2/\text{NH}_4\text{Cl}(\text{aq})$ 2M 8:1:1) dissolving a sample of the mixture in MeCN. Product spot has a yellow fluorescence

127.67, 127.41, 126.71, 126.09, 120.24, 119.78, 57.72, 56.97, 46.00, 33.08; Anal. Calcd for $C_{24}H_{24}F_{12}N_2OP_2$: C, 44.60; H, 3.74; N, 4.33. Found: C, 44.56; H, 3.82; N, 4.29.

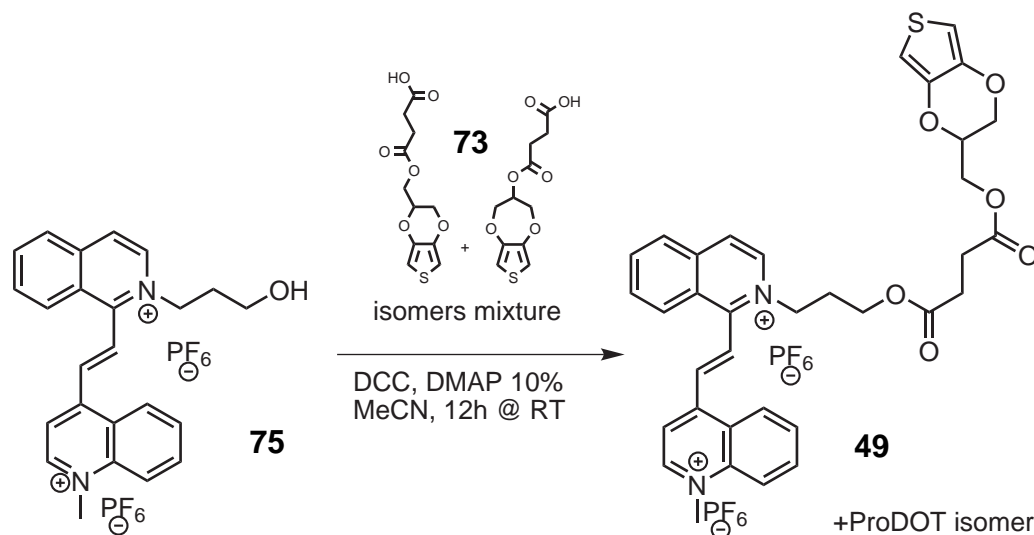
Synthesis of 4-((2,3-dihydrothieno[3,4-*b*][1,4]dioxin-2-yl)methoxy)-4-oxobutanoic acid (4-EDOT-MeO-4-oxobutanoic acid) and 4-(3,4-dihydro-2H-thieno[3,4-*b*][1,4]dioxepin-3-yloxy)-4-oxobutanoic acid (4-ProDOT-O-4-oxobutanoic acid) mixture (73)



Under nitrogen atmosphere, to an ice-cooled suspension of succinic anhydride (1.31 g, 13.1 mmol) and Me₃N·HCl (62.7 mg, 0.656 mmol) in CH₂Cl₂ (35 ml), Et₃N (0.996 g, 9.84 mmol) was added. A solution of EDOT-MeOH (58) (mixture of isomers 95:5, 1.13 g, 6.56 mmol) in CH₂Cl₂ (7 ml) was added, and the solution was stirred at 0 °C for 3 h. The mixture was extracted with 3x10 ml of HCl_(aq) 10%. The organic phase was collected, dried overnight over Na₂SO₄ and the solvent was evaporated under reduced pressure. The crude product was dissolved in 40 ml of NaHCO_{3(aq)} 0.5M, stirred for 1 h, acidified to pH<1 adding HCl_(aq) 10% and extracted with 20 ml of toluene. The organic phase was washed with 10 ml of HCl_(aq) 10%, and dried over Na₂SO₄. Product was obtained as a pale yellow solid after solvent removal under reduced pressure for 72 h (1.064 g, yield 60%).

¹H NMR (500 MHz, CDCl₃) δ [ppm]: 6.51 (s, 2H ProDOT), 6.35 (m, 2H EDOT), 5.27 (qui, 1H ProDOT), 4.40-4.31 (m, 3H EDOT), 4.25-4.21 (m, 1H EDOT + 4H ProDOT), 4.06-4.02 (m, 1H EDOT), 2.70 (m, 4H (EDOT + ProDOT)).

Synthesis of (*E*)-4-(2-(2-(3-(4-((2,3-dihydrothieno[3,4-*b*][1,4]dioxin-2-yl)methoxy)-4-oxobutanoyloxy)propyl)isoquinolinium-1-yl)vinyl)-1-methylquinolinium hexafluorophosphate (49) (ISO1)



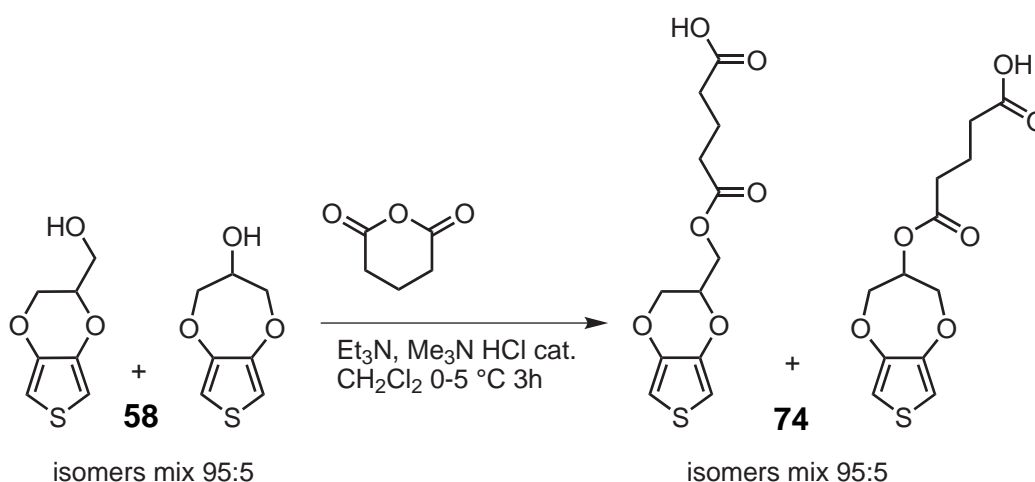
Under nitrogen atmosphere, a suspension of **73** (737 mg, 2.71 mmol), **75** (1.749 g, 2.71 mmol), DCC (615 mg, 2.98 mmol) and DMAP (35 mg, 0.29 mmol) in 10 ml of anhydrous MeCN was prepared. A white solid precipitated. The solution was kept under stirring for 6h. The mixture was filtered washing the precipitate with MeCN. The filtrate was collected and evaporated under reduced pressure obtaining a black solid which was sonicated for 15 min with Et₂O (30 ml). The product was filtered, suspended in 30 ml of EtOH and stirred for 72h*. The mixture was filtered on an Hirsh funnel obtaining the product as a pale brown solid (1.926 g, yield 76%, m.p.: 94-100 °C).

¹H NMR (500 MHz, DMSO-*d*₆) δ [ppm]: 9.68 (d, *J*=6.3 Hz, 1H (EDOT + ProDOT)), 8.92 (d, *J*=6.9 Hz, 1H (EDOT + ProDOT)), 8.80 (d, *J*=6.2 Hz, 1H (EDOT + ProDOT)), 8.71 (d, *J*=6.9 Hz, 1H (EDOT + ProDOT)), 8.67-8.60 (m, 3H (EDOT + ProDOT)), 8.50 (d, *J*=16.2 Hz, 1H (EDOT + ProDOT)), 8.45 (d, *J*=8.2 Hz, 1H (EDOT + ProDOT)), 8.41 (d, *J*=16.2 Hz, 1H (EDOT + ProDOT)), 8.34 (m, 2H (EDOT + ProDOT)), 8.10 (m, 2H (EDOT + ProDOT)), 6.79 (s, 2H ProDOT), 6.60 (m, 2H EDOT), 4.91 (t, *J*=7.3 Hz, 2H (EDOT + ProDOT)), 4.72 (s, 3H (EDOT + ProDOT)), 4.38 (m, 1H EDOT), 4.27-4.20 (m, 3H EDOT), 4.11 (t, *J*=6.0 Hz, 2H (EDOT + ProDOT)), 4.13-4.10 (4H ProDOT), 4.00-3.97 (m, 1H EDOT), 2.47 (t, *J*=7.0 Hz, 2H EDOT + ProDOT), 2.30 (m, 4H (EDOT + ProDOT)); EDOT:ProDOT ratio is

*This step is necessary to eliminate residual DMAP from the product.

21:1. Anal. Calcd for $C_{35}H_{34}F_{12}N_2O_6P_2S \cdot \frac{1}{3}CH_3CH_2OH$: C, 46.77; H, 3.96; N, 3.06; S, 3.50. Found: C, 46.93; H, 4.12; N, 3.23; S, 3.67.

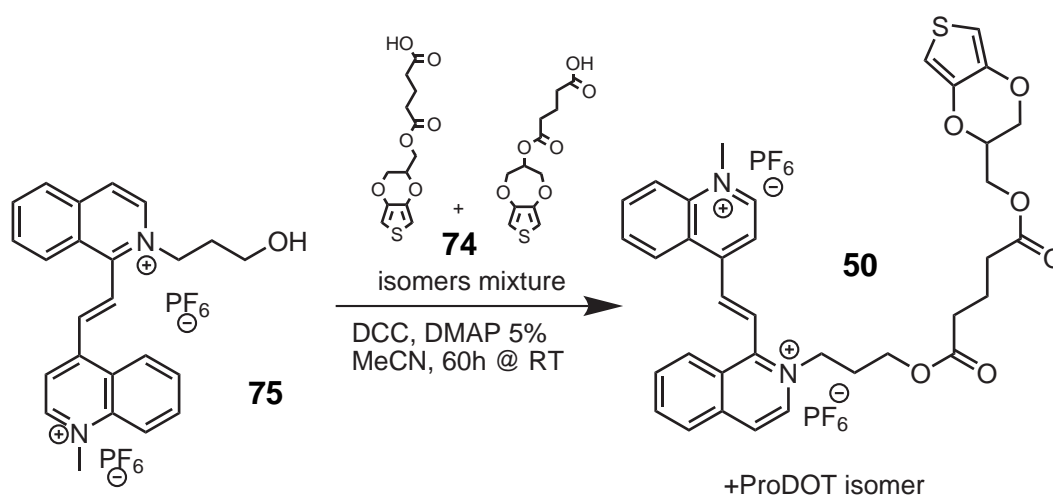
Synthesis of 5-((2,3-dihydrothieno[3,4-*b*][1,4]dioxin-2-yl)methoxy)-5-oxopentanoic acid (5-EDOT-MeO-5-oxopentanoic acid) and 5-(3,4-dihydro-2H-thieno[3,4-*b*][1,4]dioxepin-3-yloxy)-5-oxopentanoic acid (5-ProDOT-O-5-oxopentanoic acid) mixture (74)



Under nitrogen atmosphere, to an ice-cooled suspension of glutaric anhydride (1.556 g, 13.64 mmol) and $Me_3N \cdot HCl$ (65.2 mg, 0.682 mmol) in CH_2Cl_2 (20 ml), Et_3N (1.035 g, 10.23 mmol) was added. A solution of EDOT-MeOH (mixture of isomers 95:5, 1.174 g, 6.82 mmol) in CH_2Cl_2 (7 ml) was added, and the solution was stirred at $0^\circ C$ for 3 h 15 min. The mixture was extracted with 3×10 ml of $HCl_{(aq)}$ 10%. The organic phase was collected, filtered, and dried over Na_2SO_4 overnight. The mixture was filtered and the solvent was evaporated under reduced pressure. Toluene (3 ml) and water (3 ml) were added to the crude product and the mixture was kept under stirring at RT for 12 h. Toluene and water were added to the mixture till a clear phase separation occurred. The organic phase was collected and the aqueous phase if extracted with 2×10 ml of toluene. The organic phase was collected, dried over Na_2SO_4 and filtered. Product was obtained as a pale yellow viscous oil after solvent removal under reduced pressure (3 mmHg) at $60^\circ C$ for 8 h (1.394 g, yield 71%). The product slowly crystallized in 6 months to a white solid (mp.: $53-60^\circ C$). 1H NMR (500 MHz, $CDCl_3$) δ [ppm]: 6.51 (s, 2H ProDOT), 6.37 (d, $J=3.7$ Hz, 1H EDOT), 6.35 (d, $J=3.7$ Hz, 1H EDOT), 5.25 (qui, $J=4.6$ Hz, 1H ProDOT),

4.40-4.36 (m, 1H EDOT), 4.35-4.29 (m, 2H EDOT), 4.27-4.20 (m, 1H EDOT + 4H ProDOT), 4.06-4.02 (m, 1H EDOT), 2.51-2.44 (m, 4H (EDOT + ProDOT)), 2.09-1.94 (m, 2H (EDOT + ProDOT)); EDOT:ProDOT ratio is 4:1; ^{13}C NMR (125.7 MHz, CDCl_3) δ [ppm]: 178.49, 172.54, 141.26, 141.07, 100.86-99.49 (m), 71.52, 65.66, 62.48, 32.94, 32.84, 19.77; Anal. Calcd for $\text{C}_{12}\text{H}_{14}\text{O}_6\text{S}$: C, 50.34; H, 4.93. Found: C, 50.63; H, 5.58.

Synthesis of (*E*)-4-(2-(2-(3-(5-((2,3-dihydrothieno[3,4-*b*][1,4]dioxin-2-yl)methoxy)-5-oxopentanoyloxy)propyl)isoquinolinium-1-yl)-vinyl)-1-methylquinolinium hexafluorophosphate (50) (ISO2)



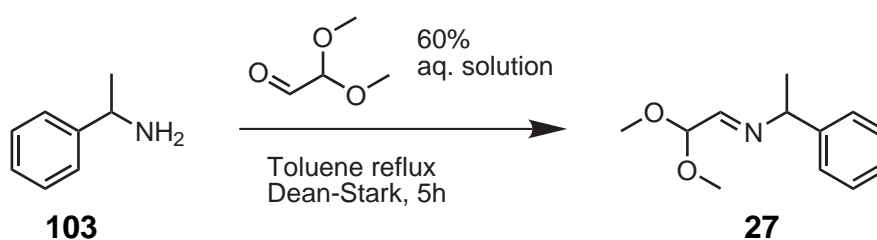
Under nitrogen atmosphere, a suspension of **74** (2.737 g, 9.56 mmol, 80:20 EDOT:ProDOT), **75** (6.000 g, 9.28 mmol), DCC (2.107 g, 10.20 mmol) and DMAP (62 mg, 0.51 mmol) in 60 ml of anhydrous MeCN was prepared. The formation of a white precipitate was observed. The solution was kept under stirring for 60h. The mixture was filtered washing the precipitate with MeCN (20 ml). The filtrate was collected and evaporated under reduced pressure obtaining a black solid which was sonicated with Et_2O (50 ml). The product was collected by filtration, suspended in 50 ml of EtOH and stirred for 72h*. The mixture was filtered on an Hirsh funnel obtaining the product as a pale light brown solid (7.338 g, yield 87%, m.p.: 77-87 °C).

^1H NMR (500 MHz, $\text{DMSO}-d_6$) δ [ppm]: 9.69 (d, $J=6.3$ Hz, 1H (EDOT + ProDOT)), 8.94 (d, $J=6.9$ Hz, 1H (EDOT + ProDOT)), 8.81 (d, $J=6.2$ Hz, 1H (EDOT + ProDOT)), 8.71 (d, $J=6.8$ Hz, 1H (EDOT + ProDOT)), 8.66-8.61 (m, 3H (EDOT + ProDOT)),

*This step is necessary to eliminate residual DMAP from the product

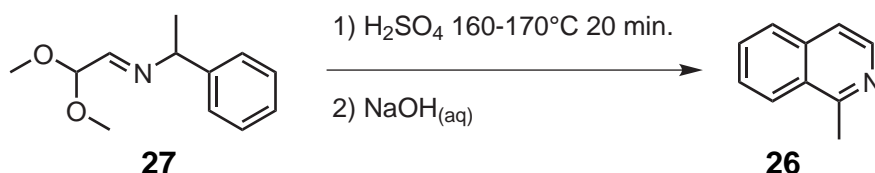
8.50 (d, $J=16.3$ Hz, 1H (EDOT + ProDOT)), 8.45 (d, $J=8.2$ Hz, 1H (EDOT + ProDOT)), 8.41 (d, $J=16.3$ Hz, 1H (EDOT + ProDOT)), 8.37-8.32 (m, 2H (EDOT + ProDOT)), 8.13-8.08 (m, 2H (EDOT + ProDOT)), 6.81 (s, 2H ProDOT), 6.61 (d, $J=3.6$ Hz, 1H EDOT), 6.60 (d, $J=3.5$ Hz, 1H EDOT), 5.12 (qui, $J=3.7$ Hz, 1H ProDOT), 4.91 (t, $J=7.5$ Hz, 2H (EDOT + ProDOT)), 4.72 (s, 3H (EDOT + ProDOT)), 4.41-4.39 (m, 1H EDOT), 4.29-4.20 (m, 2H EDOT + 4H ProDOT), 4.14-4.10 (m, 1H EDOT + 2H (EDOT + ProDOT)), 4.02-3.98 (m, 1H EDOT), 2.34-2.24 (m, 4H (EDOT+ ProDOT)), 2.12-2.07 (m, 2H (EDOT + ProDOT)), 1.62-1.54 (m, 2H (EDOT + ProDOT)); EDOT:ProDOT ratio is 4:1; ^{13}C NMR (125.7MHz, DMSO- d_6) δ [ppm]: 172.76, 156.26, 150.18, 150.06, 141.66, 141.54, 139.27, 138.16, 137.68, 137.28, 136.49, 136.08, 132.17, 130.94, 130.58, 129.23, 128.40, 127.85, 127.49, 126.75, 126.33, 120.40, 119.94, 100.62, 100.55, 71.89, 65.52, 62.64, 61.42, 56.64, 46.16, 32.77, 32.75, 29.40, 20.06; Anal. Calcd. for $\text{C}_{36}\text{H}_{36}\text{F}_{12}\text{N}_2\text{O}_6\text{P}_2\text{S} \cdot \frac{1}{3}\text{CH}_3\text{CH}_2\text{OH}$: C, 47.35; H, 4.12; N, 3.01; S, 3.45. Found: C, 47.72; H, 4.21; N, 3.39; S, 3.61.

Synthesis of (*E*)-*N*-(2,2-diethoxyethylidene)-1-phenylethanamine (27)



A mixture of α -Methylbenzylamine (**103**) (50.00 g, 0.413 mmol) and dimethoxyacetaldehyde 60% w/w aqueous solution (79.14 g, 0.454 mmol) in 250 ml of toluene were refluxed for 5h under nitrogen atmosphere, collecting water with a Dean-Stark apparatus. The mixture was cooled to room temperature and solvent was removed under reduced pressure (~ 1 mmHg) obtaining product as a yellow oil (82.97 g, 0.400 mmol, yield 97%).

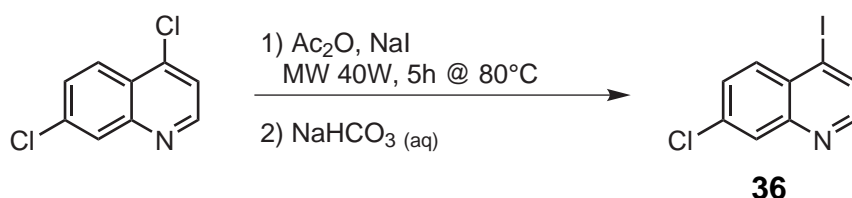
^1H NMR (500MHz, CDCl_3) δ [ppm]: 7.58 (d, $J=4.5$ Hz, 1H), 7.36-7.31 (m, 4H), 7.26-7.22 (m, 1H), 4.72 (d, $J=4.5$ Hz, 1H), 4.41 (q, $J=6.7$ Hz, 1H), 3.43 (s, 3H), 3.37 (s, 3H), 1.54 (d, $J=6.7$ Hz, 3H).



Alternative synthesis of 1-methyloisoquinoline (26)

In a 1L RBF, H₂SO₄ (300 ml) was heated to 160°C. The hot plate was switched off, and compound **27** (82.97 g, 0.400 mol) was dropwise added to the mixture maintaining temperature between 160°C and 170°C (addition took 15 minutes). A vigorous reaction with smoke evolution occurred and mixture turned to black. The mixture was stirred for further 5 min and then slowly poured in ice (800 g) cooling with an external ice bath. The solution was neutralized adding NaOH pellets till pH 10. The crude mixture (including all the precipitated Na₂SO₄) was transferred to a RBF and steam distilled. The distillate was extracted with ether (4 × 200 ml). The organic phase was collected, washed with brine (200 ml), and dried over Na₂SO₄ overnight. Solvent was evaporated under reduced pressure (5 mmHg) heating at 60°C for 3 h with an external water bath. Product was further purified by distillation (b.p.: 102.5°C at 5 mmHg). Colorless liquid (37.359 g, 0.261 mol, yield 65%).*

Synthesis of 7-chloro-4-iodoquinoline (36)



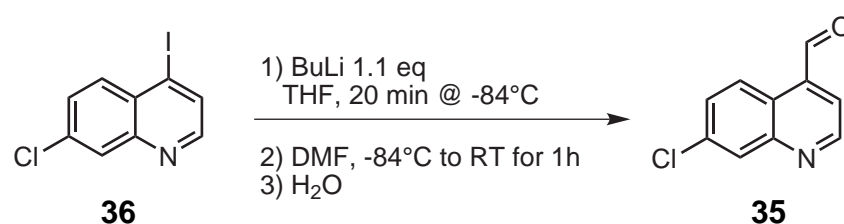
In a 35 ml microwave reaction vessel, a mixture of 4,7-dichloroquinoline (4.500 g, 22.72 mmol) and NaI (10.217 g, 68.16 mmol) in Ac₂O (5.798 g, 56.8 mmol) was prepared and heated at 80°C for 5 h in a CEM Discover microwave reactor (P_{max}=40 W, cooling off). Product was suspended in 100 ml of NaHCO₃(aq) 5% and stirred for 1 h. A 5% aqueous solution of Na₂SO₃ was added (50 ml)

*Product obtained with this route is purer than the one obtained with the Bischler-Napieralski route since it is free from 1-methyl-tetrahydroisoquinoline which can be seen in NMR spectrum (5%). This impurity was usually removed easily during crystallization of product **61** but its amount is dependent on reaction conditions. An high content of hydrogenated product can lead to a difficult purification of **61**.

followed by a 5% aqueous solution of $\text{Na}_2\text{S}_2\text{O}_3$ (50 ml). The mixture was extracted with $3 \times 30\text{ml}$ of CH_2Cl_2 , and dried over Na_2SO_4 . Solvent was evaporated under reduced pressure obtaining product as a white solid which was further purified by crystallization from EtOH (5.011 g, 17.31 mmol, yield 76%, m.p.: 123-124 °C).

^1H NMR (500 MHz, CDCl_3) δ [ppm]: 8.44 (d, $J=4.5\text{Hz}$, 1H), 8.06 (d, $J=2.1\text{Hz}$, 1H), 7.99 (d, $J=4.6\text{Hz}$, 1H), 7.97 (d, $J=9.0\text{Hz}$, 1H), 7.57 (dd, $J=8.9\text{Hz}$, $J=2.1\text{Hz}$, 1H).

Synthesis of 7-chloroquinoline-4-carbaldehyde (35)

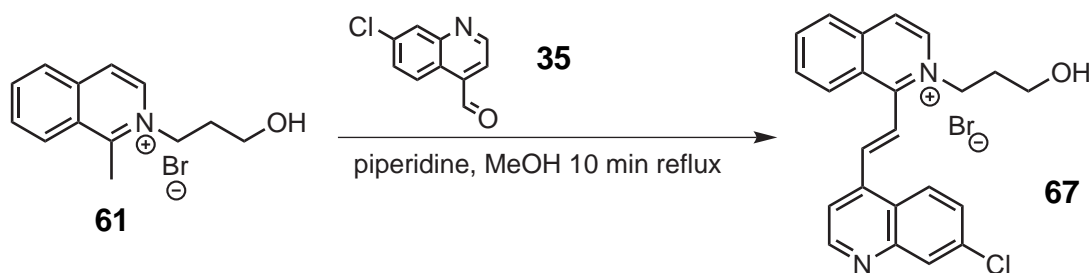


Under N_2 atmosphere, a solution of **36** (5.000 g, 17.27 mmol) in anhydrous THF (30 ml) was prepared, and cooled to -84°C with an AcOEt/ N_2 cooling bath. A 1.28 M BuLi solution in hexane (14.83 ml) was slowly added under stirring. The obtained red-brown mixture was stirred at -84°C for 20 min. Anhydrous DMF (1.262 g, 17.27 mmol) was slowly added and the mixture was allowed to warm slowly to room temperature and kept under stirring for 1 h. Water (50 ml) was added to the mixture obtaining an orange solution which was extracted with $3 \times 50\text{ml}$ of AcOEt. The organic phase was collected, washed with brine (100 ml), dried over Na_2SO_4 and evaporated under reduced pressure. The obtained product was purified by column chromatography (SiO_2 , eluent: AcOEt/n-Hex 1:3) (1.136 g, 5.93 mmol, yield 34 %, m.p.: 105-106 °C).

^1H NMR (500 MHz, CDCl_3) δ [ppm]: 10.45 (s, 1H), 9.21 (d, $J=4.2\text{Hz}$, 1H), 9.02 (d, $J=9.1\text{Hz}$, 1H), 8.22 (d, $J=2.2\text{Hz}$, 1H), 7.80 (d, $J=4.2\text{Hz}$, 1H), 7.69 (dd, $J=9.1\text{Hz}$, $J=2.2\text{Hz}$, 1H).

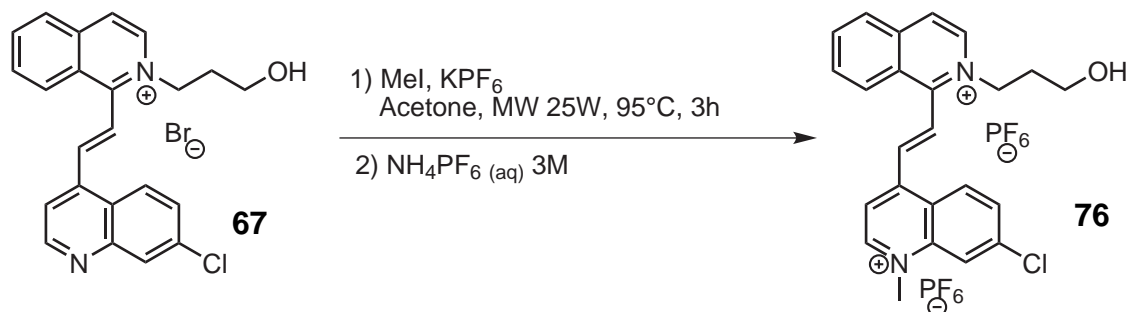
Synthesis of (E)-1-(2-(7-chloroquinolin-4-yl)vinyl)-2-(3-hydroxypropyl)isoquinolinium bromide (67)

To a mixture of **61** (700 mg, 2.37 mmol) and **35** (500 g, 2.61 mmol), a solution of piperidine (70 μl , 60 mg, 0.70 mmol) in 0.7 ml of MeOH was added. The mixture



was heated to reflux for 10 min obtaining a solid product which was washed with acetone (10ml) and filtered on an Hirsh funnel washing with 5ml of acetone and 30ml of Et₂O. Residual solvent was removed under reduced pressure at 50 °C. Product was recovered as a pale yellow solid (948 mg, 2.08 mmol, yield 88%, m.p.: 220-221 °C (dec.)).

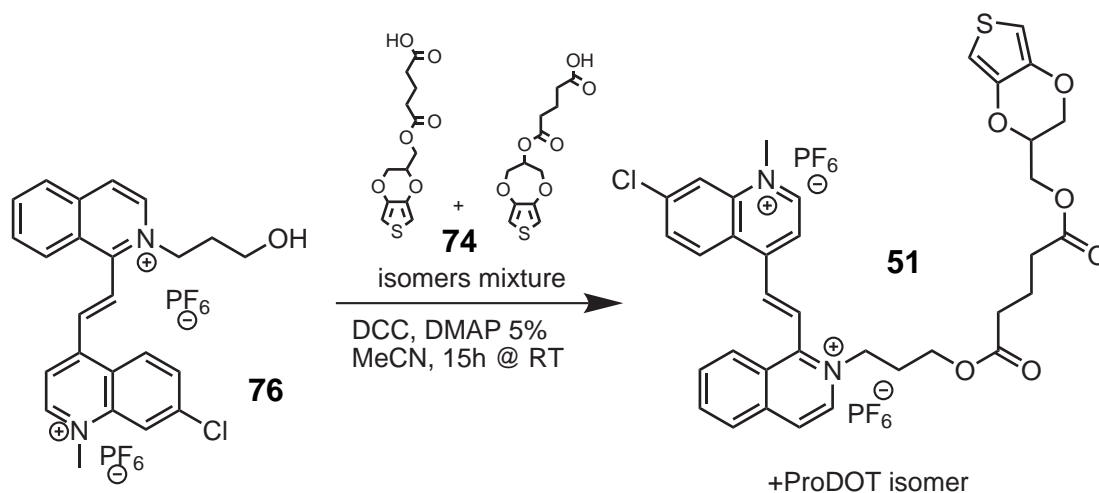
Synthesis of (*E*)-7-chloro-4-(2-(2-(3-hydroxypropyl)isoquinolinium-1-yl)vinyl)-1-methylquinolinium hexafluorophosphate (76)



A suspension of **67** (900 mg, 1.97 mmol), KPF₆ (872 mg, 4.74 mmol) in 2.5 ml of acetone was stirred at room temperature for 10 min and MeI was subsequently added (576 mg, 3.00 mmol). The mixture was heated in a CEM Discover microwave reactor for 3 h (P_{\max} =25 W, 95 °C, cooling off), and cooled to RT. The solid was filtered on an Hirsh funnel and washed with few ml of acetone and then with Et₂O. The solid was suspended in 15 ml of NH₄PF₆(aq) 30% and stirred for 1.5 days. The product was filtered and washed with 50 ml of HPLC grade water. Residual solvent was evaporated under reduced pressure (0.4 torr) at 40 °C obtaining product as a pale yellow solid (929 mg, 1.364 mmol, yield 69%, m.p.: 188-190 °C).

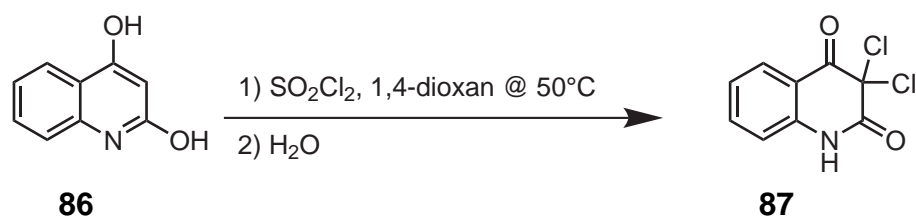
¹H NMR (500 MHz, CD₃CN) δ [ppm]: 9.20 (d, J =5.2 Hz, 1H), 8.68-8.41 (m, 6H), 8.41-8.22 (m, 2H), 8.21-7.99 (m, 4H), 4.86 (broad s, 2H), 4.61 (s, 3H), 3.61 (broad s, 2H), 2.22 (broad s, 3H)

Synthesis of (*E*)-7-chloro-4-(2-(2-(3-(5-((2,3-dihydrothieno[3,4-*b*]-[1,4]dioxin-2-yl)methoxy)-5-oxopentanoyloxy)propyl)isoquinolinium-1-yl)vinyl)-1-methylquinolinium hexafluorophosphate (51) (ISO2-Cl)



Under nitrogen atmosphere, a suspension of **74** (100 mg, 0.348 mmol, 80:20 EDOT:ProDOT), **76** (230 mg, 0.338 mmol), DCC (77 mg, 0.372 mmol) and DMAP (3 mg, 0.019 mmol) in 2 ml of anhydrous MeCN was prepared. A white solid precipitated. The solution was kept under stirring for 15h. The mixture was filtered washing the precipitate with MeCN (10 ml). The filtrate was collected and evaporated under reduced pressure obtaining a black solid which was sonicated with Et₂O (30 ml). The product was collected by filtration, suspended in 50 ml of EtOH and stirred for 5 days. The mixture was filtered on an Hirsh funnel obtaining the product as a greenish solid (254 mg, yield 79%, m.p.: 87-91 °C). ¹H NMR (500 MHz, DMSO-d₆) δ [ppm]: 9.69 (d, *J*=6.1 Hz, 1H (EDOT + ProDOT)), 8.94 (d, *J*=6.7 Hz, 1H (EDOT + ProDOT)), 8.82-8.79 (m, 2H (EDOT + ProDOT)), 8.71 (d, *J*=6.7 Hz, 1H (EDOT + ProDOT)), 8.65-8.64 (m, 2H (EDOT + ProDOT)), 8.49 (m, 3H (EDOT + ProDOT)), 8.33 (t, *J*=7.5 Hz, 1H (EDOT + ProDOT)), 8.20 (d, *J*=8.7 Hz, 1H (EDOT + ProDOT)), 8.09 (t, *J*=7.9 Hz, 1H (EDOT + ProDOT)), 6.80 (s, 2H ProDOT), 6.61-6.59 (m, 2H), 5.12 (broad s, 1H ProDOT), 4.90 (t, *J*=6.8 Hz, 2H (EDOT + ProDOT)), 4.70 (s, 3H (EDOT + ProDOT)), 4.41-4.39 (m, 1H EDOT), 4.29-4.21 (m, 2H EDOT + 4H ProDOT), 4.14-4.07 (m, 2H (EDOT + ProDOT) + 1H EDOT), 4.02-3.98 (m, 1H EDOT), 2.32-2.26 (m, 4H (EDOT + ProDOT)), 2.15-2.09 (m, 2H (EDOT + ProDOT)), 1.64-1.57 (m, 2H (EDOT + ProDOT)).

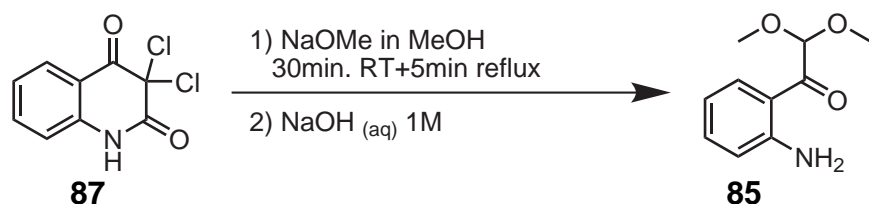
Synthesis of 3,3-dichloroquinoline-2,4(1H,3H)-dione (87)



To a suspension of 2,4-quinolinediol (**86**) (20.810 g, 129.1 mmol) in 1,4-dioxan (75 ml) at 50 °C SO₂Cl₂ (41.7 g, 308 mmol, 25.0 ml) was dropwise added under vigorous stirring. The clear yellow solution obtained was refluxed for 30 min observing HCl evolution. The mixture was cooled to RT and 300 g of ice were added. A yellow solid precipitated and was filtered on a Büchner funnel after stirring for 30 min. The solid was dried at 50 °C under reduce pressure (27.87 g, 121.1 mmol, yield 94%). The raw product contains a little amount of impurity (5%) but was suitable for next step without further purification. If needed it can be purified by crystallization from toluene.

¹H NMR (500 MHz, DMSO-d₆) δ [ppm]: 11.42 (s, 1H), 7.90 (dd, *J*=7.8 Hz, *J*=1.0 Hz, 1H), 7.69 (td, *J*=8.0 Hz, *J*=0.9 Hz, 1H), 7.21 (t, *J*=7.7 Hz, 1H), 7.15 (d, *J*=8.0 Hz, 1H).

Synthesis of 1-(2-aminophenyl)-2,2-dimethoxyethanone (85)

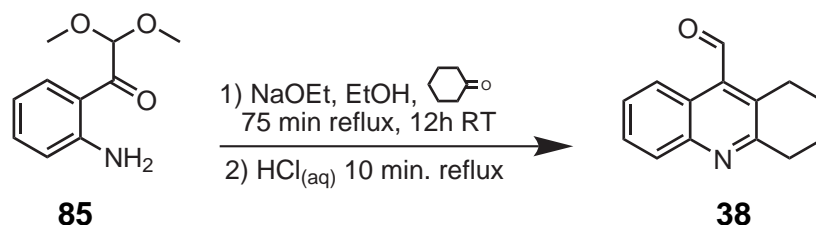


A suspension of **87** (15.000 g, 65.20 mmol) in dry MeOH was dropwise added to a stirred freshly prepared solution of NaOMe (195.6 mmol) in 50 ml of MeOH. After 30 min, the obtained orange suspension was heated to reflux for 5 min and cooled to RT. A 1 M aqueous NaOH solution (300 ml) was added to the mixture obtaining a clear solution which was stirred overnight. The solvent was distilled off till the temperature approaches 100 °C. The mixture was re-fluxed for 1 h, and cooled to room temperature. A yellow solid precipitated and was filtered on a Büchner funnel washing with water (100 ml). Product was dried at 50 °C under reduced pressure and crystallized from cyclohexane

(9.406 g, 48.2 mmol, yield 74%, m.p.: 99-100 °C).

^1H NMR (500 MHz, $\text{DMSO}-d_6$) δ [ppm]: 7.87 (d, $J=8.3$ Hz, 1H), 7.26 (t, $J=7.0$ Hz, 3H), 6.78 (d, $J=8.4$ Hz, 1H), 6.52 (t, $J=7.4$ Hz, 1H), 5.24 (s, 1H), 3.38 (s, 6H).

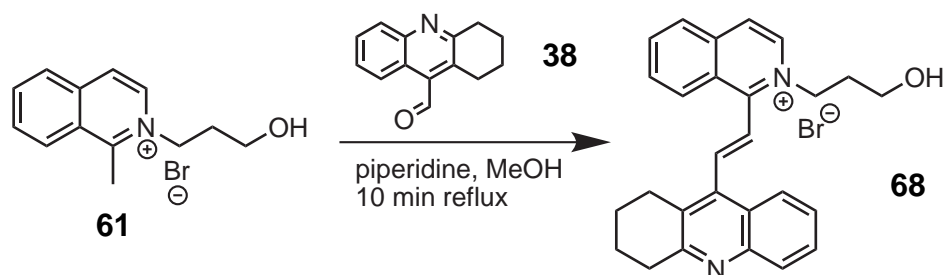
Synthesis of 1,2,3,4-tetrahydroacridine-9-carbaldehyde (**38**)



In a 100 ml RBF, under N_2 atmosphere, a solution of NaOEt in EtOH was prepared (20 ml, 13.00 mmol, 0.65 M). Cyclohexanone (1.005 g, 10.24 mmol) and compound **85** (1.000 g, 5.12 mmol) were added and the mixture was heated to reflux. The bright yellow solution turned to pale yellow after few minutes. The solution was kept under reflux for 20 min, cooled to RT and stirred for 2 h. The solvent was evaporated under reduced pressure and 50 ml of water were added to the mixture. The solution was acidified adding $\text{HCl}_{(\text{conc})}$ (4 ml) and refluxed for 7 min. The hot mixture was poured in 100 g of ice, basified with Na_2CO_3 and extracted with 100 + 3 \times 30 ml of Et_2O . The organic phase was collected, dried over MgSO_4 and evaporated under reduced pressure obtaining a yellow oil. Product was sonicated with few ml of hexane obtaining a pale yellow solid which was collected by filtration (827 mg, 3.91 mmol, yield 76%, m.p.: 76-78 °C). ^1H NMR (500 MHz, CDCl_3) δ [ppm]: 11.00 (s, 1H), 8.49 (d, $J=8.5$ Hz, 1H), 8.09 (broad s, 1H), 7.70 (t, $J=7.5$ Hz, 1H), 7.59 (t, $J=7.4$ Hz, 1H), 3.30 (t, $J=6.4$ Hz, 2H), 3.24 (t, $J=6.1$ Hz, 2H), 2.04-1.94 (m, 4H); ^{13}C NMR (125.7 MHz, CDCl_3) δ [ppm]: 194.10, 159.72, 146.40, 135.08, 132.49, 129.45, 128.73, 128.08, 123.65, 123.34, 34.03, 26.16, 22.58, 22.27.

Synthesis of (*E*)-2-(3-hydroxypropyl)-1-(2-(1,2,3,4-tetrahydroacridin-9-yl)vinyl)isoquinolinium bromide (**68**)

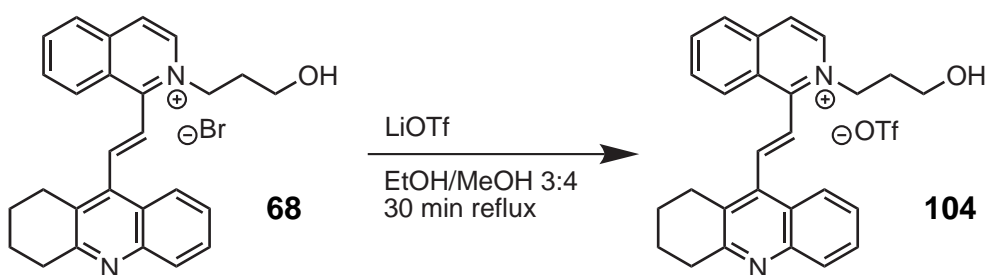
In a 100 ml RBF, to a mixture of **61** (1302 mg, 4.61 mmol) and **38** (1072 mg, 5.07 mmol), a solution of piperidine (39 mg, 0.46 mmol) in 1 ml of MeOH was added, and the mixture was heated to reflux with an external bath (100 °C). A red homogeneous solution was obtained and after 3 min it solidified to a pale yellow



solid. The mixture was refluxed for further 5 min, cooled to room temperature, sonicated with 15 ml of EtOH and filtered on an Hirsh funnel washing with EtOH and Et₂O. Residual solvent was removed under reduced pressure at 50 °C. Product was recovered as a pale yellow solid (2.005 g, 4.22 mmol, yield 91%, m.p.: 247 °C (dec.)).

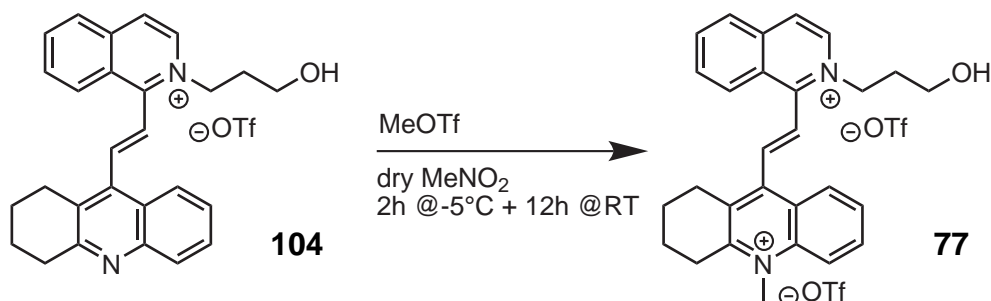
¹H NMR (500 MHz, DMSO-*d*₆) δ [ppm]: 8.87 (d, *J*=6.9 Hz, 1H), 8.76 (d, *J*=8.6 Hz, 1H), 8.61 (d, *J*=6.9 Hz, 1H), 8.43 (d, *J*=8.2 Hz, 1H), 8.31 (t, *J*=7.8 Hz, 1H), 8.22 (d, *J*=8.4 Hz, 1H), 8.12 (t, *J*=7.7 Hz, 1H), 7.99 (d, *J*=8.4 Hz, 1H), 7.84 (d, *J*=16.8 Hz, 1H), 7.74 (t, *J*=7.7 Hz, 1H), 7.64 (d, *J*=16.8 Hz, 1H), 7.59 (t, *J*=7.5 Hz, 1H), 4.87 (t, *J*=7.5 Hz, 2H), 4.79 (t, *J*=4.8, 1H), 3.51 (q, *J*=5.2 Hz, 2H), 3.13 (t, *J*=6.6 Hz, 4H), 2.17 (qui, *J*=7.0 Hz, 2H), 1.98-1.91 (m, 4H).

Synthesis of (*E*)-2-(3-hydroxypropyl)-1-(2-(1,2,3,4-tetrahydroacridin-9-yl)vinyl)isoquinolinium trifluoromethanesulfonate (104)



In a two-necked 100 ml RBF a suspension of **68** (910 mg, 1.91 mmol) was refluxed in 30 ml of EtOH and MeOH was added till complete dissolution (35 ml). A solution of LiOTf (2.986 g, 19.1 mmol) in 3 ml of MeOH was added, and the mixture was refluxed for further 30 min. The volume was reduced to 20 ml by solvent evaporation under reduced pressure and the precipitated white solid was filtered on an Hirsh funnel washing with EtOH (856 mg, 1.57 mmol, yield 82%, m.p.: 206-207 °C).

Synthesis of (*E*)-9-(2-(2-(3-hydroxypropyl)isoquinolinium-1-yl)-vinyl)-10-methyl-1,2,3,4-tetrahydroacridinium trifluoromethanesulfonate (77)

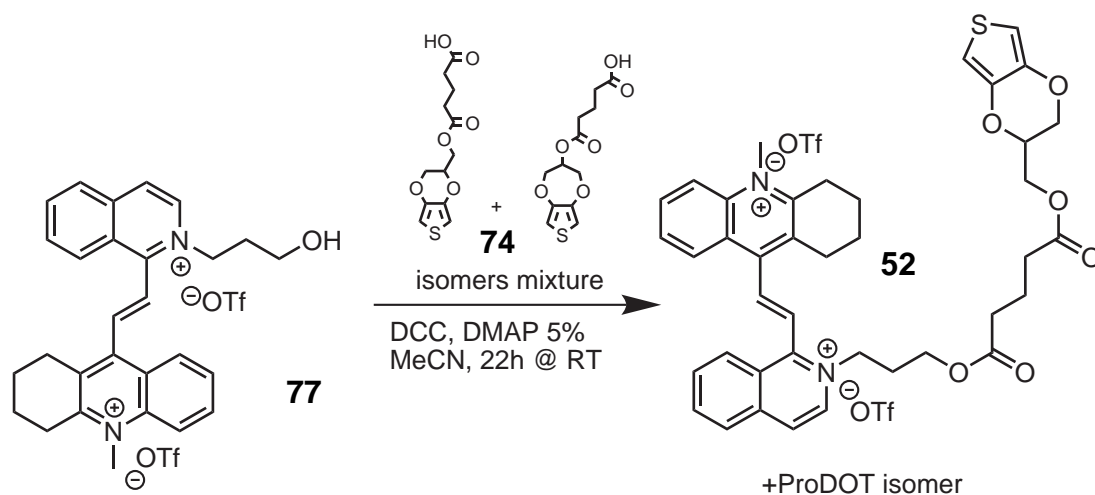


Under N_2 atmosphere, **104** (850 mg, 1.56 mmol) was suspended in dry MeNO_2 (20 ml), and the mixture was cooled to -5°C with an ice/salt bath. MeOTf (282 mg, 1.72 mmol) was dropwise added, and the mixture was stirred for 3 h at -5°C and for 12 h at RT. A white solid was obtained after stirring for 30 min with Et_2O . Product was collected by filtration on an Hirsh funnel, washed with *i*-PrOH and Et_2O , and dried in vacuum (850 mg, 1.20 mmol, yield 77%, m.p.: $173\text{-}174^\circ\text{C}$).

$^1\text{H NMR}$ (500 MHz, DMSO-d_6) δ [ppm]: 8.90 (d, $J=6.8\text{ Hz}$, 1H), 8.77 (d, $J=8.5\text{ Hz}$, 1H), 8.70-8.66 (m, 2H), 8.59 (d, $J=8.3\text{ Hz}$, 1H), 8.45 (d, $J=8.2\text{ Hz}$, 1H), 8.34 (t, $J=7.7\text{ Hz}$, 1H), 8.26 (t, $J=7.8\text{ Hz}$, 1H), 8.15 (t, $J=7.3\text{ Hz}$, 1H), 8.04-7.99 (m, 2H), 7.79 (d, $J=16.9\text{ Hz}$, 1H), 4.84 (t, $J=7.3\text{ Hz}$, 2H), 4.54 (s, 3H), 3.55-3.45 (m, 4H), 3.22 (broad s, 2H), 3.13 (broad s, 1H), 2.13 (m, 2H), 2.03 (m, 2H), 1.89 (m, 2H).

Synthesis of (*E*)-9-(2-(2-(3-(5-((2,3-dihydrothieno[3,4-*b*][1,4]dioxin-2-yl)methoxy)-5-oxopentanoyloxy)propyl)isoquinolinium-1-yl)-vinyl)-10-methyl-1,2,3,4-tetrahydroacridinium trifluoromethanesulfonate (52) (ISO3)

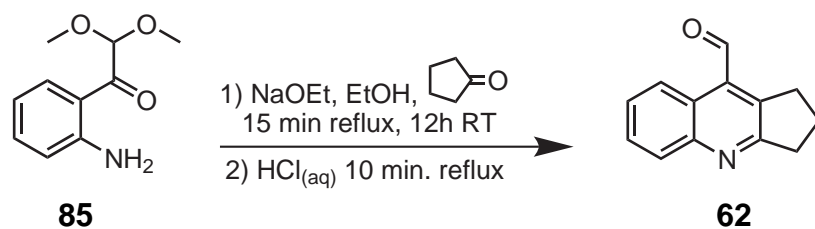
Under nitrogen atmosphere, a suspension of **74** (361 mg, 1.26 mmol, 80:20 EDOT:ProDOT), **77** (850 mg, 1.20 mmol), DCC (273 mg, 1.32 mmol) and DMAP (8 mg, 0.07 mmol) in 15 ml of anhydrous MeCN was prepared. A white solid precipitated. The solution was kept under stirring for 22 h. The mixture was filtered washing the precipitate with MeCN (60 ml). The filtrate was collected and evaporated under reduced pressure obtaining a sticky solid which was washed with Et_2O (4 ml \times 100 ml) obtaining a light green solid. The product was collected by fil-



tration, washed with Et₂O (20 ml), and dried under reduced pressure (1027 mg, 1.051 mmol, yield 83%).

¹H NMR (500 MHz, DMSO-d₆) δ [ppm]: 8.89 (d, *J*=6.3 Hz, 1H (EDOT + ProDOT)), 8.79 (d, *J*=8.1 Hz, 1H (EDOT + ProDOT)), 8.70-8.66 (m, 2H (EDOT + ProDOT)), 8.57 (d, *J*=8.1 Hz, 1H (EDOT + ProDOT)), 8.46 (d, *J*=8.0 Hz, 1H (EDOT + ProDOT)), 8.34 (t, *J*=7.3 Hz, 1H (EDOT + ProDOT)), 8.25 (t, *J*=8.3 Hz, 1H (EDOT + ProDOT)), 8.16 (t, *J*=7.2 Hz, 1H (EDOT + ProDOT)), 8.02-7.99 (m, 2H (EDOT + ProDOT)), 7.79 (d, *J*=16.6 Hz, 1H (EDOT + ProDOT)), 6.79-6.78 (m, 2H ProDOT), 6.59 (broad s, 2H EDOT), 5.18-5.12 (m, 1H ProDOT), 4.84 (s, 2H (EDOT + ProDOT)), 4.55 (s, 3H (EDOT + ProDOT)), 4.42 (s, 1H EDOT), 4.27 (s, 2H EDOT + 4H ProDOT), 4.17-4.12 (m, 1H EDOT + 2H (EDOT + ProDOT)), 4.04-4.02 (m, 1H EDOT), 3.54 (s, 2H (EDOT + ProDOT)), 2.40 (t, *J*=7.4 Hz, 2H (EDOT + ProDOT)), 2.29 (m, 2H (EDOT + ProDOT)), 2.11 (t, *J*=7.0 Hz, 2H (EDOT + ProDOT)), 2.04 (broad s, 2H (EDOT + ProDOT)), 1.90 (broad s, 2H (EDOT + ProDOT)), 1.63 (t, *J*=7.1 Hz, 2H (EDOT + ProDOT)).

Synthesis of 2,3-dihydro-1*H*-cyclopenta[*b*]quinoline-9-carbaldehyde (**62**)

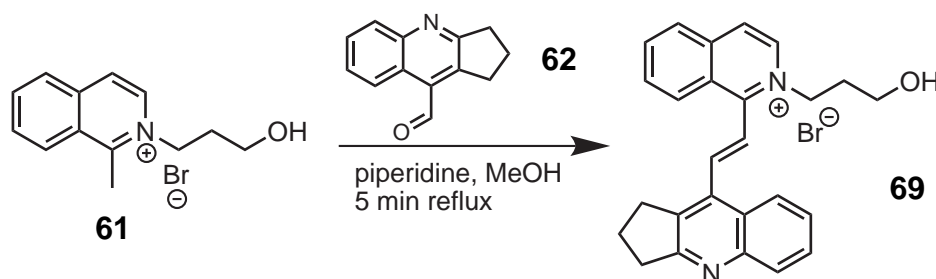


In a 100 ml round bottom flask, under N₂ atmosphere, a solution of NaOEt

in EtOH was prepared (10 ml, 6.66 mmol, 0.67 M). A solution of cyclopentanone (474 mg, 5.63 mmol) and compound **85** (1.000 g, 5.12 mmol) in dry EtOH (20 ml) was added, and the mixture was heated to reflux. The bright yellow solution turned to pale yellow after few minutes. The solution was kept under reflux for 20 min, cooled to RT. The solvent was evaporated under reduced pressure and 50 ml of water were added to the mixture. The solution was acidified adding $\text{HCl}_{(\text{conc})}$ (5 ml) and refluxed for 10 min. The mixture was rapidly cooled to RT adding ice, washed with 3×50 ml of CH_2Cl_2 , basified to pH 9 by addition of $\text{NaOH}_{(\text{aq})}$ 5%, extracted with 2×50 ml of AcOEt, dried over Na_2SO_4 and filtered over a silica plug. Product was obtained as a pale yellow solid after solvent evaporation under reduced pressure (344 mg, 1.74 mmol, yield 32%, m.p.: 110-111 °C).

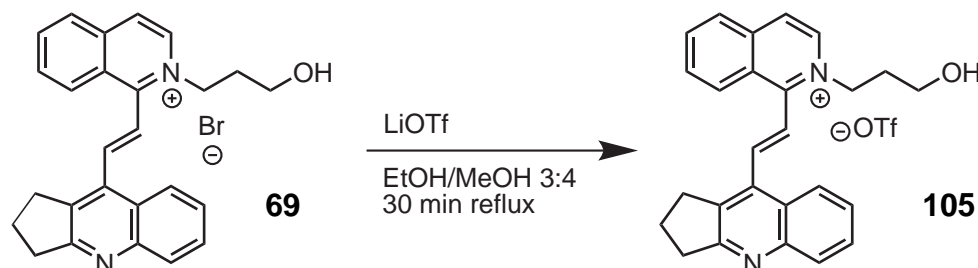
^1H NMR (500 MHz, CDCl_3) δ [ppm]: 10.81 (s, 1H), 8.78 (d, $J=8.4$ Hz, 1H), 8.06 (d, $J=8.3$ Hz, 1H), 7.68 (t, $J=7.4$ Hz, 1H), 7.59 (t, $J=7.2$ Hz, 1H), 3.41 (t, $J=7.5$ Hz, 2H), 3.18 (t, $J=7.8$ Hz, 2H), 2.27 (qui, $J=7.6$ Hz, 2H).

Synthesis of (*E*)-1-(2-(2,3-dihydro-1*H*-cyclopenta[*b*]quinolin-9-yl)-vinyl)-2-(3-hydroxypropyl)isoquinolinium bromide (**69**)



In a 100 ml round bottom flask, to a mixture of **61** (859 mg, 3.05 mmol) and **62** (650 mg, 3.29 mmol), a solution of piperidine (25 mg, 0.3 mmol) in 1 ml of MeOH was added, and the mixture was heated to reflux with an external bath (100 °C). A red homogeneous solution was obtained and after 3 min it solidified to a pale yellow solid. The mixture was refluxed for 5 min, cooled to room temperature, sonicated with 20 ml of MeOH and filtered on an Hirsh funnel washing with MeOH and Et_2O . Residual solvent was removed under reduced pressure at 50 °C. Product was recovered as a pale yellow solid (1.238 g, 2.68 mmol, yield 88%, m.p.: 262-263 °C).

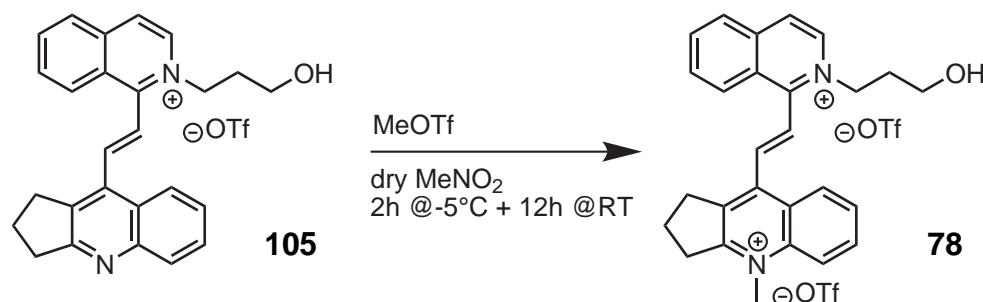
Synthesis of (*E*)-1-(2-(2,3-dihydro-1*H*-cyclopenta[*b*]quinolin-9-yl)-vinyl)-2-(3-hydroxypropyl)isoquinolinium trifluoromethanesulfonate (105)



In a two-necked 100 ml RBF a suspension of **69** (1.200 g, 2.60 mmol) was refluxed in 30 ml of EtOH and MeOH was added till complete dissolution (30 ml). A solution of LiOTf (4.056 g, 26 mmol) in 5 ml of MeOH was added, and the mixture was refluxed for further 30 min. The volume was reduced to 20 ml by solvent evaporation under reduced pressure and the precipitated white solid was filtered on an Hirsh funnel washing with EtOH (953 mg, 1.80 mmol, yield 69%, m.p.: 253-254 °C).

¹H NMR (500 MHz, DMSO-*d*₆) δ [ppm]: 8.87 (d, *J*=6.9 Hz, 1H), 8.69 (d, *J*=8.6 Hz, 1H), 8.62 (d, *J*=6.9 Hz, 1H), 8.42 (d, *J*=8.2 Hz, 1H), 8.30 (t, *J*=7.3 Hz, 1H), 8.17 (d, *J*=8.3 Hz, 1H), 8.10-8.05 (m, 2H), 8.03 (d, *J*=8.3 Hz, 1H), 7.78-7.72 (m, 2H), 7.58 (t, *J*=7.5 Hz, 1H), 4.87 (t, *J*=7.5 Hz, 2H), 4.80 (t, *J*=4.8 Hz, 1H), 3.50 (q, *J*=5.5 Hz, 2H), 3.46 (t, *J*=7.3 Hz, 2H), 3.21-3.17 (m, 2H), 2.25 (qui, *J*=7.5 Hz, 2H), 2.16 (qui, *J*=6.7 Hz, 2H).

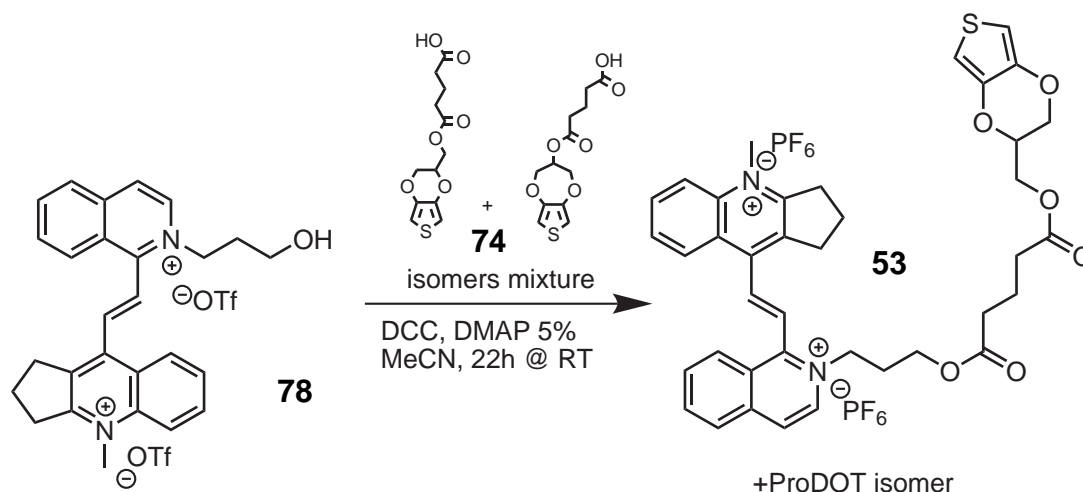
Synthesis of (*E*)-9-(2-(2-(3-hydroxypropyl)isoquinolinium-1-yl)-vinyl)-4-methyl-2,3-dihydro-1*H*-cyclopenta[*b*]quinolinium trifluoromethanesulfonate (78)



Under N₂ atmosphere, **105** (950 mg, 1.60 mmol) was suspended in dry MeNO₂ (15 ml) and cooled to -5 °C with an ice/salt bath. A solution of MeOTf (289 mg, 1.76 mmol) in MeNO₂ (6 ml) was dropwise added. After 2 h at -5 °C the mixture was warmed to RT and kept under stirring for 12 h. The mixture was cooled to -5 °C and more MeOTf (262 mg, 1.60 mmol) was added keeping the mixture under stirring at -5 °C for 4 h. Product was precipitated after addition of Et₂O, collected by filtration on an Hirsh funnel and dried in vacuum (837 mg, 1.20 mmol, yield 75%, m.p.: 169-170 °C).

¹H NMR (500 MHz, DMSO-d₆) δ [ppm]: 8.91 (d, *J*=7.0 Hz, 1H), 8.69-8.67 (m, 2H), 8.61 (d, *J*=8.9 Hz, 1H), 8.52 (d, *J*=8.0 Hz, 1H), 8.45 (d, *J*=8.45 Hz, 1H), 8.33 (t, *J*=7.6 Hz, 1H), 8.24-8.19 (m, 2H), 8.11 (t, *J*=7.8 Hz, 1H), 8.02-7.97 (m, 2H), 4.85 (t, *J*=7.4 Hz, 2H), 4.80 (broad s, 1H), 4.54 (s, 3H), 3.75 (t, *J*=7.7 Hz, 2H), 3.62 (t, *J*=7.6 Hz, 2H), 3.49 (t, *J*=5.6 Hz, 2H), 2.41 (qui, *J*=7.5 Hz, 2H), 2.15 (qui, *J*=7.0 Hz, 2H); ¹³C NMR (125.7 MHz, DMSO-d₆) δ [ppm]: 168.88, 156.31, 144.21, 138.41, 138.07, 137.95, 137.85, 136.92, 136.24, 134.10, 132.02, 130.38, 129.90, 129.53, 128.31, 127.61, 126.86, 126.75, 125.94, 119.68, 57.68, 56.95, 41.75, 35.03, 32.95, 32.00, 22.76.

Synthesis of (*E*)-9-(2-(2-(3-(5-((2,3-dihydrothieno[3,4-*b*][1,4]dioxin-2-yl)methoxy)-5-oxopentanoyloxy)propyl)isoquinolinium-1-yl)-vinyl)-10-methyl-1,2,3,4-tetrahydroacridinium hexafluorophosphate (**53**) (ISO4)

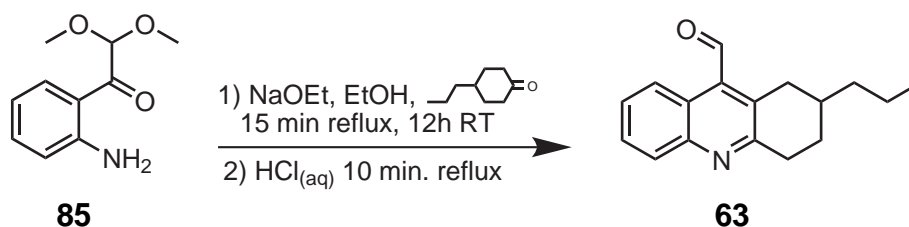


Under N₂ atmosphere, a suspension of **74** (91 mg, 0.32 mmol, 80:20 mixture), **78** (200 mg, 0.29 mmol), DCC (72 mg, 0.35 mmol) and DMAP (2 mg, 0.02 mmol)

in 3 ml of anhydrous MeCN was prepared. The solution was kept under stirring for 24h. The mixture was filtered washing the precipitate with MeCN. The filtrate was collected and evaporated under reduced pressure obtaining a sticky solid which was washed with Et₂O. Product was dissolved in EtOH (1 ml) and 1 ml of NH₄PF₆(aq) 5M solution was added. A light green solid precipitated and was collected by filtration on an Hirsh funnel and washed with 5 ml of EtOH. Residual solvent was evaporated under reduced pressure obtaining product as a white greenish solid (189 mg, 0.198 mmol, yield 68%).

¹H NMR (500 MHz, T=353 K, DMSO-d₆) δ [ppm]: 8.89 (d, *J*=6.7 Hz, 1H (EDOT + ProDOT)), 8.70-8.66 (m, 2H (EDOT + ProDOT)), 8.61 (d, *J*=8.9 Hz, 1H), 8.51 (d, *J*=8.4 Hz, 1H (EDOT + ProDOT)), 8.45 (d, *J*=8.2 Hz, 1H (EDOT + ProDOT)), 8.34 (t, *J*=7.6 Hz, 1H (EDOT + ProDOT)), 8.24-8.12 (m, 3H (EDOT + ProDOT)), 8.03-7.96 (m, 2H (EDOT + ProDOT)), 6.74 (s, 2H ProDOT), 6.55-6.52 (m, 2H EDOT), 5.15 (qui, *J*=3.2 Hz, 1H ProDOT), 4.90 (t, *J*=7.2 Hz, 2H (EDOT + ProDOT)), 4.57 (s, 3H (EDOT + ProDOT)), 4.43-4.39 (m, 1H EDOT), 4.29-4.26 (m, 2H EDOT + 4H ProDOT), 4.21-4.12 (m, 1H EDOT + 2H (EDOT + ProDOT)), 4.05-4.01 (m, 1H EDOT), 3.79 (t, *J*=7.6 Hz, 2H (EDOT + ProDOT)), 3.64 (t, *J*=7.3 Hz, 2H (EDOT + ProDOT)), 2.47 (t, *J*=7.6 Hz, 2H (EDOT + ProDOT)), 2.38 (t, *J*=7.0 Hz, 2H (EDOT + ProDOT)), 2.33-2.28 (m, 2H (EDOT + ProDOT)), 2.15 (t, *J*=7.4 Hz, 2H (EDOT + ProDOT)), 1.71-1.64 (m, 2H (EDOT + ProDOT)); ¹³C NMR (125.7 MHz, T=353 K, DMSO-d₆) δ [ppm]: 172.52, 172.47, 168.83, 168.30, 156.39, 144.56, 141.57, 138.63, 138.31, 138.20, 137.94, 137.09, 136.09, 134.21, 132.12, 130.23, 129.94, 129.40, 128.37, 127.83, 126.95, 126.85, 126.18, 119.58, 106.72, 100.31, 72.66, 71.89, 71.56, 65.61, 62.54, 61.32, 56.72, 41.64, 35.00, 32.93, 32.89, 31.93, 29.31, 22.58, 20.12.

Synthesis of 2-propyl-1,2,3,4-tetrahydroacridine-9-carbaldehyde (63)

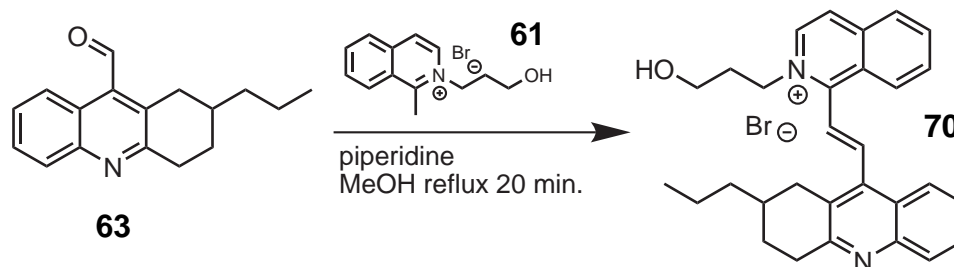


In a 250 ml RBF, under N₂ atmosphere, a solution of NaOEt in EtOH was prepared (20 ml, 13 mmol, 0.65 M). The 4-*n*-propylcyclohexanone (1.54 g, 11.0 mmol)

and compound **85** (1.095 g, 5.60 mmol) were added and the mixture was heated to reflux. The bright yellow solution turned to pale yellow after few minutes. The solution was kept under reflux for 15 min, cooled to RT and kept under stirring for 12h. The solvent was reduced to 5 ml under reduced pressure and 50 ml of water were added to the mixture. The solution was acidified to pH 1 adding $\text{HCl}_{(\text{conc})}$, refluxed for 10 min and quenched by addition of ice. The mixture was basified to pH 8 by addition of NaHCO_3 and extracted with $3 \times 30\text{ml}$ of Et_2O . The organic phase was collected, dried over MgSO_4 , and evaporated under reduced pressure obtaining a red oil. The crude product was purified by chromatography on silica plug (eluent: gradient *n*-hexane to *n*-hexane/ Et_2O 1:1). Product was obtained as a pale green solid after solvent evaporation (1.148 g, 4.53 mmol, yield 81%).

^1H NMR (500 MHz, CDCl_3) δ [ppm]: 10.98 (s, 1H), 8.47 (d, $J=8.1\text{Hz}$, 1H), 8.06 (d, $J=8.4\text{Hz}$, 1H), 7.68 (t, $J=7.7\text{Hz}$, 1H), 7.57 (t, $J=7.7\text{Hz}$, 1H), 3.47-3.42 (m, 1H), 3.34-3.29 (m, 1H), 3.19-3.12 (m, 1H), 2.81-2.75 (m, 1H), 2.16-2.12 (m, 1H), 1.88-1.83 (m, 1H), 1.62-1.54 (m, 1H), 1.50-1.42 (m, 4H), 0.96 (t, $J=6.9\text{Hz}$, 3H).

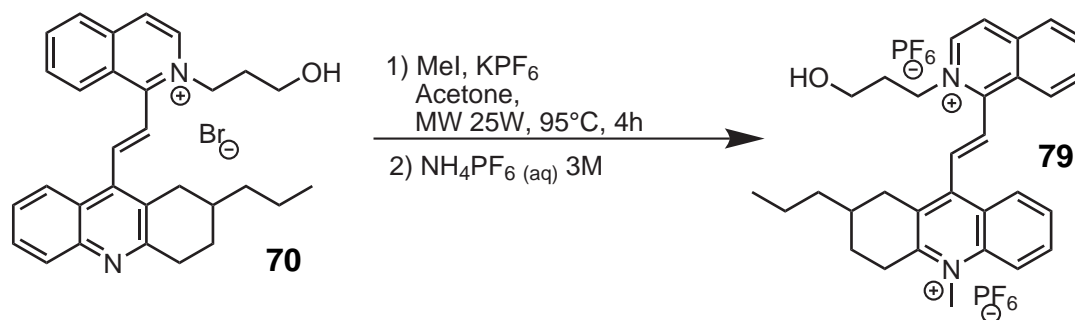
Synthesis of (*E*)-2-(3-hydroxypropyl)-1-(2-(2-propyl-1,2,3,4-tetrahydroacridin-9-yl)vinyl)isoquinolinium bromide (**70**)



In a test tube, to a mixture of **61** (736 mg, 2.61 mmol) and **63** (747 mg, 2.95 mmol), a solution of piperidine (45 mg, 0.53 mmol) in 0.6 ml of MeOH was added, and mixture was heated with an external bath (100°C). A red homogeneous solution was obtained and after 3 min it solidified to a pale yellow solid. The mixture was heated for further 15 min, cooled to room temperature, sonicated with 4 ml of acetone and filtered on an Hirsh funnel washing with acetone and Et_2O . Residual solvent was removed under reduced pressure at 60°C . Product was recovered as a white solid (1.008 g, 1.95 mmol, yield 75%, m.p.: $201\text{-}202^\circ\text{C}$). ^1H NMR (500 MHz, $\text{DMSO}-d_6$) δ [ppm]: 8.90 (d, $J=6.9\text{Hz}$, 1H), 8.77 (d, $J=8.6\text{Hz}$, 1H), 8.64 (d, $J=6.9\text{Hz}$, 1H), 8.45 (d, $J=8.2\text{Hz}$, 1H), 8.32 (t, $J=7.5\text{Hz}$, 1H), 8.25 (d,

$J=8.4\text{Hz}$, 1H), 8.11 (t, $J=7.4\text{Hz}$, 1H), 7.99 (d, $J=8.1\text{Hz}$, 1H), 7.85 (d, $J=16.8\text{Hz}$, 1H), 7.74 (t, $J=7.6\text{Hz}$, 1H), 7.66-7.58 (m, 2H), 4.89 (m, 2H), 4.80 (t, $J=4.8\text{Hz}$, 1H), 3.51 (q, $J=5.2\text{Hz}$, 2H), 3.29-3.07 (m, 3H), 2.71-2.65 (m, 1H), 2.16 (qui, $J=6.2\text{Hz}$, 2H), 2.09-2.07 (m, 1H), 1.85 (m, 1H), 1.61-1.53 (m, 1H), 1.46-1.38 (m, 4H), 0.91 (t, $J=6.9\text{Hz}$, 3H); ^{13}C NMR (125.7MHz, DMSO- d_6) δ [ppm]: 159.11, 157.10, 146.49, 141.07, 139.50, 137.98, 136.65, 136.29, 131.73, 130.31, 129.24, 128.68, 128.33, 127.74, 126.83, 125.94, 125.32, 124.92, 124.74, 57.77, 56.78, 38.66, 34.27, 33.74, 32.86, 28.88, 19.97, 14.68.

Synthesis of (*E*)-9-(2-(2-(3-hydroxypropyl)isoquinolinium-1-yl)vinyl)-10-methyl-2-propyl-1,2,3,4-tetrahydroacridinium hexafluorophosphate (79)

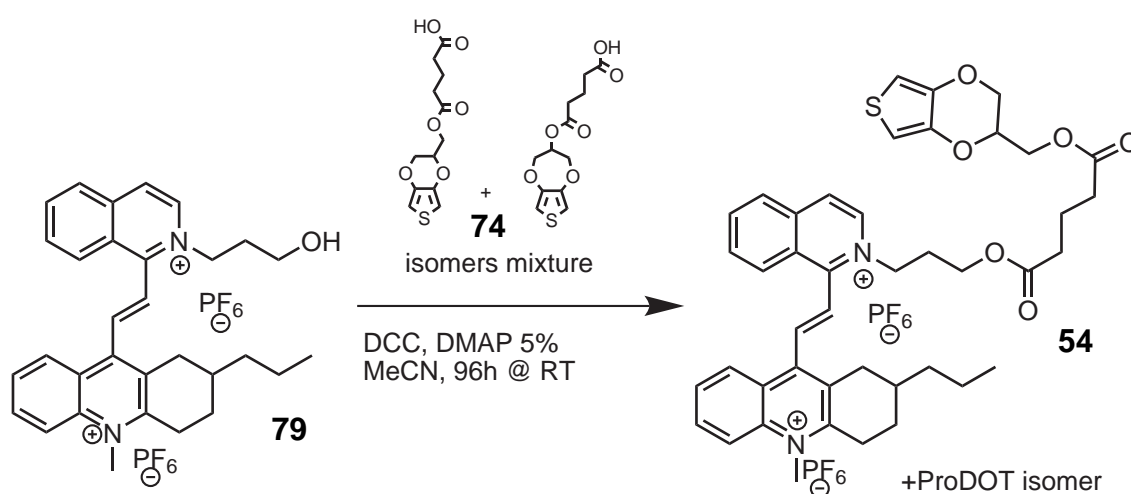


A suspension of **70** (700 mg, 1.35 mmol), KPF₆ (606 mg, 3.29 mmol) in 1.5 ml of acetone was stirred at room temperature for 15 min and MeI was subsequently added (700 mg, 4.93 mmol). The mixture was heated in a CEM Discover microwave reactor for 4 h ($P_{\text{max}}=15\text{W}$, 95°C, cooling off, 10 ml closed vessel), stirred at RT for 3 h. The solid was filtered on an Hirsh funnel and washed with acetone and then with Et₂O. Product was suspended in 4 ml of NH₄PF₆(aq) 30% and stirred for 24 h. The solid was filtered and washed with few ml of NH₄PF₆(aq) 30% and then with HPLC grade water. Residual solvent was evaporated under reduced pressure at 60°C for 12 h obtaining product as a white solid (648 mg, 0.873 mmol, yield 65%, m.p.: 156-160°C).

^1H NMR (500 MHz, CD₃CN) δ [ppm]: 8.80 (d, $J=8.6\text{Hz}$, 1H), 8.60-8.56 (m, 2H), 8.50-8.47 (m, 2H), 8.38 (d, $J=8.1\text{Hz}$, 1H), 8.32 (t, $J=7.8\text{Hz}$, 1H), 8.24 (t, $J=8.0\text{Hz}$, 1H), 8.14 (t, $J=7.6\text{Hz}$, 1H), 8.03 (t, $J=7.6\text{Hz}$, 1H), 7.78 (d, $J=16.9\text{Hz}$, 1H), 7.58 (d, $J=17.0\text{Hz}$, 1H), 4.84 (m, 2H), 4.48 (s, 3H), 3.62-3.54 (m, 3H), 3.45-3.38 (m, 1H), 3.33-3.29 (m, 1H), 2.89 (t, $J=4.5\text{Hz}$, 1H), 2.80-2.75 (m, 1H), 2.29 (m, 1H), 2.22 (t, $J=6.0\text{Hz}$, 2H), 1.92 (s, 1H), 1.71-1.62 (m, 1H), 1.48 (s, 4H), 0.97 (s, 3H); ^{13}C NMR

(125.7 MHz, T=333 K, DMSO- d_6) δ [ppm]: 160.84, 156.00, 149.66, 138.90, 138.88, 138.08, 136.84, 136.29, 134.84, 131.91, 131.81, 130.02, 129.85, 129.14, 128.44, 127.66, 126.040, 125.91, 119.74, 57.83, 57.07, 39.89, 37.45, 34.48, 33.02, 31.60, 30.69, 27.19, 19.76, 14.43.

Synthesis of (*E*)-9-(2-(2-(3-(6-((2,3-dihydrothieno[3,4-*b*][1,4]dioxin-2-yl)methoxy)-6-oxohexanoyloxy)propyl)isoquinolinium-1-yl)vinyl)-10-methyl-2-propyl-1,2,3,4-tetrahydroacridinium hexafluorophosphate mixture of isomers (54**) (ISO5)**

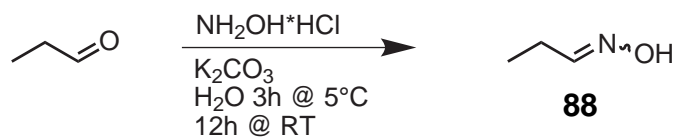


Under nitrogen atmosphere, a suspension of **74** (119 mg, 0.416 mmol, 80:20 isomers mixture), **79** (300 mg, 0.404 mmol), dicyclohexylcarbodiimide (DCC) (92 mg, 0.444 mmol) and DMAP (5 mg, 0.04 mmol) in 3 ml of anhydrous MeCN was prepared. A white solid precipitated. The solution was kept under stirring for 96 h. The mixture was filtered washing the precipitate with MeCN (10 ml). The filtrate was collected and evaporated under reduced pressure obtaining a dark oil which was sonicated with Et₂O (20 ml) obtaining a yellow solid. The product was filtered, suspended in 10 ml of EtOH and stirred for 48 h to eliminate residual DMAP. The mixture was filtered on an Hirsh funnel obtaining the product as a pale light brown solid (285 mg, 0.287 mmol, yield 69%, m.p.: 90-120 °C).

¹H NMR (500 MHz, DMSO- d_6) δ [ppm]: 8.89 (d, $J=6.9$ Hz, 1H (EDOT + ProDOT)), 8.82 (d, $J=8.6$ Hz, 1H (EDOT + ProDOT)), 8.69 (t, $J=7.0$ Hz, 2H (EDOT + ProDOT)), 8.60 (d, $J=8.6$ Hz, 1H (EDOT + ProDOT)), 8.47 (d, $J=8.2$ Hz, 1H (EDOT + ProDOT)), 8.36 (t, $J=7.5$ Hz, 1H (EDOT + ProDOT)), 8.26 (t, $J=8.2$ Hz, 1H (EDOT + ProDOT)),

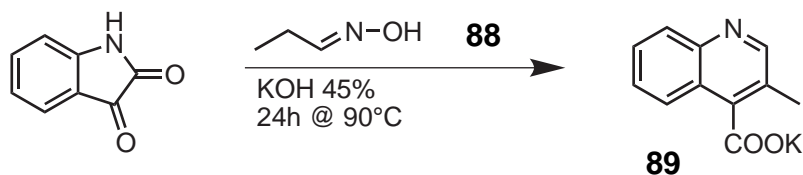
8.15 (t, $J=7.3$ Hz, 1H (EDOT + ProDOT)), 8.05-8.01 (m, 2H (EDOT + ProDOT)), 7.78 (d, $J=16.8$ Hz, 1H (EDOT + ProDOT)), 6.79 (s, 2H ProDOT), 6.62-6.60 (m, 2H EDOT), 5.12 (qui, $J=$, 1H ProDOT), 4.93-4.76 (m, 2H (EDOT + ProDOT)), 4.55 (s, 3H (EDOT + ProDOT)), 4.43-4.40 (m, 1H EDOT), 4.30-4.22 (m, 2H EDOT + 4H ProDOT), 4.15-4.10 (m, 1H EDOT + 2H (EDOT + ProDOT)), 4.03-4.00 (m, 1H EDOT), 3.62-3.57 (m, 1H (EDOT + ProDOT)), 3.56-3.36 (m, 1H (EDOT + ProDOT)), 3.36-3.25 (m, 1H (EDOT + ProDOT)), 2.81-2.75 (m, 1H (EDOT + ProDOT)), 2.33-2.25 (m, 4H (EDOT + ProDOT)), 2.23-2.18 (m, 1H (EDOT + ProDOT)), 2.10 (t, $J=7.4$ Hz, 2H (EDOT + ProDOT)), 1.92-1.81 (m, 1H (EDOT + ProDOT)), 1.67-1.55 (m, 3H (EDOT + ProDOT)), 1.49-1.34 (m, 4H (EDOT + ProDOT)), 0.91 (t, $J=6.4$ Hz, 3H (EDOT + ProDOT)), EDOT:ProDOT ratio is 4:1; ^{13}C NMR (125.7 MHz, DMSO- d_6) δ [ppm]: 172.64, 160.66, 156.19, 149.59, 141.54, 141.42, 139.32, 138.80, 138.10, 136.97, 136.27, 134.88, 132.05, 131.59, 130.25, 129.86, 128.44, 127.69, 127.54, 125.89, 125.87, 119.78, 107.15, 100.49, 100.43, 72.65, 71.79, 71.56, 65.41, 62.54, 61.27, 56.34, 37.54, 34.41, 32.66, 32.63, 32.60, 31.58, 30.76, 29.00, 27.21, 19.97, 19.78, 14.52.

Synthesis of propionaldehyde oxime (88)



To 600 ml of deionized water, cooled to 5°C with an ice water bath, $\text{NH}_2\text{OH}\cdot\text{HCl}$ (50.00 g, 719.5 mmol) was added portionwise followed by K_2CO_3 (49.72 g, 359.8 mmol) obtaining a light yellow solution. Propionaldehyde (43.87 g, 755.5 mmol) was added dropwise over 30 min. Gas evolution was observed during the addition, and the light yellow color faded away. The mixture was kept under stirring and the ice in the cooling bath was allowed to melt (3 h). The mixture was kept under stirring for further 12 h at RT and extracted with 5×50 ml of Et_2O . The organic phase was collected, dried over MgSO_4 and evaporated under reduced pressure at 30°C obtaining product as a clear liquid (36.84 g, 0.504 mol, yield 70%). ^1H NMR (500 MHz, CDCl_3) δ [ppm]: 9.10 (s, 1H E+Z), 7.43 (t, $J=5.7$ Hz, 1H, E isomer), 6.71 (t, $J=5.4$ Hz, 1H, Z isomer), 2.39 (m, 2H, Z isomer), 2.22 (m, 2H, E isomer), 1.07 (t, $J=7.6$ Hz, 3H, E+Z isomers). E/Z ratio is 1.33.

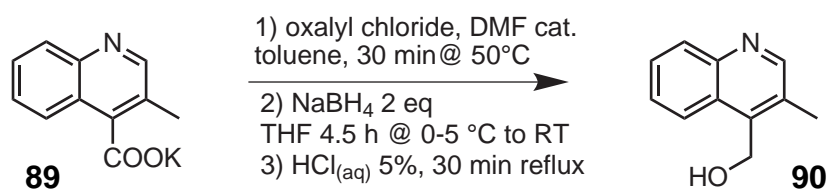
Synthesis of potassium 3-methylquinoline-4-carboxylate (**89**)



In a 1 l two-necked RBF, an aqueous KOH solution was prepared (206.6 g of KOH in 260 ml of deionized water) and isatin (64.60 g, 0.439 mol) was added. The mixture turned black and after few minutes a white solid mass was obtained. Propionaldehyde oxime (20.00 g, 0.274 mol) was added, and the mixture was heated to 90 °C. An orange homogeneous solution was obtained after few minutes. The mixture was kept under stirring at 90 °C for 24 h observing the formation of a white precipitate. The mixture was cooled to room temperature and stirred for further 3 h. The white precipitate was collected by filtration under reduced pressure on a sintered glass funnel and washed with a 30% aqueous KOH solution followed by few ml of EtOH. The residual solvent was removed under reduced pressure at 80 °C (31.00 g, 0.138 mol, yield 50%, m.p.: >400 °C)

$^1\text{H NMR}$ (500 MHz, D_2O) δ [ppm]: 8.56 (s, 1H), 7.84 (d, $J=8.4$ Hz, 1H), 7.70 (d, $J=8.3$ Hz, 1H), 7.60 (t, $J=8.3$ Hz, 1H), 7.50 (t, $J=8.1$ Hz, 1H), 2.31 (s, 3H).

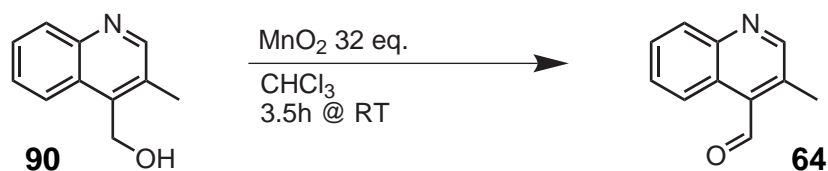
Synthesis of (3-methylquinolin-4-yl)methanol (**90**)



In a 250 ml two-necked RBF, equipped with a CaCl_2 guard tube, a suspension of **89** (15.00 g, 66.58 mmol) in 100 ml of toluene was prepared. Anhydrous DMF (100 μl) was added followed by dropwise addition of oxalyl chloride (12.67 g, 99.84 mmol). Gas evolution was observed. The mixture was heated to 50 °C on a water bath for 30 min. The mixture was cooled to RT and poured in 150 ml of saturated NaHCO_3 aqueous solution. The organic phase was separated and the aqueous one was extracted with further 50 ml of toluene. The organic phases were collected, washed with brine (50 ml), dried over MgSO_4 and evaporated

under reduce pressure obtaining a yellow oil (13.46 g, 65.45mmol). Crude product was dissolved in anhydrous THF (60ml) in a RBF equipped with CaCl₂ guard tube. The mixture was cooled to 5 °C with an ice-water bath, and NaBH₄ (5.04g, 133mmol) was added portionwise under stirring. The mixture was kept under stirring at 0-5°C for 1.5h and then allowed to warm to RT (3h). A yellow solution with a white precipitate was obtained. The mixture was poured in 300ml of water and acidified by addition of HCl_(aq) 37%. The mixture was heated to boiling and THF was distilled off. After 30min the solution was cooled to RT and basified by addition of Na₂CO₃ observing formation of a pale yellow solid. Et₂O (15ml) was added, and the mixture was kept under stirring overnight. The solid was collected by filtration under reduced pressure on a sintered glass funnel, dried in air and suspended in toluene. The mixture was refluxed removing residual water by azeotropic distillation using a Dean-Stark apparatus. The Dean-Stark was replaced by a condenser and toluene was added till clarification. The mixture was filtered hot and the obtained solution was allowed to cool to RT observing crystallization of the product which was collected by filtration under reduced pressure (4.934g). The filtrate from the filtration of the initial basified solution was extracted with 4 × 40ml of CHCl₃, dried over MgSO₄ and evaporated under reduced pressure obtaining a yellow oil which was purified by crystallization from toluene (435mg). A total of 5.369g of product was obtained (31.00mmol, yield 47%, m.p.: 170-172 °C). ¹H NMR (500MHz, CDCl₃) δ [ppm]: 8.65 (s, 1H), 8.22 (d, *J*=8.4Hz, 1H), 8.07 (d, *J*=8.3Hz, 1H), 7.66 (t, *J*=7.6Hz, 1H), 7.59 (t, *J*=7.5Hz, 1H), 5.16 (s, 2H), 2.55 (s, 3H).

Synthesis of 3-methylquinoline-4-carbaldehyde (64)

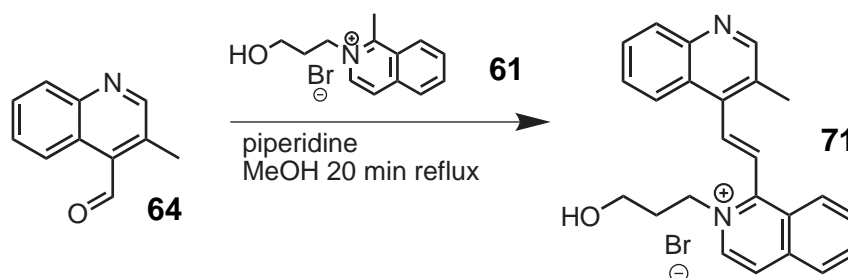


In a 250ml RBF equipped with a CaCl₂ guard tube, compound **90** (4.700g, 27.13mmol) was suspended in CHCl₃ (250ml) and activated MnO₂ was added (75g, 863mmol, Aldrich 63543). The mixture was kept under vigorous stirring for 3.5 h at RT, filtered on a sintered glass funnel and again on a paper filter to remove MnO₂. The solvent was evaporated under reduced pressure obtaining

product as a white solid (3.069 g, 17.92 mmol, yield 66%, m.p.: 97-98 °C).

^1H NMR (500 MHz, CDCl_3) δ [ppm]: 11.00 (s, 1H), 8.91 (s, 1H), 8.71 (d, $J=8.2$ Hz, 1H), 8.19 (d, $J=8.4$ Hz, 1H), 7.75 (t, $J=8.3$ Hz, 1H), 7.69 (t, $J=7.0$ Hz, 1H), 2.80 (s, 3H); ^{13}C NMR (125.7 MHz, CDCl_3) δ [ppm]: 192.85, 152.85, 132.76, 130.03, 129.66, 128.86, 124.59, 123.96, 16.72.

Synthesis of (*E*)-2-(3-hydroxypropyl)-1-(2-(3-methylquinolin-4-yl)-vinyl)isoquinolinium bromide (71)

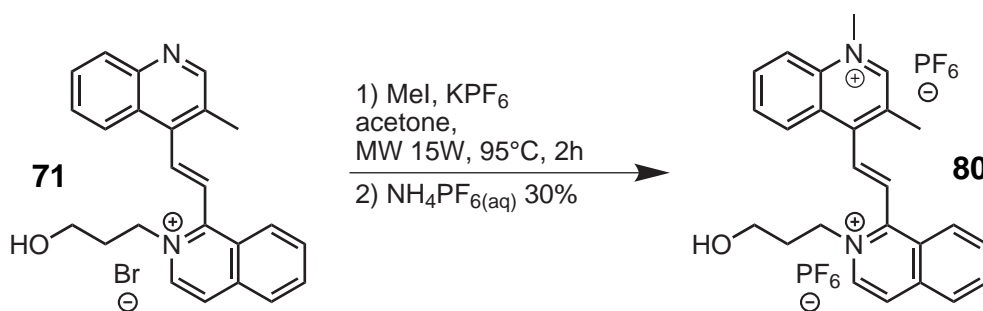


In a test tube a solution of piperidine (40 mg, 0.47 mmol) in 0.6 ml of MeOH was added to a mixture of **61** (656 mg, 2.33 mmol) and **64** (450 mg, 2.63 mmol). The mixture was heated to reflux and a red homogeneous solution was obtained. A pale yellow solid mass was obtained after 4 min. The mixture was heated for further 15 min and cooled to RT. The solid was triturated by sonication with acetone (5 ml). Product was collected by filtration under reduced pressure washing with Et_2O and residual solvent was removed at 50 °C under reduced pressure. White solid (912 mg, 2.09 mmol, yield 90%, m.p.: 253 °C (dec.)).

^1H NMR (500 MHz, $\text{DMSO}-d_6$) δ [ppm]: 8.96 (s, 1H), 8.90 (d, $J=6.9$ Hz, 1H), 8.76 (d, $J=8.6$ Hz, 1H), 8.64 (d, $J=6.9$ Hz, 1H), 8.44 (d, $J=8.2$ Hz, 1H), 8.31 (t, $J=7.3$ Hz, 1H), 8.27 (d, $J=8.3$ Hz, 1H), 8.14-8.09 (m, 2H), 7.92 (d, $J=16.8$ Hz, 1H), 7.79 (t, $J=7.1$ Hz, 1H), 7.72 (d, $J=16.8$ Hz, 1H), 7.68 (t, $J=7.7$ Hz, 1H), 4.88 (t, $J=7.5$ Hz, 2H), 4.80 (t, $J=4.8$ Hz, 1H), 3.51 (q, $J=5.3$ Hz, 2H), 2.71 (s, 3H), 2.15 (qu, $J=6.8$ Hz, 2H).

Synthesis of (*E*)-4-(2-(2-(3-hydroxypropyl)isoquinolinium-1-yl)-vinyl)-1,3-dimethylquinolinium (80)

A suspension of **71** (500 mg, 1.148 mmol), KPF_6 (516 mg, 2.84 mmol) in 1 ml of acetone was stirred at room temperature for 15 min and MeI was subsequently

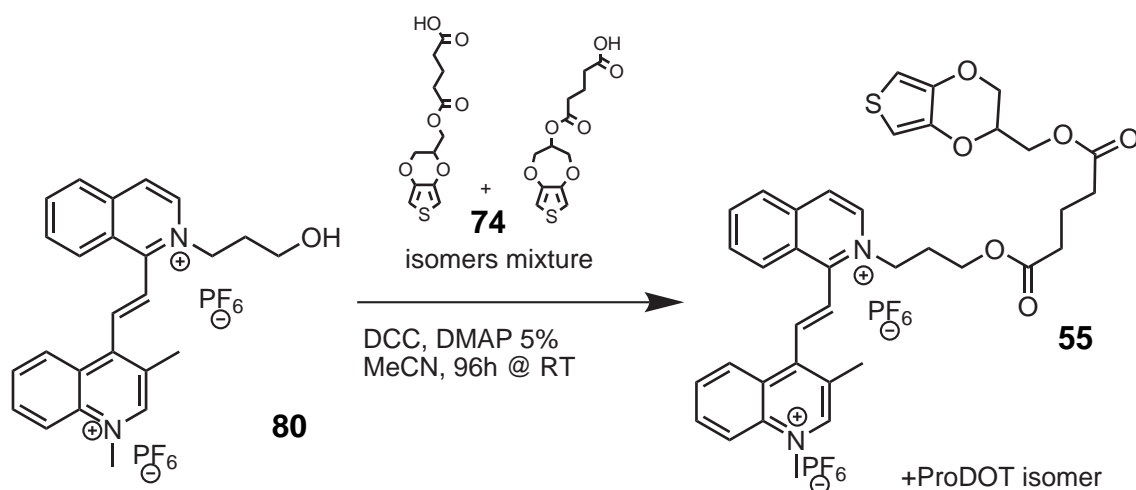


(0.30 ml, 0.68 g, 4.8 mmol). The mixture was heated in a CEM Discover microwave reactor for 30 min ($P_{\max}=15\text{W}$, 95°C , cooling off, 10 ml closed vessel). The mixture was cooled down to RT, and the solid precipitate was triturated using a spatula. The vessel was heated again in the same conditions for 1.5 h, and cooled to RT. The yellow precipitate was collected by filtration and washed with acetone and Et₂O. Product was suspended in 6 ml of an aqueous NH₄PF₆ 30% solution and stirred for 3 days. The white solid was filtered under reduced pressure and washed with few ml of NH₄PF₆(aq) 30% and with deionized water. Product was dried under reduced pressure at 60°C for 4 h (664 mg, 1.01 mmol, yield 88%, m.p.: $186\text{-}190^\circ\text{C}$).

¹H NMR (500 MHz, DMSO-*d*₆) δ [ppm]: 9.65 (s, 1H), 8.91 (d, $J=6.9\text{Hz}$, 1H), 8.78 (d, $J=8.6\text{Hz}$, 1H), 8.68 (d, $J=6.8\text{Hz}$, 1H), 8.63 (d, $J=8.5\text{Hz}$, 1H), 8.59 (d, $J=8.9\text{Hz}$, 1H), 8.46 (d, $J=8.2\text{Hz}$, 1H), 8.36-8.29 (m, 2H), 8.16-8.08 (m, 3H), 7.88 (d, $J=16.8\text{Hz}$, 1H), 4.86 (t, $J=7.4\text{Hz}$, 2H), 4.70 (s, 3H), 3.50 (t, $J=5.7\text{Hz}$, 2H), 2.81 (s, 3H), 2.15 (qui, $J=6.7\text{Hz}$, 2H); ¹³C NMR (125.7 MHz, DMSO-*d*₆) δ [ppm]: 156.16, 151.89, 150.40, 138.56, 138.08, 137.63, 136.99, 136.40, 134.85, 132.17, 130.92, 130.77, 130.43, 129.74, 128.47, 127.71, 127.62, 127.56, 125.98, 120.09, 57.80, 57.03, 45.98, 33.06, 18.30.

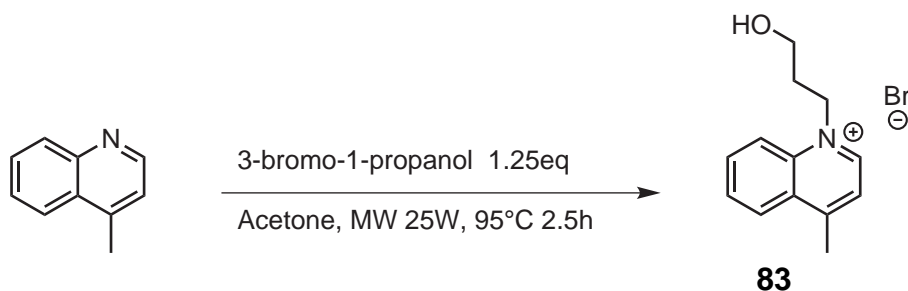
Synthesis of (*E*)-4-(2-(2-(3-(5-((2,3-dihydrothieno[3,4-*b*][1,4]dioxin-2-yl)methoxy)-5-oxopentanoyloxy)propyl)isoquinolinium-1-yl)-vinyl)-1,3-dimethylquinolinium hexafluorophosphate (ISO7) (55)

In a closed vessel a suspension of **74** (89 mg, 0.312 mmol, 80:20 isomers mixture), **80** (200 mg, 0.303 mmol), dicyclohexylcarbodiimide (DCC) (69 mg, 0.333 mmol) and DMAP (3 mg, 0.02 mmol) in 3 ml of anhydrous MeCN was prepared. A white solid precipitated. The solution was kept under stirring for 96 h. The mixture was filtered washing the precipitate with MeCN (10 ml). The filtrate was collected and evaporated under reduced pressure obtaining an dark oil



which was sonicated with Et₂O (20 ml) obtaining a pale green solid. The product was collected by filtration, suspended in 10 ml of EtOH and stirred for 48h to eliminate residual DMAP. The mixture was filtered on an Hirsh funnel obtaining the product as a pale yellow solid (229 mg, 0.246 mmol, yield 81%).

¹H NMR (500 MHz, DMSO-d₆) δ [ppm]: 9.66 (s, 1H (EDOT + ProDOT)), 8.90 (d, *J*=6.8 Hz, 1H (EDOT + ProDOT)), 8.80 (d, *J*=8.6 Hz, 1H (EDOT + ProDOT)), 8.69 (d, *J*=6.8 Hz, 1H (EDOT + ProDOT)), 8.61-8.58 (m, 2H (EDOT + ProDOT)), 8.46 (d, *J*=8.2 Hz, 1H (EDOT + ProDOT)), 8.35 (t, *J*=7.7 Hz, 1H (EDOT + ProDOT)), 8.30 (t, *J*=8.1 Hz, 1H (EDOT + ProDOT)), 8.16-8.07 (m, 4H (EDOT + ProDOT)), 7.88 (d, *J*=16.8 Hz, 1H (EDOT + ProDOT)), 6.81 (s, 2H ProDOT), 6.62-6.60 (m, 2H EDOT), 5.13 (m, 1H ProDOT), 4.84 (t, *J*=7.2 Hz, 2H (EDOT + ProDOT)), 4.70 (s, 3H (EDOT + ProDOT)), 4.44-4.39 (m, 1H EDOT), 4.30-4.22 (m, 2H EDOT + 4H ProDOT), 4.17-4.07 (m, 1H EDOT + 2H (EDOT + ProDOT)), 4.03-3.99 (m, 1H EDOT), 2.80 (s, 3H (EDOT + ProDOT)), 2.30-2.26 (m, 4H (EDOT + ProDOT)), 2.12-2.08 (m, 2H (EDOT + ProDOT)), 1.64-1.59 (m, 2H (EDOT + ProDOT)), EDOT:ProDOT ratio is 4:1; ¹³C NMR (125.7 MHz, DMSO-d₆) δ [ppm]: 172.78, 172.76, 156.33, 151.91, 150.40, 149.70, 141.66, 141.55, 138.92, 138.19, 137.58, 137.12, 136.34, 134.88, 132.26, 130.92, 130.74, 130.48, 129.64, 128.50, 127.72, 127.65, 127.51, 126.05, 120.08, 107.45, 107.25, 100.613, 100.56, 72.73, 71.90, 71.66, 65.53, 62.65, 61.40, 56.52, 45.99, 32.79, 32.72, 29.16, 20.09, 18.29.

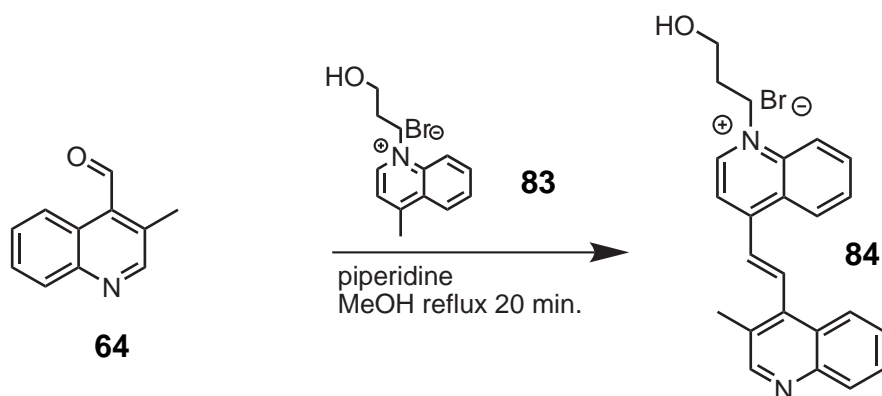


Synthesis of 1-(3-hydroxypropyl)-4-methylquinolinium bromide (83)

A mixture of 4-methylquinoline (4.00 g, 27.9 mmol), 3-bromo-1-propanol (4.84 g, 34.8 mmol) and 10 ml of acetone was heated in a CEM Discover microwave reactor for 2.5 h ($P_{\text{max}}=25\text{ W}$, 95°C , cooling off, 35 ml vessel), and cooled to RT. The vessel was kept at RT for 3 h; the white solid was filtered on a Büchner funnel, washed with acetone and then with Et_2O . Residual solvent was evaporated under reduced pressure (0.4 torr) at 40°C (5.631 g, 19.96 mmol, yield 71%, m.p.: $151\text{-}154^\circ\text{C}$).

$^1\text{H NMR}$ (500 MHz, DMSO-d_6) δ [ppm]: 9.53 (d, $J=6.1\text{ Hz}$, 1H), 8.61 (d, $J=8.9\text{ Hz}$, 1H), 8.53 (d, $J=8.5\text{ Hz}$, 1H), 8.25 (t, $J=8.9\text{ Hz}$, 1H), 8.10 (d, $J=6.2\text{ Hz}$, 1H), 8.04 (t, $J=7.9\text{ Hz}$, 1H), 5.13 (t, $J=7.2\text{ Hz}$, 2H), 4.74 (broad s, 1H), 3.53 (t, $J=5.8\text{ Hz}$, 2H), 3.00 (s, 3H), 2.13 (qui, $J=6.6\text{ Hz}$, 2H); $^{13}\text{C NMR}$ (125.7 MHz, DMSO-d_6) δ [ppm]: 159.06, 149.34, 137.34, 135.65, 130.12, 129.49, 127.75, 123.21, 119.95, 58.00, 55.34, 32.70, 20.35.

Synthesis of (*E*)-1-(3-hydroxypropyl)-4-(2-(3-methylquinolin-4-yl)-vinyl)quinolinium bromide (84)

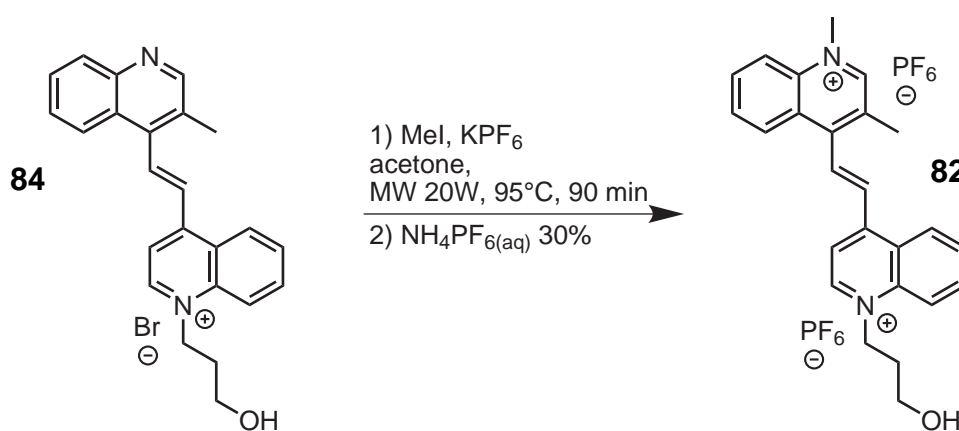


In a test tube, a solution of piperidine (20 mg, 0.23 mmol) in 0.3 ml of MeOH

was added to a mixture of **83** (328 mg, 1.16 mmol) and **64** (225 mg, 1.31 mmol). The mixture was heated to reflux and a red homogeneous solution was obtained. After 20 min the mixture was cooled to RT. A pale yellow solid product crystallized from the solution. Product was collected by filtration washing with acetone and Et₂O (330 mg, 0.758 mmol, yield 65%, m.p.: 169-170°C).

¹H NMR (500 MHz, DMSO-d₆) δ [ppm]: 9.60 (d, *J*=6.4 Hz, 1H), 8.93 (s, 1H), 8.85 (d, *J*=8.4 Hz, 1H), 8.80 (d, *J*=6.3 Hz, 1H), 8.64 (d, *J*=9.0 Hz, 1H), 8.50 (d, *J*=16.3 Hz, 1H), 8.31 (t, *J*=7.7 Hz, 1H), 8.25 (d, *J*=8.3 Hz, 1H), 8.13 (d, *J*=16.3 Hz, 1H), 8.08 (d, *J*=8.3 Hz, 1H), 8.04 (t, *J*=7.6 Hz, 1H), 7.78 (t, *J*=7.6 Hz, 1H), 7.66 (t, *J*=7.7 Hz, 1H), 5.17 (t, *J*=7.2 Hz, 2H), 4.88 (t, *J*=4.9 Hz, 1H), 3.59 (q, *J*=5.4 Hz, 2H), 2.65 (s, 3H), 2.18 (qui, *J*=6.3 Hz, 2H); ¹³C NMR (125.7 MHz, DMSO-d₆) δ [ppm]: 153.58, 152.45, 149.27, 147.08, 140.22, 138.50, 138.03, 135.88, 130.41, 130.31, 130.06, 129.31, 129.10, 127.79, 127.66, 127.42, 126.16, 125.43, 119.94, 118.74, 58.14, 55.52, 32.74, 18.20.

Synthesis of (*E*)-4-(2-(1-(3-hydroxypropyl)quinolinium-4-yl)vinyl)-1,3-dimethylquinolinium hexafluorophosphate (**82**)

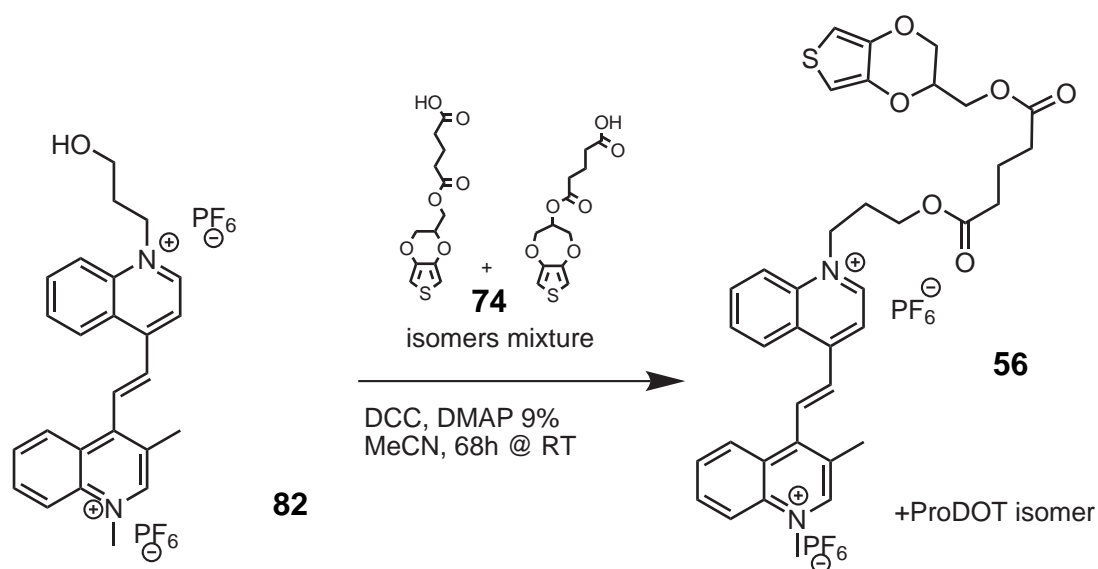


A suspension of **84** (250 mg, 0.574 mmol), KPF₆ (258 mg, 1.47 mmol) in 1.0 ml of acetone was stirred at room temperature for 20 min. MeI was added (244 mg, 1.72 mmol). The mixture was heated in a CEM Discover microwave reactor for 90 min (*P*_{max}=20 W, 95°C, cooling off, 10 ml closed vessel). The mixture was cooled down to RT. The solid precipitate was triturated using a spatula, collected by filtration, and washed with acetone and Et₂O. Product was suspended in 4 ml of an aqueous NH₄PF₆ 30% solution and stirred for 14 h. The white solid was filtered under reduced pressure, and washed with few ml of NH₄PF₆(aq) 30% and with deionized water. Product was dried under reduced pressure at

60 °C for 3 h (262 mg, 0.397 mmol, yield 69%, m.p.: 182-184 °C).

¹H NMR (500 MHz, DMSO-d₆) δ [ppm]: 9.65 (d, *J*=6.3 Hz, 1H), 9.63 (s, 1H), 8.81-8.78 (m, 2H), 8.67 (d, *J*=9.0 Hz, 1H), 8.64 (d, *J*=8.5 Hz, 1H), 8.58-8.52 (m, 2H), 8.34 (t, *J*=7.7 Hz, 1H), 8.31-8.27 (m, 2H), 8.10-8.08 (m, 2H), 5.19 (t, *J*=7.2 Hz, 2H), 4.68 (s, 3H), 3.60 (t, *J*=5.7 Hz, 2H), 2.76 (s, 3H), 2.19 (qui, *J*=6.5 Hz, 2H); ¹³C NMR (125.7 MHz, DMSO-d₆) δ [ppm]: 151.79, 151.58, 151.54, 149.57, 138.50, 137.60, 136.06, 134.98, 134.85, 133.82, 130.86, 130.76, 130.56, 127.99, 127.94, 127.85, 127.40, 120.04, 119.99, 119.54, 58.16, 55.85, 45.93, 32.77, 18.23.

Synthesis of (*E*)-4-(2-(1-(3-(5-((2,3-dihydrothieno[3,4-*b*][1,4]dioxin-2-yl)methoxy)-5-oxopentanoyloxy)propyl)quinolinium-4-yl)vinyl)-1,3-dimethylquinolinium hexafluorophosphate (ISO8) (**56**)

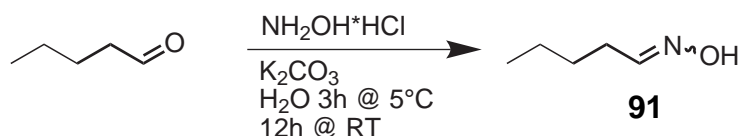


In a closed vessel a suspension of **74** (89.3 mg, 0.312 mmol, 80:20 isomers mixture), **82** (200 mg, 0.302 mmol), dicyclohexylcarbodiimide (DCC) (69.0 mg, 0.334 mmol) and DMAP (3.4 mg, 0.028 mmol) in 3 ml of dry MeCN was prepared. A white solid precipitated. The solution was kept under stirring for 68 h. The brown mixture was filtered washing the precipitate with MeCN (20 ml). The filtrate was collected and evaporated under reduced pressure obtaining a black solid which was sonicated with Et₂O (20 ml). The product was filtered, suspended in 15 ml of EtOH and stirred for 48 h to eliminate residual DMAP. Product was filtered and residual solvent was evaporated under reduced pressure at 40 °C obtaining a brown solid (197.4 mg, 0.213 mmol, yield 70%).

¹H NMR (500 MHz, DMSO-d₆) δ [ppm]: 9.66-9.60 (m, 2H (EDOT + ProDOT)),

8.78-8.77 (m, 2H (EDOT + ProDOT)), 8.67 (d, $J=8.9$ Hz, 1H (EDOT + ProDOT)), 8.62 (d, $J=8.4$ Hz, 1H (EDOT + ProDOT)), 8.57 (d, $J=8.8$ Hz, 1H (EDOT + ProDOT)), 8.50 (d, $J=16.2$ Hz, 1H (EDOT + ProDOT)), 8.34 (t, $J=7.6$ Hz, 1H (EDOT + ProDOT)), 8.30-8.23 (m, 2H (EDOT + ProDOT)), 8.11-8.06 (m, 2H (EDOT + ProDOT)), 6.75 (s, 2H ProDOT), 6.57-6.55 (m, 2H EDOT), 5.24-5.19 (m, 2H (EDOT + ProDOT)), 5.15 (qui, $J=3.8$ Hz, 1H ProDOT), 4.69 (s, 3H (EDOT + ProDOT)), 4.42-4.38 (m, 1H EDOT), 4.30-4.24 (m, 2H (EDOT + ProDOT) + 2H EDOT + 4H ProDOT), 4.15-4.14 (m, 1H EDOT), 4.02-3.98 (m, 1H EDOT), 2.76 (s, 3H (EDOT + ProDOT)), 2.44-2.36 (4H (EDOT + ProDOT)), 2.32-2.28 (m, 2H (EDOT + ProDOT)), 1.80-1.74 (m, 2H (EDOT + ProDOT)).

Synthesis of valeraldehyde oxime (91)

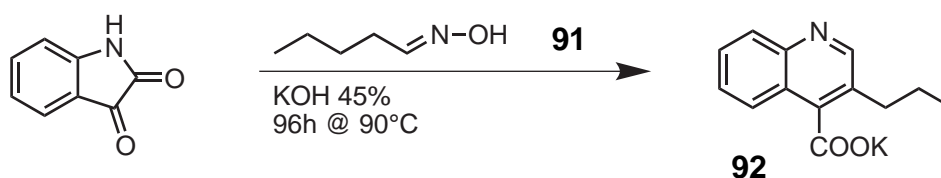


To 600 ml of deionized water, cooled to 5 °C with an ice water bath, $\text{NH}_2\text{OH}\cdot\text{HCl}$ (30.73 g, 442.3 mmol) was added portionwise followed by K_2CO_3 (30.56 g, 221.1 mmol) obtaining a light yellow solution. Pentanal (40.00 g, 464.4 mmol) was added dropwise over 30 min. Gas evolution was observed during the addition, and the light yellow color faded away. The mixture was kept under stirring and the ice in the cooling bath was allowed to melt (3 h). The mixture was kept under stirring for further 12 h at RT and extracted with 100 + 4 × 50 ml of Et_2O . The organic phase was collected, dried over MgSO_4 and evaporated under reduced pressure at 60 °C obtaining product as a white solid (38.755 g, 0.383 mol, yield 87%).

^1H NMR (500 MHz, CDCl_3) δ [ppm]: 9.21 (s, 2H E+Z), 7.41 (t, $J=6.2$ Hz, 1H, E isomer), 6.73 (t, $J=5.3$ Hz, 1H, Z isomer), 2.38 (q, $J=7.5$ Hz, 2H, Z isomer), 2.20 (q, $J=7.7$ Hz, 2H, E isomer), 1.47 (m, 2H, E+Z), 1.35 (sep, $J=7.8$ Hz, 2H, E+Z), 0.89 (q, $J=7.2$ Hz, 3H, E+Z), E/Z ratio is 1.18.

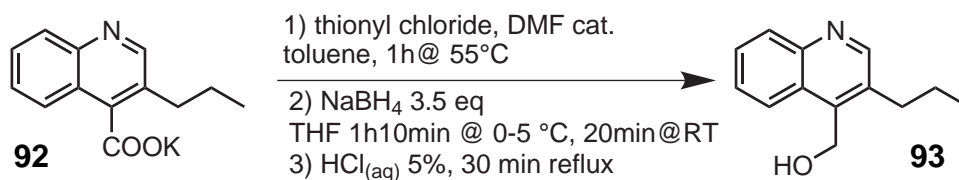
Synthesis of potassium 3-propylquinoline-4-carboxylate (92)

In a 1 L two-necked RBF, an aqueous KOH solution was prepared (223.87 g of KOH in 280 ml of deionized water), and isatin (70.00 g, 0.476 mol) was subsequently added. The mixture turned black and after few minutes a white solid



mass was obtained. Valeraldehyde oxime (30.09 g, 0.2975 mol) was added, and the mixture was heated to 90°C. An orange homogeneous solution was obtained after few minutes. The mixture was kept under stirring at 90°C for 96h observing the formation of a white precipitate. The mixture was cooled to room temperature and stirred for further 12h. The white precipitate was collected by filtration under reduced pressure on a sintered glass funnel and washed with a 30% aqueous KOH solution followed by few ml of Et₂O. The residual solvent was removed under reduced pressure at 90°C. The obtained yellow solid was suspended in refluxing acetone (200ml) for 30 min, cooled and filtered. Product was obtained as a white solid after evaporation of residual solvent under reduced pressure at 90°C (45.79 g, 0.1807 mol, yield 61%, m.p.: 297-299°C dec.) ¹H NMR (500MHz, D₂O) δ [ppm]: 8.63 (s, 1H), 7.98 (d, *J*=8.3Hz, 1H), 7.88 (d, *J*=8.3Hz, 1H), 7.58 (t, *J*=6.8Hz, 1H), 7.44 (t, *J*=7.5Hz, 1H), 2.72 (t, *J*=7.9Hz, 2H), 1.68 (sex, *J*=7.7Hz, 2H), 0.94 (t, *J*=7.4Hz, 3H).

Synthesis of (3-propylquinolin-4-yl)methanol (93)

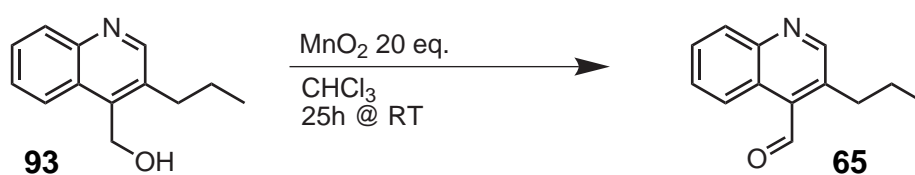


In a 250ml two-necked RBF, equipped with a CaCl₂ guard tube, a suspension of **92** (10.00 g, 39.47mmol) in 100ml of dry toluene was prepared. Anhydrous DMF (5.3ml) was added followed by dropwise addition of SOCl₂ (18.78 g, 157.9mmol). The mixture was stirred at RT for 10min and heated to 55°C on a water bath for 1h obtaining a yellow solution. The mixture was cooled to RT, poured in 200ml of water and basified with NaHCO₃. The organic phase was separated and the aqueous one was extracted with further 50ml of toluene. The organic phases were collected, washed with brine (100ml), dried over MgSO₄ and evaporated under reduce pressure obtaining a yellow oil (6.94g, 29.7mmol). Crude product was dissolved in THF (100ml) in a RBF

equipped with CaCl_2 guard tube. The mixture was cooled to 5°C with an ice-water bath, and NaBH_4 (3.93 g, 104 mmol) was added portionwise under stirring. The mixture was kept under stirring at $0-5^\circ\text{C}$ for 1 h 10 min and then allowed to warm to RT (20 min). A yellow solution with a white precipitate was obtained. The mixture was poured in 100 ml of water and acidified by addition of 150 ml of $\text{HCl}_{(\text{aq})}$ 1 M. The mixture was heated to boiling and THF was distilled off. After 30 min the solution was cooled to RT and basified by addition of Na_2CO_3 observing formation of a pale yellow solid. Et_2O (30 ml) was added, and the mixture was kept under stirring overnight. The solid was collected by filtration under reduced pressure on a sintered glass funnel, dried in air and under reduced pressure at 40°C . The solid was dissolved in refluxing toluene/*n*-hexane 1:1 mixture, filtered hot and the filtrate was allowed to cool to room temperature observing crystallization of desired product which was collected by filtration under reduced pressure. The filtrate from the filtration of the initial basified solution was extracted with 3×50 ml of CHCl_3 , dried over MgSO_4 and evaporated under reduced pressure obtaining a yellow oil which was purified by crystallization from toluene. A total of 4.087 g of product was obtained (20.31 mmol, yield 51%, m.p.: $96-97^\circ\text{C}$).

^1H NMR (500 MHz, CDCl_3) δ [ppm]: 8.51 (s, 1H), 8.28 (d, $J=8.3$ Hz, 1H), 8.06 (d, $J=8.0$ Hz, 1H), 7.64 (t, $J=7.6$ Hz, 1H), 7.59 (t, $J=7.0$ Hz, 1H), 2.80 (t, $J=7.9$ Hz, 2H), 1.62 (m, 2H), 0.97 (t, $J=7.3$ Hz, 3H).

Synthesis of 3-propylquinoline-4-carbaldehyde (65)

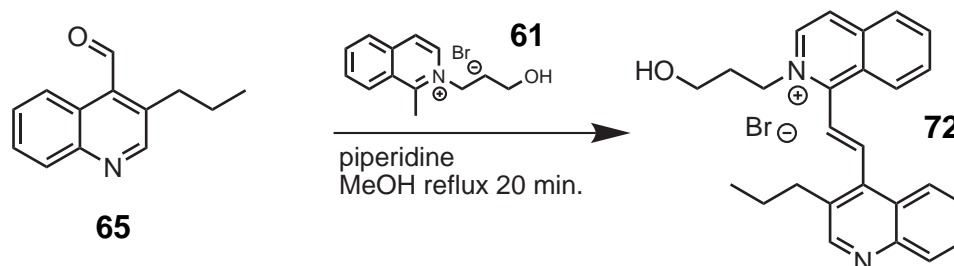


In a 250 ml RBF equipped with a CaCl_2 guard tube, compound **93** (3.800 g, 18.88 mmol) was dissolved in dry CHCl_3 (100 ml) and activated MnO_2 was added (32.8 g, 377 mmol, Aldrich 63543). The mixture was kept under vigorous stirring for 25 h at RT, filtered on a sintered glass funnel and again on a paper filter to remove MnO_2 . The solvent was evaporated under reduced pressure at 40°C obtaining product as a clear yellow liquid (2.948 g, 14.79 mmol, yield 78%).

^1H NMR (500 MHz, CDCl_3) δ [ppm]: 10.92 (s, 1H), 8.90 (s, 1H), 8.71 (d, $J=8.5$ Hz,

1H), 8.19 (d, $J=8.3$ Hz, 1H), 7.75 (t, $J=7.0$ Hz, 1H), 7.67 (t, $J=7.0$ Hz, 1H), 3.09 (m, 2H), 1.75 (sex, $J=7.4$ Hz, 2H), 1.04 (t, $J=7.4$ Hz, 3H).

Synthesis of (*E*)-2-(3-hydroxypropyl)-1-(2-(3-propylquinolin-4-yl)-vinyl)isoquinolinium bromide (**72**)

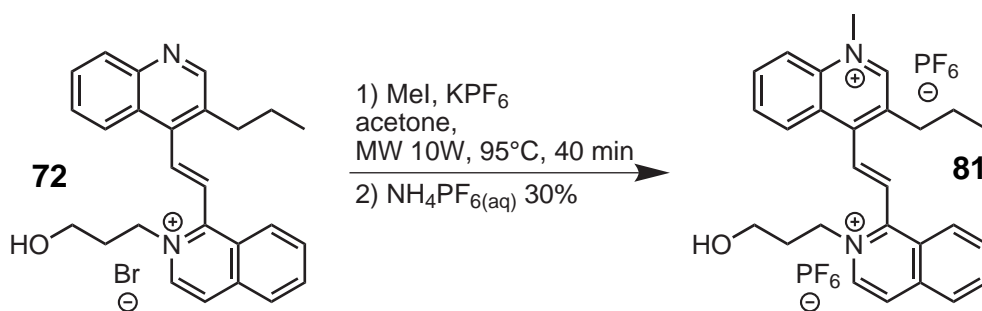


In a test tube a solution of piperidine (40 mg, 0.47 mmol) in 0.6 ml of MeOH was added to a mixture of **61** (580 mg, 2.06 mmol) and **65** (463 mg, 2.32 mmol). The mixture was heated to reflux and a red homogeneous solution was obtained. After 20 min the mixture was cooled to RT. The solvent was evaporated under reduced pressure and the obtained solid was triturated by sonication with acetone (2.5 ml). The yellow solid was collected by filtration washing with acetone and Et₂O. Crystallization from *i*-PrOH and solvent removal under reduced pressure at 60 °C yields product as a pale yellow solid (511 mg, 1.10 mmol, yield 54%, m.p.: 200-201 °C).

¹H NMR (500 MHz, DMSO-*d*₆) δ [ppm]: 8.95 (s, 1H), 8.91 (d, $J=6.9$ Hz, 1H), 8.73 (d, $J=8.6$ Hz, 1H), 8.65 (d, $J=6.9$ Hz, 1H), 8.45 (d, $J=8.2$ Hz, 1H), 8.34-8.30 (m, 2H), 8.14-8.10 (m, 2H), 7.92 (d, $J=16.8$ Hz, 1H), 7.81 (t, $J=8.3$ Hz, 1H), 7.79-7.65 (m, 2H), 4.87 (t, $J=7.6$ Hz, 2H), 4.81 (t, $J=4.8$ Hz, 1H), 3.51 (q, $J=5.3$ Hz, 2H), 2.97 (t, $J=8.0$ Hz, 2H), 2.15 (qui, $J=7.2$ Hz, 2H), 1.73 (sex, $J=7.8$ Hz, 2H), 0.99 (t, $J=7.3$ Hz, 3H); ¹³C NMR (125.7 MHz, DMSO-*d*₆) δ [ppm]: 157.10, 153.18, 147.16, 140.78, 139.09, 138.08, 136.74, 136.37, 133.37, 131.89, 130.30, 130.15, 129.42, 128.46, 127.97, 127.90, 126.24, 125.91, 125.52, 125.47, 57.87, 56.86, 33.16, 33.03, 24.92, 14.55.

Synthesis of (*E*)-4-(2-(2-(3-hydroxypropyl)isoquinolinium-1-yl)-vinyl)-1-methyl-3-propylquinolinium hexafluorophosphate (**81**)

A suspension of **72** (350 mg, 0.755 mmol), KPF₆ (356 mg, 1.933 mmol) in 1.3 ml of acetone was stirred at room temperature for 20 min obtaining a white sus-

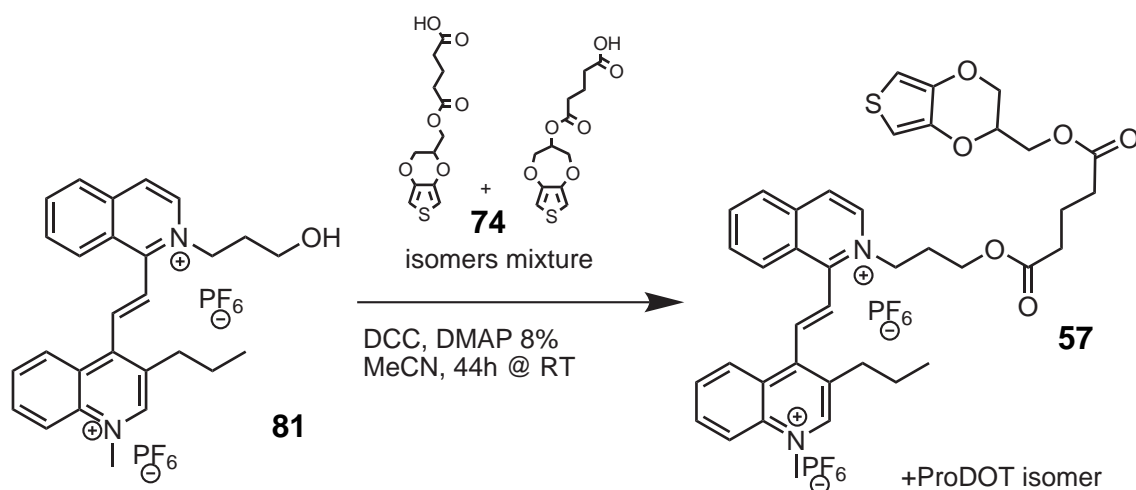


pension. MeI was added (0.20 ml, 3.21 mmol, 0.46 g). The mixture was heated in a CEM Discover microwave reactor for 40 min ($P_{\max}=10\text{ W}$, 95°C , cooling off, 10 ml closed vessel). The mixture was cooled down to RT. The solid precipitate was triturated using a spatula, collected by filtration and washed with acetone and Et₂O. Product was suspended in 4 ml of an aqueous NH₄PF₆ 30% solution and stirred for 3 days. The white solid was filtered under reduced pressure and washed with few ml of NH₄PF₆(aq) 30% and with deionized water. Product was dried under reduced pressure at 60°C for 4 h (288 mg, 0.419 mmol). Filtrate from the first filtration was allowed to evaporate and the residue was suspended in 3 ml of an aqueous NH₄PF₆(aq) 30% solution, stirred for 2 days, filtered and washed with few ml of NH₄PF₆(aq) 30% solution and water. The solid was dried under reduced pressure at 50°C obtaining more 175 mg of product. A total of 403 mg of product was obtained (0.586 mmol, yield 78%, m.p.: $193\text{-}195^\circ\text{C}$).

¹H NMR (500 MHz, DMSO-*d*₆) δ [ppm]: 9.64 (s, 1H), 8.90 (d, $J=6.9\text{ Hz}$, 1H), 8.73 (d, $J=8.6\text{ Hz}$, 1H), 8.69-8.67 (m, 2H), 8.59 (d, $J=8.9\text{ Hz}$, 1H), 8.46 (d, $J=8.2\text{ Hz}$, 1H), 8.35-8.30 (m, 2H), 8.16-8.09 (m, 3H), 7.81 (d, $J=16.8\text{ Hz}$, 1H), 4.85 (t, $J=7.5\text{ Hz}$, 2H), 4.72 (s, 3H), 3.50 (t, $J=5.7\text{ Hz}$, 2H), 3.07 (t, $J=7.9\text{ Hz}$, 2H), 2.15 (qui, $J=6.9\text{ Hz}$, 2H), 1.82 (sex, $J=7.8\text{ Hz}$, 2H), 1.03 (t, $J=7.3\text{ Hz}$, 3H).

Synthesis of (*E*)-4-(2-(2-(3-(5-((2,3-dihydrothieno[3,4-*b*][1,4]dioxin-2-yl)methoxy)-5-oxopentanoyloxy)propyl)isoquinolinium-1-yl)-vinyl)-1-methyl-3-propylquinolinium hexafluorophosphate (ISO9) (57)

In a closed vessel a suspension of **74** (98.5 mg, 0.344 mmol, 80:20 isomers mixture), **81** (230 mg, 0.334 mmol), dicyclohexylcarbodiimide (DCC) (75.8 mg, 0.367 mmol) and DMAP (3.5 mg, 0.029 mmol) in 3 ml of dry MeCN was prepared. A white solid precipitated. The solution was kept under stirring for 44 h. The mix-

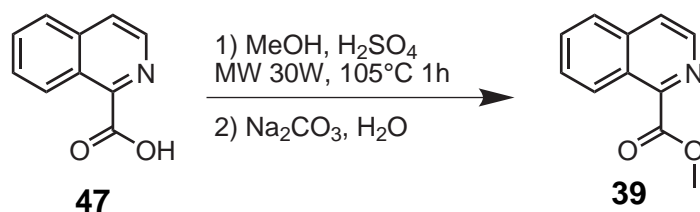


ture was filtered washing the precipitate with MeCN (20 ml). The filtrate was collected and evaporated under reduced pressure obtaining an orange glassy solid which was sonicated with Et₂O (20 ml) obtaining a pale orange solid. The product was filtered, suspended in 15 ml of EtOH and stirred for 72 h to eliminate residual DMAP. Product was collected by filtration and residual solvent was evaporated under reduced pressure at 50 °C obtaining a pale orange solid (253 mg, 0.264 mmol, yield 79%).

¹H NMR (500 MHz, DMSO-*d*₆) δ [ppm]: 9.65 (s, 1H (EDOT + ProDOT)), 8.89 (d, *J*=6.9 Hz, 1H (EDOT + ProDOT)), 8.76 (d, *J*=8.7 Hz, 1H (EDOT + ProDOT)), 8.68 (d, *J*=6.9 Hz, 1H (EDOT + ProDOT)), 8.65 (d, *J*=8.6 Hz, 1H (EDOT + ProDOT)), 8.59 (d, *J*=8.9 Hz, 1H (EDOT + ProDOT)), 8.46 (d, *J*=8.2 Hz, 1H (EDOT + ProDOT)), 8.36-8.29 (m, 2H (EDOT + ProDOT)), 8.14 (t, *J*=8.0 Hz, 1H (EDOT + ProDOT)), 8.11-8.08 (m, 2H (EDOT + ProDOT)), 7.79 (d, *J*=16.7 Hz, 1H (EDOT + ProDOT)), 6.81 (s, 2H ProDOT), 6.61 (m, 2H EDOT), 5.12 (m, 1H ProDOT), 4.81 (t, *J*=7.6 Hz, 2H (EDOT + ProDOT)), 4.71 (s, 3H (EDOT + ProDOT)), 4.42-4.40 (m, 1H EDOT), 4.30-4.24 (m, 2H EDOT + 4H ProDOT), 4.15-4.08 (m, 1H EDOT + 2H (EDOT + ProDOT)), 4.03-3.99 (m, 1H EDOT), 3.05 (t, *J*=8.0 Hz, 2H (EDOT + ProDOT)), 2.30-2.26 (m, 4H (EDOT + ProDOT)), 2.12-2.09 (m, 2H (EDOT + ProDOT)), 1.79 (sex, *J*=7.9 Hz, 2H (EDOT + ProDOT)), 1.63-1.59 (m, 2H (EDOT + ProDOT)), 1.01 (t, *J*=7.3 Hz, 3H (EDOT + ProDOT)).

Synthesis of methyl isoquinoline-1-carboxylate (**39**)

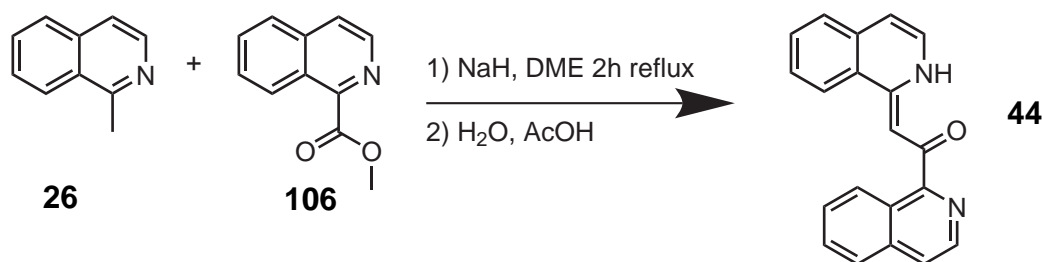
In a 250 ml RBF a suspension of **47** (10.726 g, 61.9 mmol) in 75 ml of MeOH was prepared. The mixture was cooled with an ice-water bath, and concen-



trated H₂SO₄ (24.88 g, 253 mmol) was slowly added under stirring. The mixture was stirred at room temperature for 10 min and transferred in a CEM 35 ml microwave pressure vessel (4 aliquots were used) and heated at 105°C, 30W for 1 h. The mixture was cooled to RT, slowly poured in water (300 ml) and basified to pH 10 by addition of Na₂CO₃. The mixture was extracted with 60 ml + 2 × 30 ml of CH₂Cl₂ collecting the organic phase and drying over Na₂SO₄. Product was recovered after solvent evaporation under reduced pressure and purified by vacuum distillation (b.p.: 130°C at 5 mmHg). Clear oil (8.110 g, 43.3 mmol, yield 70%).

¹H NMR (500 MHz, CDCl₃) δ [ppm]: 8.83 (d, *J*=8.5 Hz, 1H), 8.63 (d, *J*=5.5 Hz, 1H), 7.88 (d, *J*=8.1 Hz, 1H), 7.83 (d, *J*=5.5 Hz, 1H), 7.74 (t, *J*=8.1 Hz, 1H), 7.69 (t, *J*=7.8 Hz, 1H), 4.10 (s, 3H).

Synthesis of (Z)-2-(isoquinolin-1(2H)-ylidene)-1-(isoquinolin-1-yl)ethanone (44)



Under N₂ atmosphere, in an oven dried 250 ml 3-necked RBF, fitted with reflux condenser, septum and dropping funnel, a suspension of NaH* (1.406 g, 58.6 mmol) in anhydrous DME was prepared. A solution of **26** (2.00 g, 14.0 mmol) and **106** (3.14 g, 16.8 mmol) in 20 ml of anhydrous DME was dropwise added to the refluxing suspension of NaH[†]. The suspension turned to yellow and after 1 h a brown homogeneous solution was obtained. After 2 h the mixture was

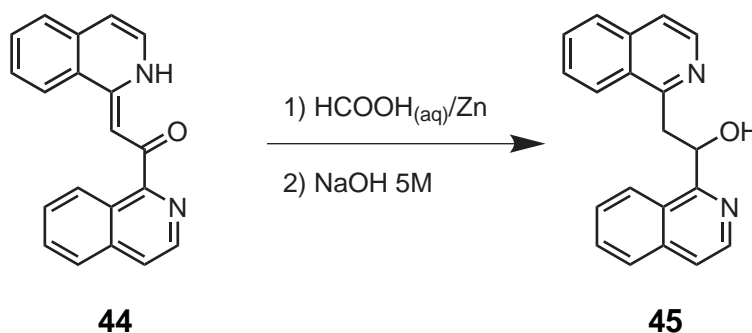
*NaH dispersion in paraffin was used. The reagent was carefully washed with ETP before solvent addition

[†]both reagents were freshly distilled under reduced pressure

cooled with an ice-water bath, and Et₂O (25 ml) was added followed by AcOH (1.74 g). After 5 min H₂O (18 ml) was added followed by more AcOH (1.74 g). The mixture was kept under stirring at RT for 1 h. The bright yellow solid was filtered on a Büchner funnel washing with Et₂O. The filtrate was extracted with 3 × 20 ml of Et₂O collecting the organic phase and washing it with 10 ml of NaHCO_{3(aq)}. The organic phase was dried over Na₂SO₄ and the volume was reduced to 5 ml under reduced pressure. The precipitate was filtered and collected. Product from the first filtration was continuously extracted with CH₂Cl₂ in a Soxhlet apparatus to remove insoluble impurities and recovered after solvent evaporation under reduced pressure. Bright yellow powder (3.399 g overall, 11.39 mmol, yield 82%, m.p.: 175.5-177.0 °C).

¹H NMR (500 MHz, C₆D₆) δ [ppm]: 16.42 (s, 1H), 9.88 (d, *J*=8.6 Hz, 1H), 8.75 (d, *J*=5.5 Hz, 1H), 8.02 (d, *J*=8.3 Hz, 1H), 7.78 (s, 1H), 7.56 (d, *J*=8.2 Hz, 1H), 7.51 (td, *J*=7.2 Hz, *J*=1.3 Hz, 1H), 7.41-7.38 (m, 2H), 7.20 (t, *J*=7.9 Hz, 1H), 7.08 (d, *J*=7.9 Hz, 1H), 7.04 (t, *J*=7.6 Hz, 1H), 6.48 (t, *J*=5.8 Hz, 1H), 6.17 (d, *J*=6.7 Hz, 1H); ¹³C NMR (125.7 MHz, DMSO-*d*₆) δ [ppm]: 186.23, 158.17, 153.84, 141.91, 137.10, 135.87, 133.10, 130.84, 129.50, 128.50, 128.26, 127.78, 127.70, 127.60, 125.94, 125.38, 124.27, 122.47, 111.66, 88.11.

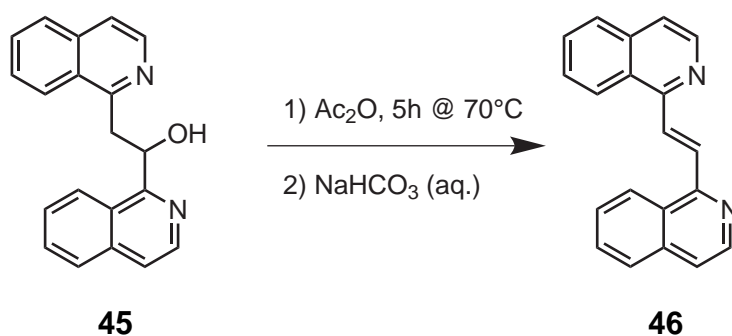
Synthesis of 2-(isoquinolin-1-yl)-1-(quinolin-4-yl)ethanol (45)



To a stirred solution of **44** (2.000 g, 6.70 mmol) in aqueous formic acid 50% (100 ml), zinc dust (2.091 g, 32.0 mmol) was added. The solution rapidly changed its colour from red to pale yellow. The mixture was kept under stirring for 25 min and filtered collecting the filtrate in an ice-cooled stirred 5 M NaOH solution (250 ml). A white solid separated and the mixture was kept under stirring for 15 min, filtered on a Büchner funnel and washed with 30 ml of 5 M NaOH solution followed by 30 ml of deionized water. The white solid was dried in an evacuated desiccator (1.890 g, 6.29 mmol, yield 94%, m.p.: 167.7-168.5 °C).

^1H NMR (500MHz, $\text{DMSO}-d_6$) δ [ppm]: 8.57 (d, $J=8.44\text{Hz}$, 1H), 8.40 (d, $J=5.6\text{Hz}$, 1H), 8.37-8.33 (m, 2H), 7.99 (d, $J=8.1\text{Hz}$, 1H), 7.94 (d, $J=8.1\text{Hz}$, 1H), 7.79-7.74 (m, 3H), 7.70 (t, $J=7.4\text{Hz}$, 1H), 7.67-7.64 (m, 2H), 6.09 (q, $J=6.3\text{Hz}$, 1H), 5.75 (d, $J=6.2\text{Hz}$, 1H), 3.97-3.89 (m, 2H); ^{13}C NMR (125.7MHz, $\text{DMSO}-d_6$) δ [ppm]: 161.93, 160.03, 142.13, 141.47, 136.70, 136.20, 130.64, 130.58, 127.86, 127.84, 127.82, 127.76, 127.64, 126.31, 126.01, 120.94, 119.68, 72.11, 41.72.

Synthesis of (*E*)-1,2-di(isoquinolin-1-yl)ethene (46)

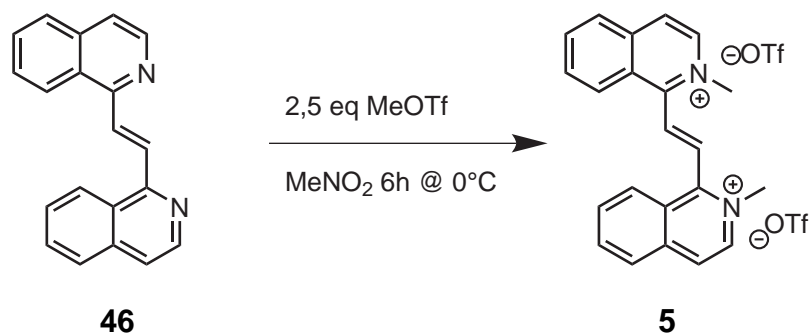


A stirred suspension of **45** (1.700g, 5.67 mmol) in Ac_2O (15 ml) was heated to 70°C with a water bath. A clear solution was obtained after 10min and a solid started to precipitate after 20min. After 5h the mixture was poured in 150ml of water and NaHCO_3 was added under stirring till pH 8. The mixture was stirred overnight, 200ml of water were added and the light brown solid was filtered on an Hirsh funnel washing with 30ml of distilled water, EtOH (10ml) and Et_2O (30ml). The solid was collected and dried in vacuum at 50°C (1.395g, 4.94mmol, yield 87%, m.p.: 260°C (dec.)).

^1H NMR (500MHz, CDCl_3) δ [ppm]: 9.03 (s, 2H), 8.67-8.65 (m, 4H), 7.88 (d, $J=7.9\text{Hz}$, 2H), 7.76-7.69 (m, 6H). ^{13}C NMR (125.7MHz, CDCl_3) δ [ppm]: 153.94, 142.23, 136.99, 130.42, 129.59, 127.73, 127.48, 127.35, 125.16, 121.10.

Synthesis of (*E*)-1,1'-(ethene-1,2-diyl)bis(2-methylisoquinolinium) trifluoromethanesulfonate (5)

Under N_2 atmosphere, MeOTf (95mg, 0.58mmol) was added to an ice-cooled stirred suspension of **46** (50mg, 0.18mmol) in dry MeNO_2 (2.0ml). The mixture was kept under stirring at 0°C for 6h obtaining a clear solution. Product was precipitated as a white solid after addition of Et_2O (6ml), collected by filtration on an Hirsh funnel, and dried in vacuum (45mg, 0.073mmol, yield 42%).



^1H NMR (500MHz, CD_3CN) δ [ppm]: 8.78 (d, $J=8.8\text{Hz}$, 2H), 8.55 (d, $J=6.9\text{Hz}$, 2H), 8.50 (d, 6.8Hz, 2H), 8.40 (d, 8.3Hz, 2H), 8.33 (t, $J=7.7\text{Hz}$, 2H), 8.16 (t, $J=7.8\text{Hz}$, 2H), 7.80 (s, 2H), 4.42 (s, 6H); ^{13}C NMR (125.7MHz, CD_3CN) δ [ppm]: 154.19, 138.38, 136.98, 136.78, 133.46, 132.32, 129.19, 128.332, 127.109, 126.352, 47.52.

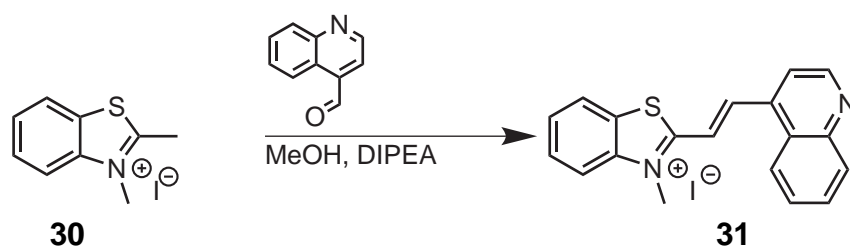
Synthesis of 2,3-dimethylbenzo[*d*]thiazol-3-ium iodide (30)



A solution of 2-methylbenzothiazole (5.000 g, 33.50 mmol) and iodomethane (5.706 g, 40.2 mmol) in 7 ml of acetone was heated in a CEM Discover microwave reactor for 75 min ($P_{\text{max}}=70\text{W}$, 110°C , cooling off, 35 ml vessel), and cooled to RT. The white solid was washed with acetone and filtered on a Büchner funnel washing with acetone and Et_2O . Residual solvent was evaporated under reduced pressure (0.4 torr) at 40°C (9.291 g, 31.91 mmol, yield 95%, m.p.: 225°C (dec.))

Synthesis of (*E*)-3-methyl-2-(2-(quinolin-4-yl)vinyl)benzo[*d*]thiazol-3-ium iodide (31)

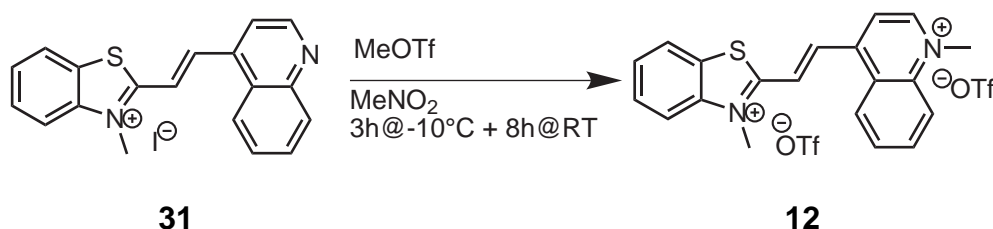
To a mixture of **30** (500 mg, 1.72 mmol) and quinoline-4-carboxyaldehyde (304 mg, 1.93 mmol), a solution of *N,N*-diisopropylethylamine (DIPEA) (29 μl , 22.23 mg, 0.172 mmol) in 1 ml of MeOH was added. The mixture was heated to reflux for 20 min obtaining a red homogeneous solution. The solution was allowed to cool to room temperature obtaining a red solid which was washed with EtOH



and filtered on an Hirsh funnel washing with EtOH and Et₂O. Product was purified by crystallization from EtOH. Residual solvent was removed under reduced pressure at 50°C. Product was recovered as a purple solid (202mg, 0.465mmol, yield 27%).

¹H NMR (500MHz, DMSO-d₆) δ [ppm]: 9.13 (d, *J*=4.5Hz, 1H), 8.92 (d, *J*=15.8Hz, 1H), 8.56 (t, *J*=7.6Hz, 2H), 8.39-8.33 (m, 2H), 8.24 (d, *J*=4.6Hz, 1H), 8.16 (d, *J*=8.4Hz, 1H), 7.97 (t, *J*=7.9Hz, 1H), 7.93-7.88 (m, 2H), 7.81 (td, *J*=7.0Hz, *J*=1.2Hz, 1H), 4.48 (s, 3H); ¹³C NMR (125.7MHz, DMSO-d₆) δ [ppm]: 171.39, 150.87, 148.83, 142.54, 142.29, 139.12, 130.63, 130.30, 130.23, 129.45, 129.22, 128.22, 125.60, 124.97, 124.53, 120.69, 119.85, 117.84, 37.48.

Synthesis of (*E*)-3-methyl-2-(2-(1-methylquinolinium-4-yl)vinyl)-benzo[*d*]thiazol-3-ium trifluoromethanesulfonate (**12**)

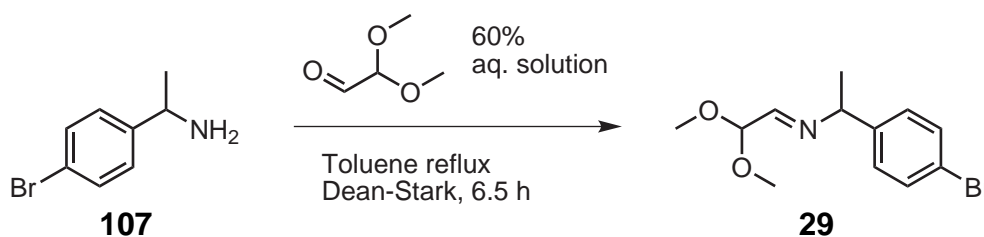


Under N₂ atmosphere, MeOTf (63 mg, 0.382 mmol) was added to a stirred suspension of **31** (60 mg, 0.139 mmol) in dry MeNO₂ (2 ml) cooled to -10°C with an ice/salt bath. The mixture was kept under stirring at -10°C for 3h obtaining a clear violet solution and stirred overnight at room temperature. Product was precipitated as a white solid after addition of Et₂O (6 ml), collected by filtration on an Hirsh funnel, and dried in vacuum (165 mg, 0.267 mmol, yield 70%).

¹H NMR (500MHz, CD₃CN) δ [ppm]: 9.24 (d, *J*=6.1Hz, 1H), 8.78-8.75 (m, 2H), 8.52-8.47 (m, 2H), 8.41 (d, *J*=8.1Hz, 1H), 8.36 (t, *J*=8.2Hz, 1H), 8.26-8.23 (m, 2H), 8.17 (td, *J*=7.3Hz, *J*=1.0Hz, 1H), 8.02 (t, *J*=7.8Hz, 1H), 7.94 (t, *J*=7.3Hz, 1H), 4.65 (s, 3H), 4.43 (s, 3H); ¹³C NMR (125.7MHz, CD₃CN) δ [ppm]: 149.42, 149.15, 142.47, 139.29, 138.97, 138.73, 136.11, 130.87, 130.69, 129.93, 129.56, 127.37,

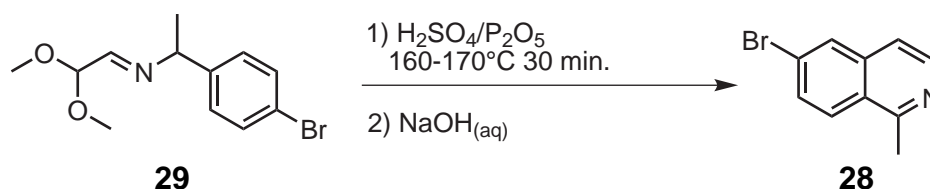
126.58, 124.61, 124.34, 122.14, 120.22, 119.49, 46.08, 37.27. Anal. Calcd for $C_{22}H_{18}F_6N_2O_6S_3$: C, 42.86; H, 2.94; N, 4.54; S, 15.6. Found: C, 43.80; H, 3.31; N, 4.62; S, 15.97.

Synthesis of (*E*)-*N*-(2,2-dimethoxyethylidene)-1-(4-bromophenyl)ethanamine (**29**)



A mixture of 1-(4-bromophenyl)ethanamine (**107**) (9.980 g, 49.88 mmol) and dimethoxyacetaldehyde 60% w/w aqueous solution (9.35 g, 53.87 mmol) in 40 ml of toluene were refluxed for 6.5 h under nitrogen atmosphere, collecting water with a Dean-Stark apparatus. The mixture was cooled to room temperature and solvent was removed under reduced pressure (~ 1 mmHg) obtaining product as a yellow oil (13.988 g, 48.88 mmol, yield 98%).

Synthesis of 6-bromo-1-methylisoquinoline (**28**)

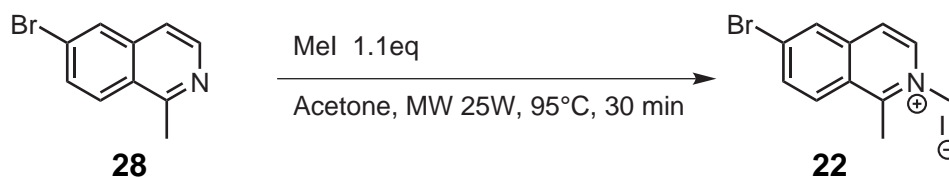


In a 250 ml RBF, **29** (11.45 g, 40.01 mmol) was slowly added, under stirring, to ice cooled H_2SO_4 (60 ml). The solution was added under stirring to a mixture of H_2SO_4 (8 ml) and P_2O_5 (22.9 g, 161.33 mmol) and heated to 160°C for 30 min. The mixture was allowed to cool to room temperature, slowly poured in ice and basified till pH 9 adding NaOH. The mixture was stirred at room temperature for 12 h and filtered. The filtrate was extracted with 3×250 ml of AcOEt collecting the organic phase and drying over $MgSO_4$. Solvent was evaporated under reduced pressure obtaining product as a pale yellow solid (5.838 g, 26.29 mmol, yield 66%, m.p.: 50-51°C).

1H NMR (500 MHz, $CDCl_3$) δ [ppm]: 8.41 (d, $J=5.9$ Hz, 1H), 8.02-8.00 (m, 2H),

7.72 (dd, $J=9.0\text{Hz}$, $J=1.9\text{Hz}$, 1H), 7.49 (d, $J=5.9\text{Hz}$, 1H), 3.01 (s, 3H); ^{13}C NMR (125.7MHz, CDCl_3) δ [ppm]: 158.73, 143.54, 137.11, 130.01, 129.40, 127.48, 125.89, 124.21, 118.04, 22.20.

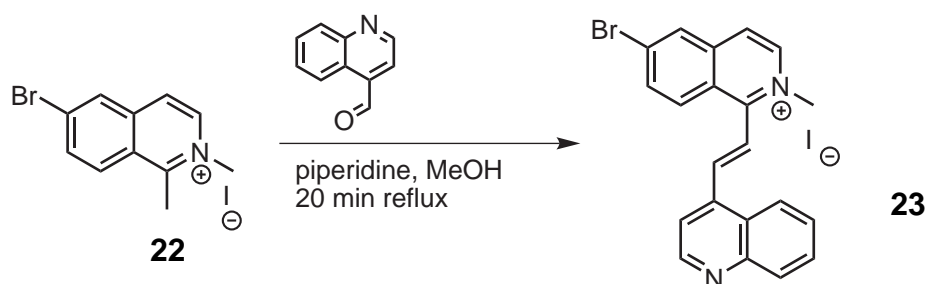
Synthesis of 6-bromo-1,2-dimethylisoquinolinium iodide (**22**)



A mixture of **28** (500 mg, 2.251 mmol), MeI (474 mg, 2.476 mmol) and 0.5 ml of acetone was heated in a CEM Discover microwave reactor for 30 min ($P_{\text{max}}=25\text{W}$, 95°C, cooling off), and cooled to RT. The white solid was filtered on an Hirsh funnel, washed with acetone and then with Et_2O . Residual solvent was evaporated under reduced pressure (0.4 torr) at 40°C (692 mg, 1.90 mmol, yield 84%, m.p.:284-285°C).

^1H NMR (500MHz, $\text{DMSO}-d_6$) δ [ppm]: 8.73-8.70 (m, 2H), 8.64 (d, $J=1.9\text{Hz}$, 1H), 8.31 (d, $J=6.9\text{Hz}$, 1H), 8.20 (dd, $J=9.2\text{Hz}$, $J=2.0\text{Hz}$, 1H), 4.37 (s, 3H), 3.20 (s, 3H).

Synthesis of (*E*)-2-(3-hydroxypropyl)-1-(2-(quinolin-4-yl)vinyl)-isoquinolinium bromide (**23**)

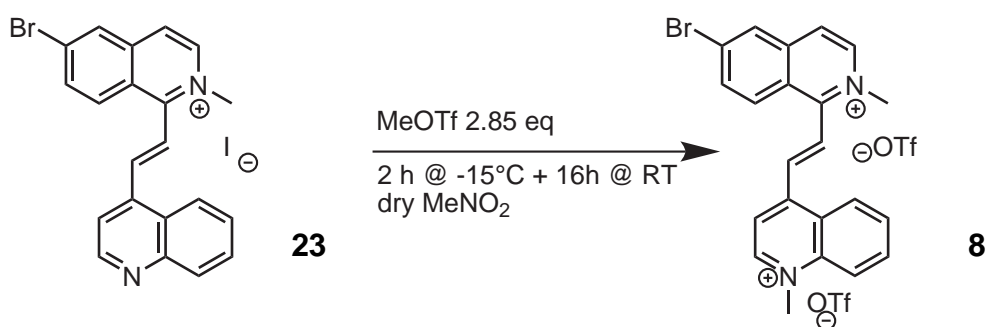


To a mixture of **22** (600 mg, 1.648 mmol) and quinoline-4-carboxaldehyde (310 mg, 1.978 mmol), a solution of piperidine (169 mg, 1.98 mmol) in 2 ml of MeOH was added. The mixture was heated to reflux for 10 min obtaining a solid. The mixture was allowed to cool to room temperature and sonicated with acetone obtaining a yellow solid. Product was filtered on an Hirsh funnel and washed with acetone and Et_2O . Residual solvent was removed under reduced

pressure at 50°C. Product was recovered as a yellow solid (621 mg, 1.23mmol, yield 75%, m.p.: 220°C (dec.)).

^1H NMR (500MHz, DMSO- d_6) δ [ppm]: 9.12 (d, $J=4.5\text{Hz}$, 1H), 8.88 (d, $J=6.9\text{Hz}$, 1H), 8.74 (d, $J=1.9\text{Hz}$, 1H), 8.60 (d, $J=9.2\text{Hz}$, 1H), 8.49 (d, $J=6.9\text{Hz}$, 1H), 8.31 (d, $J=8.1\text{Hz}$, 1H), 8.27 (d, $J=16.4\text{Hz}$, 1H), 8.19 (dd, $J=9.2\text{Hz}$, $J=2.0\text{Hz}$, 1H), 8.17 (d, $J=4.5\text{Hz}$, 1H), 8.15 (d, $J=8.1\text{Hz}$, 1H), 8.04 (d, $J=16.3\text{Hz}$, 1H), 7.87 (d, $J=7.7\text{Hz}$, 1H), 7.71 (t, $J=7.6\text{Hz}$, 1H), 4.45 (s, 3H).

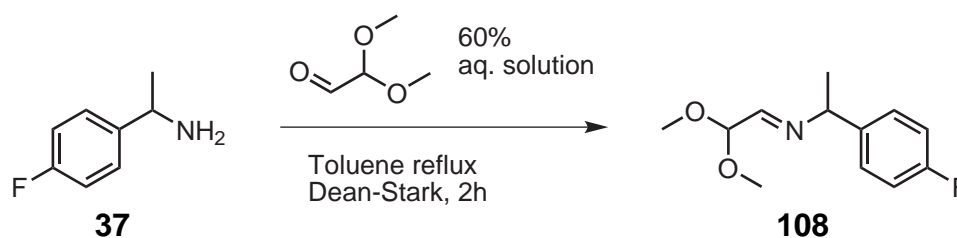
Synthesis of (*E*)-4-(2-(6-bromo-2-methylisoquinolinium-1-yl)vinyl)-1-methylquinolinium trifluoromethanesulfonate (**8**)



Under N_2 atmosphere, MeOTf (196 mg, 1.192mmol) was added to a stirred suspension of **23** (200 mg, 0.398mmol) in dry MeNO_2 (2 ml) cooled to -15°C with an ice/salt bath. The mixture was kept under stirring at -15°C for 2h obtaining a clear pale yellow solution, and stirred overnight at room temperature. Product was precipitated as a white solid after addition of Et_2O (4 ml), collected by filtration on an Hirsh funnel, and dried in vacuum (174 mg, 0.252mmol, yield 63%, m.p.: 162-163°C).

^1H NMR (500MHz, DMSO- d_6) δ [ppm]: 9.68 (d, $J=6.2\text{Hz}$, 1H), 8.93 (d, $J=6.9\text{Hz}$, 1H), 8.79-8.77 (m, 2H), 8.68 (d, $J=8.5\text{Hz}$, 1H), 8.62-8.58 (m, 2H), 8.56 (d, $J=6.9\text{Hz}$, 1H), 8.44 (d, $J=8.4\text{Hz}$, 1H), 8.38-8.32 (m, 2H), 8.23 (dd, $J=9.1\text{Hz}$, $J=1.8\text{Hz}$, 1H), 8.12 (t, $J=7.6\text{Hz}$, 1H), 4.71 (s, 3H), 4.47 (s, 3H); ^{13}C NMR (125.7MHz, DMSO- d_6) δ [ppm]: 156.59, 150.16, 150.08, 139.29, 138.96, 138.77, 137.80, 136.06, 135.14, 132.26, 131.89, 130.86, 130.50, 129.42, 127.48, 126.92, 126.32, 124.78, 120.40, 119.96, 47.68, 46.17. Anal. Calcd for $\text{C}_{24}\text{H}_{19}\text{BrF}_6\text{N}_2\text{O}_6\text{S}_2$: C, 41.81; H, 2.78; N, 4.06; S, 9.30. Found: C, 41.35; H, 3.03; N, 3.99; S, 9.20.

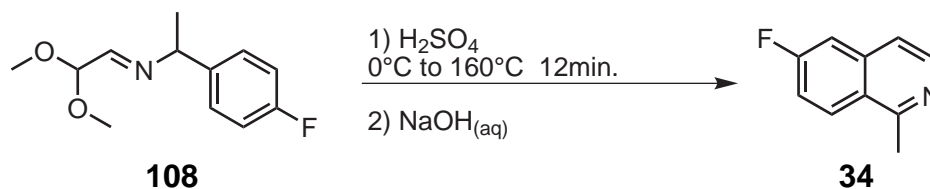
Synthesis of (*E*)-*N*-(2,2-dimethoxyethylidene)-1-(4-fluorophenyl)ethanamine (**108**)



A mixture of 1-(4-fluorophenyl)ethanamine (**37**) (5.000 g, 35.92 mmol) and dimethoxyacetaldehyde 60% w/w aqueous solution (6.856 g, 39.52 mmol) in 35 ml of toluene were refluxed for 2 h under nitrogen atmosphere, collecting water with a Dean-Stark apparatus. The mixture was cooled to room temperature and solvent was removed under reduced pressure (~ 1 mmHg) obtaining product as a yellow oil (7.66 g, 34.0 mmol, yield 95%).

^1H NMR (500 MHz, $\text{DMSO}-d_6$) δ [ppm]: 7.63 (d, $J=5.0$ Hz, 1H), 7.39-7.36 (m, 2H), 7.17-7.14 (m, 2H), 4.65 (d, $J=5.0$ Hz, 1H), 4.45 (q, $J=6.6$ Hz, 1H), 3.33 (s, 3H), 3.28 (s, 3H), 1.39 (d, $J=6.6$ Hz, 3H).

Synthesis of 6-fluoro-1-methylisoquinoline (**34**)

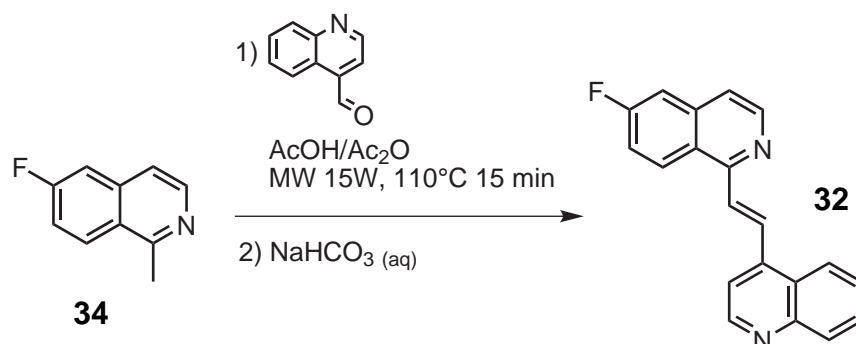


In a 500 ml RBF, **108** (7.600 g, 33.76 mmol) was slowly added, under stirring, to ice cooled H_2SO_4 (76 ml). The solution was heated to 160°C in 10 min and kept at that temperature for 2 min. The mixture was slowly poured in ice (400 g) and basified till pH 9 adding NaOH . The mixture was steam distilled till a clear distillate was obtained. The distillate was extracted with 4×200 ml of CH_2Cl_2 . The organic phase was collected, dried over Na_2SO_4 and evaporated under reduced pressure obtaining product as a colourless liquid (2.095 g, 13.00 mmol, yield 39%).

^1H NMR (500 MHz, CDCl_3) δ [ppm]: 8.37 (d, $J=5.8$ Hz, 1H), 8.12 (dd, $J=9.2$ Hz, $J=5.5$ Hz, 1H), 7.45 (d, $J=5.8$ Hz, 1H), 7.39 (dd, $J=9.3$ Hz, $J=2.5$ Hz, 1H), 7.33 (td, $J=8.7$ Hz, $J=2.5$ Hz, 1H), 2.94 (s, 3H); ^{13}C NMR (125.7 MHz, CDCl_3) δ [ppm]:

163.03 (d, $J=252.0$ Hz), 158.64, 142.92, 137.67 (d, $J=10.2$ Hz), 128.88 (d, $J=9.6$ Hz), 124.82, 119.10 (d, $J=4.9$ Hz), 117.39 (d, $J=25.0$ Hz), 110.52 (d, $J=20.5$ Hz), 22.64.

Synthesis of (*E*)-4-(2-(6-fluoroisoquinolin-1-yl)vinyl)quinoline (**32**)

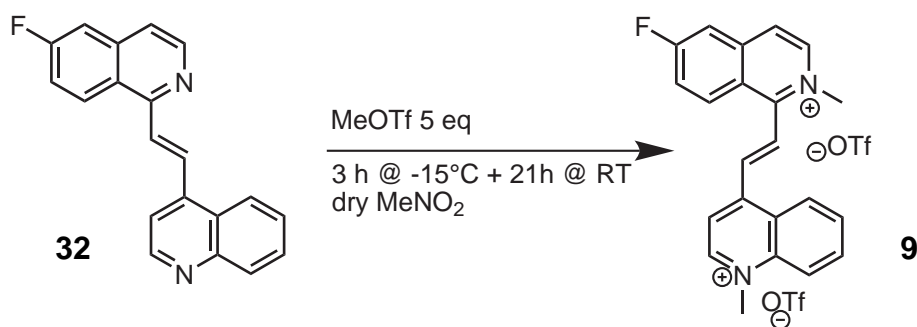


A suspension of **34** (200 mg, 1.24 mmol) and quinoline-4-carboxaldehyde (163 mg, 1.04 mmol) in a mixture of AcOH (0.5 ml) and Ac₂O (0.2 ml) was heated in a CEM discover microwave reactor for 15 min ($P_{\max}=15$ W, 110°C, cooling off). The solution was allowed to cool to RT observing the crystallization of a yellow solid which was recovered and dried on filter paper. Product was purified by crystallization from acetone/AcOH 20:1. The crystalline solid was suspended in 25 ml of a saturated NaHCO₃ aqueous solution for 30 min and extracted with 2 × 20 ml of CH₂Cl₂. The organic phase was collected, dried over Na₂SO₄ and evaporated under reduced pressure at 80°C obtaining product as a white solid (138 mg, 0.459 mmol, yield 37%, m.p.: 170-171°C).

¹H NMR (500 MHz, CDCl₃) δ [ppm]: 8.98 (d, $J=4.6$ Hz, 1H), 8.76 (d, $J=15.3$ Hz, 1H), 8.64 (d, $J=5.6$ Hz, 1H), 8.42 (dd, $J=9.3$ Hz, $J=5.3$ Hz, 1H), 8.38 (d, $J=8.3$ Hz, 1H), 8.22 (d, $J=8.4$ Hz, 1H), 8.16 (d, $J=15.3$ Hz, 1H), 7.81-7.77 (m, 2H), 7.66-7.63 (m, 2H), 7.49 (dd, $J=9.1$ Hz, $J=2.5$ Hz, 1H), 7.44 (td, $J=8.7$ Hz, $J=2.6$ Hz, 1H).
Anal. Calcd for C₂₀H₁₃FN₂: C, 79.98; H, 4.36; N, 9.33. Found: C, 80.06; H, 5.87; N, 9.22.

Synthesis of (*E*)-4-(2-(6-fluoro-2-methylisoquinolinium-1-yl)vinyl)-1-methylquinolinium trifluoromethanesulfonate (**9**)

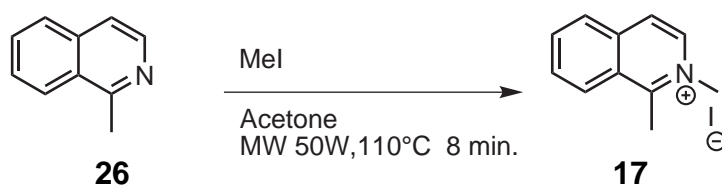
Under N₂ atmosphere, MeOTf (222 mg, 1.35 mmol) was added to a stirred suspension of **32** (80 mg, 0.266 mmol) in dry MeNO₂ (2 ml) cooled to -15°C with an ice/salt bath. The mixture was kept under stirring at -15°C for 3 h obtaining



a clear solution, and stirred for 21 h at room temperature. Product was precipitated as a pale yellow solid after addition of Et₂O (10 ml), collected by filtration on an Hirsh funnel, and dried in vacuum (120 mg, 0.191 mmol, yield 72%, m.p.: 224.4-225.5 °C).

¹H NMR (500 MHz, DMSO-d₆) δ [ppm]: 9.68 (d, *J*=6.2 Hz, 1H), 8.91 (d, *J*=6.9 Hz, 1H), 8.81 (dd, *J*=9.4 Hz, *J*=5.2 Hz, 1H), 8.77 (d, *J*=6.2 Hz, 1H), 8.68 (d, *J*=8.5 Hz, 1H), 8.62-8.59 (m, 2H), 8.44 (d, *J*=16.3 Hz, 1H), 8.38-8.32 (m, 2H), 8.29 (dd, *J*=9.1 Hz, *J*=2.5 Hz, 1H), 8.12 (t, *J*=7.7 Hz, 1H), 8.03 (td, *J*=9.2 Hz, *J*=2.1 Hz, 1H), 4.72 (s, 3H), 4.47 (s, 3H); ¹³C NMR (125.7 MHz, DMSO-d₆) δ [ppm]: 166.44 (d, *J*=260.0 Hz), 156.17, 150.233, 150.09, 140.51 (d, *J*=12.9 Hz), 139.27, 138.41, 137.64, 136.05, 134.74 (d, *J*=11.0 Hz), 130.85, 129.59, 127.47, 126.94, 125.21 (d, *J*=4.9 Hz), 124.97, 122.45 (d, *J*=25.6 Hz), 120.40, 119.96, 112.37 (d, *J*=22.4 Hz), 47.50, 46.17; Anal. Calcd for C₂₄H₁₉F₇N₂O₆S₃: C, 45.86; H, 3.05; N, 4.46. Found: C, 44.90; H, 2.75; N, 4.61. Anal. Calcd for C₂₄H₁₉F₇N₂O₆S₂: C, 45.86; H, 3.05; N, 4.46; S, 10.2. Found: C, 46.63; H, 3.41; N, 4.66; S, 11.23.

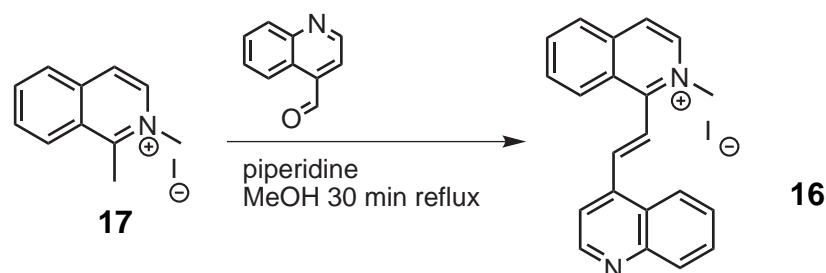
Synthesis of 1,2-dimethyloquinolinium iodide (17)



A mixture of **26** (5.00 g, 34.9 mmol), MeI (5.95 g, 41.9 mmol) and 7 ml of acetone was heated in a CEM Discover microwave reactor for 8 min ($P_{\text{max}}=50 \text{ W}$, 110 °C, cooling off, 35 ml vessel), and cooled to RT. The white solid product was washed with acetone and filtered on a Büchner funnel, washing with more acetone and then with Et₂O. Residual solvent was evaporated under reduced pressure (0.4 torr) at 40 °C (8.72 g, 30.6 mmol, yield 88%, m.p.: 210-211 °C).

^1H NMR (500MHz, $\text{DMSO}-d_6$) δ [ppm]: 8.79 (d, $J=8.7\text{Hz}$, 1H), 8.70 (d, $J=6.9\text{Hz}$, 1H), 8.40 (d, $J=6.9\text{Hz}$, 1H), 8.31 (d, $J=8.1\text{Hz}$, 1H), 8.22 (t, $J=7.7\text{Hz}$, 1H), 8.05 (t, $J=7.7\text{Hz}$, 1H), 4.40 (s, 3H), 3.22 (s, 3H).

Synthesis of (*E*)-2-methyl-1-(2-(quinolin-4-yl)vinyl)isoquinolinium iodide (**16**)

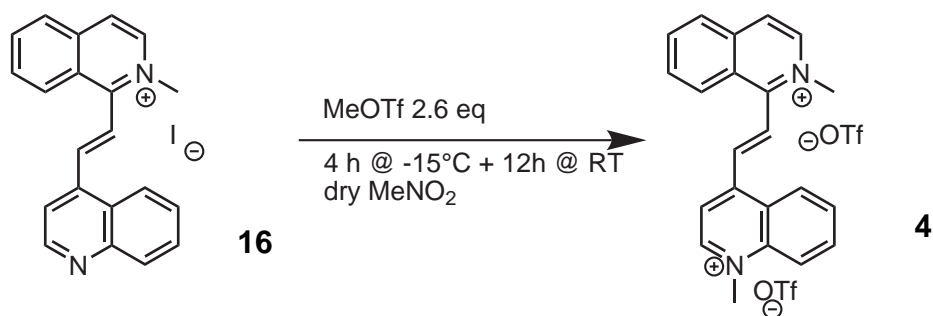


To a mixture of **17** (5.000 g, 17.53 mmol) and quinoline-4-carboxaldehyde (3.113 g, 19.80 mmol), a solution of piperidine (0.50 ml, 430 mg, 5.0 mmol) in 10 ml of MeOH was added. The mixture was heated to reflux for 30 min obtaining a solid. The mixture was allowed to cool to room temperature and 25 ml of MeOH were added. The solid was filtered on an Hirsh funnel and washed with MeOH and Et_2O . Residual solvent was removed under reduced pressure at 50°C . Product was recovered as a pale yellow solid (6.165 g, 14.53 mmol, yield 83%, m.p.: $217\text{-}218^\circ\text{C}$ (dec.)).

^1H NMR (500MHz, $\text{DMSO}-d_6$) δ [ppm]: 9.12 (d, $J=4.5\text{Hz}$, 1H), 8.87 (d, $J=6.9\text{Hz}$, 1H), 8.69 (d, $J=8.7\text{Hz}$, 1H), 8.60 (d, $J=6.8\text{Hz}$, 1H), 8.41 (d, $J=8.2\text{Hz}$, 1H), 8.33 (d, $J=8.2\text{Hz}$, 1H), 8.31-8.27 (m, 2H), 8.18 (d, $J=4.5\text{Hz}$, 1H), 8.15 (d, $J=8.1\text{Hz}$, 1H), 8.10-8.04 (m, 2H), 7.87 (t, $J=7.7\text{Hz}$, 1H), 7.71 (t, $J=7.6\text{Hz}$, 1H), 4.50 (s, 3H). ^{13}C NMR (125.7MHz, $\text{DMSO}-d_6$) δ [ppm]: 157.15, 150.97, 148.73, 140.13, 140.02, 137.85, 137.22, 136.62, 131.88, 130.38, 130.18, 130.14, 128.20, 127.88, 127.52, 126.01, 125.13, 124.42, 123.80, 119.03, 47.41.

Synthesis of (*E*)-1-methyl-4-(2-(2-methylisoquinolinium-1-yl)vinyl)quinolinium trifluoromethanesulfonate (**4**)

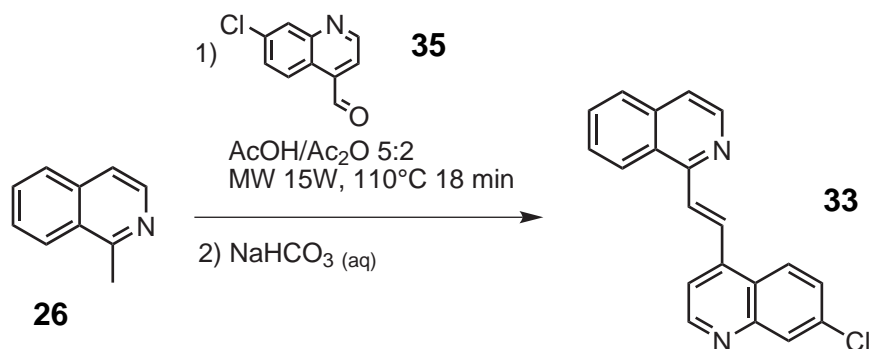
Under N_2 atmosphere, MeOTf (200 mg, 1.219 mmol) was added to a stirred suspension of **16** (200 mg, 0.471 mmol) in dry MeNO_2 (7 ml) cooled to -15°C with an ice/salt bath. The mixture was kept under stirring at -15°C for 4 h obtaining



a clear pale yellow solution, and stirred overnight at room temperature. Product was precipitated as a pale yellow solid after addition of Et₂O, collected by filtration on an Hirsh funnel, and dried in vacuum (280 mg, 0.458 mmol, yield 97%).

¹H NMR (500 MHz, DMSO-d₆) δ [ppm]: 9.68 (d, *J*=6.3 Hz, 1H), 8.92 (d, *J*=6.9 Hz, 1H), 8.78 (d, *J*=6.2 Hz, 1H), 8.71-8.66 (m, 3H), 8.62 (d, *J*=8.9 Hz, 1H), 8.47-8.43 (m, 2H), 8.38-8.30 (m, 3H), 8.13-8.09 (m, 2H), 4.72 (s, 3H), 4.30 (s, 3H); ¹³C NMR (125.7 MHz, DMSO-d₆) δ [ppm]: 156.02, 150.22, 149.97, 139.17, 137.91, 137.42, 137.27, 136.86, 135.93, 132.00, 130.74, 130.03, 129.63, 128.27, 127.37, 127.33, 126.83, 125.77, 120.28, 119.83, 47.46, 46.04; Anal. Calcd for C₂₄H₂₀F₆N₂O₆S₂ : C, 47.21; H, 3.30; N, 4.59; S, 10.50. Found: C, 47.30; H, 3.72; N, 4.61; S, 10.44.

Synthesis of (*E*)-7-chloro-4-(2-(isoquinolin-1-yl)vinyl)quinoline (33)

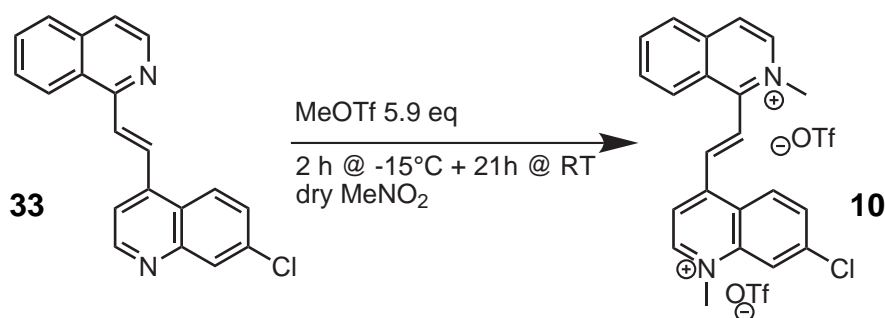


A suspension of **26** (374 mg, 2.61 mmol) and **35** (500 mg, 2.61 mmol) in 2 ml of a 5:2 AcOH/Ac₂O mixture was heated in a CEM discover microwave reactor for 18 min (*P*_{max}=15 W, 110°C, cooling off). The solution was allowed to cool to RT observing the crystallization of a yellow solid which was suspended in 30 ml of water and filtered on an Hirsh funnel. Product was purified by crystallization from acetone/AcOH 19:1. The crystalline solid was suspended in 100 ml

of 10% NaHCO₃ aqueous solution for 30 min and extracted with 3 × 50 ml of CH₂Cl₂. The organic phase was collected, dried over Na₂SO₄ and evaporated under reduced pressure obtaining product as a white solid. Product was kept for 1 day in a desiccator to remove residual water (467 mg, 1.474 mmol, yield 56%, m.p.: 163-164 °C).

¹H NMR (500 MHz, CDCl₃) δ [ppm]: 8.97 (d, *J*=4.6 Hz, 1H), 8.71 (d, *J*=15.4 Hz, 1H), 8.65 (d, *J*=5.6 Hz, 1H), 8.38 (d, *J*=8.5 Hz, 1H), 8.33 (d, *J*=9.0 Hz, 1H), 8.22 (d, *J*=15.3 Hz, 1H), 8.17 (d, *J*=2.1 Hz, 1H), 7.90 (d, *J*=8.2 Hz, 1H), 7.76-7.73 (m, 2H), 7.70-7.67 (m, 2H), 7.57 (dd, *J*=9.0 Hz, *J*=2.1 Hz, 1H).

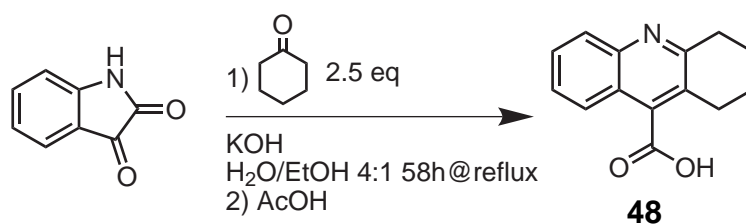
Synthesis of (*E*)-7-chloro-1-methyl-4-(2-(2-methylisoquinolinium-1-yl)vinyl)quinolinium trifluoromethanesulfonate (10)



Under N₂ atmosphere, MeOTf (310 mg, 1.89 mmol) was added to a stirred suspension of **33** (100 mg, 0.316 mmol) in dry MeNO₂ (2 ml) cooled to -15 °C with an ice/salt bath. The mixture was kept under stirring at -15 °C for 2 h obtaining a clear solution, and stirred for 21 h at room temperature. Product was precipitated after addition of Et₂O (5 ml) and acetone (1 ml), collected by filtration on an Hirsh funnel, and dried in vacuum. Product was purified by crystallization from EtOH (89 mg, 0.138 mmol, yield 44%, m.p.: 159.5-159.9 °C). ¹H NMR (500 MHz, DMSO-*d*₆) δ [ppm]: 9.68 (d, *J*=6.3 Hz, 1H), 8.91 (d, *J*=6.8 Hz, 1H), 8.79-8.78 (m, 2H), 8.71 (d, *J*=9.2 Hz, 1H), 8.67-8.66 (m, 2H), 8.45-8.41 (m, 2H), 8.36 (d, *J*=16.3 Hz, 1H), 8.32 (t, *J*=7.7 Hz, 1H), 8.20 (dd, *J*=9.2 Hz, *J*=1.9 Hz, 1H), 8.09 (t, *J*=7.3 Hz, 1H), 4.70 (s, 3H), 4.49 (s, 3H); Anal. Calcd for C₂₄H₁₉F₆N₂O₆S₂Cl : C, 44.69; H, 2.97; N, 4.34. Found: C, 44.89; H, 3.06; N, 4.41.

Synthesis of 1,2,3,4-tetrahydroacridine-9-carboxylic acid (48)

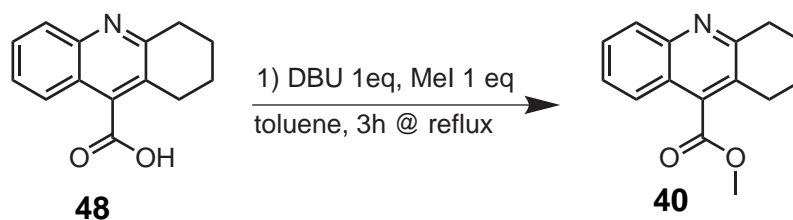
A solution of KOH (63.0 g, 1.12 mol) in EtOH/H₂O 1:4 (200 ml) was slowly added under stirring to a mixture of isatin (50.00 g, 339.8 mmol) and cyclohex-



anone (84.00 g, 849.6 mmol). The obtained deep red solution was heated to reflux observing a colour change to pale yellow after 30 min with the formation of a biphasic mixture. After refluxing for 58 h, water (200 ml) was added followed by AcOH till pH 4 observing the formation of a white precipitate. The mixture was stirred for 20 min, and the filtrate was collected by filtration on a Büchner funnel washing with water 200 ml, MeOH (200 ml) and Et₂O (50 ml). Residual solvent was evaporated under reduced pressure at 60 °C for 2 days and the solid was further dried in a desiccator over P₂O₅ for 3 days (64.13 g, 295.2 mmol, yield 87%, m.p.: >300 °C)

¹H NMR (500 MHz, DMSO-d₆) δ [ppm]: 7.93 (d, *J*=8.4 Hz, 1H), 7.72-7.69 (m, 2H), 7.57 (t, *J*=7.6 Hz, 1H), 3.18 (s, 2H), 3.06 (t, *J*=6.6 Hz, 2H), 2.90 (t, *J*=6.4 Hz, 2H), 1.94-1.89 (m, 2H), 1.87-1.82 (m, 2H).

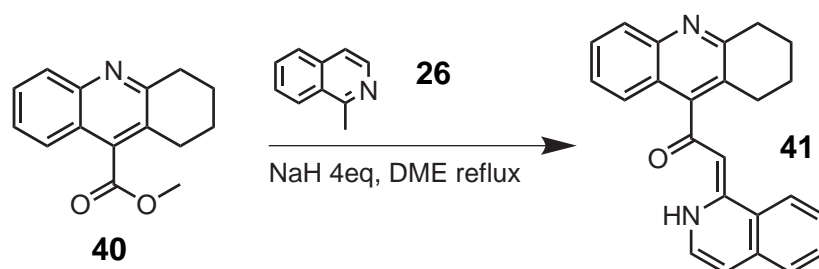
Synthesis of methyl 1,2,3,4-tetrahydroacridine-9-carboxylate (40)



To a stirred suspension of **48** (10.00 g, 44.00 mmol) and DBU (6.698 g, 44.00 mmol) in toluene (75 ml), MeI (6.245 g, 44.00 mmol) was added; the mixture was stirred at RT for 20 min and then heated to reflux for 3 h. The change in solution colour to yellow and the formation of a white precipitate were observed. The mixture was cooled to RT and filtered washing with 30 ml of toluene. The filtrate was collected, and solvent was evaporated under reduced pressure obtaining product as a pale yellow solid (8.988 g, 37.25 mmol, yield 85%, m.p.: 68-70 °C).

¹H NMR (500 MHz, CDCl₃) δ [ppm]: 8.05 (d, *J*=8.5 Hz, 1H), 7.67-7.64 (m, 2H), 7.49 (t, *J*=7.5 Hz, 1H), 4.05 (s, 3H), 3.18 (t, *J*=6.6 Hz, 2H), 2.93 (t, *J*=6.4 Hz, 2H), 2.01-1.96 (m, 2H), 1.92-1.88 (m, 2H).

Synthesis of (Z)-2-(isoquinolin-1(2H)-ylidene)-1-(1,2,3,4-tetrahydroacridin-9-yl)ethanone (41)



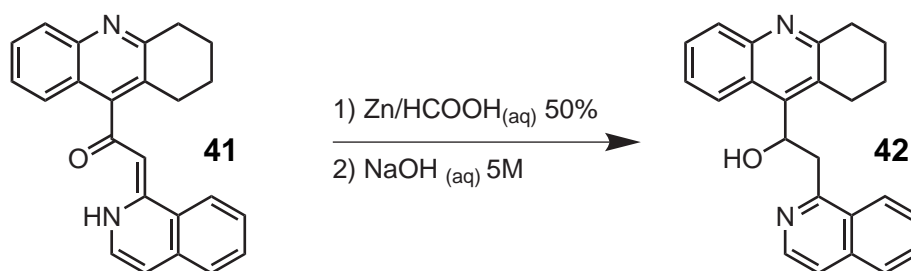
Under N₂ atmosphere, in an oven dried 250ml 3-necked RBF, fitted with reflux condenser, septum and dropping funnel, a suspension of NaH* (828g, 20.72mmol) in anhydrous DME (10ml) was prepared. A solution of freshly distilled **26** (742mg, 5.18mmol) and **40** (1.500g, 6.22mmol) in 20ml of anhydrous DME was drop wise added to the refluxing suspension of NaH. The suspension was refluxed for a total of 46h observing the formation of a bright yellow solution. The mixture was cooled with an ice-water bath, and AcOH (2.50g) was added followed by 20ml of water. A yellow solid precipitated and was filtered on a Büchner funnel washing with H₂O (50ml). Product was dried in a desiccator for 3 days and crystallized from DMF (950mg, 2.70mmol, yield 52%, m.p.: 240 °C (dec)).

¹H NMR (500MHz, CDCl₃) δ [ppm]: 15.96 (s, 1H), 8.09 (d, *J*=6.8Hz, 1H); 8.03 (d, *J*=8.4Hz, 1H), 7.94 (d, *J*=8.3Hz, 1H), 7.71 (t, *J*=7.1Hz, 1H), 7.66-7.62 (m, 2H), 7.51-7.48 (m, 2H), 7.42 (t, *J*=7.4Hz, 1H), 6.97 (d, *J*=6.8Hz, 1H), 6.20 (s, 1H), 3.24 (t, *J*=6.3Hz, 2H), 3.16-2.94 (m, 2H), 2.00 (qui, *J*=6.0Hz, 2H), 1.96-1.79 (m, 2H).

Synthesis of 2-(isoquinolin-1-yl)-1-(1,2,3,4-tetrahydroacridin-9-yl)-ethanol (42)

To a stirred mixture of **41** (900mg, 2.553mmol) and Zn (501mg, 7.661mmol), aqueous formic acid 50% (50ml) was added. The solution rapidly changed its colour from orange to pale green. The mixture was kept under stirring for 20min and filtered collecting the filtrate in an ice-cooled stirred 5M NaOH solution (150ml). A white solid separated, and the mixture was kept under stirring

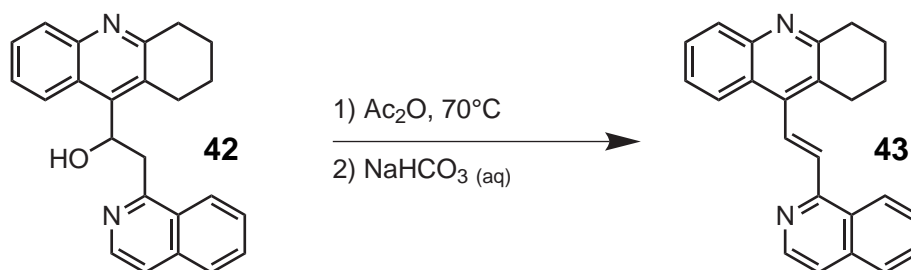
*NaH dispersion in paraffin was used. The reagent was carefully washed with ETP before solvent addition



for 15 min. The suspension was filtered on a Büchner funnel and washed with 50 ml of 5 M NaOH solution followed by 100 ml of deionized water. The white solid was dried in a desiccator for 2 days (256 mg, 0.722 mmol, yield 28%, m.p.: 80 °C (dec.)).

¹H NMR (500 MHz, CDCl₃) δ [ppm]: 8.90 (broad s, 1H), 8.51 (d, $J=5.8$ Hz, 1H), 8.02 (d, $J=8.3$ Hz, 1H), 7.96 (d, $J=8.5$ Hz, 1H), 7.87 (d, $J=8.2$ Hz, 1H), 7.71 (t, $J=7.6$ Hz, 1H), 7.65 (d, $J=5.8$ Hz, 1H), 7.62 (td, $J=8.3$ Hz, $J=1.1$ Hz, 1H), 7.56 (t, $J=7.7$ Hz, 1H), 7.44 (td, $J=7.1$ Hz, 1.4 Hz, 1H), 6.45 (d, $J=10.1$ Hz, 1H), 4.13-4.08 (m, 1H), 3.57 (dd, $J=17.4$ Hz, $J=2.0$ Hz, 1H), 3.23 (t, $J=6.4$ Hz, 1H), 3.17 (t, $J=6.4$ Hz, 2H), 1.97-1.85 (m, 6H).

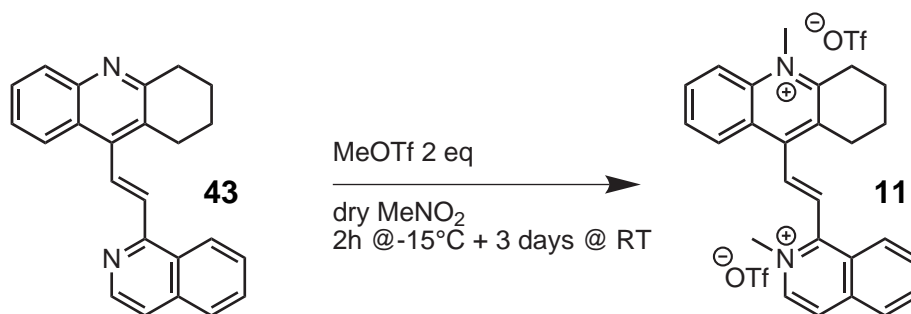
Synthesis of (*E*)-9-(2-(isoquinolin-1-yl)vinyl)-1,2,3,4-tetrahydroacridine (43)



A suspension of **42** (200 mg, 0.564 mmol) in Ac₂O (2 ml) was heated to 60 °C in a CEM Discover Microwave reactor ($P_{\max}=15$ W, cooling off) for 3 h. The formation of a white precipitate was observed. The mixture was poured in a saturated NaHCO₃ solution, stirred for 20 min, and extracted with 3 \times 25 ml of CH₂Cl₂. The organic phase was collected, washed with brine, dried over Na₂SO₄ and evaporated under reduced pressure. The obtained brown solid was sonicated with few ml of *i*-PrOH and filtered on an Hirsh funnel washing with few ml of Et₂O. Residual solvent was evaporated under reduced pressure at 50 °C (123 mg, 0.366 mmol, yield 65%. m.p.: 123.4-124.6 °C).

^1H NMR (500 MHz, CDCl_3) δ [ppm]: 8.65 (d, $J=5.6$ Hz, 1H), 8.27-8.21 (m, 3H), 7.89 (d, $J=8.2$ Hz, 1H), 7.78 (d, $J=15.9$ Hz, 1H), 7.73-7.67 (m, 3H), 7.62 (t, $J=7.6$ Hz, 1H), 7.49 (t, 7.4 Hz, 1H), 3.27 (broad s, 2H), 3.07 (t, $J=6.3$ Hz, 2H), 2.04-1.97 (m, 2H), 1.95-1.90 (m, 2H).

Synthesis of (E)-10-methyl-9-(2-(2-methylisoquinolinium-1-yl)-vinyl)-1,2,3,4-tetrahydroacridinium trifluoromethanesulfonate (11)

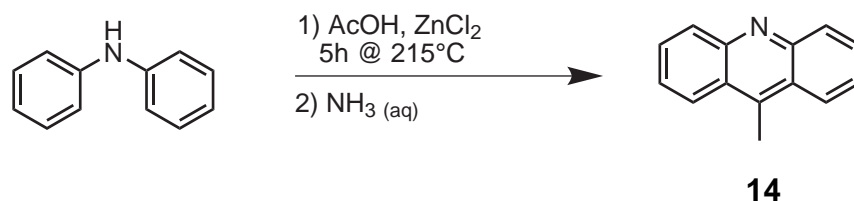


Under N_2 atmosphere, MeOTf (97 mg, 0.59 mmol) was added to an ice-cooled stirred suspension of **43** (100 mg, 0.297 mmol) in dry MeNO_2 (0.5 ml). The mixture was kept under stirring at -15°C for 2 h obtaining a clear solution. The mixture was allowed to warm to RT and kept under stirring for 3 days. Product was precipitated as a pale brown solid after addition of Et_2O (10 ml), collected by filtration on an Hirsh funnel and purified by crystallization from *i*-PrOH (20 mg, 0.030 mmol, yield 10%, m.p.: 155.2 - 156.7°C)

^1H NMR (500 MHz, CD_3CN) δ [ppm]: 8.79 (d, $J=8.6$ Hz, 1H), 8.56 (d, $J=8.4$ Hz, 1H), 8.52-8.48 (m, 2H), 8.44 (d, $J=6.7$ Hz, 1H), 8.37 (d, $J=8.2$ Hz, 1H), 8.30 (t, $J=7.9$ Hz, 1H), 8.23 (t, $J=8.1$ Hz, 1H), 8.14 (t, $J=7.6$ Hz, 1H), 8.02 (t, $J=7.6$ Hz, 1H), 7.76 (d, $J=17.0$ Hz, 1H), 7.49 (d, $J=17.0$ Hz, 1H), 4.48 (s, 3H), 4.40 (s, 3H), 3.45 (t, $J=6.3$ Hz, 2H), 3.20 (t, $J=6.3$ Hz, 2H), 2.14-2.08 (m, 4H); ^{13}C NMR (125.7 MHz, CD_3CN) δ [ppm]: 160.74, 155.66, 149.74, 138.96, 138.90, 138.28, 136.80, 136.58, 134.73, 132.37, 132.04, 129.69, 129.51, 128.79, 128.22, 127.50, 127.30, 126.04, 125.76, 119.07, 47.38, 39.36, 31.17, 28.30, 21.10, 20.51; Anal. Calcd for $\text{C}_{28}\text{H}_{26}\text{F}_6\text{N}_2\text{O}_6\text{S}_2$: C, 50.60; H, 3.94; N, 4.21. Found: C, 51.05; H, 3.77; N, 4.20.

Synthesis of 9-methylacridine (14)

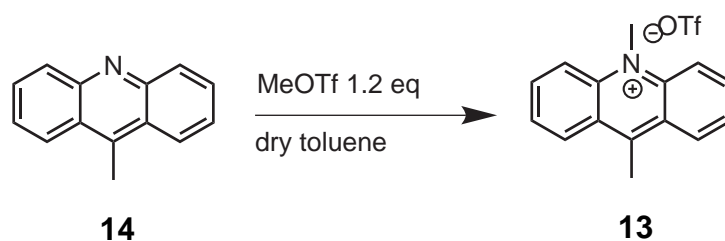
In a 1L 2-necked RBF, equipped with still head and condenser, a mixture of diphenylamine (30.00 g, 177.3 mmol), ZnCl_2 (126.2 g, 925.9 mmol) and AcOH



(29.57 g, 492.5 mmol) was heated to 215 °C, slowly distilling off the excess of acetic acid. The mixture was kept at 215 °C for 5 h and allowed to cool to room temperature rotating the flask to spread the material inside it. The black solid glassy material was sonicated with NH₃(aq) 33% until a brown powdery solid was obtained. The precipitate was collected by filtration, washed with NH₃(aq) 33% and transferred in a flask containing 500 ml of CH₂Cl₂. The mixture was stirred for 15 min, filtered to eliminate the insoluble material and washed with 5 × 50 ml of saturated NaHCO₃ aqueous solution. The organic phase was collected, dried over Na₂SO₄ and evaporated under reduced pressure. The obtained solid material was crystallized 3 times from EtOH/water 1:1 removing the black oil which separated at the beginning by hot filtration, and cooling the mixture to -18 °C. Product was recovered by filtration as pale yellow needles, and dried in a desiccator for 3 days (18.63 g, 96.4 mmol, yield 54%, m.p.: 115-116 °C).

¹H NMR (500 MHz, DMSO-d₆) δ [ppm]: 8.39 (d, *J*=9.1 Hz, 2H), 8.14 (d, *J*=8.6 Hz, 2H), 7.84 (t, *J*=7.6 Hz, 2H), 7.63 (t, *J*=7.2 Hz, 2H), 3.13 (s, 3H).

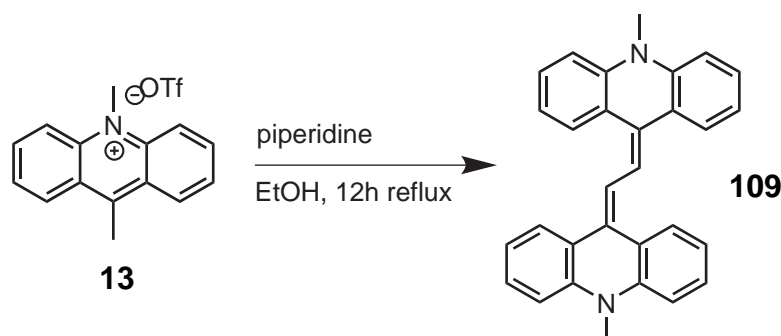
Synthesis of 9,10-dimethylacridinium (13)



Methyltrifluoromethane sulphonate (5.095 g, 31.05 mmol) was added drop wise to a solution of **13** (4.000 g, 20.70 mmol) in 30 ml of dry toluene. Colour turned from pale yellow to greenish yellow and a yellow precipitate was formed. After 24 h stirring at room temperature, the suspension was filtered under reduced pressure to give product **13** as a yellow powder (5.120 g, 14.33 mmol, 69%).

^1H NMR (200MHz, DMSO- d_6) δ [ppm]: 8.92 (d, $J=8.5\text{Hz}$, 2H), 8.75 (d, $J=8.7\text{Hz}$, 2H), 8.42 (t, $J=7.8\text{Hz}$, 2H), 8.02 (t, $J=7.1\text{Hz}$, 2H), 4.81 (s, 3H), 3.50 (s, 3H).

Synthesis of 1,2-bis(10-methylacridin-9(10H)-ylidene)ethane (**109**)

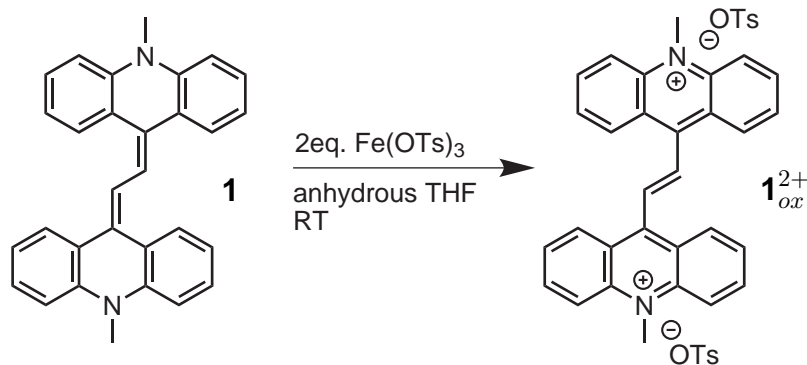


A suspension of derivative **13** (6.454g, 18.00mmol) in EtOH (100ml) was heated at the reflux temperature till complete dissolution of the suspended material was achieved. Piperidine (6ml) was added drop wise to the refluxing solution observing a gradual turning of the color from yellow to deep red. After a total 12h at the reflux temperature the red suspension was cooled to room temperature and the red precipitate was filtered off under reduced pressure. The crude product was dissolved in 70ml of toluene and filtered through a short silica plug. The filtrate was collected and the solvent was removed under reduced pressure obtaining product **109** as a red crystalline solid (1.561g, 3.77mmol, 42%).

^1H NMR (500MHz, C_6D_6) δ [ppm]: 8.18 (dd, $J=7.7\text{Hz}$, $J=1.4\text{Hz}$, 2H), 7.88 (dd, $J=7.7\text{Hz}$, $J=1.2\text{Hz}$, 2H), 7.50 (s, 2H), 7.29-7.26 (m, 2H), 7.19-7.14 (m, 4H), 7.01 (t, $J=7.8\text{Hz}$, 2H), 6.74 (d, $J=8.3\text{Hz}$, 2H), 6.66 (d, $J=8.2\text{Hz}$, 2H), 2.86 (s, 6H); ^{13}C NMR (125.7MHz, C_6D_6) δ [ppm]: 142.83, 141.16, 132.03, 129.19, 128.24, 127.40, 124.71, 123.54, 122.02, 121.47, 120.34, 112.67, 112.60, 32.92; Anal. Calcd for $\text{C}_{30}\text{H}_{24}\text{N}_2 \cdot 2\text{H}_2\text{O}$: C, 80.33; H, 6.29; N, 6.25. Found: C, 80.27; H, 5.75; N, 6.82.

Chemical oxidation of 1,2-bis(10-methylacridin-9(10H)-ylidene)ethane (**1_{ox}²⁺**)

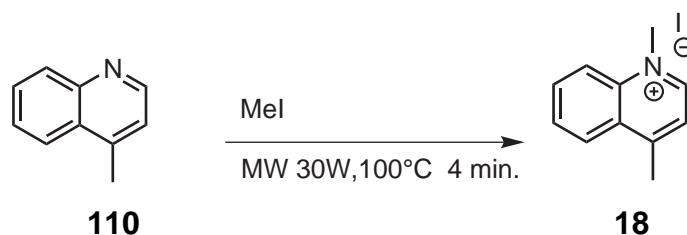
Under N_2 atmosphere, a solution of $\text{Fe}(\text{OTf})_3$ (276mg, 0.485mmol) in 5ml of anhydrous THF were dropwise added to a solution of **1** (100mg, 0.424mmol) in the same solvent. The solution immediately turned orange and the formation



of a precipitate was observed after 10 min. The mixture was stirred for 2 h. The precipitate was collected by filtration and washed with THF. Residual solvent was evaporated under reduced pressure obtaining product as a yellow solid (20 mg, 0.026 mmol, yield 6%)

$^1\text{H NMR}$ (500 MHz, DMSO-d_6) δ [ppm]: 8.95 (m, 8H), 8.53 (m, 6H), 8.05 (m, 4H), 7.43 (d, $J=7.9$ Hz, 4H), 7.10 (d, $J=7.9$ Hz, 4H), 4.98 (s, 6H), 2.25 (s, 6H).

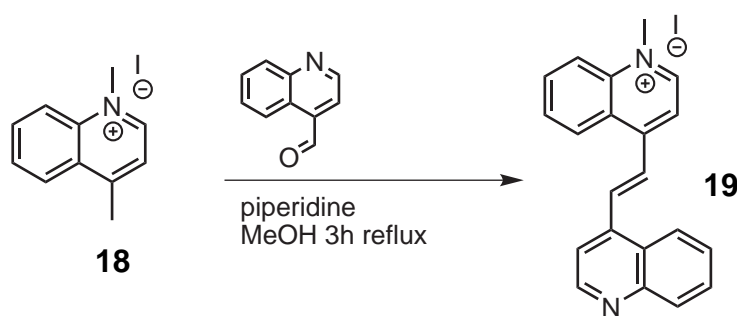
Synthesis of 1,4-dimethylquinolinium iodide (**18**)



A mixture of **110** (1.000 g, 6.98 mmol), MeI (3.960 g, 27.9 mmol) was heated in a CEM Discover microwave reactor for 4 min ($P_{\text{max}}=30$ W, 100°C , cooling off), and cooled to RT. The pale yellow solid product was washed with toluene and filtered on a Büchner funnel, washing with more toluene and then with Et_2O . Residual solvent was evaporated under reduced pressure (0.4 torr) at 40°C (1.783 g, 6.25 mmol, yield 90%, m.p.: $176\text{--}177^\circ\text{C}$).

Synthesis of (*E*)-1-methyl-4-(2-(quinolin-4-yl)vinyl)quinolinium iodide (**19**)

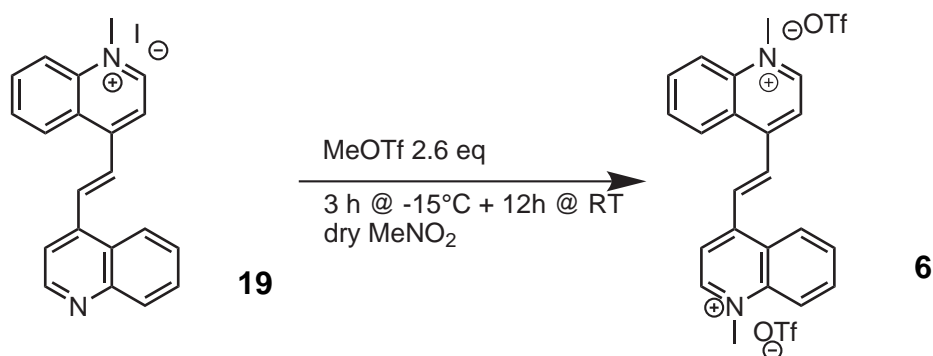
A mixture of **18** (1.200 g, 4.21 mmol) and quinoline-4-carboxyaldehyde (728 mg, 4.631 mmol) in MeOH (5 ml) was heated to reflux, and piperidine (2 drops) was added. The mixture was heated to reflux for 1 h obtaining a red solution. The



mixture was allowed to cool to room temperature; the volume was reduced to 3 ml evaporating the solvent under reduced pressure and refluxed again for more 2h. The solution was cooled with an ice-water bath obtaining a precipitate which was filtered on an Hirsh funnel and washed with cold MeOH and Et₂O. Residual solvent was removed under reduced pressure at 50 °C. Product was recovered as an orange solid (336 mg, 0.792 mmol, yield 19%, m.p.: 227 °C (dec.)).

¹H NMR (500 MHz, DMSO-d₆) δ [ppm]: 9.53 (d, *J*=6.4 Hz, 1H), 9.10 (d, *J*=8.5 Hz, 1H), 9.07 (d, *J*=4.6 Hz, 1H), 8.90-8.87 (m, 2H), 8.69 (d, *J*=8.4 Hz, 1H), 8.65 (d, *J*=15.8 Hz, 1H), 8.53 (d, *J*=8.9 Hz, 1H), 8.35-8.31 (m, 2H), 8.14-8.10 (m, 2H), 7.87 (t, *J*=7.1 Hz, 1H), 7.77 (t, *J*=7.2 Hz, 1H), 4.64 (s, 3H).

Synthesis of (*E*)-4,4'-(ethene-1,2-diyl)bis(1-methylquinolinium) trifluoromethanesulfonate (**6**)

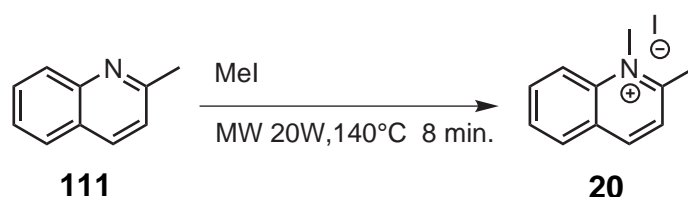


Under N₂ atmosphere, MeOTf (200 mg, 1.219 mmol) was added to a stirred suspension of **19** (200 mg, 0.471 mmol) in dry MeNO₂ (7 ml) cooled to -15 °C with an ice/salt bath. The mixture was kept under stirring at -15 °C for 3h and stirred overnight at room temperature. After a while a clear solution was obtained but later precipitation of a yellow solid was observed. More product

was precipitated after addition of Et₂O, collected by filtration on an Hirsh funnel, and dried in vacuum (250 mg, 0.409 mmol, yield 87%).

¹H NMR (500 MHz, DMSO-d₆) δ [ppm]: 9.64 (d, *J*=6.4 Hz, 2H), 9.14 (d, *J*=8.3 Hz, 2H), 8.99-8.98 (m, 4H), 8.60 (d, *J*=8.9 Hz, 2H), 8.38 (t, *J*=8.1 Hz, 2H), 8.19 (t, *J*=7.5 Hz, 2H), 4.69 (s, 6H); ¹³C NMR (125.7 MHz, DMSO-d₆) δ [ppm]: 150.58, 149.57, 139.32, 135.85, 133.19, 130.52, 127.43, 127.03, 120.24, 119.72, 45.89.

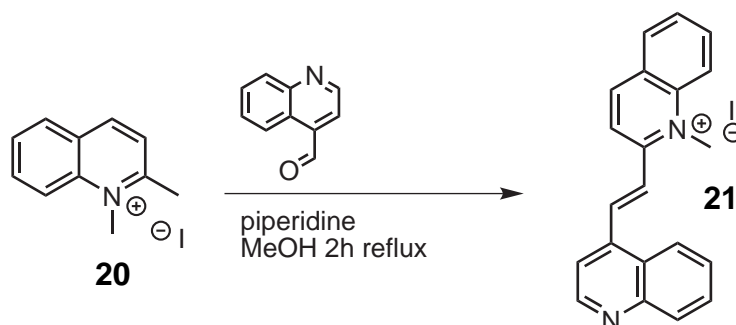
Synthesis of 1,2-dimethylquinolinium iodide (20)



A mixture of **111** (1.000 g, 6.98 mmol), MeI (3.960 g, 27.9 mmol) was heated in a CEM Discover microwave reactor for 8 min (P_{\max} =20 W, 140 °C, cooling off), and cooled to RT. The pale yellow solid product was washed with toluene and filtered on a Büchner funnel, washing with more toluene and then with Et₂O. Residual solvent was evaporated under reduced pressure (0.4 torr) at 40 °C (1.452 g, 5.09 mmol, yield 73%, m.p.: 197 °C (dec.)).

¹H NMR (500 MHz, DMSO-d₆) δ [ppm]: 9.10 (d, *J*=8.5 Hz, 1H), 8.60 (d, *J*=9.0 Hz, 1H), 8.40 (d, *J*=8.1 Hz, 1H), 8.24 (t, *J*=8.13 Hz, 1H), 8.12 (d, *J*=8.5 Hz, 1H), 8.00 (t, *J*=7.7, 1H), 4.45 (s, 3H), 3.08 (s, 3H).

Synthesis of (*E*)-1-methyl-2-(2-(quinolin-4-yl)viny)quinolinium iodide (21)

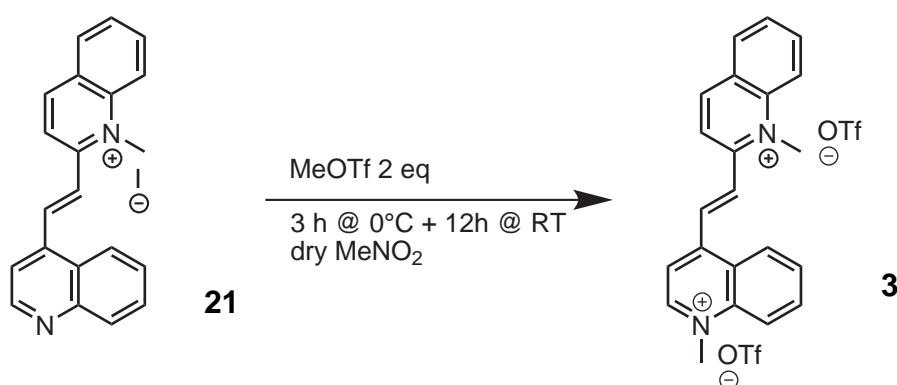


A mixture of **20** (1.200 g, 4.21 mmol), quinoline-4-carboxaldehyde (728 mg, 4.631 mmol) and piperidine (3 drops) in MeOH (8 ml) was heated to reflux for

2h. The solution was cooled with an ice-water bath obtaining a greenish precipitate which was filtered on an Hirsh funnel and washed with cold MeOH and Et₂O. Residual solvent was removed under reduced pressure (1.87 g, 2.56 mmol, yield 61%).

¹H NMR (500 MHz, DMSO-d₆) δ [ppm]: 9.27 (d, *J*=8.8 Hz, 1H), 9.10 (d, *J*=4.5 Hz, 1H), 8.91-8.86 (m, 2H), 8.68-8.66 (m, 2H), 8.47 (dd, *J*=8.1 Hz, *J*=1.2 Hz, 1H), 8.30-8.24 (m, 3H), 8.15 (d, *J*=8.4 Hz, 1H), 8.05 (t, *J*=7.6 Hz, 1H), 7.89 (t, *J*=7.7 Hz, 1H), 7.79 (t, *J*=7.6 Hz, 1H), 4.68 (s, 3H); ¹³C NMR (125.7 MHz, DMSO-d₆) δ [ppm]: 155.75, 150.93, 148.82, 145.55, 140.41, 139.97, 139.71, 135.88, 130.69, 130.48, 130.20, 130.04, 128.95, 127.95, 126.50, 125.95, 124.68, 122.85, 120.04, 119.46, 41.07.

Synthesis of (*E*)-1-methyl-4-(2-(1-methylquinolinium-2-yl)vinyl)-quinolinium trifluoromethanesulfonate (**3**)

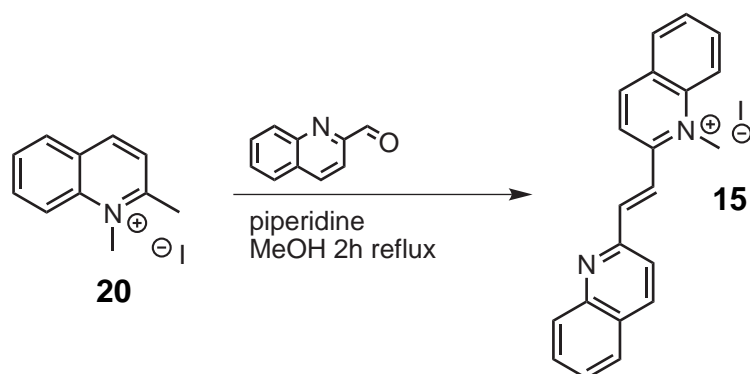


Under N₂ atmosphere, MeOTf (700 mg, 4.26 mmol) was added to a stirred suspension of **21** (900 mg, 2.12 mmol) in dry MeNO₂ (15 ml) cooled to 0°C with an ice bath. The mixture was kept under stirring at 0°C for 3h, and stirred overnight at room temperature. After a 15 min a clear solution was obtained but later precipitation of a yellow solid was observed. More product was precipitated after addition of Et₂O, collected by filtration on an Hirsh funnel, and dried in vacuum (1.137 g, 1.86 mmol, yield 88%, m.p.: 266-268 °C).

¹H NMR (500 MHz, CD₃CN) δ [ppm]: 9.22 (d, *J*=6.2 Hz, 1H), 9.18 (d, *J*=8.6 Hz, 1H), 8.77 (d, *J*=8.6 Hz, 1H), 8.58 (d, *J*=15.9 Hz, 1H), 8.53-8.45 (m, 4H), 8.43 (d, *J*=8.2 Hz, 1H), 8.38-8.30 (m, 2H), 8.22 (d, *J*=15.9 Hz, 1H), 8.16 (t, *J*=7.4 Hz, 1H), 8.09 (t, *J*=7.7 Hz, 1H), 4.65 (s, 3H), 4.62 (s, 3H); ¹³C NMR (125.7 MHz, CD₃CN) δ [ppm]: 154.67, 150.66, 149.05, 146.70, 139.88, 139.24, 136.67, 136.40, 135.99,

131.58, 130.71, 130.65, 130.36, 129.47, 127.54, 126.53, 122.80, 119.77, 119.47, 119.07, 45.96, 41.01.

Synthesis of (*E*)-1-methyl-2-(2-(quinolin-2-yl)vinyl)quinolinium iodide (**15**)

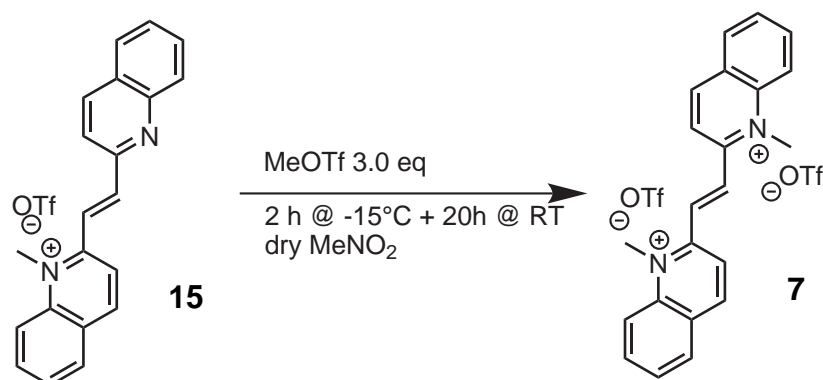


A mixture of **20** (824 mg, 2.89 mmol), quinoline-2-carboxaldehyde (500 mg, 3.18 mmol) and piperidine (2 drops) in MeOH (8 ml) was heated to reflux for 2 h. The solution was cooled with an ice-water bath obtaining an orange precipitate which was filtered on an Hirsh funnel and washed with cold MeOH and Et₂O. Residual solvent was removed under reduced pressure at 50 °C (596 mg, 1.405 mmol, yield 49%, m.p.: 220 °C (dec.)).

¹H NMR (500 MHz, DMSO-*d*₆) δ [ppm]: 9.22 (d, *J*=8.8 Hz, 1H), 8.71 (d, *J*=8.8 Hz, 1H), 8.66 (d, *J*=9.0 Hz, 1H), 8.59 (d, *J*=8.5 Hz, 1H), 8.46-8.43 (m, 2H), 8.30-8.23 (m, 3H), 8.14 (d, *J*=8.5 Hz, 1H), 8.08 (d, *J*=8.1 Hz, 1H), 8.04 (t, *J*=7.6 Hz, 1H), 7.87 (td, *J*=7.0 Hz, *J*=1.2 Hz, 1H), 7.71 (t, *J*=7.5 Hz, 1H), 4.67 (s, 3H); ¹³C NMR (125.7 MHz, DMSO-*d*₆) δ [ppm]: 156.05, 153.60, 148.11, 145.64, 145.61, 139.75, 137.85, 135.86, 131.06, 130.70, 129.96, 129.72, 128.88, 128.54, 128.46, 128.40, 125.16, 122.38, 121.99, 119.96, 40.96.

Synthesis of (*E*)-1-methyl-4-(2-(1-methylquinolinium-2-yl)vinyl)quinolinium trifluoromethanesulfonate (**7**)

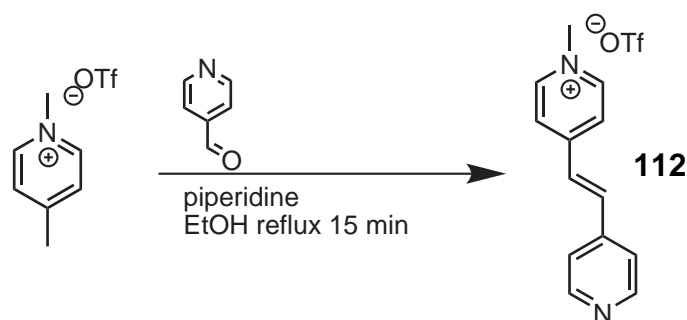
Under N₂ atmosphere, MeOTf (464 mg, 2.83 mmol) was added to a stirred suspension of **15** (400 mg, 0.94 mmol) in dry MeNO₂ (4 ml) cooled to -15 °C with an ice bath. The mixture was kept under stirring at -15 °C for 2 h, and stirred overnight at room temperature. After a 15 min a clear solution was obtained. More product was precipitated after addition of Et₂O, collected by filtration on



an Hirsh funnel, dried in vacuum and crystallized twice from EtOH (91 mg, 0.149 mmol, yield 16%, m.p.: 287-288 °C).

$^1\text{H NMR}$ (500 MHz, CD_3CN) δ [ppm]: 9.20 (d, $J=8.6$ Hz, 2H), 8.53 (d, $J=9.0$ Hz, 2H), 8.44 (dd, $J=8.2$ Hz, $J=1.1$ Hz, 2H), 8.42 ($J=8.6$ Hz, 2H), 8.34 (t, $J=8.12$ Hz, 2H), 8.18 (s, 2H), 8.10 (t, $J=7.4$ Hz, 2H), 4.62 (s, 6H); $^{13}\text{C NMR}$ (125.7 MHz, CD_3CN) δ [ppm]: 153.97, 147.20, 140.00, 136.74, 134.94, 130.83, 130.65, 129.78, 122.98, 119.19, 41.34.

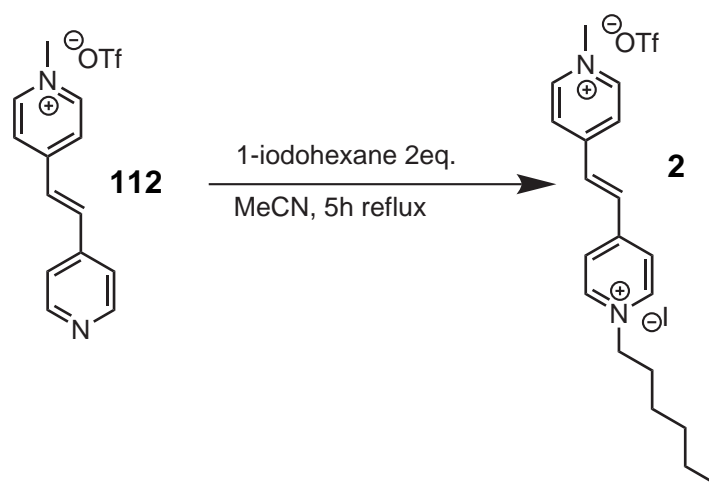
Synthesis of (*E*)-1-methyl-4-(2-(pyridin-4-yl)vinyl)pyridinium trifluoromethanesulfonate (112)



A mixture of 1,4-dimethylpyridine (5.000 g, 19.40 mmol) and pyridine-4-carboxaldehyde (3.05 g, 28.45 mmol) in EtOH (5 ml) was heated to reflux, and piperidine (1.1 ml, 948 mg, 11.1 mmol) was drop wise added. The resulting red/purple solution was refluxed for 15 min, and cooled with an ice-water bath obtaining a precipitate. The mixture was filtered on an Hirsh funnel, and washed with cold EtOH. Product was purified by crystallization from EtOH, filtered and washed with CHCl_3 . Residual solvent was removed under reduced pressure at 50 °C obtaining product as a white solid (2.687 g, 7.76 mmol, yield 40%, m.p.: 217-218 °C).

^1H NMR (500MHz, DMSO-d_6) δ [ppm]: 8.94 (d, $J=6.7\text{Hz}$, 2H), 8.71 (d, $J=6.0\text{Hz}$, 2H), 8.29 (d, $J=6.7\text{Hz}$, 2H), 7.96 (d, $J=16.4\text{Hz}$, 1H), 7.77 (d, $J=16.4\text{Hz}$, 1H), 7.67 (d, $J=6.0\text{Hz}$, 2H), 4.30 (s, 3H); ^{13}C NMR (500MHz, DMSO-d_6) δ [ppm]: 151.89, 151.03, 145.99, 142.63, 138.12, 128.20, 124.76, 122.20, 47.70.

Synthesis of (*E*)-1-hexyl-4-(2-(1-methylpyridinium-4-yl)vinyl)pyridinium trifluoromethanesulfonate iodide (**2**)

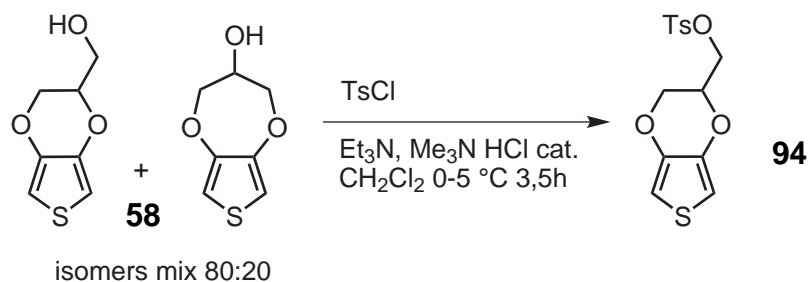


Under N_2 atmosphere, to a refluxing solution of **112** (1.00 g, 2.89 mmol) in MeCN (10 ml) a solution of 1-iodohexane (1.22 g, 5.75 mmol) in 2 ml of anhydrous MeCN was drop wise added. The mixture was refluxed for 5 h and cooled to room temperature observing the formation of a reddish precipitate. The solid product was collected by filtration, and washed with Et_2O (949 mg, 1.70 mmol, yield 59%, m.p.: 247°C (dec.)).

^1H NMR (500MHz, DMSO-d_6) δ [ppm]: 9.14 (d, $J=6.8\text{Hz}$, 2H), 9.04 (d, $J=6.7\text{Hz}$, 2H), 8.36 (d, $J=6.7\text{Hz}$, 2H), 8.33 (d, $J=6.7\text{Hz}$, 2H), 8.12 (s, 2H), 4.59 (t, $J=7.4\text{Hz}$, 2H), 4.35 (s, 3H), 1.95 (t, $J=6.4\text{Hz}$, 2H), 1.31 (broad s, 6H), 0.88 (t, $J=6.8\text{Hz}$, 3H); ^{13}C NMR (125.7MHz, DMSO-d_6) δ [ppm]: 150.90, 150.49, 146.44, 145.56, 134.46, 134.26, 125.94, 125.54, 60.87, 48.14, 31.02, 30.98, 25.53, 22.31, 14.30.

Synthesis of (2,3-dihydrothieno[3,4-*b*][1,4]dioxin-2-yl)methyl 4-methylbenzenesulfonate (**94**)

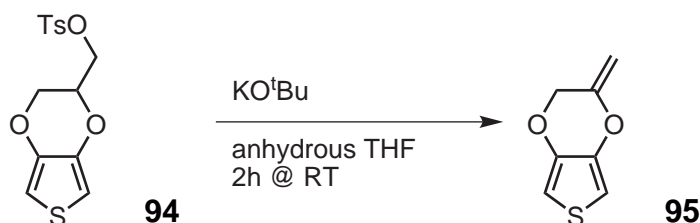
Under N_2 atmosphere, to an ice-cooled suspension of $\text{Me}_3\text{N} \cdot \text{HCl}$ (3.325 g, 34.8 mmol) and EDOT-MeOH (**58**) (mixture of isomers 80:20, 40.00 g, 232.3 mmol) in dry



CH₂Cl₂ (80 ml), TsCl (53.07, 278.4 mmol) was added portion wise under stirring. After 10 min Et₃N (35.2 g, 348 mmol) was added drop wise and the mixture was stirred at 0 °C for 3.5 h. The mixture was allowed to warm to RT, and CH₂Cl₂ (100 ml) was added. After stirring for 15 min at RT, water (100 ml) was added to the mixture followed by HCl_(aq) 10% till pH 2. The organic phase was collected, and the aqueous one was extracted with further 100 ml of CH₂Cl₂. The organic phases were washed with HCl_(aq) 5% (50 ml) followed by a saturated NaHCO₃ aqueous solution. The organic solution was dried over Na₂SO₄ and evaporated to dryness obtaining a brown solid. The obtained solid was crystallized twice from MeOH obtaining pure product as colourless crystals (39.596 g, 121.3 mmol, yield 65%, m.p.: 93.5-94.0 °C).

¹H NMR (500 MHz, CDCl₃) δ [ppm]: 7.80 (d, *J*=6.7 Hz, 2H), 7.36 (d, *J*=7.9 Hz, 2H), 6.31 (d, *J*=3.6 Hz, 1H), 6.26 (d, *J*=3.6 Hz, 1H), 4.38-4.34 (m, 1H), 4.24-4.22 (m, 1H), 4.19-4.14 (m, 2H), 4.04-4.01 (m, 1H); ¹³C NMR (125.7 MHz, CDCl₃) δ [ppm]: 145.46, 141.00, 140.45, 132.37, 130.13, 128.16, 100.35, 70.86, 67.00, 65.04, 21.83; Anal. Calcd for C₁₄H₁₄O₅S₂: C, 51.52; H, 4.32. Found: C, 51.50; H, 4.59.

Synthesis of 2-methylene-2,3-dihydrothieno[3,4-*b*][1,4]dioxine (95)

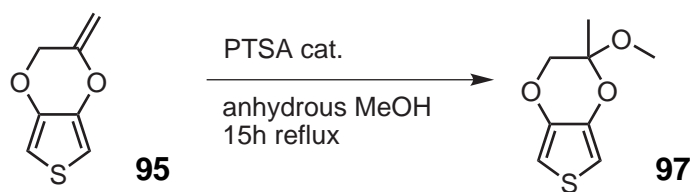


Under nitrogen atmosphere, to a stirred solution of **94** (10.02 g, 30.638 mmol) in anhydrous THF (50 ml), a solution of KO^{*t*}Bu (3.95 mg, 35.233 mmol) in THF (60 ml) was drop wise added under stirring. After 15 min the formation of a white precipitate was observed, 70 ml of THF were added and the mixture was

stirred at RT for 2h. ETP (200ml) was added, and the mixture was extracted with 4×100 ml of brine. The organic phase was collected, dried over Na_2SO_4 , and evaporated to dryness. The obtained liquid product was purified by filtering on a silica plug (SiO_2 , eluent: ETP/ Et_2O 8:1). Product was obtained as a colourless liquid after solvent removal under reduced pressure (4.139g, 27.17mmol, yield 87%).

^1H NMR (500MHz, CDCl_3) δ [ppm]: 6.44 (d, $J=3.6$ Hz, 1H), 6.39 (d, $J=3.6$ Hz, 1H), 4.77 (d, $J=1.93$ Hz, 1H), 4.49 (d, $J=0.49$ Hz, 2H), 4.42 (d, $J=2.09$ Hz 1H); ^{13}C NMR (125.7MHz, CDCl_3) δ [ppm]: 149.71, 142.02, 140.74, 100.64, 100.06, 92.74, 65.38; Anal. Calcd for $\text{C}_7\text{H}_6\text{O}_2\text{S} \cdot 3\text{H}_2\text{O}$: C, 52.48; H, 4.19. Found: C, 52.58; H, 4.20.

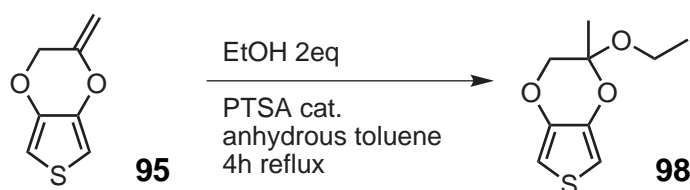
Synthesis of 2-methoxy-2-methyl-2,3-dihydrothieno[3,4-*b*][1,4]-dioxine (97)



Under nitrogen atmosphere, a deaerated solution of **95** (300 mg, 1.945 mmol) and anhydrous PTSA (55.5 mg, 0.322 mmol) in anhydrous MeOH (100 ml) was refluxed for 15h. The mixture was cooled to RT and saturated $\text{NaHCO}_3(\text{aq})$ (5 ml) was added. The volume was reduced to 10 ml evaporating the solvent under reduced pressure, and Et_2O (5 ml) was added. The organic phase was collected, washed 2×10 ml $\text{NaHCO}_3(\text{aq})$ and brine (10 ml). The solution was dried over MgSO_4 and evaporated under reduced pressure obtaining a pale yellow solid. Product was purified by column chromatography (SiO_2 , eluent: Et_2O /ETP 2:1) obtaining product as a white solid after solvent removal (198 mg, 1.06 mmol, yield 54%, m.p.: 63-64 °C).

^1H NMR (500MHz, CDCl_3) δ [ppm]: 6.35 (s, 2H), 4.10 (d, $J=11.25$ Hz, 1H), 3.85 (d, $J=11.28$ Hz, 1H), 3.36 (s, 3H), 1.49 (s, 3H); ^{13}C NMR (125.7MHz, CDCl_3) δ [ppm]: 140.94, 140.13, 100.36, 99.78, 96.49, 70.15, 49.48, 18.91; Anal. Calcd for $\text{C}_8\text{H}_{10}\text{O}_3\text{S}$: C, 51.60; H, 5.41. Found: C, 51.61; H, 5.60.

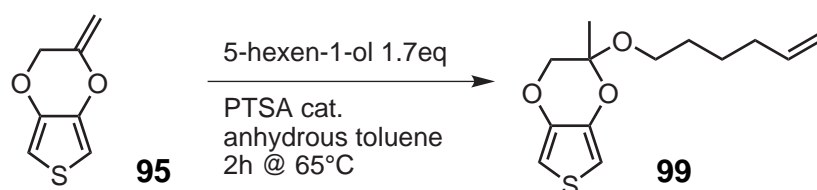
Synthesis of 2-ethoxy-2-methyl-2,3-dihydrothieno[3,4-*b*][1,4]dioxine (98)



Under nitrogen atmosphere, a deaerated solution of **95** (294 mg, 1.91 mmol), EtOH (179 mg, 3.89 mmol) and anhydrous PTSA (55.5 mg, 0.322 mmol) in anhydrous toluene (100 ml) was refluxed for 4 h. The mixture was cooled to RT and saturated $\text{NaHCO}_3(\text{aq})$ (5 ml) was added. The organic phase was washed 2×40 ml $\text{NaHCO}_3(\text{aq})$ and brine (40 ml). The solution was dried over Na_2SO_4 , and evaporated under reduced pressure obtaining a pale yellow solid. Product was purified by column chromatography (SiO_2 , eluent: $\text{Et}_2\text{O}/\text{ETP}$ 1:2) obtaining product as a white solid after solvent removal (109 mg, 0.544 mmol, yield 28%, m.p.: 49-50°C).

^1H NMR (500 MHz, CDCl_3) δ [ppm]: 6.34 (d, $J=3.65$ Hz, 1H), 6.32 (d, $J=3.63$ Hz, 1H), 4.10 (d, $J=11.19$ Hz, 1H), 3.84 (d, $J=11.20$ Hz), 3.68 (m, 2H), 1.50 (s, 3H), 1.12 (t, $J=7.11$ Hz, 3H); ^{13}C NMR (125.7 MHz, CDCl_3) δ [ppm]: 141.02, 140.39, 100.07, 99.55, 96.49, 70.29, 57.57, 10.76, 15.60; Anal. Calcd for $\text{C}_9\text{H}_{12}\text{O}_3\text{S}$: C, 53.98; H, 6.04. Found: C, 54.45; H, 5.79.

Synthesis of 2-(hex-5-enyloxy)-2-methyl-2,3-dihydrothieno[3,4-*b*][1,4]dioxine (99)

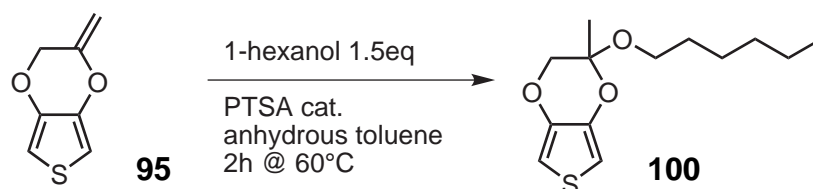


Under nitrogen atmosphere, a deaerated solution of **95** (300 mg, 1.95 mmol), 5-hexen-1-ol (333 mg, 3.33 mmol) and anhydrous PTSA (55.5 mg, 0.322 mmol) in anhydrous toluene (50 ml) was heated for 2 h at 65°C on a water bath. The mixture was cooled to RT and saturated $\text{NaHCO}_3(\text{aq})$ (5 ml) was added. The organic phase was washed 2×10 ml $\text{NaHCO}_3(\text{aq})$ and brine (20 ml). The solution was dried over Na_2SO_4 and evaporated under reduced pressure obtaining a red

oil. Product was purified by column chromatography (SiO₂, eluent: Et₂O/ETP 1:2) obtaining product as a colourless oil after solvent removal under reduced pressure (208 mg, 0.818 mmol, yield 42%).

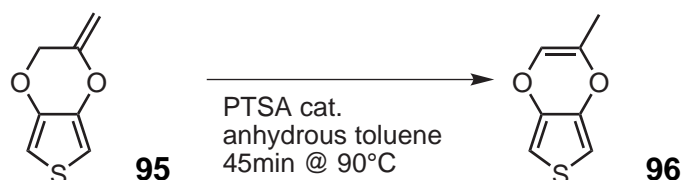
¹H NMR (500 MHz, CDCl₃) δ [ppm]: 6.33 (d, *J*=3.65 Hz, 1H), 6.32 (d, *J*=3.66 Hz, 1H), 5.71 (m, 1H), 4.92 (m, 2H), 4.09 (d, *J*=11.11 Hz, 1H), 3.84 (d, *J*=11.21 Hz, 1H), 3.60 (m, 2H), 1.95 (m, 2H), 1.49 (m, 2H), 1.48 (s, 1H), 1.26 (m, 2H); ¹³C NMR (125.7 MHz, CDCl₃) δ [ppm]: 141.11, 140.35, 138.83, 114.49, 100.18, 99.40, 96.34, 70.30, 61.58, 33.39, 29.19, 25.20, 19.66; Anal. Calcd for C₁₃H₁₈O₃S: C, 61.39; H, 7.13. Found: C, 61.73; H, 7.10.

Synthesis of 2-(hexyloxy)-2-methyl-2,3-dihydrothieno[3,4-*b*][1,4]-dioxine (100)



Under nitrogen atmosphere, a deaerated solution of **95** (300 mg, 1.95 mmol), 1-hexanol (298 mg, 2.918 mmol) and anhydrous PTSA (55.5 mg, 0.322 mmol) in anhydrous toluene (50 ml) was heated for 2 h at 60°C on a water bath. The mixture was cooled to RT and saturated NaHCO_{3(aq)} (5 ml) was added. The organic phase was washed 2 × 10 ml NaHCO_{3(aq)} and brine (20 ml). The solution was dried over Na₂SO₄ and evaporated under reduced pressure obtaining a red oil. Product was purified by column chromatography (SiO₂, eluent: Et₂O/ETP 1:4) obtaining product as a colourless oil after solvent removal under reduced pressure (388 mg, 1.279 mmol, yield 66%).

¹H NMR (500 MHz, CDCl₃) δ [ppm]: 6.33 (d, *J*=3.61 Hz, 1H), 6.31 (d, *J*=3.65 Hz, 1H), 4.09 (d, *J*=11.20 Hz, 1H), 3.84 (d, *J*=11.11 Hz, 1H), 3.59 (m, 2H), 1.49 (s, 3H), 1.49-1.45 (m, 2H), 1.17 (m, 6H), 0.83 (t, *J*=7.05 Hz, 3H); ¹³C NMR (125.7 MHz, CDCl₃) δ [ppm]: 141.12, 140.39, 100.14, 99.37, 96.34, 70.32, 61.84, 31.57, 29.77, 25.67, 22.70, 19.67, 14.12; Anal. Calcd for C₁₃H₂₀O₃S: C, 60.91; H, 7.86. Found: C, 61.01; H, 8.28; N, 0.44.

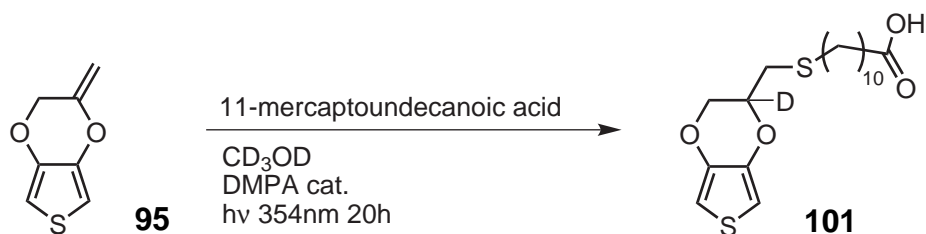


Synthesis of 2-methylthieno[3,4-*b*][1,4]dioxine (96)

Under nitrogen atmosphere, a deaerated solution of **95** (360 mg, 2.334 mmol) and anhydrous PTSA (25 mg, 0.145 mmol) in anhydrous toluene (35 ml) was heated for 45 min at 90 °C on a water bath. The mixture was cooled to RT, filtered to remove the insoluble material, and washed 2 × 10 ml NaHCO_{3(aq)} and brine (20 ml). The organic phase was dried over Na₂SO₄ and evaporated under reduced pressure obtaining product as a colourless oil (160 mg, 1.037 mmol, yield 45%).

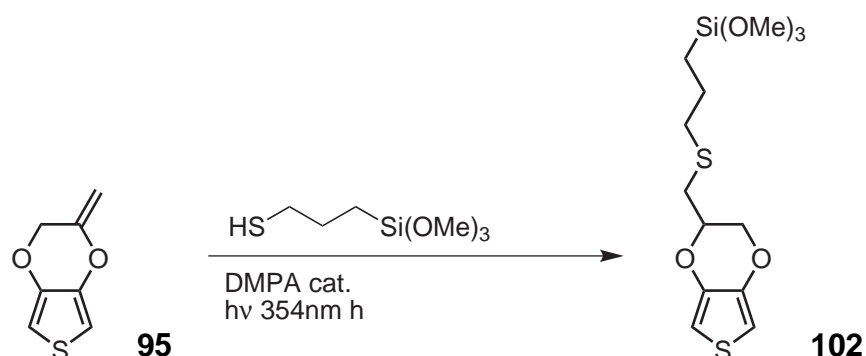
¹H NMR (500 MHz, CDCl₃) δ [ppm]: 6.27 (d, *J*=3.70 Hz, 1H), 6.23 (d, *J*=3.6 Hz, 1H), 5.76 (d, *J*=1.40 Hz, 1H), 1.73 (d, *J*=1.39 Hz, 3H); ¹³C NMR (125.7 MHz, CDCl₃) δ [ppm]: 139.90, 139.16, 132.86, 119.99, 100.62, 100.39, 14.83.

Synthesis of 11-((2,3-dihydrothieno[3,4-*b*][1,4]dioxin-2-yl)methylthio)undecanoic acid (101)



In a NMR tube, a solution of **95** (68 mg, 0.446 mmol), 11-mercaptoundecanoic acid (102 mg, 0.469 mmol) and 2,2-dimethoxy-1,2-diphenylethane (DMPA) (1.66 mg, 4.4 μmol) in CD₃OD (0.7 ml) was irradiated for a total of 20 h at 354 nm using an handheld UV lamp. The reaction was monitored using NMR spectroscopy observing a conversion higher than 90%.

¹H NMR (500 MHz, CD₃OD) δ [ppm]: 6.36 (d, *J*=3.70 Hz, 1H); 6.35 (d, *J*=3.6 Hz, 1H), 4.25 (d, *J*=11.64 Hz, 1H), 4.03 (d, *J*=11.6 Hz, 1H), 2.82 (d, *J*=14.0 Hz, 1H), 2.72 (d, *J*=14.1 Hz, 1H), 2.62 (m, 2H), 2.29 (m, 2H), 1.63-1.57 (m, 4H), 1.42-1.32 (m, 12H).

Synthesis of (3-((2,3-dihydrothieno[3,4-*b*][1,4]dioxin-2-yl)methylthio)propyl)trimethoxysilane (102)

In a test tube, a mixture of **95** (149.4 mg, 0.969 mmol), (3-Mercaptopropyl)-trimethoxysilane (MPTMS) (190.4 mg, 0.970 mmol) and 2,2-dimethoxy-1,2-diphenylethanone (DMPA) (2.20 mg, 8.58 μ mol) was irradiated for 20 min at 354 nm using an handheld UV lamp. Product was recovered as a pale yellow oil (339.8 mg, 0.97 mmol, quantitative yield)

¹H NMR (500 MHz, CDCl₃) δ [ppm]: 6.33 (s, 2H), 4.27-4.24 (m, 2H), 4.05 (dd, $J=11.35$, $J=6.7$ Hz, 1H), 3.57 (s, 9H), 2.84 (dd, $J=13.87$ Hz, $J=5.5$ Hz, 1H), 2.70 (dd, $J=13.8$ Hz, $J=7.5$ Hz, 1H), 2.63 (td, $J=7.2$ Hz, $J=2.2$ Hz, 2H), 1.73 (quin, $J=7.8$ Hz, 2H), 0.76 (t, $J=8.3$ Hz, 2H).